INFLUENCES OF LIPID SIGNALING ON NUCLEOCYTOPLASMIC TRANSPORT

By

Randolph Solomon Faustino

A Thesis
Submitted to the Faculty of Graduate Studies
in Partial Fulfillment of the Requirements
for the Degree of

DOCTOR OF PHILOSOPHY

Department of Physiology
Faculty of Medicine
University of Manitoba
and the Division of Stroke and Vascular Disease
St. Boniface General Hospital Research Centre
Winnipeg, Manitoba, Canada

Influences of Lipid Signaling on Nucleocytoplasmic Transport

BY

Randolph Solomon Faustino

A Thesis/Practicum submitted to the Faculty of Graduate Studies of The University of Manitoba in partial fulfillment of the requirement of the degree

Of

DOCTOR OF PHILOSOPHY

DEDICATION

First and foremost, I would like to dedicate this body of work to God. Science has given me skills and knowledge, but beyond that, it has given me a greater appreciation of the complexity of life and for the Creator that has orchestrated it.

To my parents – two of the most stalwart foundations during my time in graduate school. Their support, selflessness and excitement for me and my accomplishments can never be measured.

To my younger brother, who kept me striving to be the best older brother and role model that I could be.

Finally, this is dedicated to those who dare to follow the path of the scientist. The "road to discovery" is embarked upon for the improvement of humanity and is filled with all manners of detours and sidetracking and dead ends. Despite this, the scientific pursuit can still be succinctly and aptly described by this encouraging passage:

"Ask, and you will receive;

Seek, and you will find;

Knock, and the door will be opened to you."

(Matthew 7:7)

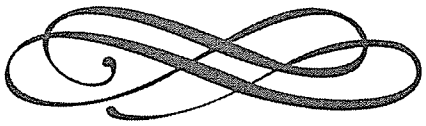

TABLE OF CONTENTS

ABSTRACT

Cellular functions are governed by constant molecular trafficking between the nucleus and the cytoplasm of the cell. Nucleocytoplasmic transport is essential in maintaining cellular homeostasis and in responding to metabolic signals. Modulation of transport, therefore, can directly influence gene expression and regulation of transport can happen in a global or specific manner.

As calcium has been demonstrated to affect nuclear pore functioning, we investigated the presence of calcium binding proteins within nuclear pore complex fractions isolated from rat hepatocytes. No calcium binding proteins were identified. However, a variety of MAP kinase substrates were found to co-purify with the nuclear pore complex fraction. Treatment of permeabilized cells did not demonstrate any effects on nuclear import, so it was surmised that the phosphoproteins within the purified pore fraction may play a role in structural dynamics or export.

The role of ERK-2 in nuclear protein import regulation via modification of a cytosolic substrate in vascular smooth muscle cells was investigated. An unusual dose-dependent effect of MAP kinases on nuclear protein import was observed. For ERK-2, p38 and JNK, higher concentrations (1 μg/ml) stimulated nuclear protein import whereas lower concentrations (0.04 μg/ml) inhibited import. This was observed in both permeabilized cell assays and microinjection studies. The targets for the actions of ERK-2 were investigated. RanGAP was identified as a candidate protein responsible for mediating the effects of ERK-2. After pre-treatment with high concentrations of ERK-2, RanGAP activity was significantly increased by 50%. In contrast, low concentrations of ERK-2

significantly attenuated RanGAP activity by 15% - 20%. These results identify a unique ERK-2 kinase dependent mechanism of nuclear transport regulation.

Lysophosphatidylcholine (LPC) stimulates vascular smooth muscle cell (VSMC) proliferation, but its mechanism of action is unclear. Import of proteins from the cytoplasm into the nucleus of a given cell is integral to the regulation of gene expression. LPC was hypothesized to exert its effects through alterations in nuclear protein import. VSMCs were pre-incubated with LPC and then microinjected with a marker protein for nuclear import. A significant stimulation of nuclear protein transport was observed. We hypothesized that the mechanism involved an action of LPC on a cytosolic component of the transport machinery. A cytosolic nuclear import cocktail was treated with various concentrations of LPC and then used in a conventional nuclear protein import assay in permeabilized VSMC. A significant stimulation of import by LPC was again observed. This effect was not observed with other lysophosphatidyl species. The stimulation was blocked with PD-98059, a MEK inhibitor. The downstream cytosolic target for LPC-induced MAPK activation was found to be an augmentation of GTP hydrolysis by RanGAP, a RanGTPase activating protein and a critical regulatory component of nuclear protein import. We conclude that LPC may alter gene expression and cell proliferation through striking effects on nuclear protein import via a MAPK induced activation of RanGAP. This may play an important role in atherosclerosis and other disorders involving accelerated cell growth/proliferation.

Ceramide has an anti-proliferative and apoptotic action, but its mechanism is unclear. The effect of ceramide on nuclear protein import in vascular smooth muscle cells (VSMCs) was studied as a potential mechanism. Cytosol pre-treated with ceramide

significantly inhibited nuclear import. This was reversed with SB-202190, a p38 MAP kinase inhibitor and PD-98059, a MEK antagonist. Microinjection of ceramide into VSMCs also inhibited import (by ~80%) and was reversed by the addition of SB-202190. The target for ceramide-mediated MAPK activation was further investigated. CAS modulates nuclear protein import by regulating nucleocytoplasmic cycling of importin-α. CAS is localized at the nuclear rim in control VSMC. Ceramide treatment eliminated this localization. Treatment of cells with ceramide ± SB-202190 or PD-98059 normalized CAS to the nuclear periphery. Ceramide therefore inhibits nuclear protein import in VSMCs via p38 or MEK kinase activation. CAS appears to be a target of MAP kinase activity and mediates the inhibitory effects of ceramide on nuclear protein import.

MAP kinases were identified as regulators of nuclear import in vascular smooth muscle cells. Two lipid species were reported to influence nuclear transport via MAP kinase signaling and the results of this work demonstrate previously uncharacterized MAPK-dependent effects of lipids on nucleocytoplasmic transport.

ACKNOWLEDGEMENTS

A body of work such as this is a significant undertaking that cannot possibly be accomplished without the assistance and guidance of so many individuals. The first big thank you goes without question to my advisor and mentor, Dr. Grant Pierce. I have said this before, but I will say it here again to be recorded for posterity's sake: Grant is not only a superb mentor, but an extremely generous individual, both with his time and resources. He is a consummate gentleman, scientist, businessman, negotiator and captain of his ship, and he does this all with equal facility. Beyond all this, however, he remains one of the best things of all: a good friend. Thank you Grant!

With me every step of the way from the beginning of my career in graduate studies were the members of my advisory committee: Drs. James Gilchrist, Larry Hryshko and Elissavet Kardami. I could not have possibly had a more encouraging and supportive group of individuals backing me up, whether through constructive criticism of my work, or by keeping me on my toes during annual evaluations that were laced with just the right amount of humour to help me maintain my sanity. Their collegial guidance, advice and friendship over the years has been invaluable and extremely appreciated.

The beginning of my graduate studies was earmarked with the technical know-how of a scientific initiate – which is to say, next to nil! This was remedied by the instruction of a certain PhD student whose surname I could not humanly pronounce at the time. However, as I can now properly say (and spell!) it, a big thank you goes to Dr. Michael Czubryt. The lion's share of the techniques I learned which I used to complete my project

was taught to me by an extremely patient and intelligent senior student who is now a good friend and a rising star himself. Thanks, Mike!

The scientific method is not exclusively technical and is punctuated at times with a bit of politics. For all the insightful and de-stressing conversations on just this topic, I would like to thank not only Dr. Czubryt, but Dr. Jeff Wigle, and my fellow doctoral candidate, Marjorie Zettler. An important component in maintaining graduate sanity is the ability to discuss these kinds of things and Jeff, Mike and Marj contributed immensely in this regard. For your time and your friendship, thank you guys!

Doctoral candidates rarely reach the successful completion of their program without the aid and assistance of their colleagues in the lab. In this respect, I was blessed with not only the technical skills of talented co-workers but had the added benefit of their friendship as well. To the trio (Mel L., Annette, and Michele), how could I have possibly done this without you three??? Mel, you ARE my nuclear transport partner-in-crime, and my work would be half of what it is without you. Thank you so much for your help and your friendship! Annette, I have told you this before, and I tell you again – you are the Cell Culture Goddess who makes cells listen. How do you do it? Thank you so much for all the work you've done, not just for me, but for the whole lab as well! Michele – of the three, you've known me the longest and helped me so much in the beginning of this endeavour. You have seen the ups and downs and you remain a great friend! Thank you, thank you, thank you!

Any graduate student can tell you that deadlines are a grad student's worst enemy. In the Division of Stroke and Vascular disease, Janet Labarre is THE Administrative

Assistant and a good friend who helped deal with all those and more. To Janet, your help from beginning to end has been greatly appreciated! Thank you!

Finally, I want to express a big thank you to all the members of the Division of Stroke and Vascular Disease and the 4th floor who made my time as a doctoral candidate enjoyable, amusing, educational and memorable and continue to do so in my newly minted PhD state! Apologies in advance to those I may have missed – many, many thanks to the (current and former) members of my lab: Cecilia, Chantal, Brad, Nicole, Thane, Elena, Satoru, Andrea, Mel K., Alex, Helen, Justin, Riya, Sandeep and Paul – all of you are amazing and wonderful people to work with and I'm thankful I had the opportunity to meet and know you. A great lab is measured by two things: great productivity and great people. You guys make the lab what it is, and I am extremely grateful for being a part of it!

LIST OF FIGURES

LIST OF TABLES

REVIEW OF LITERATURE

Nuclear Transport Signal Sequences

Nuclear localization signals (NLS)

Nuclear transport generally describes the process by which molecules move back and forth between the nuclear and cytoplasmic spaces. It is a bidirectional and energy dependent phenomenon, with specific regulatory mechanisms distributed within the soluble portion of the cell as well as at the nuclear envelope. Nucleocytoplasmic trafficking is initiated upon recognition of a specific signal sequence that directs the molecule to either be imported into the nucleus from the cytoplasm or exported in the opposite direction.

The first signal sequence identified was a monopartite, polybasic amino acid motif (PKKKRKV) directly responsible for the nuclear localization of the SV40 large T antigen (3). This nuclear localization signal, or NLS, was a polylysine motif known as the "classical" signal sequence (Table 1). NLSs also exist in a bipartite form. Dingwall *et al* first characterized the existence of a bipartite NLS in nucleoplasmin (4) and would later demonstrate that it contained polybasic sequences homologous to the NLS of the SV40 large T antigen (5).

The discovery of the NLS provided the impetus for the identification of other signal sequences responsible for nuclear import, but distinct from those of the SV40 variety. A glycine rich, novel sequence that did not contain any "classical" NLS-type basic amino acids was found in the pre-mRNA/mRNA binding protein hnRNP A1 (6) and was

Import receptor	Signal sequence/motif
Importin-α	(monopartite) PKKKRKV (3) (bipartite) KRPAAIKKAGQAKKKK (7)
Importin-β	RQARRNRRRRWR (8)
Transportin	NQSSNFGPMKGGNFGGRSSGPY GGGGQYFAKPRNQGGY (8)
Snurportin1	trimethylguanosine cap (m_3G) (9)
XRIPα	DNA binding domain (10)

Table 1. Examples of nuclear import sequences and their cognate receptors

Importin-α is the primary receptor for the "classical" polybasic amino acid motif which occurs as a monopartite or bipartite signal sequence (see text and above). Once importin-α binds its substrate, an importin-β binding domain on the alpha subunit is exposed, leading to the formation of a heterotrimeric receptor-substrate complex. Importin-β is a primary receptor as well and can bind to individual proteins without the need of an adaptor protein. Other import receptors recognize nuclear localization signals distinct from the polylysine type and are depicted above.

designated M9 and recognized by transportin (Table 1). Attachment of this sequence to two cytosolic enzymes, pyruvate kinase and beta-galactosidase, was sufficient to enable their import into the nucleus. A listing of selected NLSs and their cognate receptors are given in Table 1.

Nuclear export signals (NES)

Proteins exported from the nucleus typically possess a leucine-rich signaling motif called the nuclear export signal. Similar to NLSs, a variety of signaling motifs exist that are capable of mediating nuclear export (11). Instead of amino acid sequences, RNA species possess structural motifs recognized by specialized exportin molecules that direct them towards the cytoplasm (12). Examples of various nuclear export signals are shown (Table 2).

Due to the variety of transport signals available for import and export, nucleocytoplasmic trafficking remains a tightly controlled process. The primary level of regulation occurs at the nuclear transport signal by controlling access to the NLS/NES. With respect to the localization signal, the eukaryotic cell has evolved various mechanisms to control nuclear trafficking. Phosphorylation, dephosphorylation and regulated proteolysis are some of the common regulatory processes that play a role in regulating nuclear transport at one or more levels (13-19). The processes of phosphorylation and dephosphorylation will be focused upon because of their relevance to the research carried out in this thesis.

Export receptor	Signal sequence/motif	Molecule exported
Crm1	LPPLERLTLD (20) LALKLAGLDI (21) LQKKLEELELE (22)	Rev PKI MEK1
CAS	CGGLDKIE (23)	importin-α
Calreticulin	CGGGKVFFKRAVEGQHNLY (24)	glucocorticoid receptor
TAP Mex67p	RNA stem-loop structure (25) Polyadenylated RNA (26)	RNA

Table 2. Selected nuclear export signals and their receptors

Exportins are responsible for delivering proteins to the cytosol from the nucleus. Crm1 (also known as exportin-1) has been well characterized as a nuclear exporter. Other proteins have been identified that bind signals distinctly different from those recognized by Crm1. RNA molecules are exported from the nucleus once their receptor recognizes distinct molecular features (see above).

Regulation of NLSs and NESs

A common method of regulation within the eukaryotic cell is phosphorylation of a target substrate. In all phosphorylation and dephosphorylation cycles, there are two classes of enzymes responsible for adding and removing phosphate groups, called kinases and phosphatases, respectively.

A diverse number of kinases exist that can be regulated by cyclic AMP and GMP (27-29), calcium (30) and lipids (31-33). The process of phosphorylation begins when a protein substrate possesses a motif recognized by the kinase. Upon association of the kinase with its target, ATP is recruited to the complex and the terminal phosphate (designated as the γ phosphate) is transferred to the recipient protein, generating the phosphoprotein, ADP or AMP, plus an inorganic phosphate as reaction products. The amino acids phosphorylated in mammalian systems are referred to as O-phosphates and include tyrosine, threonine and serine (34). O-phosphates are phosphoproteins in which the hydrogen on the hydroxyl moiety of the R-group has been substituted with an anionic phosphate group. More than one of these phosphoaminoacids within a given protein may be phosphorylated, as is the case with activated MAP kinases which are dually phosphorylated on both threonine and tyrosine residues (35). While the three O-phosphates are by far the most commonly studied, other phosphoaminoacids, such as phosphohistidine, exist as well (34). Phosphoaminoacids which flank the nuclear localization signal within a protein can affect the affinity of a transport receptor for the NLS upon phosphorylation. For example, phosphorylation of the residues adjacent to the NLS of the SV40 large T antigen regulates nuclear import of the large T antigen (36).

The removal of phosphate groups is carried out by protein phosphatases (37). Phosphatases can be regulated by calcium and calmodulin (38) and can be classified into four different families based on substrate specificity and degree of conservation within their catalytic domains (39). With respect to nuclear transport, dephosphorylation functions in a manner similar to that of phosphorylation. In this case, the removal of a phosphate group can unmask the transport motif, leading to its recognition and binding by the appropriate transport receptor. For example, dephosphorylation of NFAT exposes its NLS, subsequently leading to its nuclear translocation (14). Furthermore, recent work has identified an association between protein phosphatase 2A and members of the importin-β superfamily (40), which may indicate the existence of generalized phosphatase-dependent regulation on nuclear transport machinery.

Regulation of nucleocytoplasmic transport occurs within the cytosol and possibly at the nuclear envelope. A brief overview of transport receptors, their subclasses, and a short review on the nuclear pore complex are presented in the following sections.

Nuclear Transport Receptors

The proteins responsible for the movement of molecules back and forth between the nuclear and cytosolic compartments are collectively referred to as importins (41). Identification of the first importins, also known as karyopherins, occurred in the early 1990's. It was the isolation and characterization of importin-β (or karyopherin β1) (42, 43) that unequivocally demonstrated the requirement of a cytosolic factor in the nuclear import process. As more transport receptors were discovered in subsequent years, it became apparent that all of them could be categorized into one family. The importin-β superfamily is the *de facto* designation describing these related proteins. For mechanistic reasons, transport receptors responsible for the export of molecules out of the nucleus into the cytoplasm also fall within this importin superfamily (41).

Importin-β

The prototypical importin-β protein was first isolated and identified as a 97kDa molecule in bovine erythrocytes (42), and was subsequently found to be essential to nuclear protein import (42, 44). Structural analyses of importin-β revealed that it contains nineteen tandem HEAT repeats, arranged so that the tertiary conformation of the molecule is a right handed superhelical protein with a high degree of flexibility (45). Functionally, it can bind to nuclear pore proteins containing the FxFG motif and possesses an amino-terminal Ran binding domain (46-48). With respect to nuclear import, importin-β participates as part of a trimeric complex formed when a protein bearing a "classical" polybasic NLS is recognized by its receptor, importin-α (49).

Interaction of the NLS with its cognate receptor causes importin-α to undergo a conformational shift which then promotes its binding to the carboxy terminus of importin-β by virtue of an importin-β binding (IBB) domain at its N-terminus (45, 50). Formation of the importin heterodimer causes mutual conformational changes in both subunits which ultimately promote nuclear protein import (50) in a Ran and energy dependent manner.

Alternatively, a protein may directly bind importin-β without the use or need of adaptor proteins such as importin-α (41). Several viral proteins (51-53) are able to bind directly to the IBB domain and form a heterodimeric complex which is imported into the nucleus. Additionally, other endogenous eukaryotic proteins use this mechanism to be imported (54, 55). Based on these observations, the importin-β superfamily can be subdivided into two categories: those that are capable of binding a molecule directly for import/export and those which utilize adaptor proteins. Adaptor proteins themselves can be further classified into importin-α type NLS receptors, or non-importin-α type receptors.

Adaptors: Importin-α

Importin-α is the prototypical adaptor protein that recognizes both mono- and bipartite "classical" NLSs (56, 57) and was simultaneously isolated and identified with importin-β, as mentioned previously (42). This molecule consists of ten tandem ARM motifs, with the main NLS recognition sites residing within the second and fourth ARM repeats (58). At the C-terminus is an acidic domain required for binding to CAS, the endogenous

nuclear exporter of importin-α (23, 59, 60). At its N-terminus, importin-α possesses the IBB domain required for interaction with importin-β (23, 45).

Identification of a polybasic sequence within the IBB (61) led to the hypothesis that importin-α may also possess autoinhibitory activity in addition to binding to importin-β. This was confirmed by a later study which reported that a Lys-Arg-Arg sequence within the IBB domain binds to the NLS recognition domain within importin-α (62). This highly conserved sequence was identified in several forms of importin-α from yeast, mouse and human sources (62). Using a variety of plasmids encoding different mutations of this IBB domain, Harreman *et al* demonstrated that this sequence was essential in promoting NLS-cargo release within the nucleus and it was suggested that the autoinhibitory properties of the IBB domain prevents futile cycling of unloaded importin-α/β complexes (62).

More than one form of importin-α exists. In humans, six forms have been identified, each of which are separate gene products (63), as is the case for the various mouse isoforms of importin-α that have been identified (64). Since tissue specific distribution of the importin-α isoforms has been observed, it is possible that each isoform is responsible for the import of a specific group or subset of proteins. For example, RanGEF/RCC1 is a constitutively nuclear enzyme that is preferentially imported by importin-α3 (63, 65). Future studies investigating specific importins and their respective cargoes will provide a more comprehensive understanding of the diversity of import receptors involved in nuclear transport.

Adaptors: Non-importin-α receptors

There are other adaptor proteins with specific cargoes distinct from those mediated by the importin α/β complex. In some ways, these molecules possess similar characteristics to those of importin-α. For example, they possess an IBB domain as well as the ability to bind to their respective cargoes. However, the recognition motif by which they bind is typically quite different.

Snurportin1 was identified as the adaptor responsible for importing m_3G capped U snRNPs into nuclei (9). Similar to importin-α, snurportin1 possesses an IBB domain. However, it is distinct from the former in that it allows Ran- and energy- independent nuclear protein import (66). In order to illustrate that this ability was characteristic of the snurportin1 IBB, Huber *et al* (9) generated a snurportin1 mutant that possessed the importin-α IBB and demonstrated that ribonucleoprotein import became Ran dependent.

Histone H1 is a small (~22 kDa) basic protein that is consitutively nuclear and actively transported despite its small size (67-69). Also known as linker histones, they are involved in both the maintenance of chromatin structure as well as transcriptional regulation (69) and are the exclusive ligands of the importin-7 receptor (68, 70). Several portions of histone H1 possess stretches of basic amino acids that, on their own, serve as NLSs that can functionally interact with individual import factors (68). However, import of the entire complex requires a heterodimeric receptor composed of both importin-β and importin-7, the latter being the adaptor specific for histone H1 (68). It is believed that in addition to serving as an import receptor, the importin-β/-7 complex may also serve as a chaperone for histone H1 (68).

The XRIPα adaptor protein is responsible for importing replication protein A (RPA) (10). RPA is a single stranded DNA binding protein composed of three subunits (71) that

is essential for chromosomal DNA replication (72), repair (73) and recombination (74-76). The adaptor was originally identified using a yeast two hybrid assay by Jullien *et al* (10). Briefly, several domains of the RPA holoenzyme were fused to the Gal4 DNA-binding domain to form the "bait" constructs that were used to screen a *Xenopus* oocyte cDNA library. The identified adaptor was found to specifically bind RPA and possessed an IBB structurally distinct from that of the importin-α IBB (10). Like previously characterized importin-β binding domains, the IBB of XRIPα is located at the N-terminus and contains an arginine-rich, basic motif (10). The similarities end there, however, as the arginines in this particular receptor do not form continuous stretches of basic amino acids as found in the IBBs of HIV Tat and Rev proteins (53).

It is clear from these examples that although members within the importin family share some properties, they each possess individualized characteristics which contribute to the recognition of a broad and diverse array of substrates. While this observation has been made for molecules which mediate nuclear import, it also holds true for the members of the importin-β superfamily which are responsible for nuclear export.

Exportins

Exportins are members of the importin-β family that are responsible for the movement of proteins, RNA and ribonucleoproteins from the nucleus into the cytoplasm (41, 77). They are generally similar to the importins in that they recognize a localization signal, bind to Ran and interact with proteins of the nuclear pore complex (NPC). Upon closer investigation of the exportin molecule, differences become apparent.

CRM1/exportin-1 is the prototypical exportin molecule responsible for nuclear transport of the bulk of exported substrates. It recognizes a nuclear export signal (NES), which is different from the polybasic NLS mentioned earlier (78). NESs are typically leucine rich sequences found on a protein destined for transport into the cytosol (21). The first such NES was identified in the HIV Rev protein (79). In nuclear export, CRM1 binds to the NES and associates with RanGTP to form a stable export complex, similar to the mechanism of nuclear import. This heterotrimeric complex is then directed to the nuclear basket on the nucleoplasmic face of the NPC (80) and subsequently exported to the cytoplasm. Once there, RanGAP activates the intrinsic GTPase activity of Ran (81). Hydrolysis of GTP to form RanGDP promotes dissociation of the nuclear export complex, releasing the cargo into the cytoplasm. Although this pathway is recognized as the "workhorse" pathway of nuclear export, other CRM1-independent transport mechanisms exist.

One such example is the nuclear export of importin-α. Kutay *et al* identified CAS as an essential protein required to transport importin-α from the nucleus back to the cytosol following a round of nuclear import (60). Subsequent studies confirmed the functionality of CAS as a nuclear exporter (82-85). Calreticulin is another nuclear export receptor identified by Holaska *et al* (24). Although indirectly involved in nuclear import of NFAT3 (86) and MEF2C (87), calreticulin directly exports nuclear, steroid, non-steroid hormone and orphan receptors (88, 89) from the nucleus in a calcium dependent manner (90). This observation was surprising, given the constitutive localization of calreticulin to the endoplasmic/sarcoplasmic reticulum (91). Calreticulin possesses an ER/SR retention signal which limits its presence in the cytosol (91). Walther *et al* examined calreticulin-

mediated export of the glucocorticoid receptor (GR) using a heterokaryon assay and reported that transient permeabilization of the ER membrane allowed calreticulin to leave the ER lumen (88). Calreticulin release led to increased nuclear export of GR compared to rates observed in control cells and it was hypothesized that calreticulin-mediated export was a normal physiological mechanism used to rapidly clear the nucleus of receptors prior to mitosis (88). The role of calreticulin as a nuclear export receptor remains debatable because no identifiable nuclear localization signal or import mechanism has been characterized for calreticulin. Resolution of these issues will solidify the role of calreticulin as a genuine export receptor.

Proteins are not the only molecules subject to exportin mediated transport. The export of RNA species involves completely different sets of receptors. The transport of tRNAs is mediated specifically by exportin-t (92, 93) and to a lesser extent, exportin-5 (94). Both exportin-t and exportin-5 co-operatively bind RanGTP and the tRNA molecule directly, without the need for adaptors. Similar to tRNAs, mRNAs possess specific proteins which direct them out of the nucleus in a CRM1- and Ran- independent manner.

Messenger RNA is delivered to the cytosol by the TAP receptor (95). This exportin forms a complex with another molecule, NXT1, to form a heterodimer that mediates the movement of mRNA out of the nucleus (96-98). However, transport of mRNA is slightly more complex, as other factors which participate in splicing, elongation and termination of the nascent mRNA transcript are required to mediate the association between the TAP/NXT1 complex and mRNA (77, 99, 100).

The descriptions in the previous sections demonstrate the diverse nature of nuclear transport receptors and adaptors. Many others exist that are either still being

characterized or remain to be identified (101). This body of knowledge concerning nucleocytoplasmic trafficking has come primarily from studies which have examined regulatory processes on the cytosolic machinery, but there is increasing evidence suggesting that modifications at the membrane bound, nuclear pore complex may also regulate nuclear trafficking (102). The nuclear pore complex and related elements are discussed next.

The Nuclear Pore Complex

Structure & Composition

Nuclear transport is a complex process involving both soluble, cytosolic machinery and membrane bound components. Molecules which localize from cytosolic to nucleoplasmic compartments and vice versa must cross both the outer and inner nuclear membranes of the nuclear envelope (NE) to reach their destination. For this purpose, a large multiproteinaceous structure called the nuclear pore complex, or NPC, spans both membranes of the NE and serves as the "gateway" through which these molecules pass (2, 103-111) (Figure 1). Electron microscopy of a nuclear envelope in cross section demonstrates how the nuclear pore complex serves as a proteinaceous "rivet" connecting both outer and inner nuclear membranes of the NE (Figure 2). Immunocytochemistry using mAb414, an antibody that recognizes nuclear pore complex proteins, demonstrates intense staining of the nucleus as well as pore complex proteins within the annulate lamellae in the cytoplasm (Figure 3). Confocal microscopy of smooth muscle cells at a higher magnification illustrates regular distribution of NPCs across the surface of the nuclear envelope (Figure 4). The nuclear pore complex is a dynamic and highly regulated structure which shows a high degree of evolutionary conservation across various species (108). Most of the information on NPC composition and architecture has been garnered from yeast (111) and *Xenopus* (112, 113) but the primary focus of this section will be on mammalian NPCs.

Mammalian NPCs are estimated to be roughly 125MDa in mass and composed of 100 - 200 nuclear pore proteins called nucleoporins (108). It measures ~120 nm in diameter

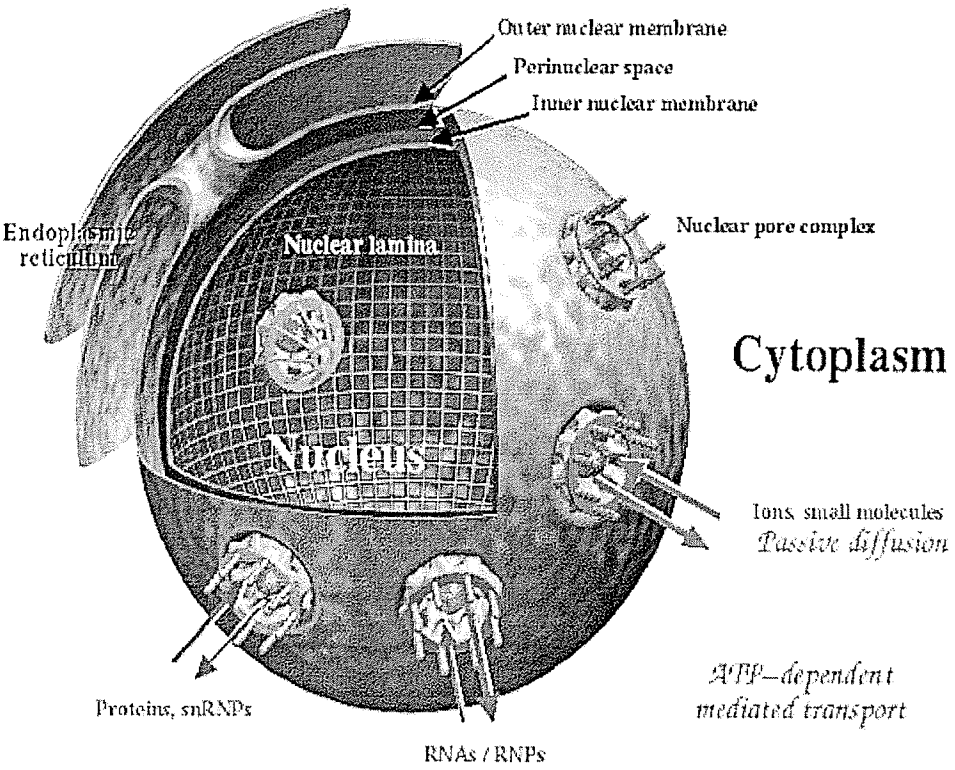

Figure 1. Nuclear pore complexes within the nuclear envelope

A schematic cutaway diagram of a nucleus is depicted above. Nuclear pore complexes sit astride the two membranes of the nuclear envelope, connecting the nuclear and cytosolic compartments. This allows for the movement of ions, small molecules, proteins, RNA, ribonucleoproteins (RNP), and small nuclear RNP (snRNP) between the two compartments (shown above). Also shown are the ER (the lumen of which is contiguous with the periplasmic space of the nucleus) as well as the nuclear lamina (which associates with the nuclear ring of the NPC). Image taken from Panté & Aebi (2).

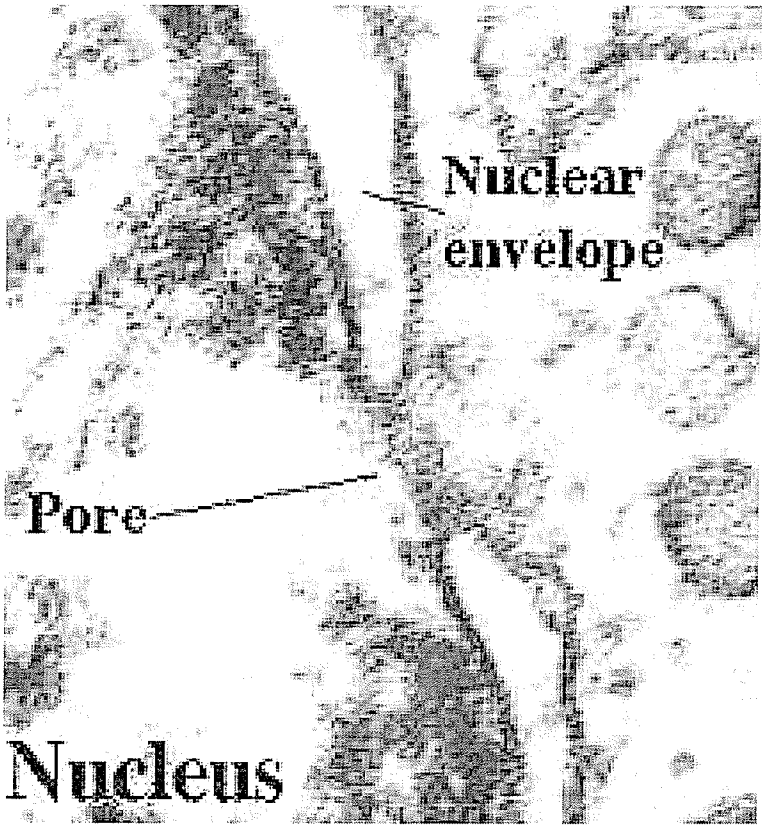

Figure 2. Electron microscopy of a nuclear pore complex in cross section

The nuclear pore complex is visualized as a distinctive, "rivet"-like feature joining the outer and inner membranes of the nuclear envelope. Shown is a section of nuclear membrane in cross-section.

Image source: http://www.cytochemistry.net/Cell-biology/nuclear_envelope.htm

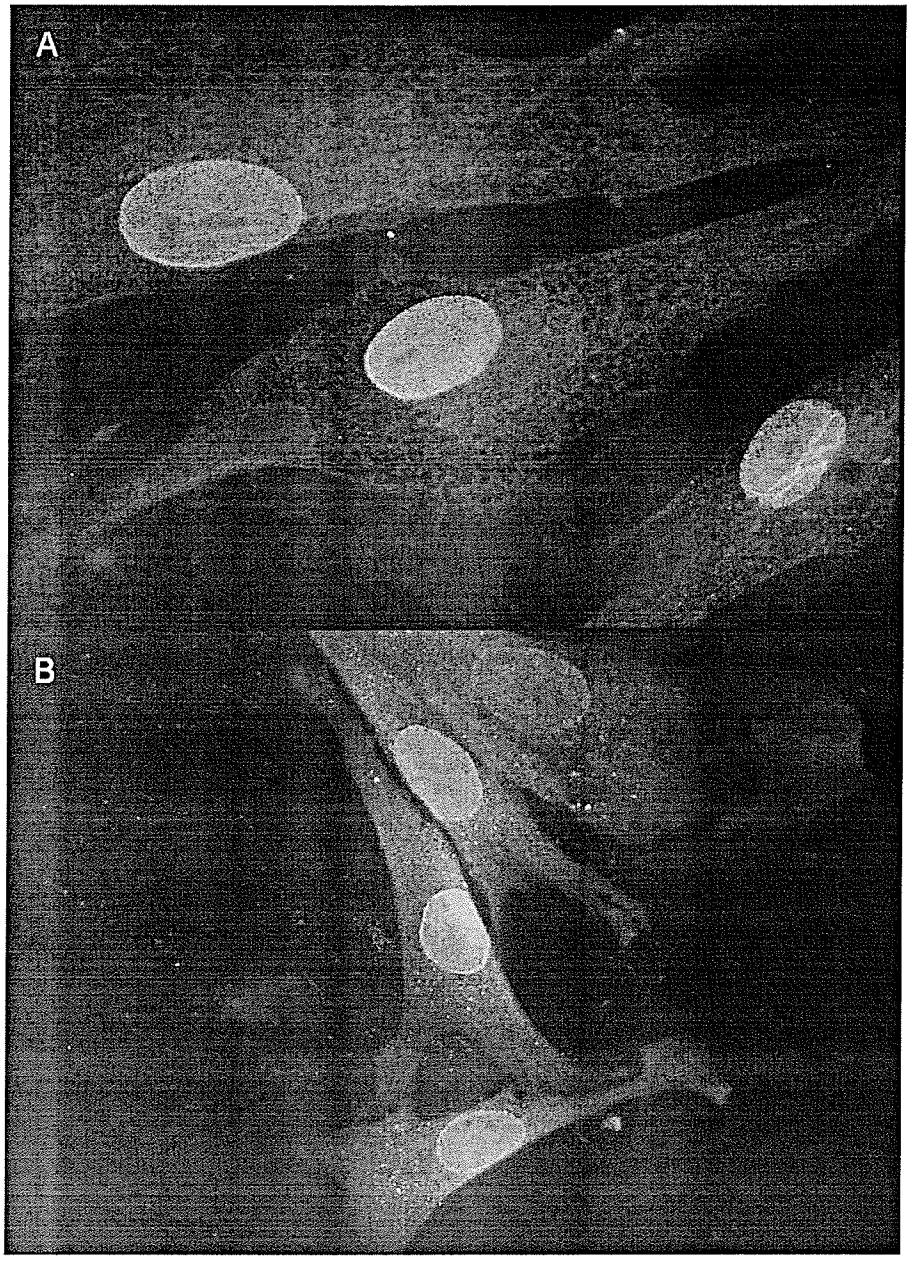

Figure 3. Smooth muscle cells stained with mAb414 and visualized using indirect immunofluorescence

Smooth muscle cells (SMC) from rabbit aortic explants were cultured and then stained for nuclear pore complex proteins using the monoclonal antibody, mAb414. This antibody recognizes the FG repeat motif common to various nuclear pore proteins (nucleoporins). (A) – quiescent SMC exhibit distinct nuclear staining. (B) – proliferating cells show a more diffuse cytosolic localization in addition to staining at the nuclear membrane. Magnification: 63x (oil immersion fluorescent objective).

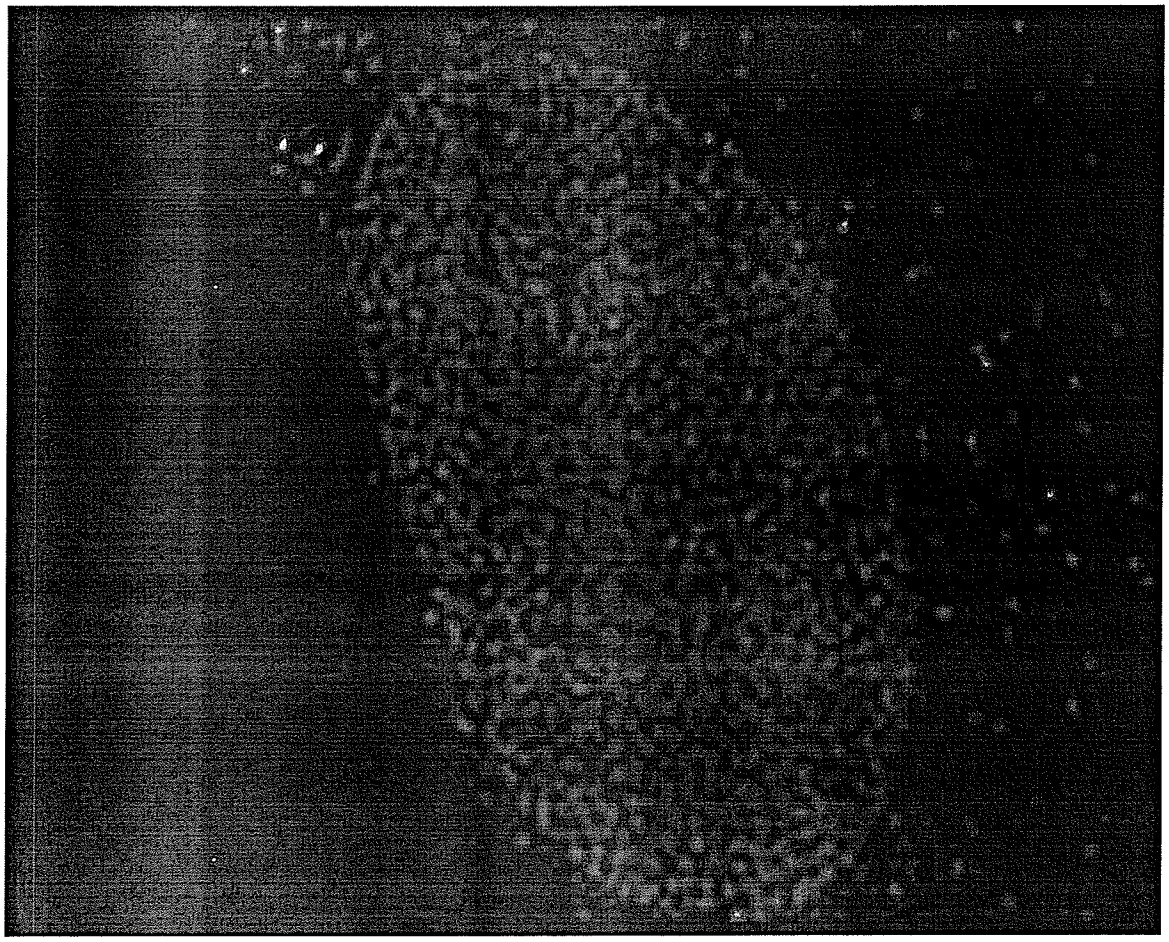

Figure 4. Visualization of a vascular smooth muscle cell nucleus using confocal microscopy

Images of mAb414 stained nuclei were taken via confocal microscopy at 100x magnification. Punctate staining of the nuclear envelope is immediately apparent, which is a distinctive NPC staining pattern. Cytosolic staining of pore proteins within annulate lamellae is also seen.

by ~70 nm deep (Figure 5). At its core, it is composed of eight multimeric subunits arranged in an annular configuration (Figure 6). This distinctive barrel-like shape leaves a functionally dynamic aqueous central channel about ~9-11nm in diameter under normal conditions (114, 115). Electron microscopy of prepared nuclear envelopes illustrates the octagonal symmetry of the pore when viewed *en face* (Figure 7). The central pore can dilate to accommodate larger cargoes in transit (116, 117) as well as in response to calcium fluxes (118, 119). In addition to the main central channel (1, 120), peripheral channels exist which are hypothesized to permit the flow of various small molecules and ions (105, 121) (Figure 6 & 8). One feature of the NPC core that remains contested is the pore "plug" (Figure 5, 7, 8). In some preparations, electron and atomic force microscopy have revealed the presence of a large molecule occluding the central channel of the pore (2). It is unclear if this pore plug is a *bona fide* structural component of the pore or simply trapped cargo, but the observations made by Stoffler *et al* suggest that the central plug may actually be a composite of both a molecule caught in transit and the distal ring structure (122).

On the nuclear and cytoplasmic faces of the pore are ring structures from which filaments extend into their respective compartments (105) (Figure 8). The cytoplasmic and nuclear ring-filament assemblies are asymmetrical and possess distinct structural variations. The cytoplasmic filaments are regularly spaced around the ring and extend into the cytosol for ~50 nm (122). They also contain nucleoporins which serve as docking sites for pre-transport import complexes (123-126).

The nuclear filaments are also evenly distributed around the nuclear ring, which in turn interacts with the nuclear lamina (127) (Figure 8). The nuclear filaments extend

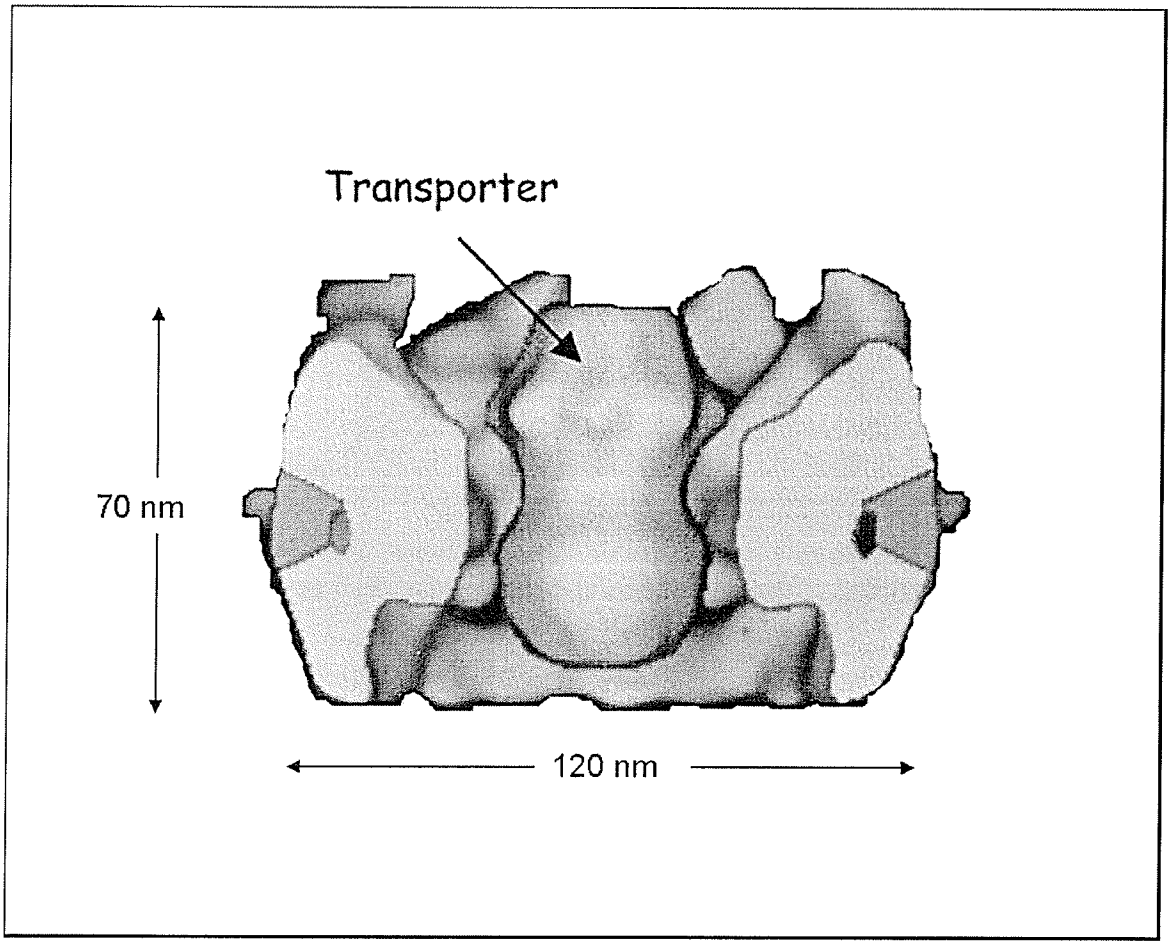

Figure 5. Dimensions of the mammalian nuclear pore complex

Illustrated are the general dimensions of the core region of the NPC. Also shown is the putative "transporter" in the central channel (see text). Image modified from Mazzanti *et al* (1).

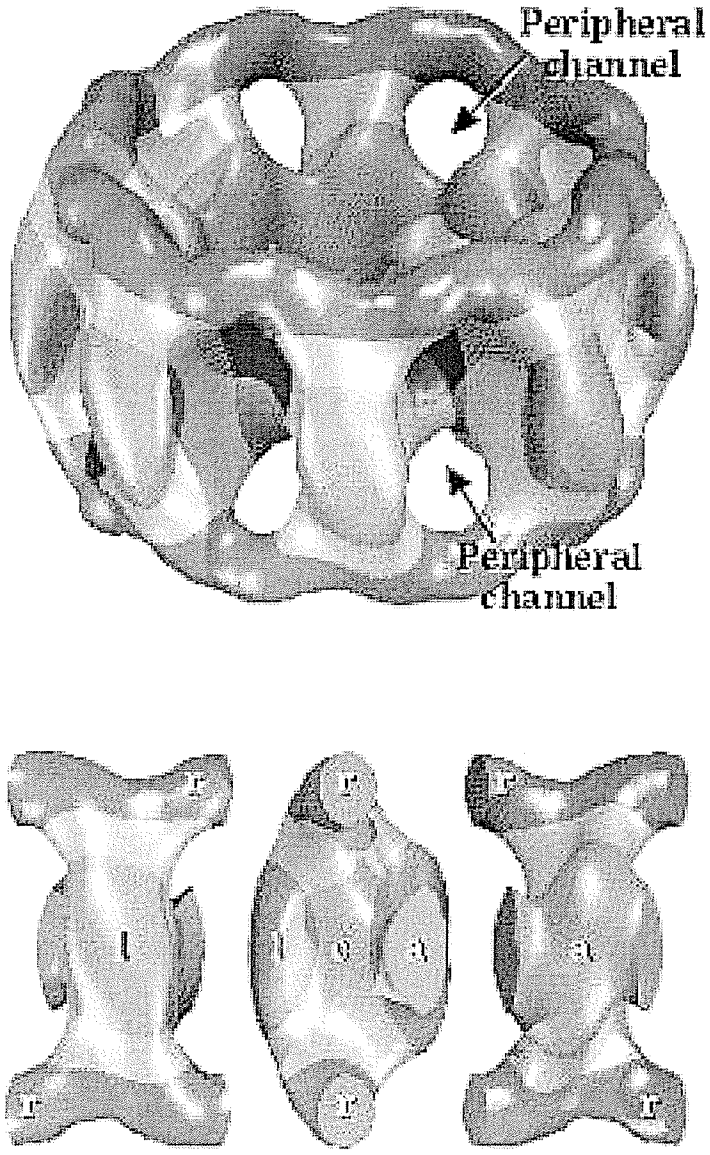

Figure 6. Core structure of nuclear pore

Above – The central component of the nuclear pore is composed of 8 identical protein subunits arranged in a distinctive, barrel-like formation. The subunits themselves are composed of 30-50 individual nuclear pore proteins, some of them functionally redundant. *Below* – A schematic illustration of an individual subunit is shown with several views rotated around a central axis. Abbreviations indicate regions of the subunit in relation to pore architecture: (r) – radial (connected to cytosolic and nuclear rings), (a) – forms the central aqueous channel, (c) – forms peripheral channels and (l) – exposed to the lumen of the periplasmic space. Image taken from Panté & Aebi (2).

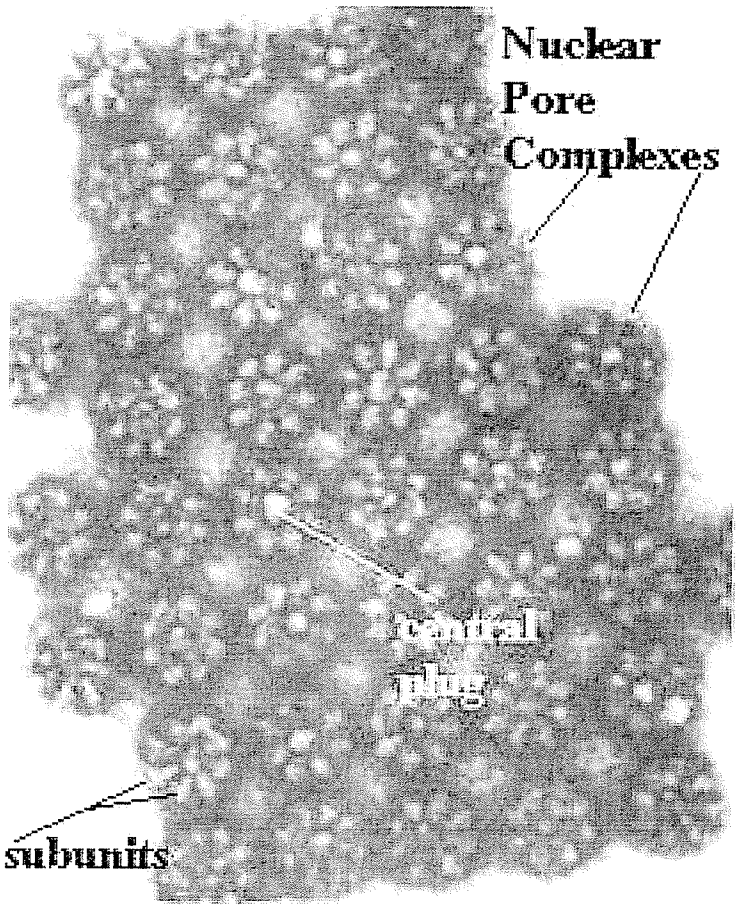

Figure 7. Electron microscopy of NPCs

Nuclear pore complexes visualized by electron microscopy show a regular, array-like distribution on the nuclear surface. Illustrated is the cytosolic face of the nuclear envelope. Prominently shown are the octameric arrangements of each pore as well as the nuclear "plug" in some pores.

Image source: http://www.cytochemistry.net/Cell-biology/nuclear_envelope.htm

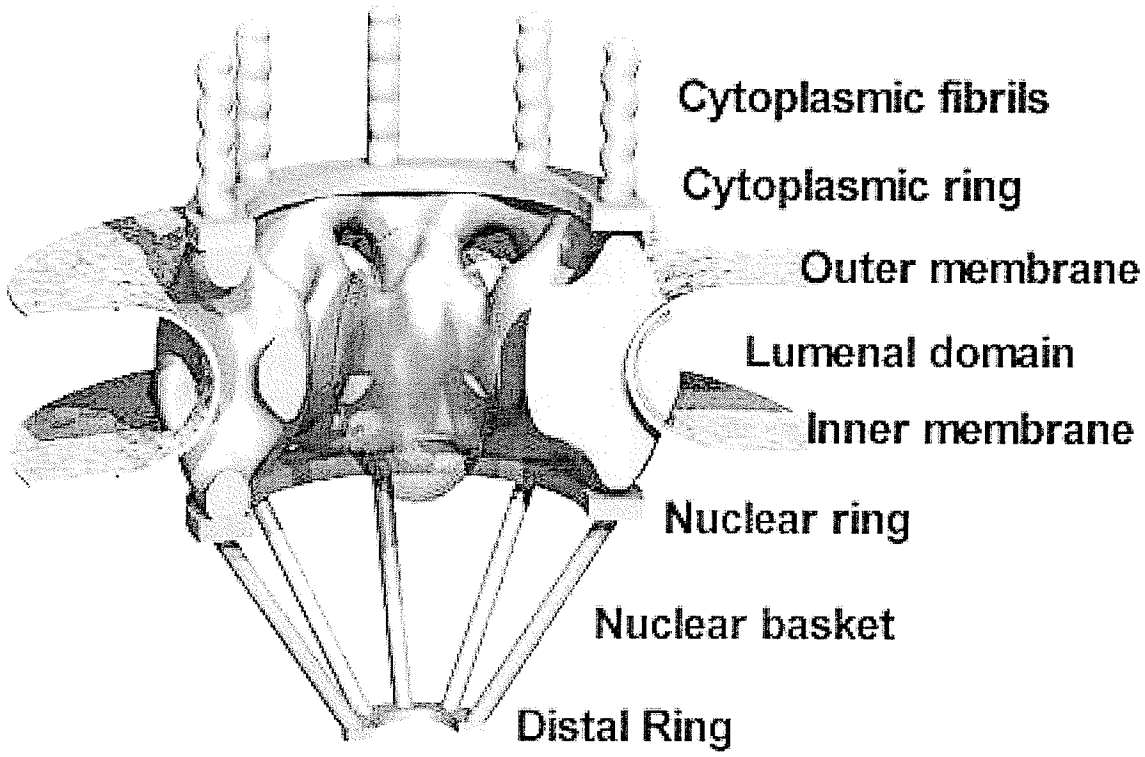

Figure 8. Cross sectional view of NPC

The nuclear pore complex is an asymmetrical structure that bridges both membranes of the nuclear envelope. The cross sectional schematic diagram above illustrates orientation of the pore in the nuclear envelope. Filaments extending from the cytoplasmic ring contain docking sites for molecules being imported/exported between the nuclear and cytosolic compartments. Nuclear filaments are joined by a distal ring forming the nuclear basket structure. Also shown is the hypothetical nuclear pore "plug" (green ovoid) which has been found in some NPC preparations. Image modified from Mazzanti *et al* (1).

much farther into the nucleoplasm than their cytoplasmic counterparts and are joined at their distal ends by another, smaller ring, termed the distal ring (104, 105, 122, 127). This entire assembly is called the nuclear basket (104, 105) (Figure 8). Sites on the distal ring and at the distal ends of the nuclear filaments serve as initial docking sites for export complexes and serve a similar function as their cytosolic counterparts (128). Another unique feature of the nuclear face of the NPC is its association with both the nuclear lamina (via the nuclear ring) and the nuclear envelope lattice (via the distal ring) (127). The function of the nuclear lamina in this respect is to anchor the NPCs within the nuclear envelope (129). The role of the nuclear envelope lattice is more obscure. Goldberg and Allen first identified this second matrix in both *Triturus* and *Xenopus* preparations using electron microscopy (127) but could ascribe no functional significance to it. The purpose of the nuclear envelope lattice remains enigmatic.

Dynamics

The nuclear pore is a highly dynamic structure that changes in response to a variety of stimuli (130-133). The presence or absence of the central "transporter" in response to the depletion or repletion of periplasmic calcium stores, respectively, is an excellent example of NPC dynamics (118, 119). It has been proposed that this pore transporter, or "plug", may represent a calcium-sensitive multimer composed of nucleoporin gp210 (130). Others have suggested that this feature was perhaps a preparative artefact since it was not observed in other experiments and was postulated to be molecular cargo that had become trapped in the pore (133). Numerous studies investigating the role of calcium in NPC

regulation, however, have demonstrated a definite calcium sensitive mechanism responsible for closing and opening the pore (118, 119). These independent observations support the notion that the NPC is dynamically regulated by calcium fluxes in and around the nucleus (118, 119, 134).

Nucleoporins are capable of diffusing from one membrane system to another within the same cell. Partial pore complexes and individual nucleoporins have been localized to the cytoplasmic annulate lamellae (AL), an organelle associated with components of the Ran cycle and potentially involved in nucleoporin distribution (135-137). Morphologically, the AL are multilayered membrane structures (129, 137, 138). Harel *et al* demonstrated that imbalances in cellular RanGTP concentrations lead to the excessive formation of annulate lamellae in cells which previously had none (136), so the presence of AL may be a secondary effect of nuclear assembly processes. However, the identification of partial pore complexes within the annulate lamellae suggests that the AL may serve as a distributor and repository for pre-assembly nuclear pore complex proteins (137). This was based on the observation that immunofluorescent staining for nucleoporins visualized proteins within the nuclear pore complex as well as within the annulate lamellae (139). Belgareh and Doye reported transnuclear diffusion of a nuclear pore protein in a binucleate heterokaryon (140), demonstrating that some nucleoporins are capable of translocating from one membrane system to another. This finding provides evidence in support of the hypothetical role of the annulate lamellae as a distributor of nucleoporins and demonstrates that the NPC is not static.

Interphasic nuclear pore complexes have low turnover in living cells and are replaced after a round of mitosis (129). Some nucleoporins are free to laterally diffuse within the

nuclear envelope and the annulate lamellae (129, 141). In untreated cells, individual NPCs possess limited lateral movement and show heterogeneous distribution because they are anchored to the nuclear lamina via the nuclear ring (129). They are capable, however, of shifting in waves around the entire surface of the nucleus as a single entity (129). One can envision this as a net covering a ball. Although the entire net can freely move around the surface of the ball, the interconnecting points are not significantly displaced with respect to each other. Abnormal spatial distribution of nuclear pore complexes has been reported in conjunction with alterations or defects in nuclear lamins (142, 143). Mutations in a specific subset of nucleoporins can also result in NPC clustering instead of the normal heterogeneous distribution (140, 144-146). These observations imply that although NPCs maintain specific distributions under normal conditions, they are capable of collectively undergoing significant spatial re-arrangement and are not static structures. Additionally, the density of nuclear pore complexes can change according to the metabolic needs of the cell (147-149). Clearly, changes in the nuclear pore can be correlated with growth requirements and/or changes in mitosis.

The link between nuclear pore complex dynamics and mitosis has been further strengthened by work that has demonstrated the redistribution of integral nucleoporins to the kinetochore during mitosis (150-152). The trigger responsible for relocalizing these nuclear pore complex proteins has been presumed to be nuclear envelope breakdown (152), which releases the nucleoporins allowing them to associate with the mitotic machinery (152). The cell can then proceed past the spindle checkpoint and subsequent steps in mitosis can continue unimpeded. From these observations, it is clear that

individual nuclear pore proteins are mobile in both interphase and mitosis, significantly more so in the latter.

Early research had demonstrated that nucleoporins which comprise the NPC possessed common amino acid sequences, composed of FG repeats as well as GLFG and FxFG motifs (153). These sequences are highly conserved between NPCs of different species and allow a researcher to search for homologous proteins in organisms other than yeast. The interaction of nucleoporins with soluble components of the nuclear transport machinery occurs through one or more of these repeats (154-156). This type of interaction formed the basis of several models of nuclear transport discussed below.

Models of Transport

Brownian affinity model

Despite our present knowledge of the structure and characteristics of the nuclear pore, the process by which a molecule enters and exits the nucleus still remains largely uncharacterized. Several models have been proposed which attempt to explain nucleocytoplasmic trafficking.

A thorough analysis of the yeast nuclear pore complex was completed by Rout *et al* (111) and they observed that the yeast nuclear pore complex contains about 30-40 different nucleoporins, the majority of which are located on both nuclear and cytoplasmic faces. Based on the number and distribution of nucleoporins observed in their work, Rout *et al* suggested the Brownian affinity model as a potential mechanism of transport (111).

Nucleoporins contain FG repeats, which in addition to FxFG and GLFG motifs are sequences shared by the majority of nuclear pore proteins (153). Aside from being a characteristic sequence by which potential nucleoporins may be identified, these sequences also bind transport receptors with varying degrees of affinity (157). Rout's model proposes that as import or export complexes bind to proteins within the nuclear pore complex, their residence time at the pore opening is increased, thus raising the probability of their entry into the channel and subsequent translocation through the central channel by Brownian motion (111). However, the inherent weakness with this model is that it does not explain the movement of large cargoes through a relatively narrow space.

Selective phase model

Another model that attempts to take into account the movement of both large and small cargoes is the selective phase model proposed by Ribbeck and Görlich (158). This model hypothesizes the existence of an interconnected meshwork between nucleoporins that are connected to each other via their FG repeats within the channel (158). Transport cargoes are able to traverse this meshwork because they are able to interact with the FG repeats themselves, thus breaking the connection between nucleoporins within the mesh. Additionally, the "holes" within the mesh act as a molecular sieve and together with the hydrophobic nature of the channel serve to exclude both inert (receptor-less) cargo and molecules beyond the size limit of the pore (158). However, the existence of this molecular sieve network has yet to be demonstrated.

"Oily spaghetti" model

A third model put forth by Macara (159) combines elements of the selective phase model with the assumption that the pore is a patent channel. Called the "oily spaghetti" model (159), nucleoporins exposing their FG repeats comprise the "spaghetti" in the core of the channel instead of the "mesh" in the selective phase model. This arrangement excludes cargoes without the transport receptors and similar to the mechanism proposed by Ribbeck and Görlich, importins and/or exportins are able to pass through by associating with the FG repeats on the nuclear pore proteins.

The three mechanisms proposed above function with one common underlying assumption – that nuclear translocation is randomly driven by facilitated diffusion. None of these models takes into account the contribution of the RanGTP gradient across the

nuclear envelope which provides directionality. For the above models to be valid, transport processes would have to proceed unimpeded following an alteration in the RanGTP gradient. Collapse of the gradient can stop transport (160-163). Additionally, the direction of transport can be reversed in the presence of high cytosolic concentrations of RanGTP (164).

Binding affinity model

Ben-Efraim and Gerace proposed a model that would take into account size exclusion limits, binding affinities and the RanGTP gradient (157). In their model, transport cargoes bound to RanGTP move up an increasing affinity gradient to end up at terminal docking sites in their predestined compartment (80, 157, 165-167). This has proved to be one of the most attractive models to explain the movement of molecules across the nuclear envelope, as it reconciles current observations with the biophysical parameters of the transport machinery (157).

Ran and Nuclear Transport

Ran is a small GTPase intimately involved with nucleocytoplasmic trafficking (73, 163, 168, 169). Located predominantly in the nucleus, it is also capable of shuttling back and forth between the nuclear and cytoplasmic compartments (170, 171). Nuclear Ran is bound to GTP and delivered to the cytosol in conjunction with an export complex (172). Once there, it is converted to RanGDP (81, 173). This is extremely important, as hydrolysis of RanGTP promotes the dissociation of exportins from their cargo when they reach the cytosol.

While cytoplasmic delivery of Ran occurs via its participation in an export complex, import of Ran requires the RanGDP specific import factor called p10/NTF2. First identified in *S. cerevisiae* by Nehrbass and Blobel (174), this molecule was shown by these and other authors to bind to the FxFG repeats of isolated nucleoporins (175, 176). Further work clarified the role of p10/NTF2 as a nuclear import receptor for Ran in its GDP bound form (177-179), as it was observed that NTF2 specifically bound RanGDP and not RanGTP (174). NTF2 is located primarily at the nuclear envelope, bound to nucleoporins (176), since the Ran-binding and nucleoporin binding domains are discrete regions of the protein (175). It is also distributed between the cytoplasm and the nucleus (175). The concentration of NTF2 at the nuclear envelope is on the order of ~20 μM and it exists in a dimerized form, whereas it is monomeric in the cytoplasm and the nucleus, at a concentration of 0.3 μM and 0.6 μM, respectively (175). These differences in concentration affect the monomer-dimer equilibrium of NTF2, as Chaillan-Huntington *et*

al reported a dissociation constant of ~1.1 μM for NTF2 (175). At concentrations below this K_D, the dimer dissociates and significantly weakens the affinity of NTF2 for RanGDP (175), releasing it into the nucleoplasm, which can then be recharged with GTP by RCC1.

Ran has weak inherent GDP/GTP exchange activity as well as intrinisic GTP hydrolyzing capabilities (180). In order for Ran to maintain its distinct GTP and GDP bound states in the nucleus and cytoplasm, respectively, a host of accessory proteins exist which regulate and enhance both the hydrolyzing ability of Ran as well as its nucleoside binding capacity. Within the nucleus is the RanGEF/RCC1 enzyme. It is constitutively imported and maintains its nuclear localization by associating with chromatin (181). This enzyme is responsible for replacing GDP with GTP, and maintains Ran in a GTP bound form (182). Binding of RanGTP to importin-β entering the nucleus promotes dissociation of the import complex and subsequent release of the NLS bearing cargo into the nucleus (183). Export complexes are formed only in the presence of RanGTP (172, 184). RCC1 is imported into the nucleus by two distinct mechanisms – one which depends on importin-α3 (63) and another which does not depend on energy or pre-existing Ran gradients (185).

RanGTP that exits the nucleus in association with an export complex is converted to RanGDP by the concerted action of several co-activating proteins. Chief among these proteins is RanGAP1 (81), which, together with the Ran binding protein RanBP1 (186), increases the intrinsic hydrolytic activity of Ran. RanGAP1 exists in two forms, a soluble cytosolic form and a SUMOylated, NPC-associated form (18, 19). At the NPC, another Ran binding protein called RanBP2/Nup358 is part of the cytoplasmic filaments of the

complex which also acts co-operatively with SUMO-RanGAP1 (18, 19). These elements maintain Ran in a GDP bound form in the cytoplasm. The nuclear components of the Ran cycle maintain high nuclear concentrations of RanGTP. It has been estimated that the concentration of RanGTP is over 200-fold greater in the nucleus than in the cytoplasm (187). Together, the cytoplasmic and nuclear elements of the Ran cycle establish a steep RanGTP gradient across the nuclear envelope. This is the source of energy for active nuclear transport as well as the element that specifies the vectorial movement of transport cargo.

The majority of nucleocytoplasmic trafficking requires a functional Ran cycle to operate (Figure 9). Exceptions exist, however, and Ran independent transport has been identified for a variety of different proteins (188, 189). The nuclear import receptor transportin enters the nucleus by a Ran unassisted mechanism (189). IκBα, a regulator of NFκB transport, is imported without Ran (190). Other non-transport proteins, such as beta catenin (191) and the U1A and U2B" spliceosome proteins (192) also enter the nucleus by a pathway independent of Ran.

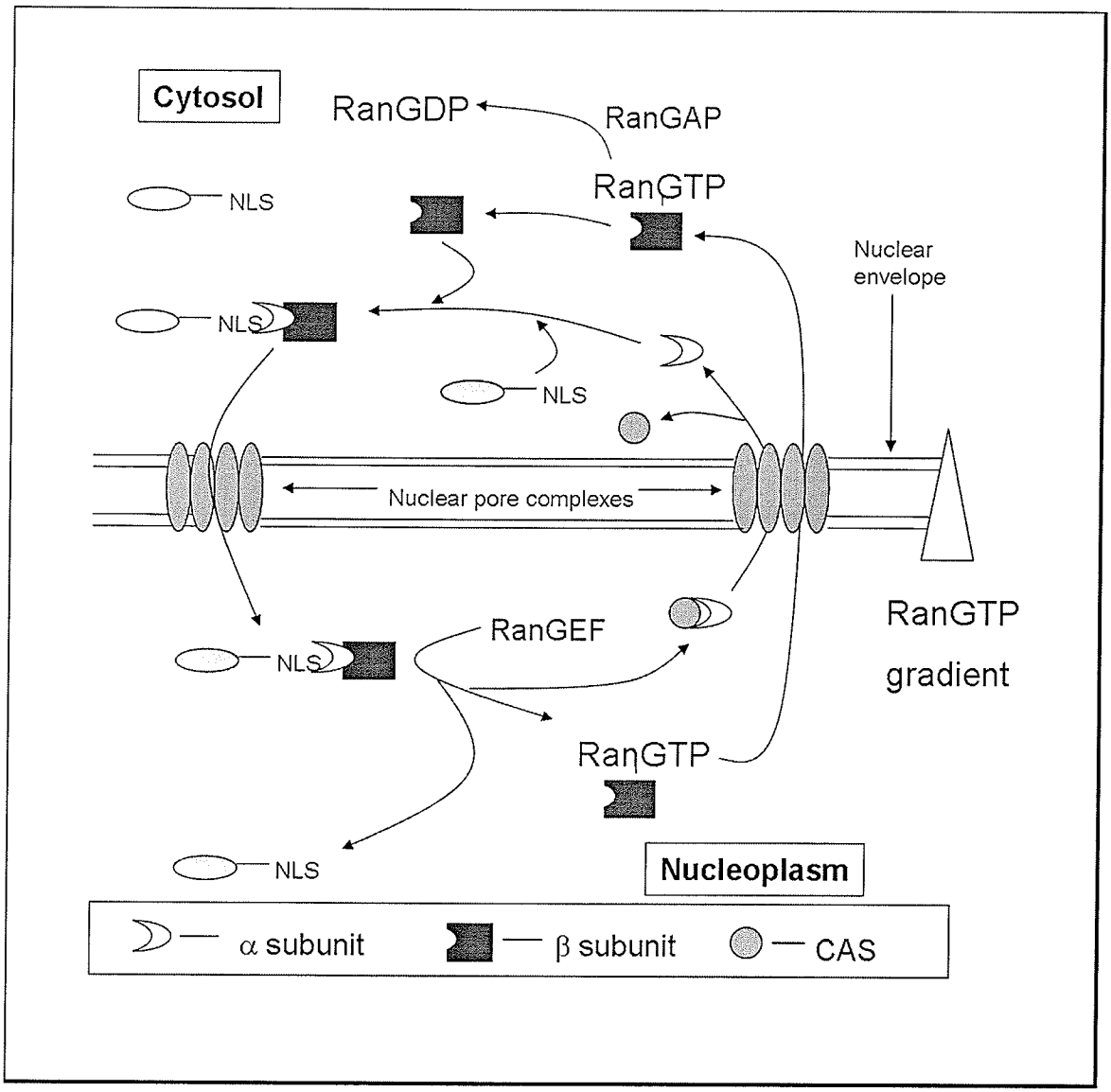

Figure 9. Ran cycle

The classic mechanism of import requires a functional Ran cycle. The Ran gradient across the nuclear envelope provides directionality and motive force to drive nuclear transport. RanGDP is imported into the nucleus by NTF2, where GDP is exchanged for GTP by RanGEF/RCC1 (see text). RanGTP is then exported from the nucleus, either in conjunction with an export complex or with importin-β. In the cytosol, RanGAP co-activates Ran, generating RanGDP and the cycle continues. CAS is the import receptor for importin-α and recycles it back to the cytosol.

Vascular Cell Growth and Disease

Cell Growth

Normal cellular growth is dependent upon regulated proliferative signaling. Extracellular signals are transduced to the nucleus where they affect gene expression leading to alterations in cell growth. This signal may be biochemical (193) or mechanical (194) in nature and can be distributed in a temporally dependent manner (195).

Biochemical factors can be secreted in an autocrine, paracrine or endocrine manner that regulate cellular development and proliferation (193, 196-199). For example, smooth muscle cells release epiregulin, a potent factor that dedifferentiates neighbouring cells as well as the secreting cell itself, thus affecting cell growth in an autocrine and paracrine manner (199). Mechanosensory stimuli are also capable of affecting cell growth. Cyclic and shear stresses (194, 200), cell-cell contact (201, 202), and interaction with extracellular matrix proteins (203-205) are the kinds of biomechanical signals capable of influencing cellular growth.

Both biochemical and mechanical modes of stimulation can occur chronically and acutely. Such a temporal distribution of the signal can significantly affect cellular growth. Chronic and acute exposures to biochemical signals can upregulate or downregulate the proliferative response depending on the nature of the signaling molecule (206), while phenomena such as (cyclic) stretching (207-211) and chronic hypertension (212) within the vasculature provide examples of temporally distributed mechanostimuli.

Uncontrolled, hyperproliferative signaling causes a pathophysiological increase in cell numbers (213, 214). Proliferative disorders in vascular smooth muscle cells are of particular relevance to this review and their effect on the vasculature is discussed next.

Proliferative Vascular Disease

Different cell types comprise the vasculature, with the primary cell types being endothelial cells, fibroblasts and smooth muscle cells (Figure 10). Endothelial cells form a semi-permeable barrier between the lumen of the blood vessel and the vasculature proper called the endothelium, which is capable of releasing both vasoactive and proliferative factors (215). Another cell type within the vascular wall, the fibroblast, primarily deposits the extracellular matrix, which is a cellular substrate and anchor (216, 217).

Smooth muscle cells are vascular contractile cells that imbue the arterial tree with the ability to generate a peristaltic, pulsatile flow of blood (218) as well as the capacity to dynamically adjust vascular tone and contractility (219-221). Smooth muscle cells possess phenotypes ranging from synthetic to contractile (222-224) which correspond to their differentiated and de-differentiated states, respectively. A morphologically distinct, heterogeneous population of smooth muscle cells exists at any given time within the vasculature, rather than being derived from a single population (225). Control of cell growth is a finely tuned, evolutionarily honed process and dysregulated cellular growth of any of the vascular cell types can lead to vascular disease. Proliferative disorders in smooth muscle cells may lead to vascular pathologies such as restenosis (226, 227) and atherosclerosis (228).

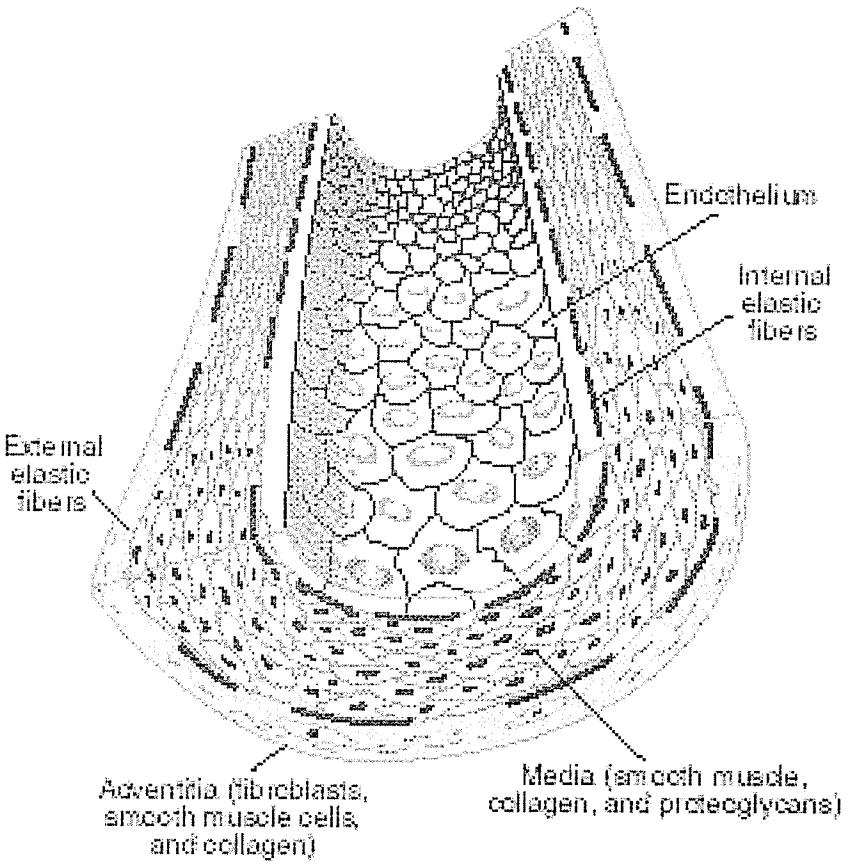

Figure 10. Layers of the vascular wall

The vascular wall is composed of the intimal, medial and adventitial layers (see above). The intimal layer contains the endothelium – a semi-permeable barrier that regulates the flow of molecules between the lumen of the blood vessel and the vascular tissue, vascular tone and also secretes autocrine and paracrine growth factors. Next is the medial layer (bordered on its proximal and distal surfaces by the internal and external elastic lamina, respectively) and the major cell type it contains are smooth muscle cells which provide contractility to the vasculature. Finally is the adventitial layer, where fibroblasts are the primary cell type. These cells are responsible for depositing components of the extracellular matrix. The adventitia also contains smooth muscle cells.

Image source:http://www.unitoday.com/library/usana_magazine/99Mar/1.html

Obstructive lesions within the vascular tree are heterogeneous occlusions that can cause a mild to a severe narrowing, or stenosis, of the blood vessel lumen (229). Stenotic vessels such as these may be widened by balloon angioplasty or stent implantation (230) or the lesion can be removed by surgical interventions such as percutaneous transluminal coronary angioplasty (PTCA) (231). The drawback to these therapies is that the vascular response which follows results in a reocclusion of the lumen, sometimes to a worse extent than the original. This narrowing of the blood vessel after a surgical intervention is called restenosis and several mechanisms are proposed to be responsible for this vascular response (227, 232). The abnormal proliferation of vascular cells is probably the most important cause of restenosis. It is primarily due to neointimal hyperplasia, especially in the case of in-stent restenosis (227).

Atherosclerosis is a multifactorial disease. Its etiology has not been fully characterized, but several models have been put forward that take into account the role of dysregulated smooth muscle cell proliferation in the formation and progression of an atherosclerotic lesion. It was originally hypothesized that monoclonal expansion of a dedifferentiated smooth muscle cell caused atherosclerosis (233, 234). However, mounting evidence indicates that atherosclerosis is the result of a heterogeneous population of smooth muscle cells that dedifferentiate to a synthetic phenotype and subsequently migrate out of the arterial media into the subendothelial intimal space (225). Once there, they proliferate and can cause abnormal vascular remodeling by vessel calcification (235) and deposition of extracellular matrix proteins (236). Smooth muscle cells also differentiate into foam cells which contribute to the development of an atherosclerotic plaque (237).

Many risk factors are associated with atherosclerosis and its progression. Smoking, diabetes, hypertension and hypercholesterolemia are among the most important factors identified (200). The latter is of particular relevance, since the emphasis of this discussion is lipid signaling.

Cholesterol is a component of cellular membranes (238, 239) and is essential in steroid hormone synthesis (240, 241). However, elevated plasma cholesterol arising from dietary imbalances and/or genetic factors can lead to atherosclerosis. Cholesterol moves within the plasma and is delivered to cells as a component of low density lipoproteins (LDL) by a receptor mediated process (242, 243). Oxidized forms of LDL initiate the formation and contribute to the progression of an atherosclerotic plaque (244, 245). However, LDL is complex and composed of other lipids in addition to cholesterol that participate in atherosclerotic development (246-249). Sphingolipids and lysophosphatidylcholine are important examples of LDL-associated lipids that can affect cell growth and are discussed in the next section.

Lipid Signaling

Ceramide and Sphingosine-1-phosphate

Ceramides belong to a class of lipids known as sphingolipids and are synthesized *de novo* from serine and palmitoyl-coA precursors (250). Alternatively, they may be made through the conversion of sphingomyelin by the enzyme sphingomyelinase (251, 252). *De novo* synthesis of ceramide begins when serine and palmitoyl-CoA form 3-ketosphinganine via serine palmitoyl-transferase (Figure 11). 3-ketosphinganine then undergoes a reductive step to form dihydrosphingosine (sphinganine). Ceramide synthase converts sphinganine to dihydroceramide which is subsequently acylated to form ceramide by dihydroceramide desaturase. Ceramide can also be synthesized by the removal of a phosphocholine group from sphingomyelin, catalyzed by sphingomyelinase. Ceramides serve as the building block for other sphingolipids, namely ceramide-1-phosphate, glucosylceramide and sphingosine-1-phosphate (S1P), in addition to sphingomyelin (251). A listing of each step of the metabolic pathway of ceramide synthesis and its respective enzyme can be found in (Table 3). Ceramide is a stable sphingolipid species with a half-life of ~2 hrs (253) and is primarily made via *de novo* synthesis and sphingomyelin breakdown. Interconversion between ceramide and its four metabolic products does occur, however, as ceramide is a branch point within the sphingolipid pathway (Figure 11).

Ceramide has the capacity to induce growth arrest and apoptosis in a variety of cell types (254-257). In a variety of non-vascular cells, levels of ceramide were observed to increase following UVA/B irradiation, subsequently leading to apoptosis (258, 259). One

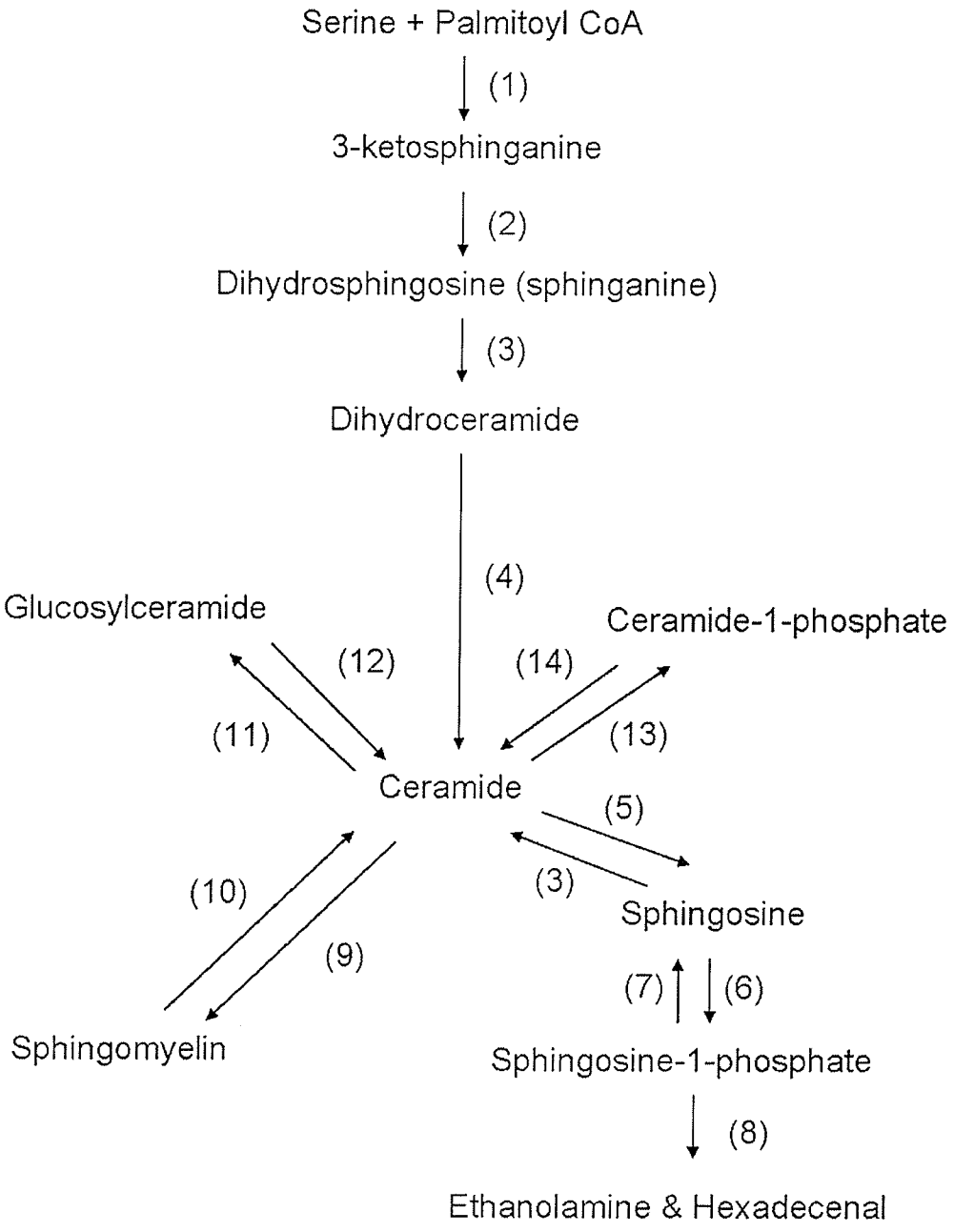

Figure 11. Pathway of sphingolipid metabolism

Reaction step	Enzyme
(1)	Serine palmitoyl - transferase
(2)	3-ketosphinganine reductase
(3)	Ceramide synthase
(4)	Dihydroceramide synthase
(5)	Ceramidase (acidic, neutral, or alkaline)
(6)	Sphingosine kinase (1 and 2)
(7)	S1P phosphatase
(8)	S1P lyase
(9)	Sphingomyelin synthase
(10)	Sphingomyelinase (acidic or neutral)
(11)	Glucosylceramide synthase
(12)	Glucosylceramidase
(13)	Ceramide kinase
(14)	Ceramide-1-phosphate phosphatase

Table 3. Enzymes involved in sphingolipid metabolism

group of scientists incubated ceramine, a non-hydrolysable analogue of ceramide, with mouse fibroblast cells and found that levels of apoptosis increased by approximately sevenfold when compared to cells incubated with hydrolysable ceramide (260). The anti-proliferative and apoptotic effects of ceramide have been linked to activation of stress activated MAP kinases, most notably p38 and JNK (254, 261-263). In addition to this, a variety of new substrates for ceramide have been identified including ceramide activated protein kinases (264) and ceramide activated protein phosphatases (265). Both of these protein classes may also affect cellular proliferation.

In addition to serving as a second messenger that activates apoptotic signaling cascades, ceramide has demonstrated membrane altering properties that may play a part in causing irreversible apoptosis. Siskind *et al* first demonstrated that ceramide could form large conductance channels in artificial planar membranes (266) that were large enough to permit the release of pro-apoptotic factors (267). The extremely high ceramide concentrations used by Siskind *et al* to produce these effects may limit the physiological relevance of their observations. Despite this limitation, it is clear from these studies and others that ceramide has a strong pro-apoptotic activity.

These apoptotic effects of ceramide have great pathological relevance for the vasculature. Apoptosis is involved in vascular development and is suggested to be involved in atherosclerosis, as microarray analyses by Kockx *et al* demonstrated a distinct overexpression of pro-apoptotic death associated protein kinase in atherosclerotic samples (268). Ceramide-induced apoptosis may be involved, therefore, in the atherosclerotic process. Ceramide signaling is important in cell growth in other pathological states as well. For example, ceramide signaling was impaired in genetically

hypertensive animals, and it was hypothesized that this deficiency could be responsible for the accelerated smooth muscle cell proliferation observed in the hypertensive vessel (256).

A large body of evidence also implicates the role of sphingosine-1-phosphate as an important signaling molecule. Sphingosine-1-phosphate is a mitogen involved in proliferative signaling (269, 270) in a variety of cells (260, 271-274). S1P activates ERK-1 and ERK-2, both of which are known proliferative MAP kinases (273). In addition to S1P possessing mitogenic properties, it also participates in cell survival and has been shown to protect against apoptotic signaling in mouse fibroblasts (260). Thus, the signaling properties of both ceramide and sphingosine-1-phosphate are directly opposed. However, they are also part of the same system, as these two molecules are directly interconvertible. Thus, it has been proposed that the balance between cellular levels of ceramide and sphingosine-1-phosphate is a cellular "rheostat" responsible for balancing the signals from both the mitogenic, S1P dependent side and the apoptogenic, anti-proliferative ceramide dependent side (275). Evidence for this rheostat model is provided by the observation that addition of exogenous sphingosine-1-phosphate rescued ceramide-mediated apoptosis (260). Additionally, "classic" proliferative signals from growth factors and cytokines can upregulate the activities of ceramidase and sphingosine kinase, two enzymes essential to the production of sphingosine-1-phosphate. Concomitant with this upregulation, the same signals downregulated the activity of enzymes involved in ceramide synthesis (276). Other studies have also demonstrated a similar differential regulation of the ceramide and S1P synthetic pathways by the same

stimulus, whether that stimulus is proliferative or apoptotic. These data argue in support of the ceramide/S1P rheostat model.

While numerous evidence exists demonstrating the role of both proliferative and apoptotic enzymes involved in sphingolipid signaling, the exact mechanisms by which this occurs still need to be identified. The action of ceramide and/or sphingosine-1-phosphate on membrane topology and membrane potential are a few ways in which these molecules may exert their effects on cellular function. The properties of sphingolipids in cellular metabolism are a complex area that requires further study to clarify their role in determining cell fate.

Lysophosphatidylcholine

Lysophosphatidylcholine (LPC) is produced from the phospholipase A_2-mediated hydrolysis of phosphatidylcholine (277, 278). It is also synthesized by lecithin-cholesterol acyltransferase (LCAT), which removes a fatty acid from phosphatidylcholine and transfers it to cholesterol (279). LPC stimulates intracellular calcium release and activates non-selective cation channels (280, 281) and plays a diverse role in cell signaling (282), chemotaxis (283) and adhesion (284-286). Cell proliferation has been attributed to stimulation by LPC (214). This is significant because LPC is believed to play a role in the progression of atherosclerosis, a proliferative disorder of the cells in the vasculature (287-289).

Work by Bassa *et al* have demonstrated that phospholipase Cγ (PLCγ–1) is phosphorylated and subsequently activated *in vivo* in response to incubation with LPC (290). Active PLC produces DAG, which is a co-activator for PKC. When PKC was

depleted (290) or pharmacologically inhibited by the PKC-specific antagonist, GF109203-X (GFX) (290) the effects of LPC treatment were attenuated. PKC can also activate Raf-1, the upstream activator of the ERK-1/2 signaling cascade (290). Jing *et al* demonstrated that ERK -1/2 was phosphorylated in response to incubation with LPC (291), while Yamakawa *et al* examined downstream effects and reported that levels of AP-1, a DNA binding complex composed of the ERK kinase-induced *c-fos* and *c-jun* genes, was increased (292). Together, these observations provided more evidence that LPC mediates its actions on cell proliferation via the ERK -1/2 signaling cascade (292).

Lysophosphatidylcholine is also capable of entering and initiating a signaling cascade within the cellular interior. LPC enters cells via a receptor-mediated pathway (293-295). The first LPC specific receptors were identified by Kabarowski *et al* (294). The receptor is a G-protein-coupled tyrosine kinase, which supports other evidence showing inhibition of LPC stimulation by a protein tyrosine kinase inhibitor (290). Work with oxidized LDL induced macrophages demonstrated that the oxLDL scavenger receptor is also capable of internalizing LPC (296).

While it seems that receptor mediated uptake of LPC is the primary means of internalization, an alternative entry pathway exists. LPC can cross the plasmalemma via a plasma membrane "flippase" (297). Work by vanderLuit *et al* tested the ability of LPC to rescue HeLa cells from alkyl-lysophospholipid-induced apoptosis (297). They noted that the apoptogenic alkyl-lysophospholipid was internalized after forming lipid rafts, but they observed that LPC (a) did not form lipid rafts and (b) traversed the plasma membrane in both a receptor-independent and an endocytosis-independent manner (297). A "flippase" mediating transbilayer movement of phosphatidylcholine has been found in

the ER membrane (298). Therefore, it was hypothesized that a similar protein or isoform of this PC "flippase" that could transport lyso-PC was present in the plasma membrane (297). This existence of this enzyme has yet to be demonstrated.

The effects of sphingolipids and LPC discussed previously occur via the MAP kinase pathway (261, 269, 270, 273). The MAP kinase signaling cascade is a common convergence point for many proliferative stimuli (299-302) and is essential in mediating cellular responses to extracellular stimulation. Relevant to this review, it is discussed in the following section.

MAP Kinases and Cell Signaling

Mitogen activated protein (MAP) kinases are a group of enzymes involved in proliferative signaling cascades in eukaryotic cells. They are a diverse group of proteins, but can be classified into three main families: the extracellular regulated kinases (ERK), p38, and Jun N-terminal kinase (JNK) families (302). The latter two are involved primarily in stress related proliferative signaling, such as that caused by toxic shock (303), UV irradiation (304) and osmotic shock (305). The ERK family mediates proliferative signaling in response to mitogenic factors (306-308) under non-stress conditions. MAP kinases play a role in cellular development/differentiation (309-312), regeneration/wound healing (313-315) and adaptive/compensatory cell growth (316-318). Apoptosis is another vital cellular process influenced by MAP kinase activity (319).

The first step in a MAP kinase signaling cascade involves activation of an initiating kinase by growth factors or stress stimuli (302) (Figure 12). This is the first of several kinases in a MAPK activating module that are activated in series by an extracellular stimulus (302). Downstream of the initiating kinase is the MEKK enzyme, followed by MEK (MAPK kinase) and finally ERK-1/2 (302) (Figure 12). Although each of the three main families of MAP enzymes possesses a specific upstream activator, there is considerable crosstalk among the three signaling pathways upstream of MEK (302).

Dual phosphorylation of a threonine/serine or threonine/tyrosine motif within MAP kinase by MEK is required for full activation (35). Dimerization of MAP kinase follows activation (35), and the enzyme can enter the nucleus autonomously (35) using an unknown import mechanism. Inactivation of MAP kinases is accomplished as part of a

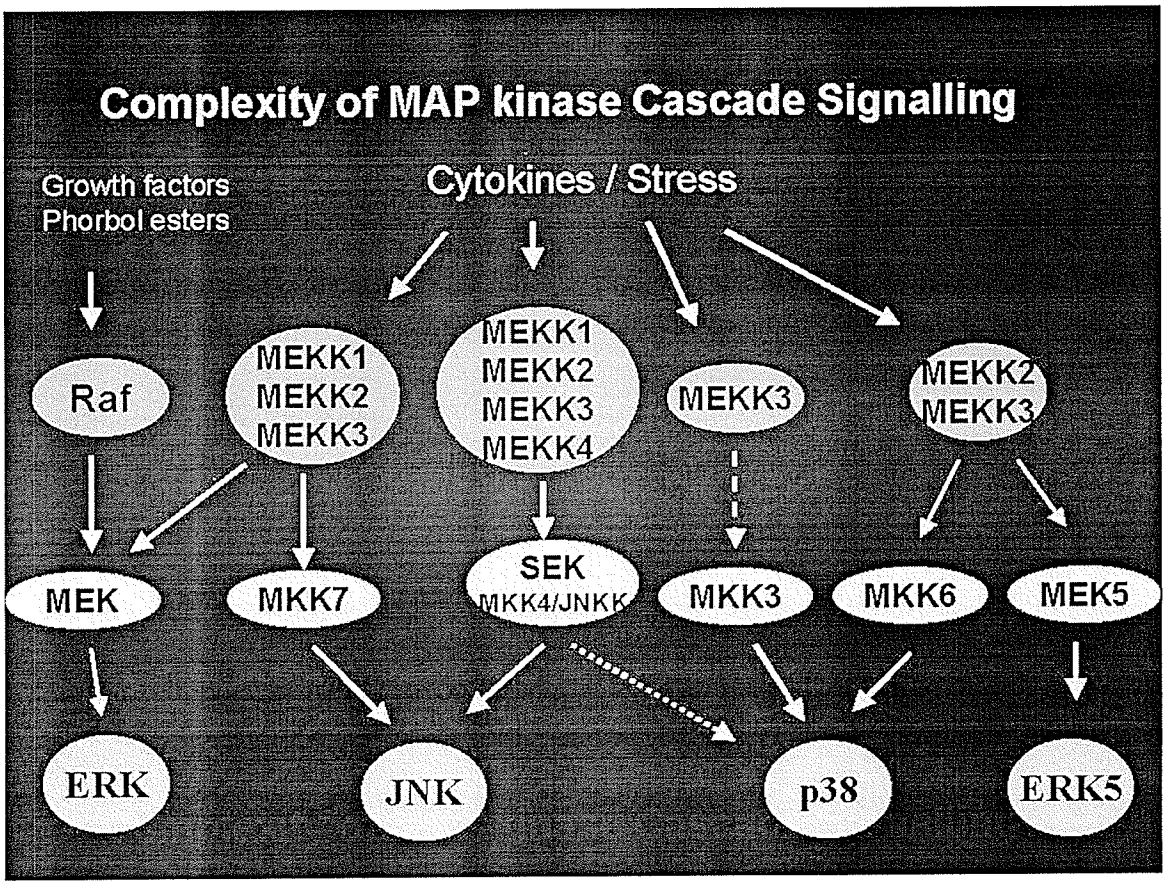

Figure 12. MAP kinase signaling pathways

Image taken from: http://www.brad.ac.uk/staff/agraham/pagenov.htm

negative feedback loop and involves MAP kinase phosphatase (MKP-1) (320). MAP kinases are classified as proline-directed serine/threonine kinases, indicating that serine or threonine residues immediately adjacent to or in close proximity to a proline residue are phosphorylated (302). Additionally, the majority of phosphosubstrates share a consensus sequence that is recognized by MAP kinases (302, 321).

Elucidation of the role of the MAP kinase cascade in signal transduction pathways has been facilitated by the use of a variety of commercially available pharmacological inhibitors. Several MAP kinase antagonists were used in this study and are briefly reviewed here. A broad range inhibitor of the ERK-1/2 branch of the MAP kinase family is apigenin (322-324). It was characterized as a significant inhibitor of cell proliferation and prevented tumor growth by pleiotropic inhibition of the MAP kinase pathways and its downstream oncogenes. One of the best characterized MAP kinase inhibitors in the literature is the MEK inhibitor, PD98059 (325, 326). It was originally identified by screening a library of artificial compounds for substances that would inhibit phosphorylation of myelin basic protein (MBP) (326). Its high degree of specificity was due to allosteric conformational shifts it imposed on MEK, as it did not compete for ATP or for ERK-1/2 (326). A novel and potent competitive inhibitor of ERK-1/2 is 5-iodotubercidin (327). Its reported K_i with respect to ERK-2 is 530 nm and at lower values (K_i = 30 nm), it inhibits protein kinase A, adenosine kinase and casein kinases 1 and 2 (328, 329). It has also been reported to inhibit insulin receptor kinase fragment at values ranging from 0.4 – 28 μM (328). SB-202190 is a specific competitive inhibitor for the α and β isoforms of p38 MAP kinase (330) and has been used to successfully inhibit

phosphorylation and activation of MAPKAPK-2, a downstream target of p38 MAP kinase (331).

Although investigation of the role of MAP kinases with respect to nuclear trafficking has centered primarily on phosphorylation of amino acids adjacent to nuclear transport signals (332, 333), a growing body of evidence reveals that MAP kinase phosphorylation may also occur within the cytosolic machinery as well as the nuclear pore complex in a physiologically relevant manner (102, 332-336).

HYPOTHESES

This aims of this project will test the following hypotheses:

1. Calcium binding proteins are present within the nuclear pore complex.
2. Phosphosubstrates exist within the nuclear pore complex.
3. MAP kinase phosphosubstrates exist within the nuclear pore complex.
4. Phosphorylation of factors involved in nuclear transport will influence the rate of nuclear import in vascular smooth muscle cells.
5. Treatment with MAP kinases will influence nuclear transport in vascular smooth muscle cells.
6. Treatment with sphingolipids will influence nuclear import in vascular smooth muscle cells.
7. Treatment with lysophosphatidylcholine (LPC) will regulate the rate of nuclear protein import in vascular smooth muscle cells.

In order to prove/disprove these hypotheses, the objectives are:

- to identify calcium binding proteins within the nuclear pore complex
- to identify phosphosubstrates within the nuclear pore complex
- to identify phosphosubstrates for MAP kinase within the nuclear pore complex
- to determine the effects of NPC phosphorylation on nuclear protein import in smooth muscle cells
- to identify nuclear transport phosphosubstrates within the cytosol

- to determine whether phosphorylation of exogenously added cytosol can influence nuclear import in vascular smooth muscle cells
- to identify putative phosphosubstrates that may affect nuclear protein import
- to determine the effects of MAP kinase treatment on nuclear protein import
- to determine the effects of sphingolipids on nuclear protein import
- to determine the effects of LPC on nuclear protein import

MATERIALS

Product	Company Name
[Ala-286]-Ca2+/Calmodulin Kinase II inhibitor	Calbiochem-Novabiochem (La Jolla, CA)
5-iodotubercidin	Biomol (Hornby, ON)
Adenosine triphosphate (ATP)	Sigma-Aldrich Canada Ltd. (Oakville, ON)
$ALEXA_{488}$ conjugated goat anti-mouse antibody	Molecular Probes (Eugene, OR)
$ALEXA_{488}$ BSA conjugate	Molecular Probes (Eugene, OR)
Ammonium molybdate	Mallinckrodt Inc. (St. Louis, MO)
Ammonium persulfate	Sigma-Aldrich Canada Ltd. (Oakville, ON)
ANS (1-amino 2-naphthal 4-sulfonic acid)	Sigma-Aldrich Canada Ltd. (Oakville, ON)
anti-BSA	Sigma-Aldrich Canada Ltd. (Oakville, ON)
anti-CAS	BD Transduction Laboratories (Lexington, KY)
anti-karyopherin beta	BD Transduction Laboratories (Lexington, KY)
anti-lamin A/C	Covance (Princeton, NJ)
anti-lamin A/C	Santa Cruz Biotechnology (Santa Cruz, CA)
anti-lamin B1	Zymed Laboratories Inc. (San Francisco, CA)
anti-NTF2	BD Transduction Laboratories (Lexington, KY)
anti-nup153	Covance (Princeton, NJ)
anti-p38	Santa Cruz Biotechnology (Santa Cruz, CA)
anti-p62	BD Transduction Laboratories (Lexington, KY)
anti-p97	Affinity Bioreagents Inc. (Golden, CO)
anti-phospho-p44/p42 antibody	New England Biolabs (Pickering, ON)
anti-phosphoserine	Sigma-Aldrich Canada Ltd. (Oakville, ON)
anti-phosphoserine	Zymed Laboratories Inc. (San Francisco, CA)
anti-phosphothreonine	Sigma-Aldrich Canada Ltd. (Oakville, ON)
anti-Ran	BD Transduction Laboratories (Lexington, KY)
anti-RanGAP-1	Zymed Laboratories Inc. (San Francisco, CA)
anti-Rch1	BD Transduction Laboratories (Lexington, KY)
anti-smooth muscle actin	Sigma-Aldrich Canada Ltd. (Oakville, ON)
Apigenin	Calbiochem-Novabiochem (La Jolla, CA)
Autocamtide-2	Calbiochem-Novabiochem (La Jolla, CA)
Autocamtide-2 Related Inhibitory Peptide	Calbiochem-Novabiochem (La Jolla, CA)
Axiovision Viewer	Zeiss (North York, ON)
Beckman Coulter LS 6500	Beckman Coulter (Mississauga, ON)
Benchmark prestained protein ladder	Gibco BRL (Burlington, ON)
BioRad Laboratories phosphoimaging screen	BioRad Laboratories (Mississauga, ON)
bis-Tris	Sigma-Aldrich Canada Ltd. (Oakville, ON)
Bovine serum albumin (BSA)	Sigma-Aldrich Canada Ltd. (Oakville, ON)
C_{16}-Ceramide	Biomol (Hornby, ON)
Calcium chloride	Fisher Scientific (Nepean, ON)
Calcium-45	NEN Life Sciences Products (Guelph, ON)

Product	Company Name
Calmodulin	Biomol (Hornby, ON)
CaMK inhibitory peptide	Calbiochem-Novabiochem (La Jolla, CA)
Capillary tubes	World Precision Instruments (Sarasota, FL)
Ceramide	Biomol (Hornby, ON)
Ceramide-1-phosphate	Biomol (Hornby, ON)
Ceramine	Biomol (Hornby, ON)
Chelerythrine chloride	Calbiochem-Novabiochem (La Jolla, CA)
c-Jun N-Terminal Kinase	Calbiochem-Novabiochem (La Jolla, CA)
Confocal laser scanning microscope	BioRad Laboratories (Mississauga, ON)
Coomassie Brilliant Blue R-250	LKB Bromma (Sweden)
DC Protein Assay Kit	BioRad Laboratories (Mississauga, ON)
Dextrose	Fisher Scientific (Nepean, ON)
Diacylglycerol (DAG)	Biomol (Hornby, ON)
Digitonin	Sigma-Aldrich Canada Ltd. (Oakville, ON)
Dimethylsphingosine	Biomol (Hornby, ON)
Dimethylsulfoxide (DMSO)	Sigma-Aldrich Canada Ltd. (Oakville, ON)
Dithiothreitol	Sigma-Aldrich Canada Ltd. (Oakville, ON)
DNAse I	Worthington Biochemicals (Freehold, NJ)
D-Salt Excellulose Plastic Desalting Columns	Pierce (Rockford, IL)
Dulbecco's Modified Eagle Medium (DMEM)	Gibco BRL (Burlington, ON)
EDTA	Sigma-Aldrich Canada Ltd. (Oakville, ON)
EGTA	Sigma-Aldrich Canada Ltd. (Oakville, ON)
ERK-2 (activated)	Calbiochem-Novabiochem (La Jolla, CA)
Ethyl acetate	Fisher Scientific (Nepean, ON)
Fetal bovine serum (FBS)	Gibco BRL (Burlington, ON)
Fluorsave	Calbiochem-Novabiochem (La Jolla, CA)
Formamide	Sigma-Aldrich Canada Ltd. (Oakville, ON)
Fungizone	Gibco BRL (Burlington, ON)
GelCode Blue Stain Reagent	Pierce (Rockford, IL)
Glycine	Gibco BRL (Burlington, ON)
Goat anti-mouse HRP conjugate	BioRad Laboratories (Mississauga, ON)
GST-tagged p38 MAP kinase	Calbiochem-Novabiochem (La Jolla, CA)
HEPES	Sigma-Aldrich Canada Ltd. (Oakville, ON)
Hoescht 33258	Sigma-Aldrich Canada Ltd. (Oakville, ON)
holo-Transferrin	Sigma-Aldrich Canada Ltd. (Oakville, ON)
Hydrochloric acid	Mallinckrodt Inc. (St. Louis, MO)
Imidazole	Sigma-Aldrich Canada Ltd. (Oakville, ON)
Insulin	Sigma-Aldrich Canada Ltd. (Oakville, ON)
Isopropanol	Fisher Scientific (Nepean, ON)
L-ascorbate	Mallinckrodt Inc. (St. Louis, MO)
Liquid nitrogen	Vitalaire (Winnipeg, MB)
Lysophosphatidylcholine (LPC)	Doosan Serdary Research Laboratories (Korea)
mAb414 (primary antibody against nucleoporins)	Covance (Princeton, NJ)

Product	Company Name
Magnesium acetate	Fisher Scientific (Nepean, ON)
Magnesium chloride	Fisher Scientific (Nepean, ON)
Mannose-6-phosphate	Sigma-Aldrich Canada Ltd. (Oakville, ON)
MAPP	Biomol (Hornby, ON)
MES	Sigma-Aldrich Canada Ltd. (Oakville, ON)
Methanol	Stanchem (Reading, UK)
Molecular Dynamics Imagespace software	Molecular Dynamics (Sunnyvale, CA)
Monoclonal mouse anti-phosphoserine	Biomeda Corporation (Foster City, CA)
Monoclonal mouse anti-phosphothreonine	Biomeda Corporation (Foster City, CA)
MS314 micromanipulator	Fine Science Tools (Vancouver, BC)
NAP-5 columns	Pharmacia Biotech (Oakville, ON)
Nitrocellulose membrane	Gibco BRL (Burlington, ON)
Nitrocellulose membranes (circular)	Whatman (Clifton, NJ)
N-oleoylethanolamide (NOE)	Biomol (Hornby, ON)
Paraformaldehyde	TAAB Laboratories Equipment Ltd. (Reading, UK)
para-iodonitrotetrazolium violet (p-INT)	Sigma-Aldrich Canada Ltd. (Oakville, ON)
PD-98059	Calbiochem-Novabiochem (La Jolla, CA)
Phenylmethylsulfonyl fluoride (PMSF)	Sigma-Aldrich Canada Ltd. (Oakville, ON)
Phosphorous-32 (GTP)	Mandel Scientific (Guelph, ON)
Phosphorous-32 (ATP)	Mandel Scientific (Guelph, ON)
Phytoceramide	Biomol (Hornby, ON)
p-nitrophenol	Sigma-Aldrich Canada Ltd. (Oakville, ON)
p-nitrophenolphosphate	Sigma-Aldrich Canada Ltd. (Oakville, ON)
Polyoxyethylenesorbitan monolaurate (Tween-20)	Sigma-Aldrich Canada Ltd. (Oakville, ON)
Ponceau S stain	Sigma-Aldrich Canada Ltd. (Oakville, ON)
Potassium acetate	Fisher Scientific (Nepean, ON)
Potassium chloride	Fisher Scientific (Nepean, ON)
Potassium phosphate	Sigma-Aldrich Canada Ltd. (Oakville, ON)
Protease inhibitor cocktail	Sigma-Aldrich Canada Ltd. (Oakville, ON)
Protein A-Agarose	Calbiochem-Novabiochem (La Jolla, CA)
Protein G PLUS-Agarose	Oncogene Research Products (San Diego, CA)
PV830 Pneumatic PicoPump	World Precision Instruments (Sarasota, FL)
Pyruvic acid	Sigma-Aldrich Canada Ltd. (Oakville, ON)
Ran (recombinant protein)	Sigma-Aldrich Canada Ltd. (Oakville, ON)
RNAse A	Sigma-Aldrich Canada Ltd. (Oakville, ON)
SB-202190	Calbiochem-Novabiochem (La Jolla, CA)
SB-202190 (2002)	Biomol (Hornby, ON)
Selenium	Sigma-Aldrich Canada Ltd. (Oakville, ON)
Sigma pre-colored protein standards	Sigma-Aldrich Canada Ltd. (Oakville, ON)
Silver Stain	BioRad Laboratories (Mississauga, ON)
Skim milk powder	Carnation/Nestle Foods (USA)
Sodium acetate	Fisher Scientific (Nepean, ON)
Sodium azide	Sigma-Aldrich Canada Ltd. (Oakville, ON)

Product	Company Name
Sodium bisulfite	Sigma-Aldrich Canada Ltd. (Oakville, ON)
Sodium chloride	Fisher Scientific (Nepean, ON)
Sodium dodecyl sulfate	Gibco BRL (Burlington, ON)
Sodium hydroxide	Sigma-Aldrich Canada Ltd. (Oakville, ON)
Sodium succinate	Sigma-Aldrich Canada Ltd. (Oakville, ON)
Sodium sulfite	Sigma-Aldrich Canada Ltd. (Oakville, ON)
SpectraPor 1 dialysis membranes	Spectrum (Laguna Hills, CA)
Sphingomyelin	Biomol (Hornby, ON)
Sphingosine	Biomol (Hornby, ON)
Sphingosine-1-phosphate	Biomol (Hornby, ON)
Stains-All	Sigma-Aldrich Canada Ltd. (Oakville, ON)
Sucrose	Mallinckrodt Inc. (St. Louis, MO)
Sulfo-SMCC	Pierce (Rockford, IL)
Sulfuric acid	Fisher Scientific (Nepean, ON)
SuperSignal Substrate	Pierce (Rockford, IL)
Trichloroacetic acid	Sigma-Aldrich Canada Ltd. (Oakville, ON)
Triethanolamine	Sigma-Aldrich Canada Ltd. (Oakville, ON)
Tris-(2-carboxyethyl) phosphine (TCEP)	Sigma-Aldrich Canada Ltd. (Oakville, ON)
Tris-OH	Sigma-Aldrich Canada Ltd. (Oakville, ON)
Triton X-100	Fisher Scientific (Nepean, ON)
Trypsin-EDTA	Gibco BRL (Burlington, ON)
X-OMAT film	Eastman Kodak (Rochester, NY)
Zeiss Axioskop 2 MOT microscope	Zeiss (North York, ON)

METHODS

Isolation of hepatic tissue and nuclei

Hepatic nuclei were obtained using the following protocol (337). Sprague-Dawley rats were anesthetized by injection with a ketamine (60mg/kg) and xylazine (10mg/kg) cocktail and sacrificed by decapitation. Livers were harvested and snap frozen in liquid N_2 for immediate storage or use in the nuclei isolation protocol. Frozen hepatic tissue was pulverized prior to thawing by suspension in 250 mM STM buffer (250 mM sucrose, 50 mM bis-Tris and 5 mM $MgCl_2$, pH 7.4) containing a final concentration of 1 μg/ml each of the following protease inhibitors: leupeptin, pepstatin A and aprotinin. Fresh or thawed liver tissue was scissor-minced and homogenized using a teflon-coated pestle. The resulting homogenate was strained through a double layer of cheesecloth and spun for 10 min at 3000 rpm. The supernatant was discarded and the pellet was resuspended in 250 mM STM and spun again for 10 min at 3000 rpm. The pellet from the second spin was resuspended in 22 mls of 250 mM STM and brought up to 66 mls with 2.3 M STM. The resulting mixture was layered onto a 5 ml cushion of 2.3 M STM (2.3 M sucrose, 50 mM bis-Tris, 5 mM $MgCl_2$, pH 7.4). A total of 11 mls was loaded onto each 5 ml cushion. The cushion also contained the same protease inhibitors mentioned earlier. The layer of 2.3 M STM was initially loaded into six pre-cooled SW28 tubes. Gradient centrifugation was then performed on the samples for 40 min at 16,000 rpms. The supernatant was drawn off and the pellet resuspended in 150 μl of 250 mM STM. The nuclei were pooled into one cryovial, snap frozen in liquid N_2 and stored at -80°C for later use in the

isolation of the nuclear pore complex. Samples stored in this manner remained viable for several years.

Enzyme marker assays

Enzyme marker assays were used to determine membrane contamination from plasmalemma, endoplasmic reticulum and mitochondrial sources in the nuclear fraction. Purified samples of plasmalemma, endoplasmic reticulum/sarcoplasmic reticulum (ER/SR) and mitochondria were used as comparative controls.

K^+-pNPPase assay

K^+-pNPPase activity can be used to assay the degree of sarcolemmal contamination (338). Duplicate tubes were prepared containing 200 ml pNPPase cocktail (250 mM sucrose, 25 mM $MgCl_2$, 5 mM EGTA, pH 7.8) at 37°C. To each tube, the following were added: 550 µl of H20 + 50 µl sample, 100 µl 200 mM KCl. To the tubes used as blanks 100 µls H_2O were added instead of KCl. Following this, 100 µl 50 mM *p*-nitrophenolphosphate was added and tubes were vortexed and placed in a 37°C water bath for ~ 6 min (record time). Tubes were transferred to an ice bath for 30 s and 2 ml of 1.0 N NaOH was added to each to stop the reaction. Again, tubes were vortexed, warmed to room temperature and then read at 490 nm. Blanks contained 600 µl H_2O and standards were prepared with 5 µl 10 mM *p*-nitrophenol + 995 µl H_2O and activity was calculated using standard equations (339).

Mannose-6-phosphatase assay

Membranes derived from the endoplasmic or sarcoplasmic reticulum may contaminate a nuclear preparation and can be assayed as previously described (337). Briefly, tubes were prepared according to the following: blanks – 260 µl 50 mM MES, pH 6.5; samples – 240 µls 50 mM MES, pH 6.5 + 20 µl crude nuclei; control – 250 µls 50 mM MES, pH 6.5 + 10 µl sarcoplasmic/endoplasmic reticulum or nuclear envelope. Once this had been prepared, the following were added: 40 µl of 100 mg/ml BSA (suspended in 50 mM MES, pH 6.5) and 100 µl of 10mM mannose-6-phosphate. Tubes were incubated at 30°C for 30 min and the reaction was quenched by adding 200 µl of 10% SDS. After SDS quenching, 200 µl 0.9% ascorbate and 200 µl 1.25% ammonium molybdate (made in 6.5% H_2SO_4) was added to each tube, insuring there was a 30 s delay between each tube (to allow enough time to read the tubes sequentially after). Tubes were incubated at room temperature for 30 min, and then centrifuged for 5 min at low speed to sediment any particulate material. Absorbance of the sample was read at 660 nm, each tube being read 30 s apart. A standard concentration curve was prepared using KH_2PO_4 and Pi concentration was calculated (337).

Succinic dehydrogenase assay

Mitochondrial contamination was assessed using the succinic dehydrogenase assay (338). On ice, 0.5 mg/ml *p*-iodonitrotetrazolium violet (INT) was dissolved in SDH cocktail (50 mM KH_2PO4, 50 mM sodium succinate, 50 mM sucrose, pH 7.4) to create the INT/SDH solution for use later in the assay procedure. Test tubes were prepared according to the following: blank(s) – 50 µl H_20 + 1 ml INT/SDH; sample – 50 µl sample + 1 ml INT/SDH. Tubes were then incubated at 37°C and a timer was started. The test

tube rack was transferred to an ice bath once suitable color had developed and time required for colorimetric development was recorded. After ~ 1min on ice, the following were added in this order: 0.3 ml 20% TCA, followed by 3.0 ml ethyl acetate. Tubes were vortexed to extract the color into the organic layer and then centrifuged at low speed for 10min at 4° C. Subsequent to centrifugation, the tubes were then warmed to room temperature and the top layer was read at 490 nm. The activity of SDH was calculated using the constant $\varepsilon_{INT}=1.85x10^4$ according to published formulae (340).

Preparation of rat liver cytosol

Hepatic cytosol from rats was prepared for use in the nuclear import assay as previously described (341). Briefly, supernatant from the rat liver nuclei isolation procedure (after a 10 min spin at 3000 rpm) was collected and re-centrifuged in JA-20 tubes at 5000xg (6500 rpm) for 15min. The resulting supernatant was centrifuged in a SW28 rotor at 27000 rpm for 1 hr. The transparent supernatant from this spin (cytosol) was removed and dialyzed against 1x nuclear import buffer (20 mM HEPES, 110 mM K^+ acetate, 5 mM Na^+ acetate, 2 mM Mg^{2+} acetate, 0.5 mM EGTA, pH 7.5) overnight (vol = 4 litres) containing the same inhibitors as used for the nuclei isolation. The dialysis tubing used was SpectraPor 1 membrane (MWCO 6000 – 8000, preboiled for 5 minutes). The next day, the dialyzed cytosol was divided into 1 ml aliquots and stored at -80° C.

Isolation of nuclear pore complexes

Nuclear pore complexes can be isolated by the method of Berrios (342) following nuclear isolation and purification (338). Briefly, nuclei from rat liver were pelleted and

resuspended in a tube with nuclease digestion buffer (10 mM TEA, 0.23 M sucrose, 0.1mM $MgCl_2$, pH 8.5) containing ~4 μg/ml of DNase I and RNase A. The tube was then incubated at 37° C for 30 min, with occasional shaking. The suspension was centrifuged for 10 min at 1000xg and the supernatant discarded. The pellet was resuspended in 0.9 volumes of nuclear extraction buffer (10 mM TEA, 0.29 M sucrose, 0.1 mM $MgCl_2$, pH 7.5). One volume is defined by digested nuclear pellets, where the volume of one pellet is equivalent to one volume. After resuspension, 0.1 volumes of cold 20% Triton X-100 (v/v) was added and incubated on ice for 10 min. This mixture was re-centrifuged for 10 min at 1000xg and the supernatant discarded. The remaining pellet was resuspended in five volumes of nuclear extraction buffer and an equal volume of 2.0 M NaCl. This mixture remained on ice for 10 min, and was then centrifuged for 10 min at 10,000xg. The supernatant was discarded and the previous step was repeated (Figure 13). The final pellet was resuspended in 500 μls of 250 mM STM (250 mM sucrose, 50 mM TRIS, 5 mM $MgCl_2$, pH 7.5), snap frozen in liquid N_2, and stored at -80°C.

Protein assay

Protein concentrations of nuclear and nuclear pore fractions were determined using the DC Protein Assay Kit.

Tissue explant & cell culture

The method of obtaining smooth muscle cells from aortic tissue explants was adapted from Czubryt *et al* (341). In detail, New Zealand white rabbits were anesthetized by administration of 5% halothane in 2L/min O_2 followed by 3% halothane in 2L/min O_2

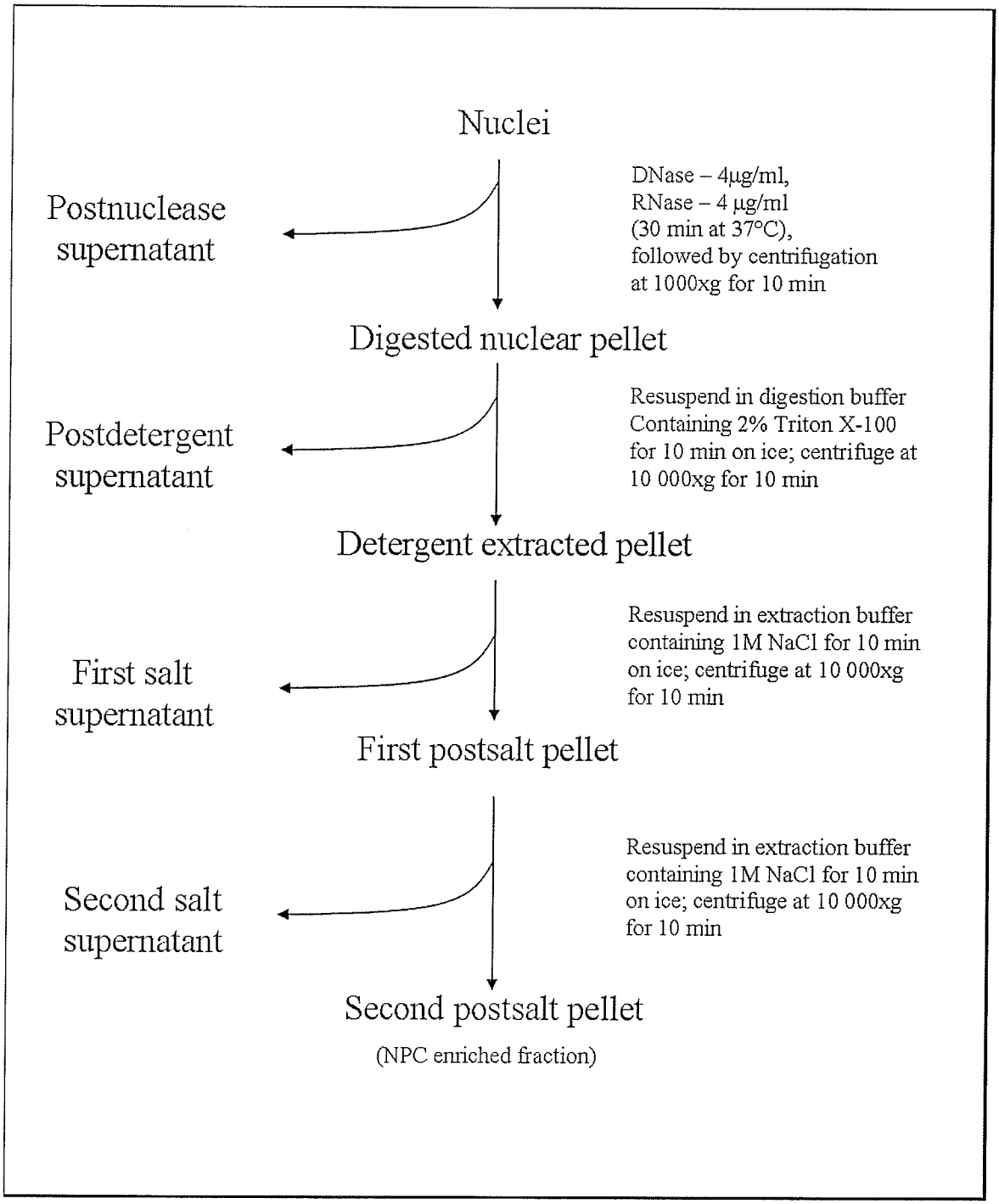

Figure 13. Nuclear pore complex isolation protocol

delivered by face mask. The thoracic aorta was dissected out and suspended in 1xPBS (137 mM NaCl, 2.7 mM KCl, 10 mM Na_2HPO_4, 1.8 mM KH_2PO_4, pH 7.4). After several rinses with PBS, excess fatty and connective tissue were removed and the aorta cut into ~1 mm rings. Aortic rings were placed into a small 10 ml beaker containing 1xPBS. Next, 1xPBS was aspirated off and 10 mls of a 20% Fungizone-PBS solution (8 ml of sterile 1xPBS + 2ml Fungizone) was added to the rings. Rings were allowed to equilibrate in this solution for 15 min, and then the solution was changed and repeated once again. During this incubation period, another Petri dish was prepared containing 10.5 mls DMEM, 20% FBS (3 mls) and 10% Fungizone (1.5 mls) for a total volume of 15 mls. Aortic rings were rinsed several times with 1xPBS, transferred using sterile forceps to the dish containing 20% FBS, and then placed in the incubator for 5-8 days. After the first 3-4 days, the concentration of Fungizone was reduced to 8%. The day that cell growth commenced was taken to be Day 1 (about 7 days after the tissue explant). Tissue was transferred to a new dish containing 20% FBS + 2% Fungizone on Day 7 and monitored for cell growth. Once the dish had reached 60% - 70% cell confluency, the tissue was removed and the media was changed to feeding solution (5% FBS + 1% Fungizone). In order to passage, cells were lifted off using 1 ml of a trypsinization solution (Trypsin-EDTA) for ~5 min at 37°C. To stop the trypsinization reaction, ~3-4 mls of 20% FBS was added and a hemacytometer was used to determine cell counts. From this, seeding densities were calculated for passaging onto coverslips to be used in the nuclear import assay.

Circular 25 mm coverslips were acid sterilized for 2-3 hours, followed by a minimum of 10 rinses with double distilled H_2O (ddH_2O) (pH was monitored to ensure complete

removal of acid). After acid sterilization, coverslips were autoclaved in ddH_2O and aseptically transferred to sterile Petri dishes. Cells were passaged onto these coverslips at the desired seeding densities and then synchronized by incubating in starvation solution made in DMEM containing 1% Fungizone, 1% supplement (0.5 mg/ml holo-Transferrin, 0.017 mg/ml selenium, 4 mg/ml L-ascorbate, 1.1 mg/ml pyruvic acid) and 10 µl insulin (from a 1mg/ml stock) for ~3-4 days. Our lab has previously demonstrated successful isolation of smooth muscle cells using this technique and confirmed it using several markers for smooth muscle cells (unpublished observations). To confirm the presence of smooth muscle cells in culture, cells were stained with anti-smooth muscle actin and smooth muscle myosin heavy chain (Figure 14) and visualized by indirect immunofluorescence. After starvation, cells were fed prior to use in the nuclear import assay, as described in detail below.

Vascular smooth muscle cells isolated from New Zealand white rabbits were seeded on acid rinsed coverslips at initial seeding densities (ISD) of $2.0x10^5$ or $1.9x10^5$ cells per coverslip and starved for 3 days before feeding. Coverslips seeded with $2.0x10^5$ cells were fed with 10 mls of DMEM containing 5% FBS + 1% Fungizone 24 hrs prior to use in the nuclear import assay, whereas coverslips seeded with $1.9x10^5$ cells were similarly fed 2-3 days before use. Cells for use in microinjection experiments were seeded at initial seeding densities of $1.5x10^5$ cells/coverslip.

Preparation of nuclear import substrate

The import substrate was constructed as previously described (341). The import substrate used was a fluorescently tagged $ALEXA_{488}$-BSA molecule coupled to the

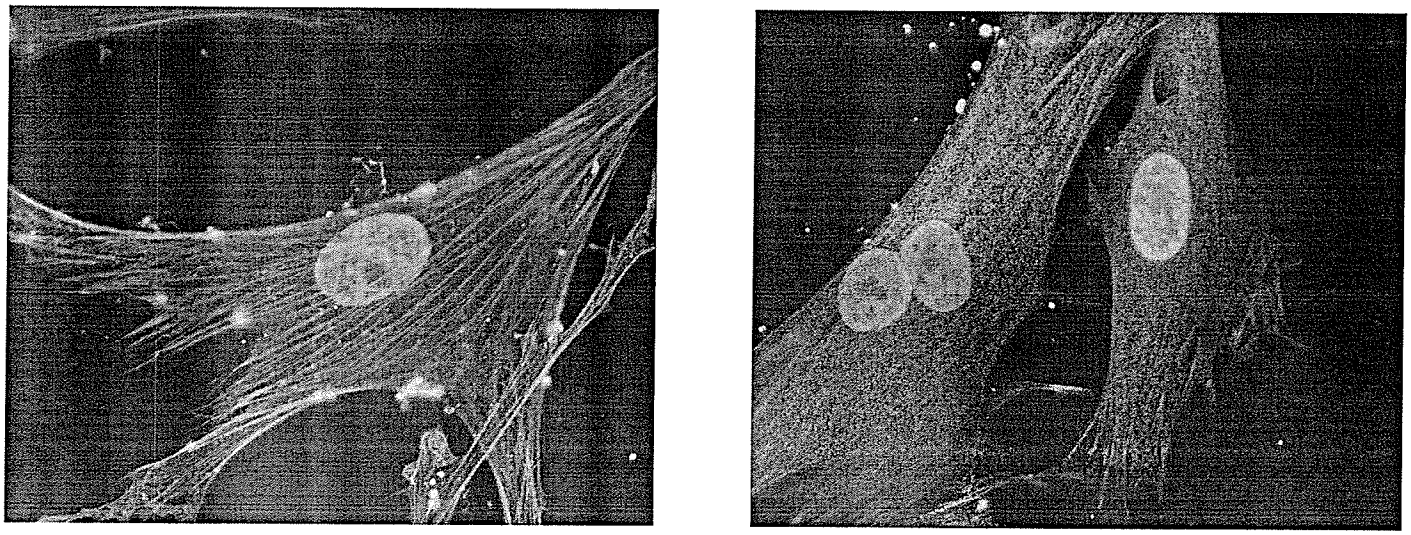

Figure 14. Smooth muscle cell stained with smooth muscle cell markers

Left: Cultured cells were stained with smooth muscle actin antibodies to confirm their identity. *Right:* Staining of cells against smooth muscle myosin heavy chain. Illustrated above are vascular smooth muscle cells from coverslips seeded with an ISD of $1.9x10^5$ cells (see text). Staining for smooth muscle actin and smooth muscle myosin heavy chain was performed 3 days after feeding and are readily distinguished after indirect immunofluorescence using an $ALEXA_{488}$-conjugated secondary antibody. Nuclei were stained using Hoescht. Magnification: 63x (oil immersion)

"classical" SV40 large T antigen nuclear localization signal, i.e. – PKKKRKV. The NLS used in the present study was custom designed with an N-terminus CGGG sequence in order to provide the signal with a –SH reactive conjugation point and and a C-terminus ED cap to protect the sequence during synthesis. The final peptide sequence was CGGGPKKKRKVED. To generate the substrate, 4 mg of $ALEXA_{488}$-BSA was suspended in 500 µl PBS and 1mg of a cross-linking agent (sulfosuccinimidyl 4-[N-maleimidomethyl]cyclohexane-1-carboxylate) was added. The solution was incubated at 37°C for 30 minutes and then desalted on a 5 ml Excellulose column that had been equilibrated with 5 column volumes of PBS prior to use. Using PBS as an eluant, aliquots were collected in 500 µl fractions and those containing the fluorescent tag were identified by their bright yellow/orange color. Two milligrams of NLS were suspended in 500 µls of coupling buffer (50 mM MES, 0.4 mM tris-(2-carboxyethyl) phosphine HCl, pH 5.0) and incubated for 30 min at 37° C. Once the incubation was complete, the solution containing the NLS was combined with the previously isolated $ALEXA_{488}$-BSA fractions. The resulting solution was placed in a dark bottle and allowed to conjugate overnight at 4° C with gentle stirring in a darkened environment. The following day, the conjugated solution was passed through another 5 ml Excellulose column equilibrated with a second elution buffer (10 mM HEPES, 110 mM potassium acetate, pH 7.3). Eight fractions of 500 µl each were collected, using the second elution buffer as eluant. To prevent overloading of the column, smaller volumes of the conjugated solution were added and the elution step was done once on each of the smaller volumes. Once again, fractions containing the fluorophore were identified by their bright yellow/orange color (typically the second to the fifth fractions) and were pooled together (Figure 15). To

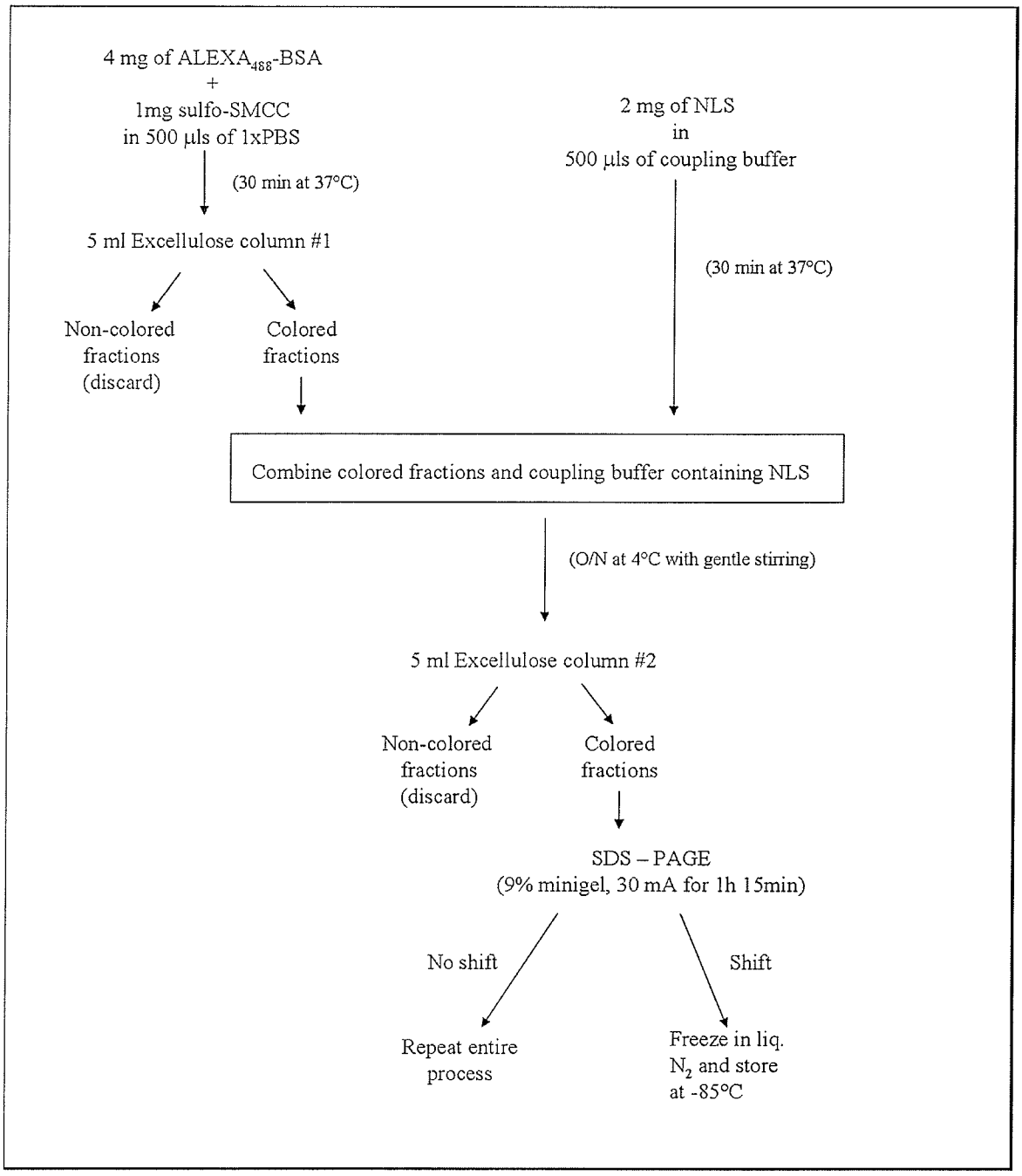

Figure 15. Fluorescent substrate synthesis

determine whether or not the conjugation had been successful, the original $ALEXA_{488}$-BSA and the NLS-$ALEXA_{488}$-BSA conjugate were run on a 9% SDS-PAGE at 30 mA for 45 min and stained with Coomassie Brilliant Blue R-250. A gel shift of the conjugated fluorophore when compared to the original indicates successful conjugation and allows for estimation of the number of NLS molecules linked to the fluorescently tagged protein (Figure 16). Approximately 10-15 NLSs were calculated to be attached to each $ALEXA_{488}$-BSA molecule, using the ratio of 1.5kDa:1 NLS. The final conjugate was aliquoted as necessary, frozen in liquid N_2 and stored at -85° C.

Nuclear import assays

The permeabilized cell assay (343) was used to measure nuclear import in cultured smooth muscle cells. Nuclear import mix containing nuclear import buffer (20 mM HEPES, 110 mM K^+ acetate, 5 mM Na^+ acetate, 2 mM Mg^{2+} acetate, 0.5 mM EGTA, pH 7.5) and 50% rat liver cytosol was added to untreated, digitonin-permeabilized smooth muscle cells and used as controls. Permeabilized cells or exogenously added import mix were treated separately to determine their effects on nuclear transport. Treatments included incubation with 0.04 μg/ml (low) and 1 μg/ml (high) of activated ERK-2, p38 and JNK. The dose dependent effects of ERK-2 on nuclear import were further tested by including 0.4 μg/ml and 0.8 μg/ml of ERK-2.

The concentration and time dependent effects of lysophosphatidylcholine on nuclear import were tested by incubating 1-50 μM LPC for 15-60 min at 37° C. In some experiments, 20 μM PD-98059 was co-incubated with LPC. Other lysolipids were also used. The effects of treating import cocktail with 10 μM lysophosphatidylethanolamine

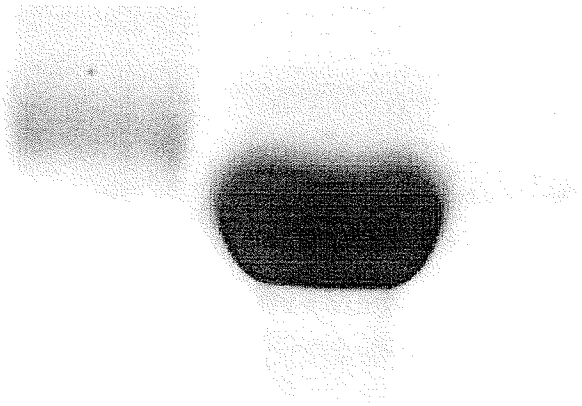

Figure 16. Gel shift of conjugated substrate

Successful conjugation of the NLS peptide to fluorescent BSA can be assessed using SDS-PAGE and will be heavier than non-conjugated BSA. *Above* – left lane loaded with NLS-conjugated $ALEXA_{488}$-BSA shows an upward shift compared to non-conjugated BSA (right).

(LPE), lysophosphatidylinositol (LPI), lysophosphatidylserine (LPS), or lysoplasmenylcholine (LPLC) for 30 min at 37° C were also tested. For the above experiments, import mix was treated prior to the import assay being carried out. Alternatively, the import cocktail was not treated, and instead permeablized cells were treated directly with either 1 or 10 μM LPC for 30 min at 37° C prior to the addition of import mix to initiate nuclear protein import.

Nuclear import mix incubated with 0.1 μM, 1 μM and 10 μM ethanol-solubilized ceramide was used to examine its dose dependent effect on nuclear import, while treatments using a constant concentration of 1 μM ceramide for 15, 30 and 60 min were used to examine its time dependent effects. The same regimen was used to determine the effects of other metabolites of the sphingolipid pathway, as follows: 1 μM of ceramide-1-phosphate (C1P), sphingomyelin (SM), and the inhibitor N-oleoylethanolamide (NOE) were each pre-incubated separately with the nuclear import mix prior to initiation of nuclear import to determine their effects on transport. Ceramide was selected for further studies and the effects of various MAP kinase inhibitors were examined.

For these experiments, 1 μM ceramide plus 1 μM SB-202190, 1 μM 5-iodotubercidin, or 20 μM PD-98059 was added to the nuclear import mix prior to use in the nuclear import assay. Alternatively, exogenous recombinant p38 MAP kinase was added at a final concentration of 0.04 μg/ml ± 1 μM SB-202190 and pre-incubated with nuclear import mix for 30 min at 37° C prior to use in the nuclear import assay.

Nuclear import was initiated by inverting the coverslips on 50 μl drops of treated import mix plus 5 μls of fluorescent substrate in a parafilm lined box and incubating at 37°C. After import, cells were fixed with 3.7% paraformaldehyde for 15 min and

subsequently visualized on a BioRad MRC600 confocal laser scanning microscope (CLSM) using the 488nm laser line and the VHS filter block. Nuclear fluorescence was assessed using Molecular Dynamics Imagespace 3.2.1 software on a Silicon Graphics O_2 Workstation and images were processed using Confocal Assistant v3.0.

Confocal Microscopy

After fixing the cells, coverslips were placed in a Leyden chamber and 1.0 ml of nuclear import buffer was added to prevent the samples from drying out. Using a BioRad MRC-600 confocal microscope, the 488 laser (at 10% transmission) and a small pinhole size (~3.0 – 5.0 units) were used to visualize the localization of the import substrate. Each of the images acquired were Kalman filtered three times per field to remove background noise originating from the photomultiplier and were initially obtained using a 40x, N.A. 1.3 oil immersion objective lens. The images were processed on an SGI workstation using the Molecular Dynamics Imagespace image analysis software.

The SGI software assigned a numerical value to the fluorescence in control and treated cells. Changes in the rate of nuclear transport were determined by comparing the fluorescence of treated to nontreated cells and reported as a percentage of the control. In this manner, the results of 3 – 4 different experiments were averaged and reported as a mean value plus or minus the standard error of the mean. Typically, each of these experiments contained numerical values of fluorescence intensity from 75 – 150 cells.

Microinjection

Coverslips containing smooth muscle cells were placed in a Leyden dish and 1 ml of pre-warmed perfusate buffer (6 mM KCl, 1 mM $MgCl_2$, 1 mM $CaCl_2$, 10 mM dextrose, 6 mM HEPES, pH 7.4) was added. Temperature was maintained at 37° C in a microperfusion chamber. Micropipettes were loaded for injection using a 1 ml syringe to add approximately 10 μl of fluorescent substrate (ALEXA-BSA-NLS) in nuclear import buffer containing either 1 μg/ml (high ERK-2) or 0.04 μg/ml (low ERK-2), ensuring that no bubbles were present in the tip. Using an MS314 micromanipulator (Fine Science Tools), the pipette was inserted into the cell cytoplasm in close proximity to the nucleus and microinjected. The microinjector used in our study was a PV830 Pneumatic PicoPump (World Precision Instruments) and settings were as follows: injection hold pressure – 40 psi; ejection pressure – 60 psi; range – 100 ms; period – 80 ms. Cells were injected 4x and the pipette was slowly removed from the cell. Images of the microinjected cell were acquired on a BioRad MRC600 CLSM under the same settings described previously for nuclear import assays. Images were taken of pre- and post-injection cells followed by set time points to observe the rate of nuclear import for each cell over time. Final images were analyzed and processed as described for nuclear import assays.

RanGAP assay

The RanGAP assay was used as previously described (81, 344, 345), with several minor modifications. Briefly, human recombinant Ran (approximately 1 μg) was loaded with [γ-^{32}P]GTP (10mCi/mmol) in the presence of loading buffer (10 mM EDTA, 2 mM ATP, 4 mM DTT, 50 mM HEPES, pH 7.4) for a total of 20 μls. Loading mixture was

incubated at room temperature for 30 min, then diluted 10-fold into GAP buffer (5 mM $MgCl_2$, 1 mM DTT, 0.1 mg/ml BSA, 0.005% Tween-20, 50 mM HEPES, pH 7.4). Unbound GTP was removed on a NAP-5 column and eluted with GAP buffer. Reaction mixtures containing GAP buffer, 1.5% rat liver cytosol and a 10-fold dilution of radioactive RanGTP were vortexed and incubated at room temperature for 30 min. Reactions were performed in triplicate and 40 µl aliquots were taken at 0, 2.5, 5, and 10 min and vacuum filtered using 0.45 µm nitrocellulose filters. Filters were washed with 2 mls of rinsing buffer (150 mM NaCl, 5 mM $MgCl_2$, 1 mM DTT, 10 mM TRIS, pH 7.5) three times and radioactivity was quantified using a Beckmann-Coulter LS 6500 scintillation counter. Results were reported as percent of control GTP bound to the membrane.

Phosphorylation Assay and SDS-PAGE

NPC phosphorylation was investigated using a phosphorylation assay described previously (346) with minor modifications. Typically, 40 µg of sample was incubated with or without (1 µg/ml) ERK-2, JNK, or p38 in phosphorylation buffer (40 mM HEPES, 10 mM $MgCl_2$, 1 mM DTT, pH 7.5) and 2.0 µCi of ^{32}P for a total volume of 50 µls. To investigate endogenous phosphorylation, samples were incubated either alone or with various kinase inhibitors. The inhibitors were used at the following concentrations: 1 µM autocamtide-2 related inhibitory peptide (AIP), 1 µM CaM kinase inhibitory peptide (CKI), 20 µM PD-98059, 0-100 µM apigenin and 0-1000 nM SB-202190. The reaction mixture was allowed to incubate at room temperature for 1 hr and the reaction was stopped immediately by the addition of an equivalent amount of 2x sample buffer.

Samples were boiled for 5 min at 95° C and then loaded onto a 4%-15% gradient gel or a 10% minigel for SDS-PAGE. Samples were separated by electrophoresis at 60 mA, 550V for ~3-4 hrs or 30 mA for 90 min, respectively. Gels were stained with either Coomassie Brilliant Blue or Stains All stain as required, then dried and exposed to KODAK X-OMAT film overnight at -80° C. (Gels stained with Stains All were not dried, but kept in solution). Film was developed the following day. Gels were also visualized using the Molecular Dynamics Phosphoimager.

Immunoprecipitation

The nuclear pore complex was immunodepleted of lamins by immunoprecipitation (Figure 17), carried out as previously described (346). The NPC/lamin enriched fraction was pre-cleared by incubating 1.0 μg of normal mouse serum IgG and 20 μls of Protein G-agarose overnight at 4° C with end-over-end rotation. Samples were then centrifuged at 1000xg for 5 min. The supernatant was transferred to a new tube and 2 μg of anti-lamin A/C (Santa Cruz Biotechnology, Inc.) and 10 μls each of Protein A and Protein G agarose conjugate was added. The fraction was incubated overnight at 4° C with end-over-end rotation. The following day, the tube was centrifuged at 1000xg for 5 min to sediment the antibodies. Again, the supernatant was transferred to a new tube and the immunoprecipitation step was repeated, this time using 5 μls of a 1 mg/ml solution of anti-lamin B_1 antibody. After overnight incubation, the tube was re-centrifuged for 5 min at 1000xg to pellet out the anti-lamin B_1. All pellets were saved in addition to the final lamin-precipitated NPC fraction.

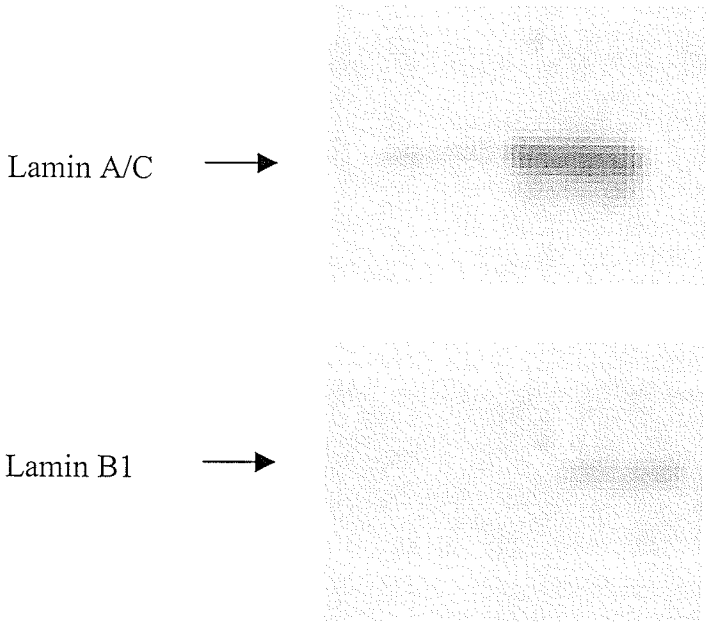

Figure 17. Immunodepletion of lamins from NPC fraction

Nuclear pore complex fractions were immunodepleted of nuclear lamins prior to use in the phosphorylation assays. Illustrated above are representative immunoblots of nuclear pore complex fractions that were immunodepleted and then blotted for lamins A/C or B1. In both cases, lamins were effectively removed. Pre-immunodepletion samples were loaded on the right for comparison.

Immunoblotting

SDS-PAGE was performed as described earlier on both the precipitated and non-precipitated NPC fractions. After completing electrophoresis, the gel was placed in Towbin's buffer (25 mM TRIS-OH, 192 mM glycine, 20% (v/v) methanol, pH 8.3) and allowed to soak for 15-20 min. Proteins were then transferred onto a nitrocellulose membrane at 50 V for 45 min. After the transfer was completed, the membrane was placed in 10% blocking buffer (10% (w/v) skim milk powder, 0.1% (v/v) Tween-20, 1xPBS) for 1 hr at room temperature with shaking. Blocking buffer was then decanted and the membrane was washed every 10 min for 30 min with wash buffer (1x PBS, 0.1% (v/v) Tween-20). Following transfer, the nitrocellulose membrane was incubated in Ponceau S stain for 10 min to visualize proteins and assess transfer efficiency. Ponceau S was rinsed off the membrane with several changes of PBS and the membrane was transferred to wash solution containing primary antibody for immunoblotting

The membrane was incubated with primary antibody diluted in 1% blocking buffer (1% (w/v) skim milk powder, 0.1% (v/v) Tween-20, 1xPBS) for 1 hr at room temperature with constant shaking. After incubation, the primary antibody was poured off and the membrane was washed again for 30 min every 10 min. A goat anti-mouse HRP conjugate was the secondary antibody used in this experiment and was added to the membrane at a dilution of 1:20,000 in 1% blocking buffer and incubated for 1 hr at room temperature with shaking. The membrane was washed as mentioned earlier and then incubated for 15 min with the Pierce SuperSignal Substrate Working Solution. The nitrocellulose was then placed in a protective plastic sheet and exposed to film for 60 s to determine working exposure. Primary antibodies used and their dilutions: mAb414 (1:10,000), anti-p38 (1:10,000), anti-lamin A/C (1:10,000) anti-lamin B_1(1:10,000), anti-

karyopherin β (1:1000). For immunoblots using anti-karyopherin β, all buffers and antibody dilutions were done using 1xTBS (10 mM TRIS, 100 mM NaCl, 0.1% (v/v) Tween-20, pH 7.5) instead of phosphate buffered saline solutions as noted above.

$^{45}Ca^{2+}$ overlay

Ca^{2+} binding to specific proteins was measured using the $^{45}Ca^{2+}$ overlay technique (338). After Western blotting, the membrane was placed in overlay buffer (60 mM KCl, 10 mM imidazole, 5 mM $MgCl_2$, pH 6.8) for 20 min and transferred to another solution of overlay buffer containing 2 μCi of $^{45}Ca^{2+}$ for 15 min. The membrane was subsequently rinsed with ddH_2O and dried overnight by sandwiching the membrane between 4 sheets of filter paper (2 above, 2 below). The next day, the membrane was placed in a developing cassette and exposed to 2 sheets of X-OMAT film for approximately 10-14 days.

Immunocytochemistry

Cells and nuclear import mix were prepared as described for the nuclear import assay, with minor modifications. For these experiments, the ALEXA-BSA-NLS substrate was not included. Immunofluorescent reactions were detected as previously described (346), with the following modifications. After cells were fixed with 3.7% paraformaldehyde, they were incubated in blocking buffer (1x PBS, 2% skim milk, 0.1% Triton X-100) for 30 min at room temperature. Coverslips were washed 3x with wash buffer (1x PBS, 2% skim milk) and inverted on 50 μls of wash buffer containing a 1:100 dilution of the appropriate antibody in a parafilm-lined box. Coverslips were incubated for 1 hr at room

temperature, washed 3x and then incubated with a 1:1000 dilution of ALEXA conjugated goat anti-mouse secondary for 1hr. Coverslips were rinsed with 1x PBS and mounted on glass slides using Fluorsave. After drying, cells were visualized using a 63x objective lens and a 488 nm filter block on a Zeiss Axioskop 2 MOT microscope. Images were captured using a Zeiss Axiocam and pseudocolored using Axiovision Viewer v3.0.

RESULTS

Isolation and characterization of nuclear pore complexes from rat liver nuclei

Hepatic tissue from normal Sprague-Dawley rats was used as source material for the nuclei isolation procedure. Nuclei isolated from rat hepatocytes may contain contaminating membrane fractions from plasmalemma and mitochondria. Enzyme marker assays to measure the amount of these membrane contaminants in the nuclear fraction showed minimal contamination by non-nuclear membranes (Table 4). Isolated nuclear pore complexes (342) showed negligible amounts of membrane contaminants (Table 4). Immunoblotting confirmed the presence of nuclear pore complex proteins using the monoclonal antibody, mAb414 (Figure 18). This antibody recognizes the FG motif common among nucleoporins (347) and was used as a diagnostic tool to determine the presence of NPC proteins as well as to measure purification. Aliquots of different fractions from the NPC isolation procedure demonstrated sequential purification of nuclear pore complex proteins (Figure 18). Protein staining shows a concomitant reduction in overall protein content. Together with the increased signal observed in Western blotting, this is indicative of an enrichment of proteins within the nuclear pore complex fraction (Figures 19, 20).

Nuclear pore complex studies

Calcium

	Control	Nuclei	NPC fraction
K^+-pNPPase (μmol/mg/hr)	28.55	$5.5x10^{-3} \pm 9.0x10^{-4}$	$3.5x10^{-3} \pm 7.0x10^{-3}$
Mannose-6-phosphatase (nmol/mg/hr)	345	38.53 ± 4.32	15.44 ± 2.56
Succinic dehydrogenase (nmol/mg/hr)	0.487	$3.37x10^{-3} \pm 2.2x10^{-4}$	$2.87x10^{-3} \pm 5.8x10^{-4}$

Table 4. Results of enzyme marker assays for nuclei and nuclear pore complex fractions

Assays measuring levels of sarcolemmal/plasmalemmal, mitochondrial and sarcoplasmic/endoplasmic reticulum membranes demonstrated insignificant or no membrane contaminants in purified nuclei and enriched NPC fractions. Controls used were purified SL/PL membrane, SR, and mitochondria for the K^+-pNPPase, mannose-6-phosphatase and mitochondrial assays, respectively.

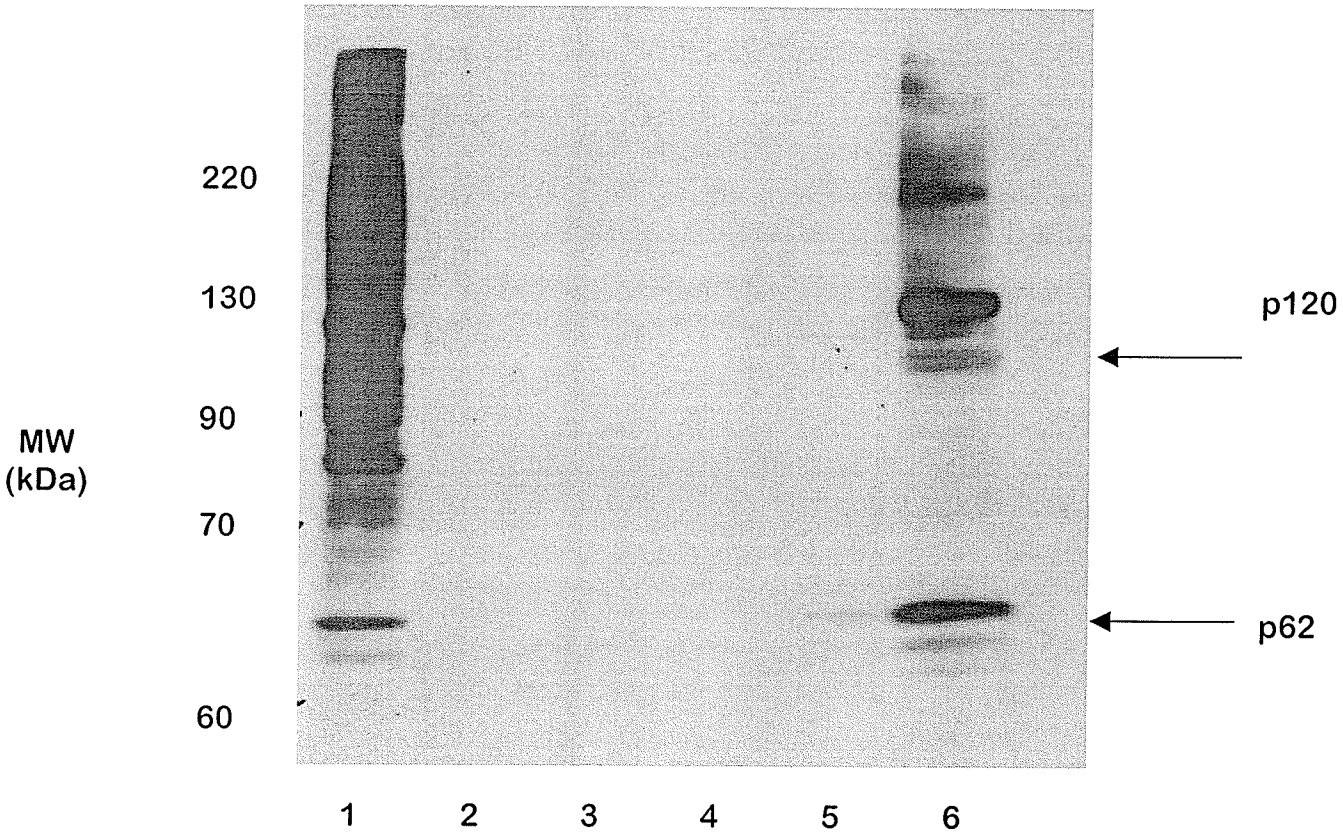

Figure 18. Western blot of fractions from the nuclear pore complex isolation protocol

Fractions from the nuclear pore complex isolation protocol were loaded onto SDS-PAGE (50 μg per lane) and then immunoblotted using mAb414. Crude nuclei (lane 1) show staining of p62 (arrow), a nucleoporin recognized by mAb414, with subsequent enrichment in the final NPC rich fraction (lane 6). *Lane assignments*: *1* – crude nuclei, *2* – supernatant from nuclease digested nuclei, *3* – supernatant from detergent extracted nuclei, *4* – supernatant from first salt wash, *5* – supernatant from second salt wash, *6* – purified NPC/lamina fraction. Other proteins recognized by mAb414 are also visible, i.e. – 120 kDa. Numbers to the left indicate molecular mass markers.

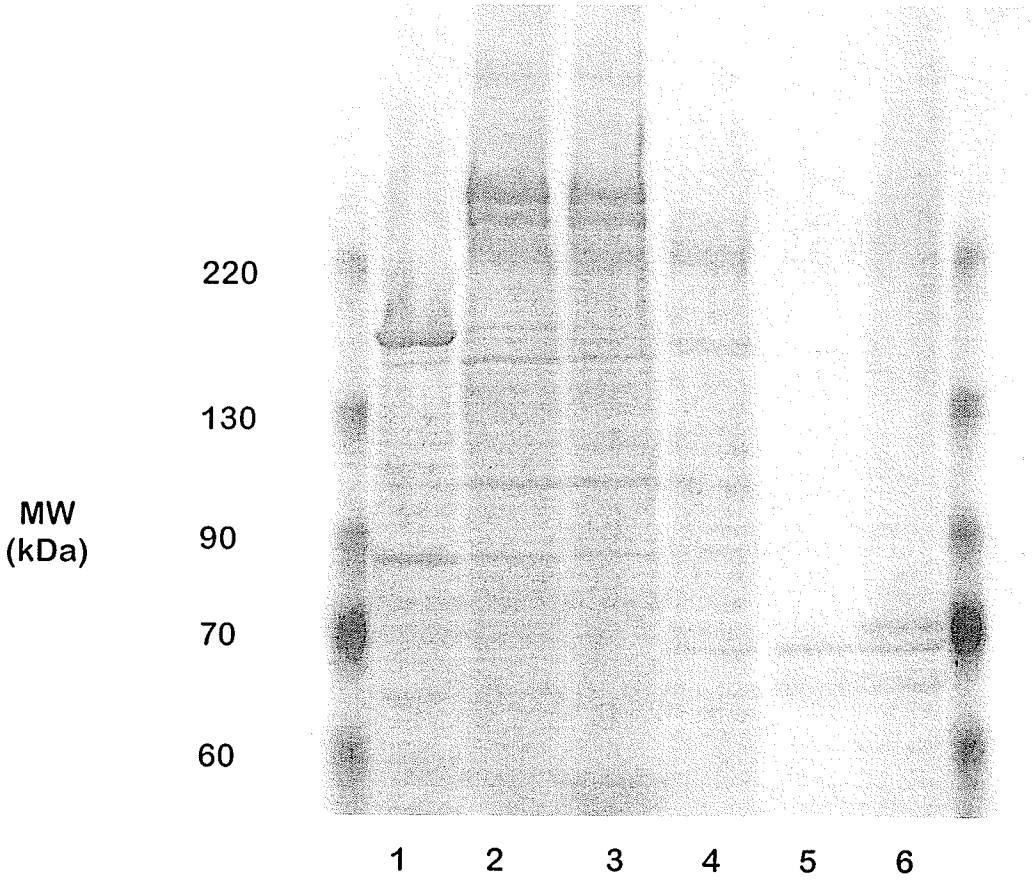

Figure 19. Enrichment of NPC/karyoskeletal fraction

Fractions from the NPC protocol were stained with a proprietary protein stain called GelCode Blue and exhibit a decrease in overall protein content. Molecular weight in kDa is shown on the left. *Lane assignments: 1* – nuclei, *2* – nuclease digested nuclei, *3* – detergent extraction (supernatant), *4* – detergent extracted nuclei, *5* – first salt wash (supernatant), *6* – enriched NPC/lamina fraction. (For details on fractions, see Figure 13). Prestained protein standards are shown on the right and left sides of the gel. Numbers to the left indicate molecular mass markers.

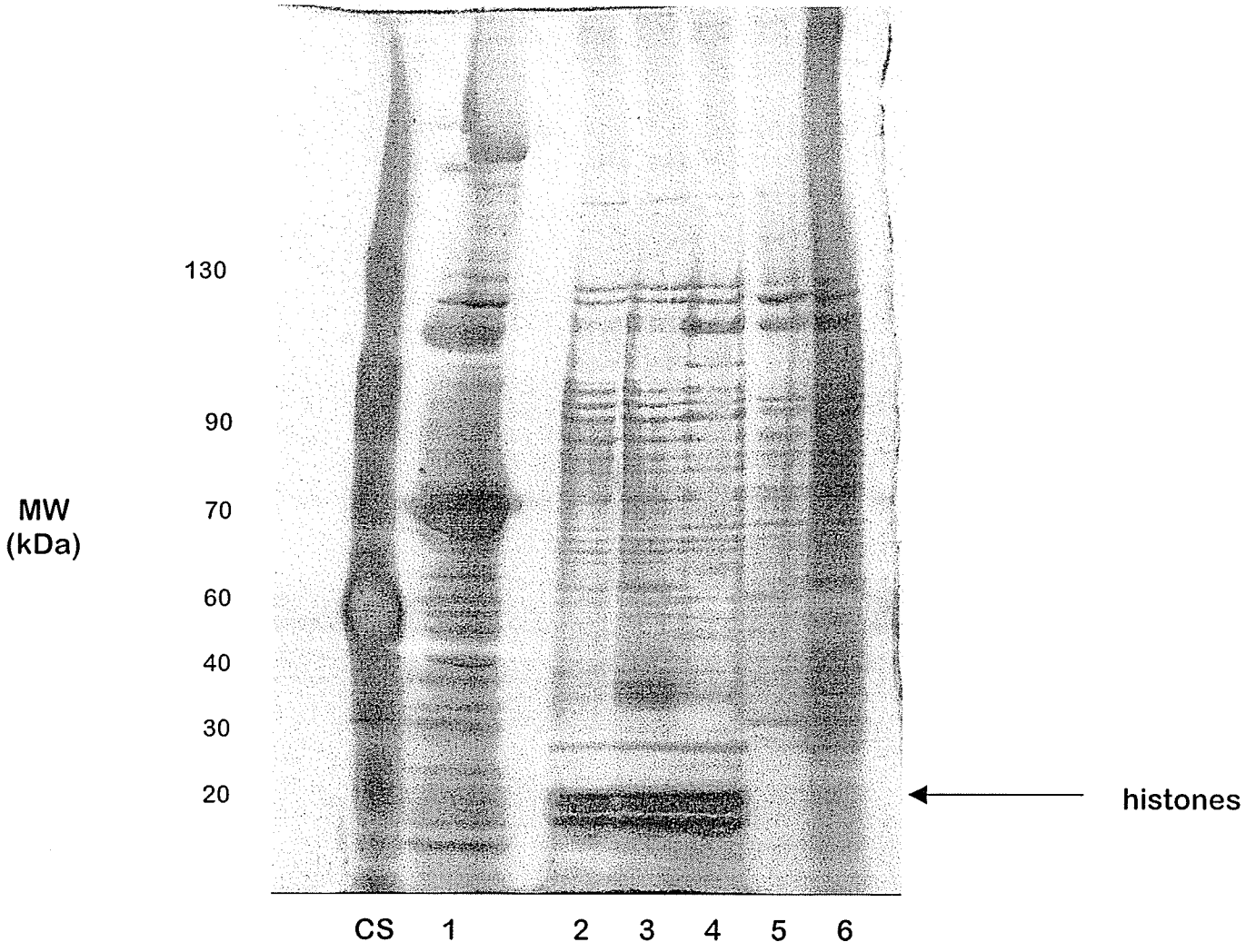

Figure 20. Silver stained gel of fractions from NPC protocol

Silver staining reveals the purification of proteins within the final fraction after two salt washes. Salt washing removes highly charged and loosely associated proteins from the final fraction, as evidenced by the loss of histone proteins when comparing lanes 2-4 with 5,6. *Lane assignments: 1* – sarcoplasmic reticulum (SR), *2* – nuclease digested nuclei, *3* – detergent extraction (supernatant), *4* – detergent extracted nuclei, *5* – first salt wash (supernatant), *6* – enriched NPC/lamina fraction. CS – colored protein standard. Numbers to the left indicate molecular mass markers.

Calcium dependent regulation of pore size and conformation has been documented (118, 119). The presence of calcium binding proteins within the fraction containing purified nuclear pore complex proteins was investigated. Stains-All revealed the presence of acidic proteins within the NPC fraction (Figure 21), but radioactive calcium overlays on the same fractions did not detect any calcium binding proteins (Figure 22).

This was not due to an inability to detect Ca^{2+} binding proteins using this technique. Lanes containing control SR fraction displayed strong Ca^{2+} binding capacity using the $^{45}Ca^{2+}$ overlay technique (Figure 22). The possibility that the calcium sensitivity of the nuclear pore was due to a calcium dependent kinase was considered. Phosphorylation of pore proteins has previously been demonstrated (334, 335). There were no differences in endogenous phosphorylation of the nuclear pore fraction over 30 min in the presence of calcium or EGTA (Figures 23, 24). Furthermore, the incubation of specific CaM kinase antagonists with the NPC fraction did not inhibit NPC phosphorylation (Figure 25). However, the addition of exogenous CaM kinase demonstrated a time dependent phosphorylation of NPC proteins (Figure 26).This argues against the presence of an endogenous CaM kinase associated with the isolated NPC but suggests the presence of several CaM kinase phosphonucleoporins of 60, 65, 70 and 72 kDa in mass (Figure 26).

Phosphorylation

Various pharmacological inhibitors were used to determine the nature of the observed endogenous kinase activity within the NPC fraction. Of all inhibitors tested, apigenin displayed the most striking inhibition of endogenous phosphorylation (Figures 25, 27). Apigenin is a broad range MAP kinase antagonist (322). Therefore, specific MAP kinase

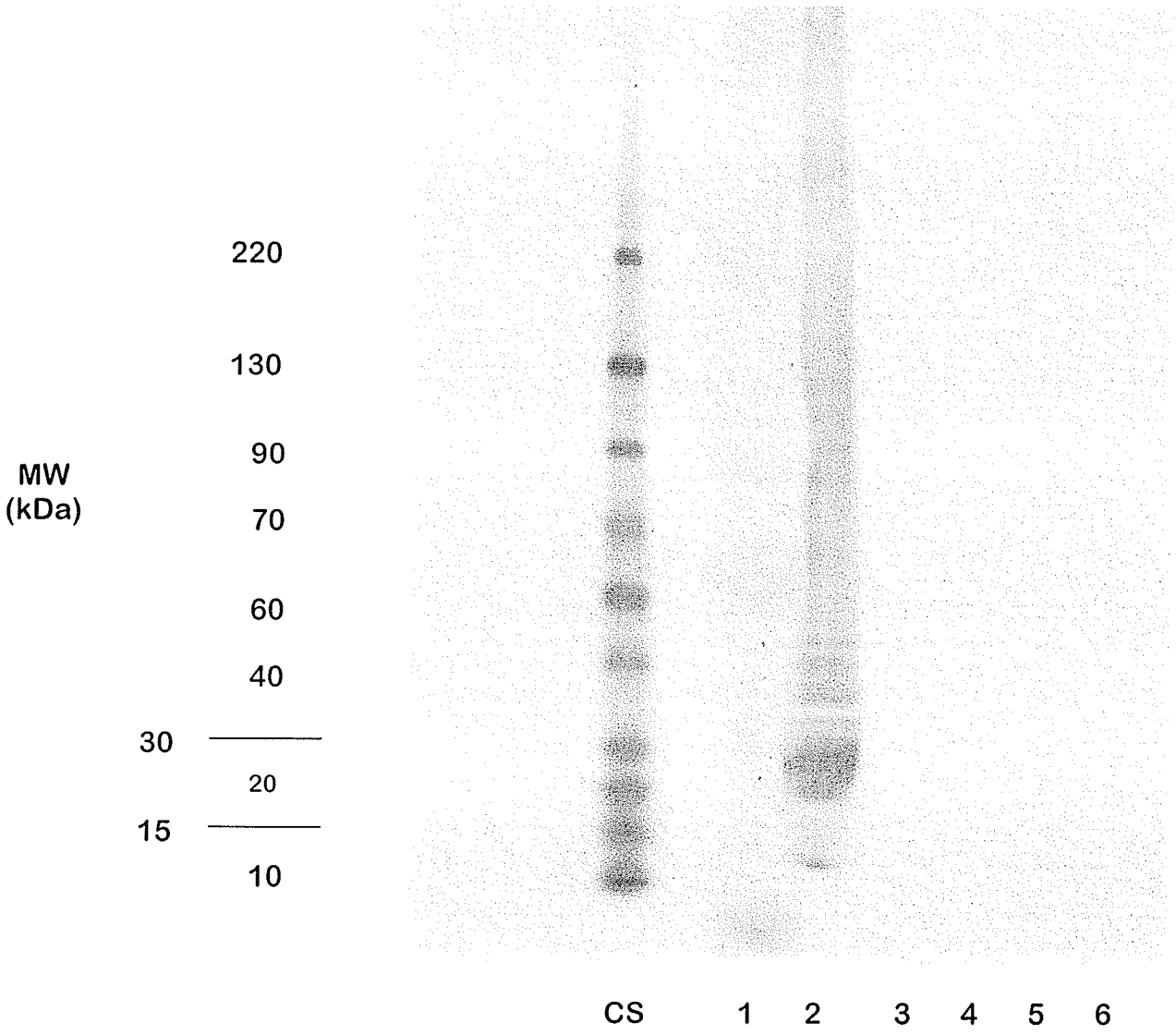

Figure 21. Stains-All staining

Stains All staining was used as a preliminary method of determining the presence of calcium binding proteins. Each lane was loaded with 50 μg protein per lane. Purified sarcoplasmic reticulum was used as control in lane 1. Stains All recognizes acidic proteins other than calcium binding proteins and visualizes histones in lane 2. No proteins were detected in the remaining lanes containing latter fractions from the NPC isolation protocol. *Lane assignments: 1* – sarcoplasmic reticulum (SR), *2* – nuclease digested nuclei, *3* – detergent extraction (supernatant), *4* – detergent extracted nuclei, *5* – first salt wash (supernatant), *6* – enriched NPC/lamina fraction. CS – colored protein standard. Numbers to the left indicate molecular mass markers.

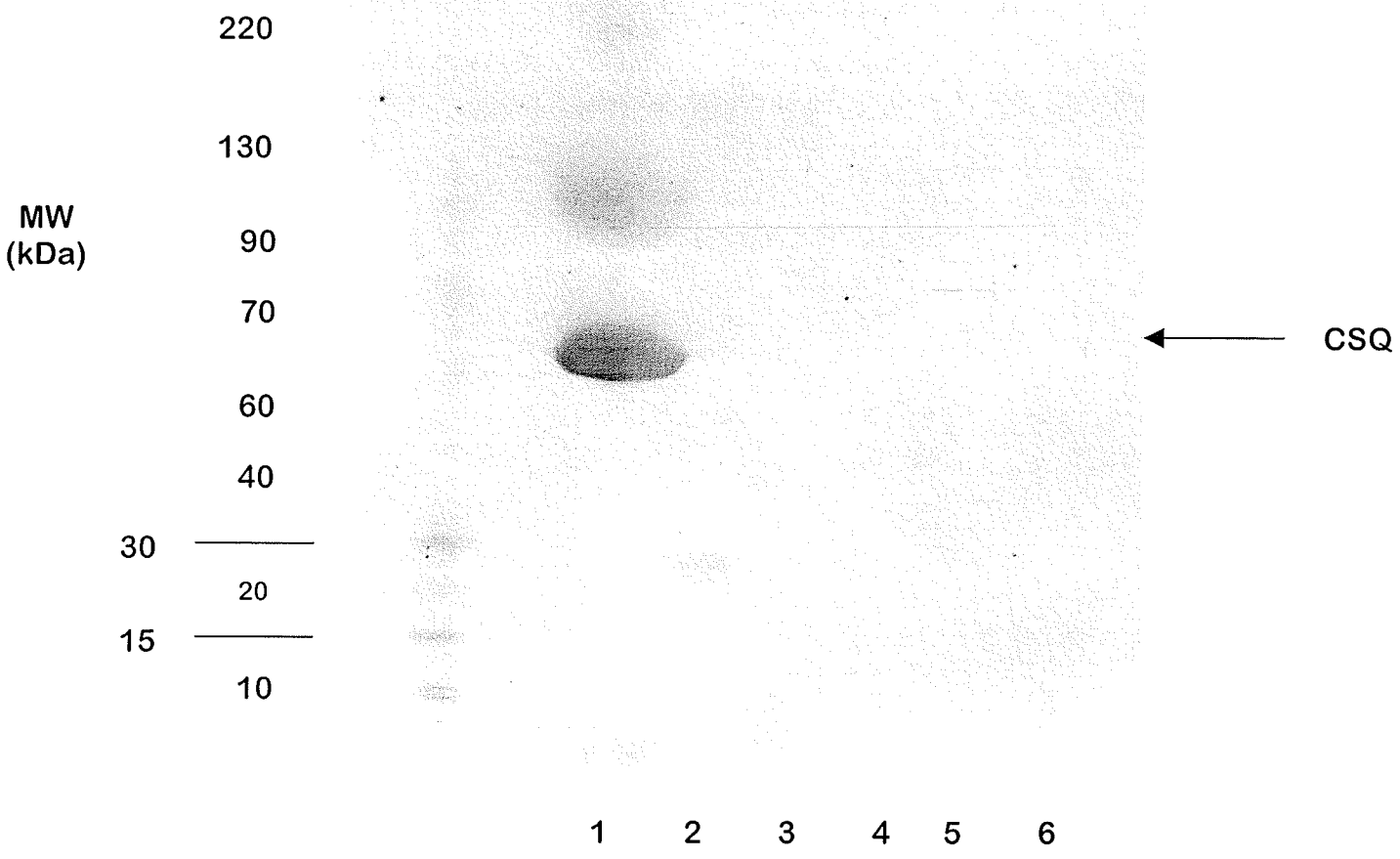

Figure 22. Calcium overlay

To determine the presence of calcium binding proteins, a radioactive calcium overlay was used. The SR fraction exhibits a strong signal due to calcium binding activity of the SERCA pump. A slight signal is detected in the initial wash fraction from the isolation procedure and no signal is seen in the final, enriched fraction. *Lane assignments: 1* – sarcoplasmic reticulum (SR), *2* – nuclease digested nuclei, *3* – detergent extraction (supernatant), *4* – detergent extracted nuclei, *5* – first salt wash (supernatant), *6* – enriched NPC/lamina fraction. CS – colored protein standard, CSQ – calsequestrin. Numbers to the left indicate molecular mass markers.

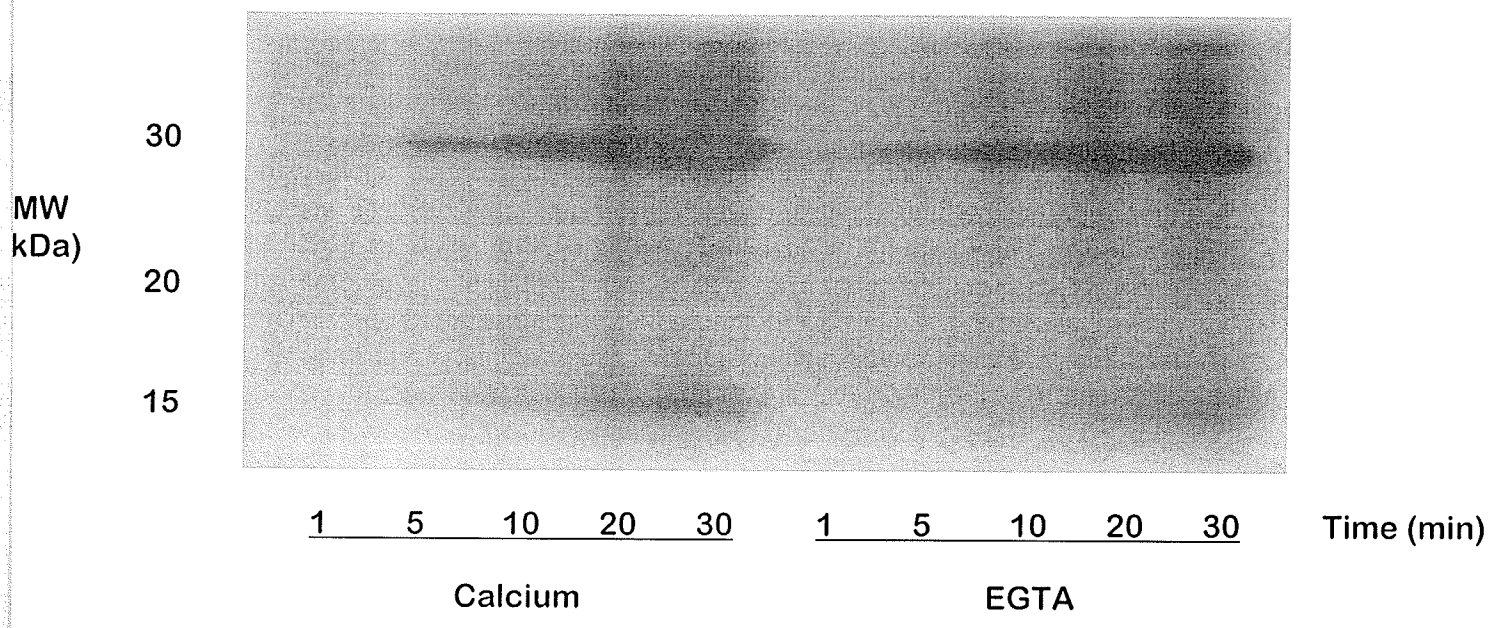

Figure 23. Endogenous phosphorylation of NPC fraction

The purified NPC fraction was incubated in kinase reaction buffer for different times before stopping with 2% SDS in the presence or absence of 5mM calcium. Endogenous phosphorylation of a 30kDa protein within the purified NPC fraction does not show any calcium dependency. Incubation of the reaction mixture in the presence of 5 mM EGTA, a chelating agent, does not show any attenuation in phosphorylation after 30 minutes.

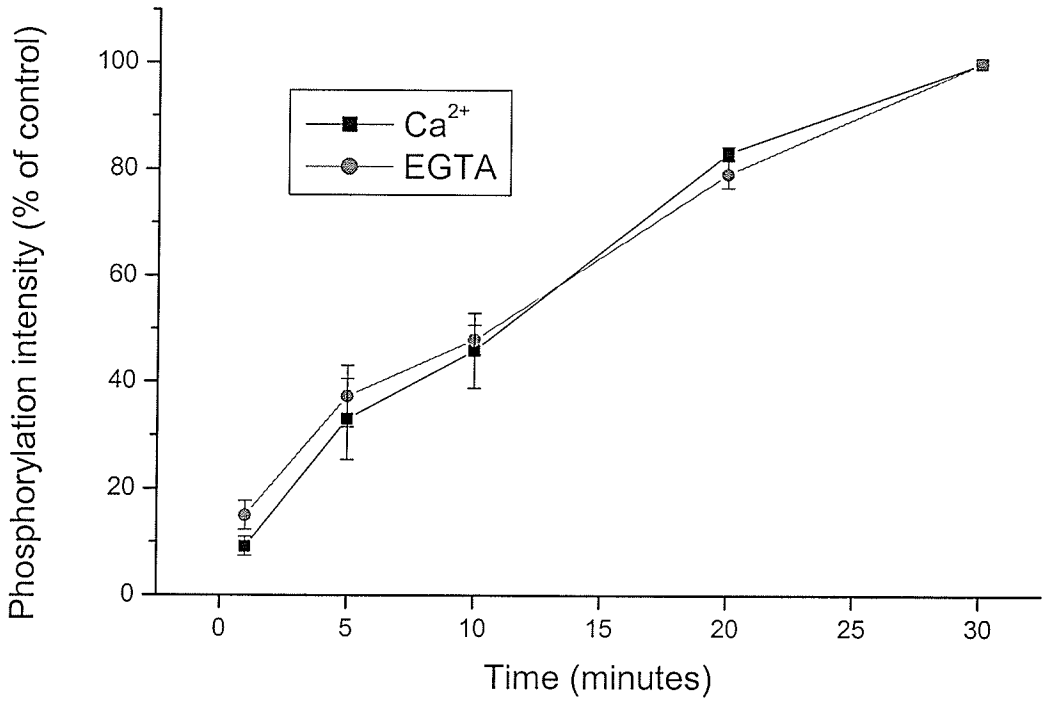

Figure 24. The NPC phosphoprotein is not modified by calcium dependent kinases

Graphical analysis of phosphorylation intensity demonstrates no significant difference in phosphorylation profile of a 30 kDa protein in the presence of 5 mM calcium or 5 mM EGTA. Densitometric analysis of protein after 30 min of phosphorylation was taken to be control.

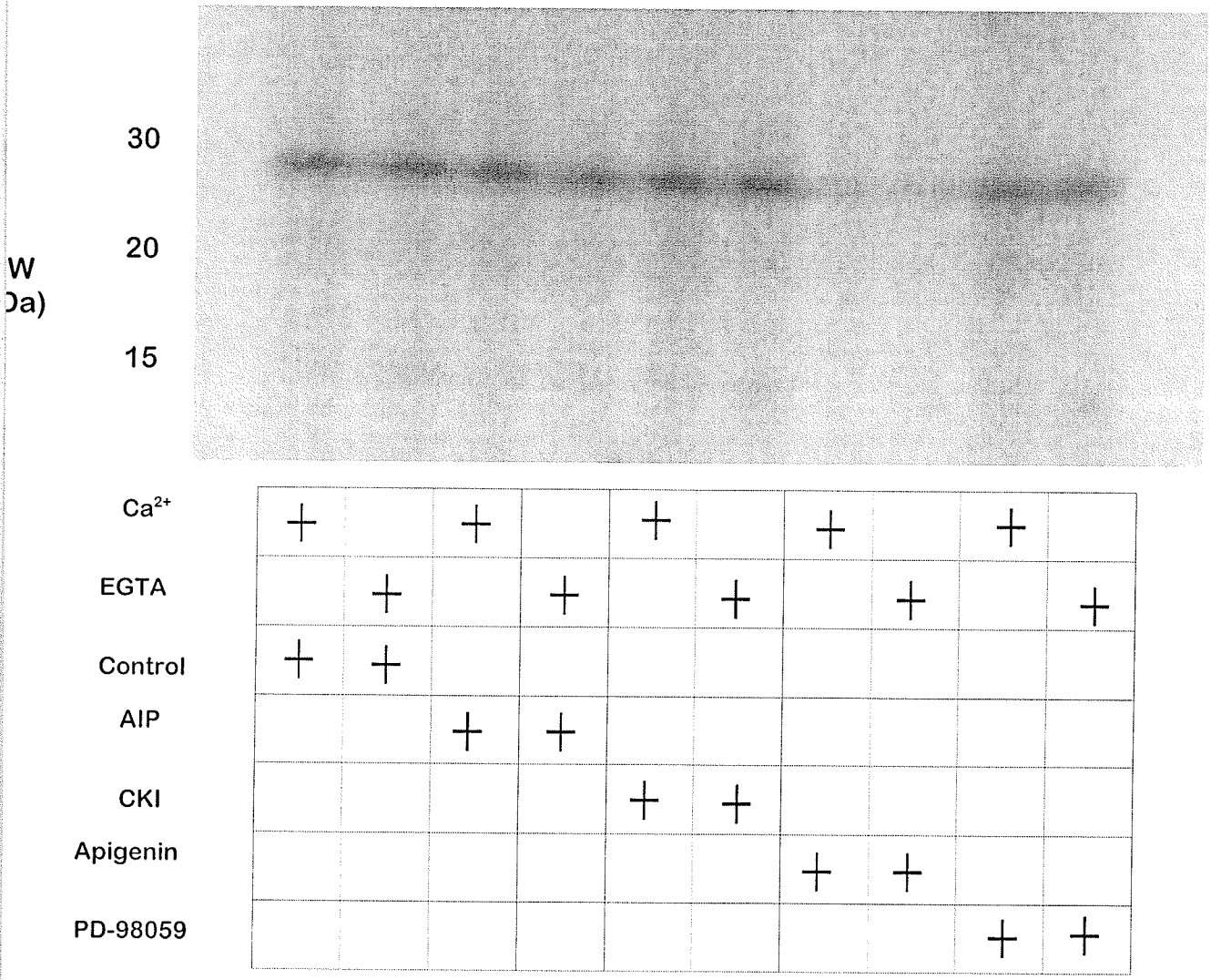

Figure 25. Pharmacological inhibition of endogenous phosphorylation

Various pharmacological antagonists were incubated with the final, purified NPC fraction in the presence and absence of EGTA. Endogenous phosphorylation of a protein within the NPC fraction was significantly inhibited by apigenin, a broad range MAP kinase inhibitor. Controls contained no inhibitor and consisted solely of purified NPCs. Inhibitors used – autocamtide-2 related inhibitory peptide (AIP)(30 nM) ; CaM kinase peptide inhibitor (CKI)(40 μM), apigenin (50 μM), PD-98059 (40 μM)

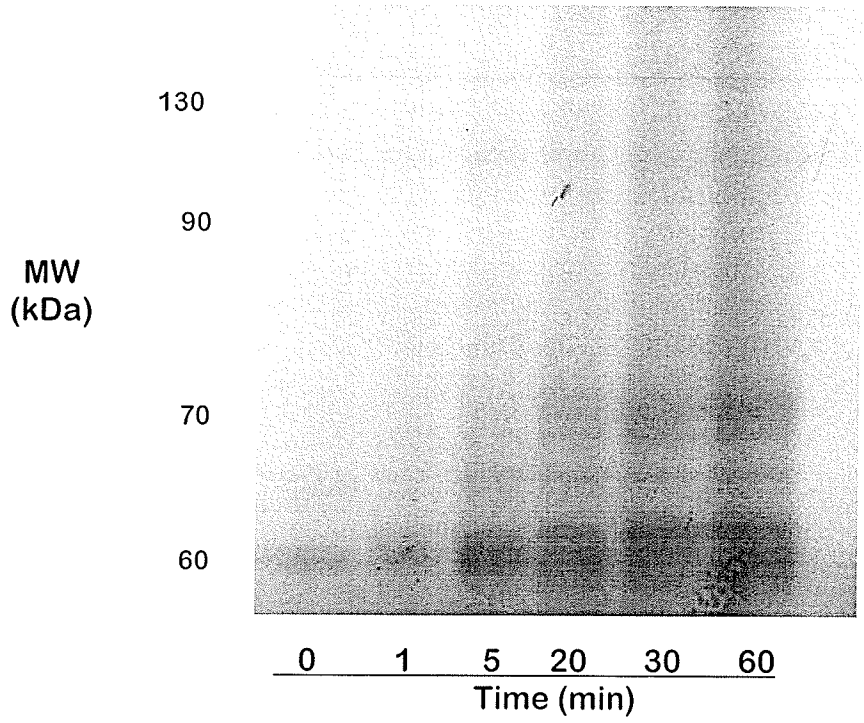

Figure 26. Exogenous CaM kinase phosphorylates proteins within the NPC fraction

A substrate for exogenously added CaM kinase was identified within the NPC fraction. Incubation of purified NPC fractions with exogenously added CaM kinase (1 μg/ml) demonstrates time-dependent phosphorylation of 60 kDa and 70 kDa proteins within the purified NPC.

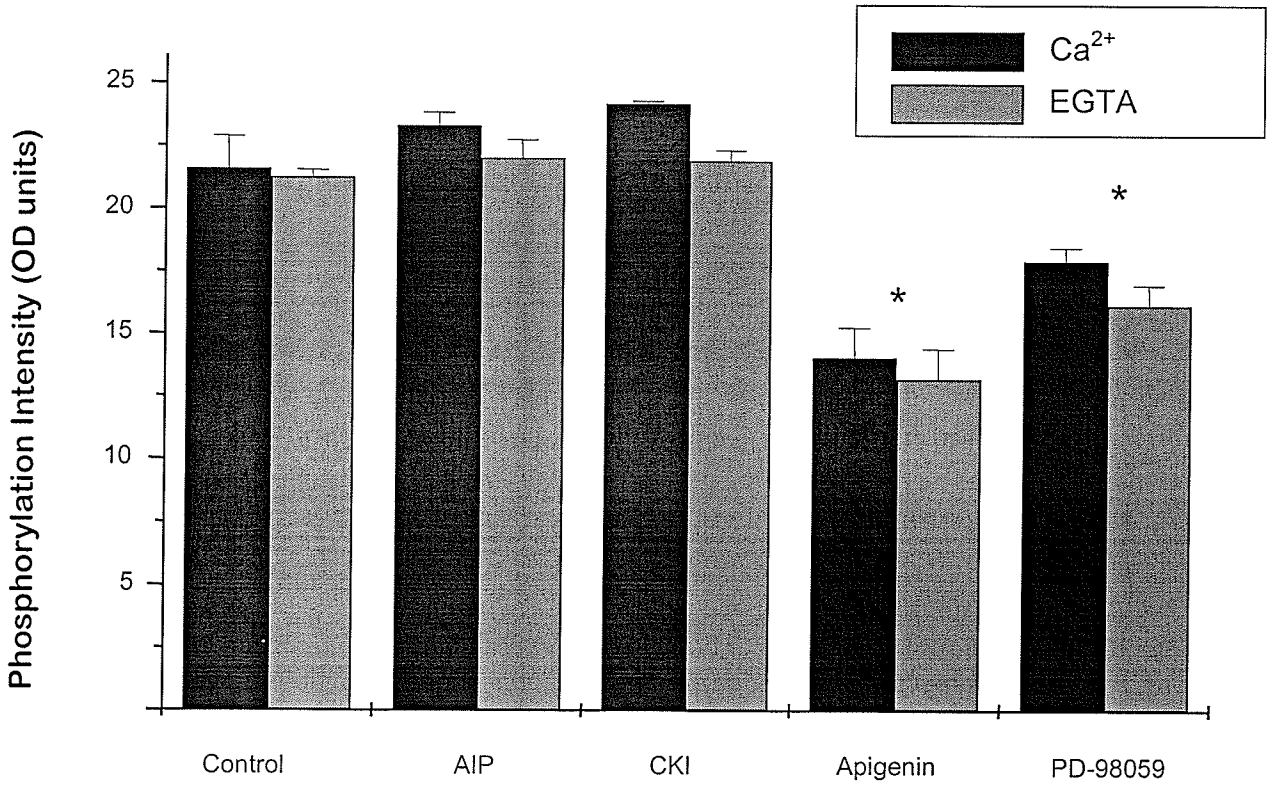

Figure 27. MAP kinase antagonists inhibit endogenous kinases within the NPC

Endogenous phosphorylation is significantly inhibited by apigenin and PD-98059. Apigenin is a broad range MAP kinase inhibitor that significantly attenuated the phosphorylation of a 30 kDa protein within the purified NPC fraction. Another inhibitor of the MAP kinase pathway was used to examine its effects on endogenous NPC phosphorylation. PD-98059 (PD) is a pharmacological antagonist of MEK, the activating kinase upstream of ERK-1/2. PD also inhibited endogenous kinase activity. Controls contained no inhibitor and consisted solely of purified NPCs. Inhibitors used – autocamtide-2 related inhibitory peptide (AIP)(30 nM) ; CaM kinase peptide inhibitor (CKI)(40 μM) , apigenin (50 μM), PD-98059 (40 μM). Data were reported as mean ± SEM. *$p<0.05$ vs. control, $n = 3$.

inhibitors were used to identify members of the MAP kinase family putatively involved in the endogenous phosphorylation of the NPC fraction. SB-202190, a potent and specific p38 MAP kinase inhibitor was selected. Both apigenin and SB-202190 inhibited the phosphorylation of a 30 kDa protein in a dose-dependent manner (Figures 28, 29).

If endogenous phosphorylation occurs in a MAP kinase-dependent fashion, Western blotting should reveal the presence of MAP kinases in the isolated NPC fraction. Nuclear pore complex fractions were analyzed by sending samples to Kinexus, a company that specializes in screening for phosphoproteins. Their proprietary screening process revealed the presence of various kinases and phosphatases in addition to a large variety of unclassified enzymes (Table 5). Consistent with our previous data, ERK, p38 and JNK p38 MAP kinases were present in the purified NPC fraction (Figures 27-29).

Phosphorylation and nuclear protein import

MAP kinase phosphosubstrates within the nuclear pore complex that were endogenously phosphorylated by MAP kinases should also be phosphorylated by exogenously added enzyme. The phosphorylation assay was carried out in the presence of exogenous ERK, p38 and JNK. Prior to adding the exogenous enzymes, the nuclear pore complex fractions were immunodepleted of lamins A/C and B1. These proteins are phosphosubstrates (348-350) that co-purify with nucleoporins (342) and could potentially mask the presence of phosphoproteins within the NPC. Additionally, the enzymes used were capable of autophosphorylation, so one lane contained enzyme and radioactive ATP to serve as control. We observed that there were non-lamin proteins phosphorylated by exogenously added MAP kinases (Figure 30).

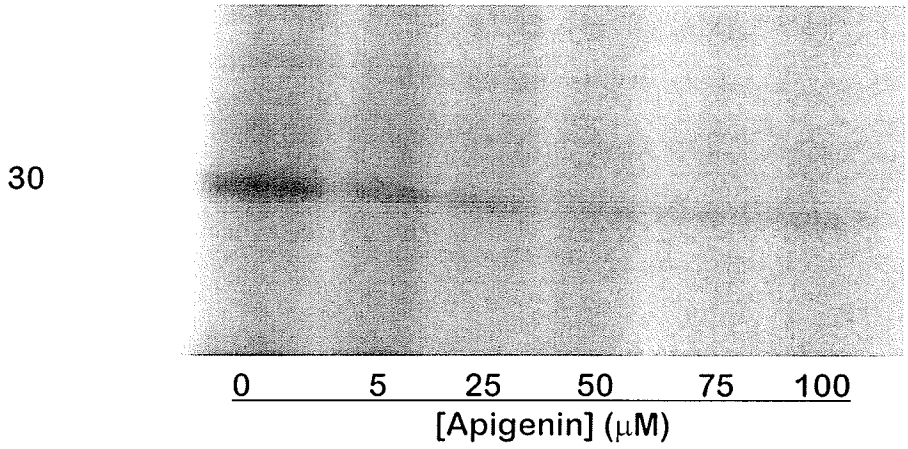

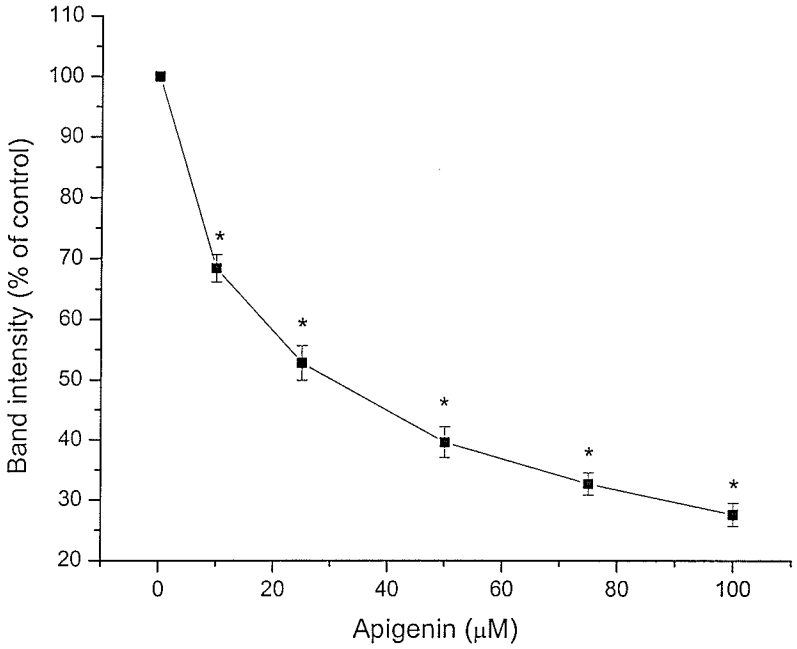

Figure 28. Dose dependent inhibition of endogenous NPC phosphorylation by apigenin

Above: The 30 kDa protein within the NPC fraction was inhibited in a concentration dependent manner using increasing amounts of apigenin. Molecular weight is given on the side in kDa. *Below:* Graphical analysis reveals potent inhibition of endogenous kinase activity with increasing doses. Data were reported as mean ± SEM. *$p<0.05$ vs. control, $n = 3$. Controls were taken to be band intensity of the protein in the absence of apigenin.

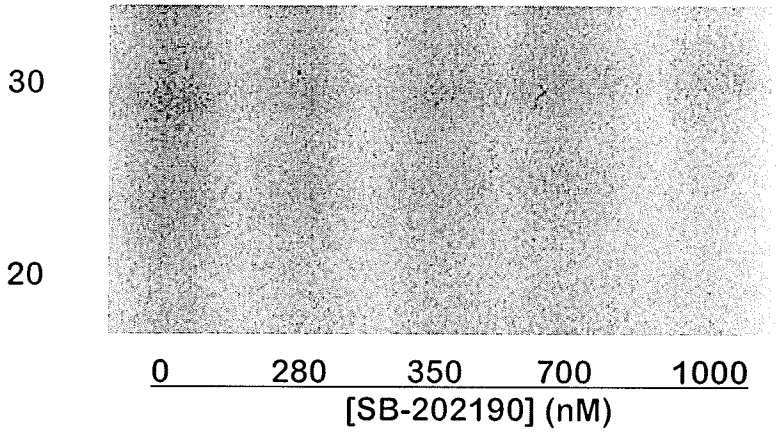

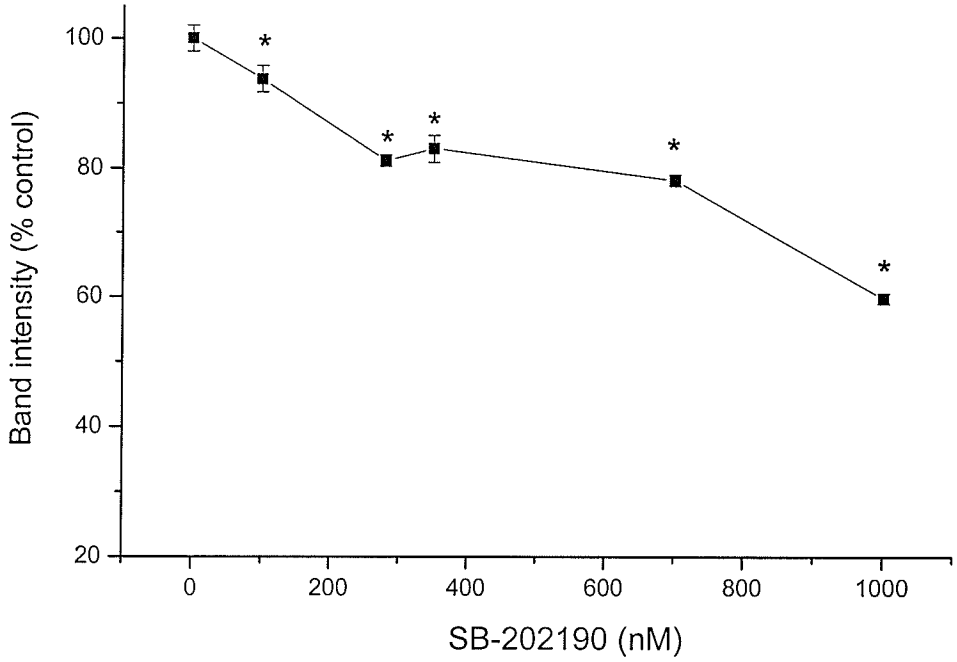

Figure 29. Dose dependent inhibition of endogenous NPC phosphorylation by SB-202190.

Above: SB-202190 is a specific inhibitor for p38 MAP kinase. Incubation of the phosphorylation reaction mixture with this inhibitor also attenuated the endogenous phosphorylation of the 30 kDa band in the NPC fraction, although to not as great an extent as apigenin. Molecular weight is given on the side as kDa. *Below:* Data were reported as mean ± SEM. *$p<0.05$ vs. control, $n = 3$. Controls were taken to be phosphorylation intensity of the protein in the absence of SB-202190.

Kinases	Phosphatases
ERK	PP1 (α, β, and γ isoforms)
p38	PP5
JNK	MAPK phosphatase 1
ZIP	PP2A (A subunit)
Cdk 7	PP2X (catalytic subunit)
PKC (ε and ζ isoforms)	

Table 5. Kinases and phosphatases identified in the purified NPC fraction

Several kinases and phosphatases were consistently present in the purified NPC fraction. The MAP kinases ERK, p38 and JNK were identified in the fraction. No CaM kinases or calcium dependent phosphatases were found.

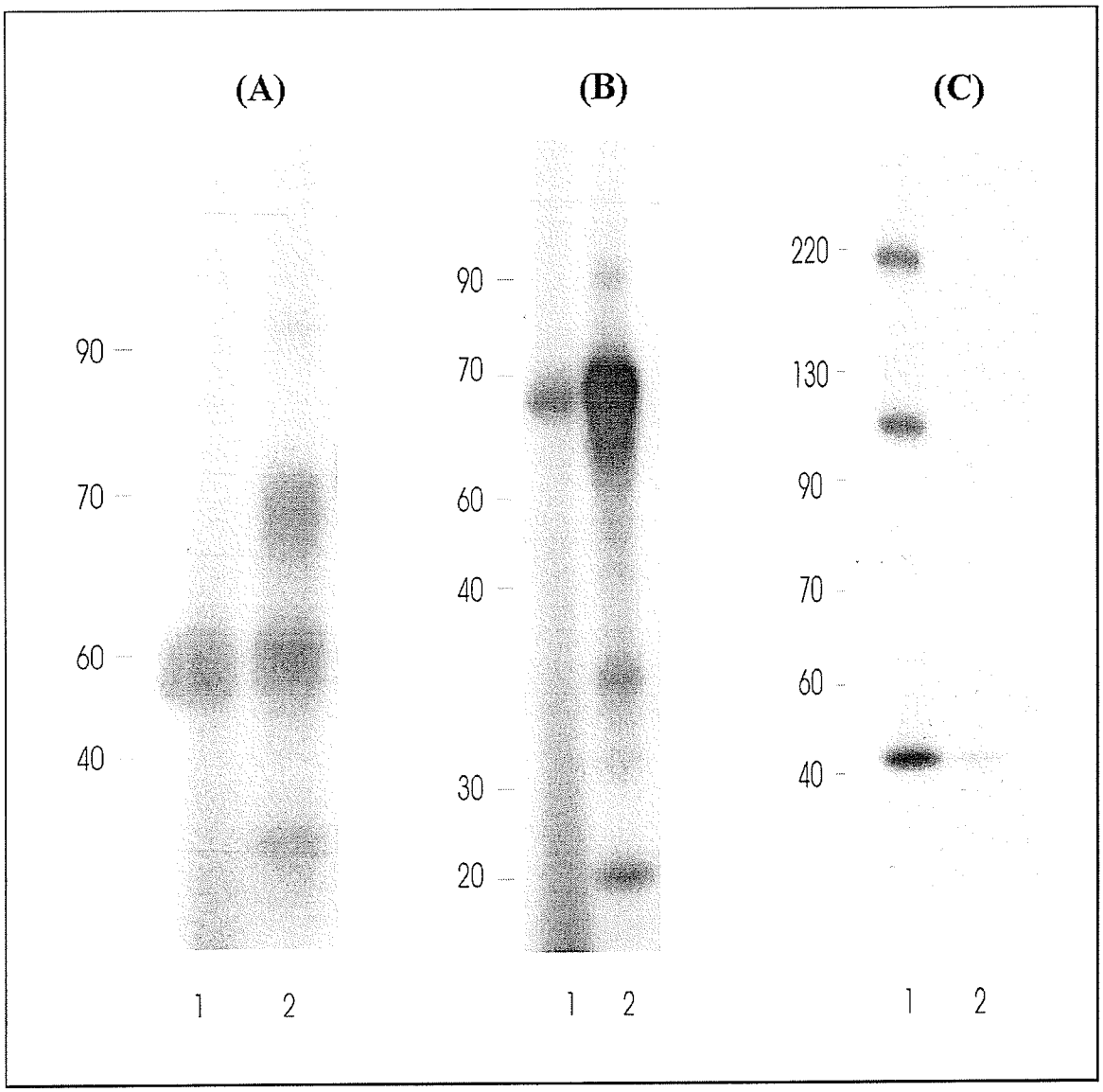

Figure 30. Phosphorylation of NPC fraction proteins by exogenous MAP kinases

Exogenous MAP kinases were added to purified, lamin-depleted NPC fractions. For each sample, another lane containing only exogenous kinase was run to distinguish autophosphorylated enzyme from nuclear pore phosphosubstrates. Molecular weight in kDa is listed to the left of each figure. (A) JNK phosphorylates proteins of 35 kDa and 90 kDa. JNK also specifically phosphorylates a 70 kDa protein within the final fraction. *Lane 1* – autophosphorylated JNK, *lane 2* – JNK + NPC fraction. (B) p38 also phosphorylates proteins of 35 kDa and 90 kDa. Additionally, a specific substrate for p38 MAP kinase migrated at 20 kDa. *Lane 1* – autphosphorylated p38-GST (recombinant GST tagged kinase), *lane 2* – p38-GST + NPC fraction. (C) ERK-2 phosphorylated proteins at 110 kDa and 220 kDa. *Lane 1* – ERK-2 + NPC fraction, *lane 2* – autophosphorylated ERK-2.

Immunocytochemistry of cultured smooth muscle cells demonstrated nuclear localization of activated ERK-2 and p38 in proliferating cells (Figure 31). Staining with anti-phosphoserine and anti-phosphothreonine showed a constitutive nuclear and quiescence-dependent localization, respectively (Figure 32). Nucleoporin phosphorylation was hypothesized to affect nuclear import, so the permeabilized cell assay was used to assess rates of nuclear import in proliferating cultured vascular smooth muscle cells after pre-treatment with MAP kinases. In this assay, the permeabilized cell or exogenously added cytosol may be treated separately to investigate effects at the nucleus or within the cytosol, respectively (Figure 33). After treating permeabilized cells with exogenous MAP kinase, no changes in the rate of nuclear import was observed (Table 6 & Figure 33A - 33C). The same MAP kinases were then pre-incubated with cytosol to determine the effects of phosphorylation on the soluble components of the nuclear transport machinery. A significant increase in the rate of nuclear import was induced by 1 μg/ml ERK (Figure 34D – 34F). Augmented rates of nuclear import were observed as early as 15 min and were sustained for 1 hr (Figure 35).

Previous work in our laboratory (341) demonstrated that the incubation of 0.04 μg/ml of exogenous ERK-2 kinase with the cytosol resulted in a significant decrease in the rate of nuclear protein import. These results are in contrast to the stimulatory effects presently observed. To address this discrepancy, the effects of ERK-2 were examined as a function of its concentration. Lower concentrations of ERK-2 inhibited import but higher concentrations significantly stimulated import. Intermediate concentrations induced intermediate effects (Figure 36). To insure that these observations had physiological significance, we microinjected VSMCs with both high and low concentrations of ERK-2

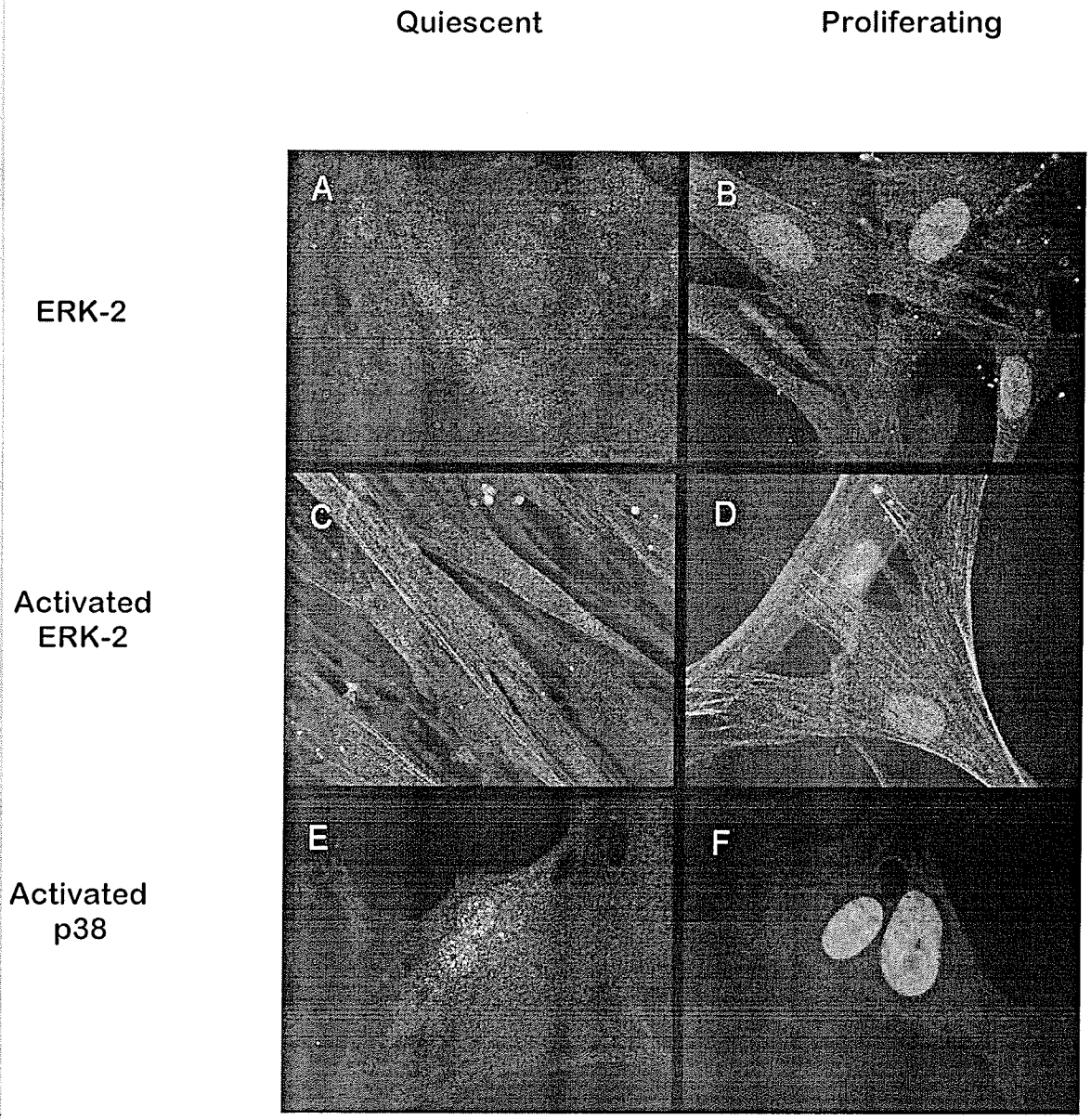

Figure 31. Immunolocalization of MAP kinases in quiescent and proliferating smooth muscle cells

Cultured smooth muscle cells were stained to visualize the distribution of MAP kinases within quiescent and proliferating smooth muscle cell. (A) Quiescent cells exhibited a diffuse, cytosolic localization of non-activated ERK-2 that was concentrated within the nucleus in proliferating cells (B). Activated ERK-2 demonstrated a distribution pattern reminiscent of actin staining in quiescent cells (C) and additionally stained the nucleus upon proliferation (D). Activated p38 showed diffuse cytosolic and speckled nuclear staining in quiescent cells (E) which became exclusively nuclear in proliferating cells (F).

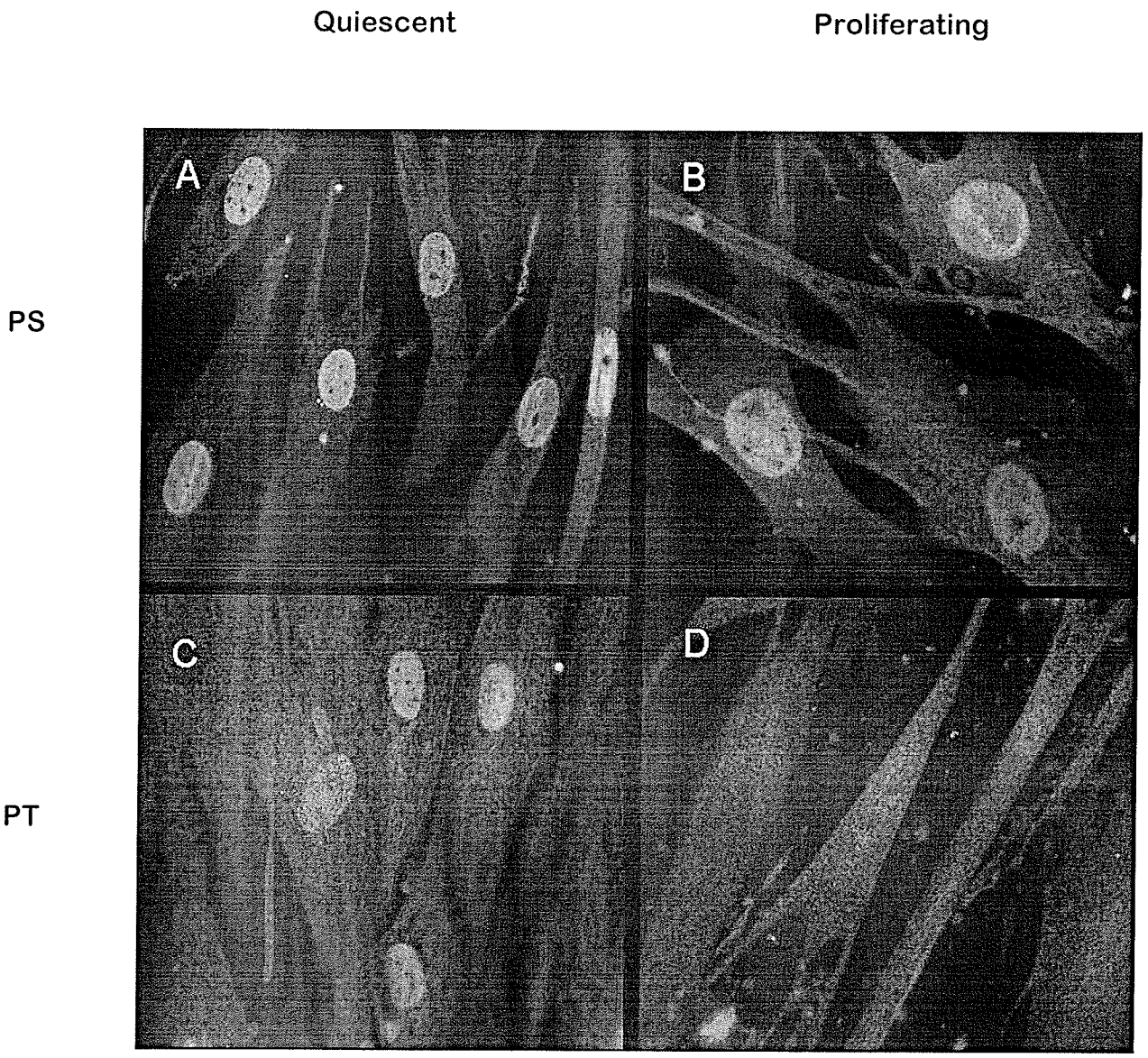

Figure 32. Phosphoproteins within smooth muscle cells

Smooth muscle cells were stained using antibodies against phosphoserine and phosphothreonine. (A) In quiescent cells, phosphoserine (PS) containing proteins were localized primarily to the nucleus with very faint cytosolic staining. (B) Proliferation causes a moderate increase in cytosolic distribution of phosphoserine, but still maintains a nuclear presence. (C) Quiescent cells stained for phosphothreonine (PT) shows diffuse cytosolic and nuclear staining as well, but (D) exhibits a complete loss of nuclear signal in proliferating cells.

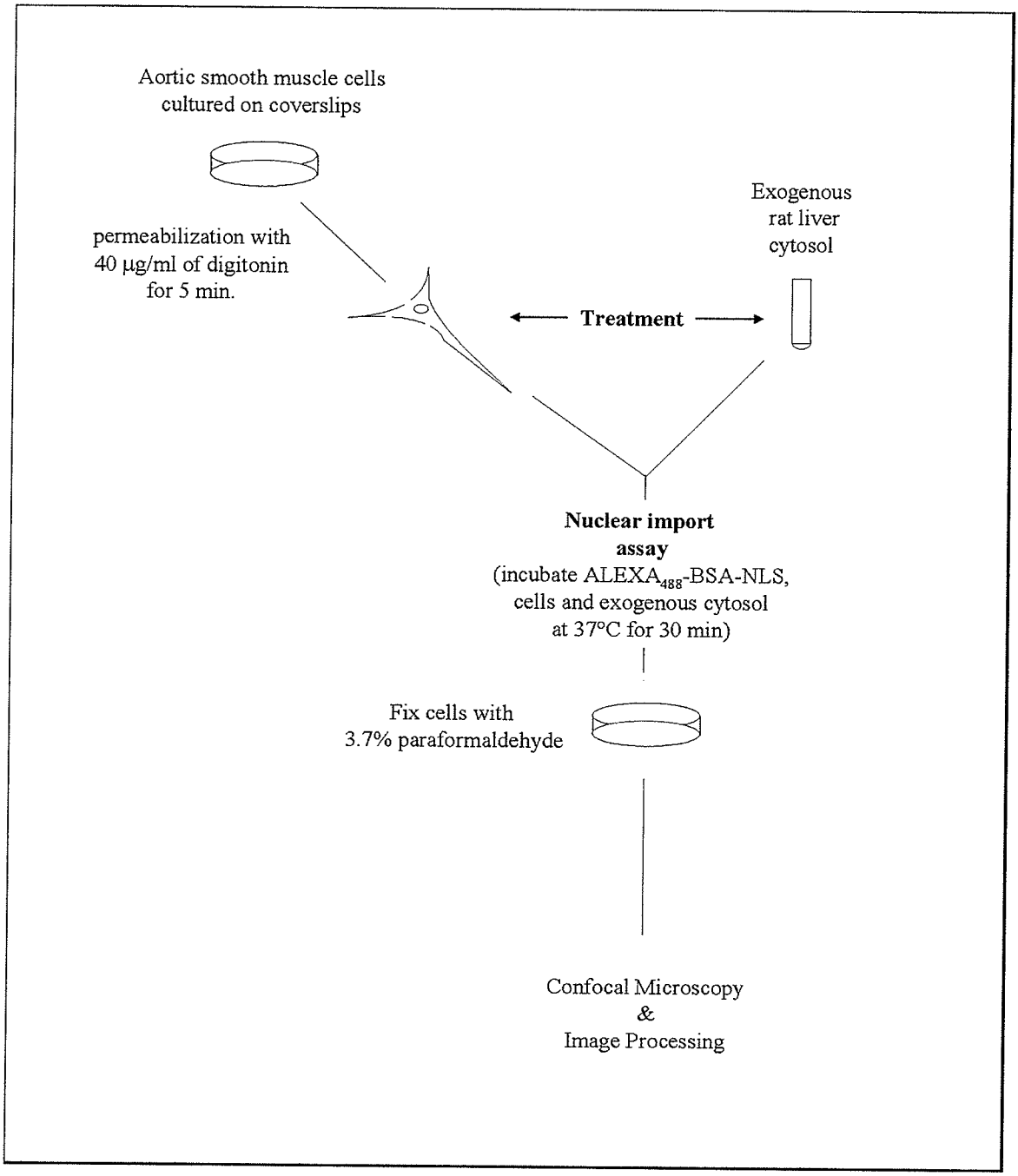

Figure 33. Nuclear import assay

Steps in the nuclear import assay illustrate how two different steps in the procedure allows an experimenter to test the permeabilized cell or the exogenously added cytosolic mix. Treatments can then be used to distinguish effects occurring at the nuclear envelope/membrane bound machinery or within the soluble fraction.

	Nuclear fluorescence (% control)		
Time (min)	**ERK-2**	**p38**	**JNK**
0	100 ± 1.6	100 ± 1.8	100 ± 1.3
15	92 ± 1.9	101.4 ± 1.9	101.4 ± 2.1
30	94.1 ± 2.3	100.6 ± 1.8	99.1 ± 1.8
60	99.9 ± 2.2	104.1 ± 2.6	97.1 ± 1.7

Table 6. Treatment of permeabilized cells with MAP kinase does not affect nuclear import

Permeabilized cells were pre-treated for different lengths of time over 60 min with 1 μg/ml of exogenous ERK-2, p38 and JNK. Visualization of nuclear fluorescence was reported as % of control, using untreated cells (0 min) as control. No significant changes in nuclear transport were observed over 60 min for any of the MAP kinases studied.

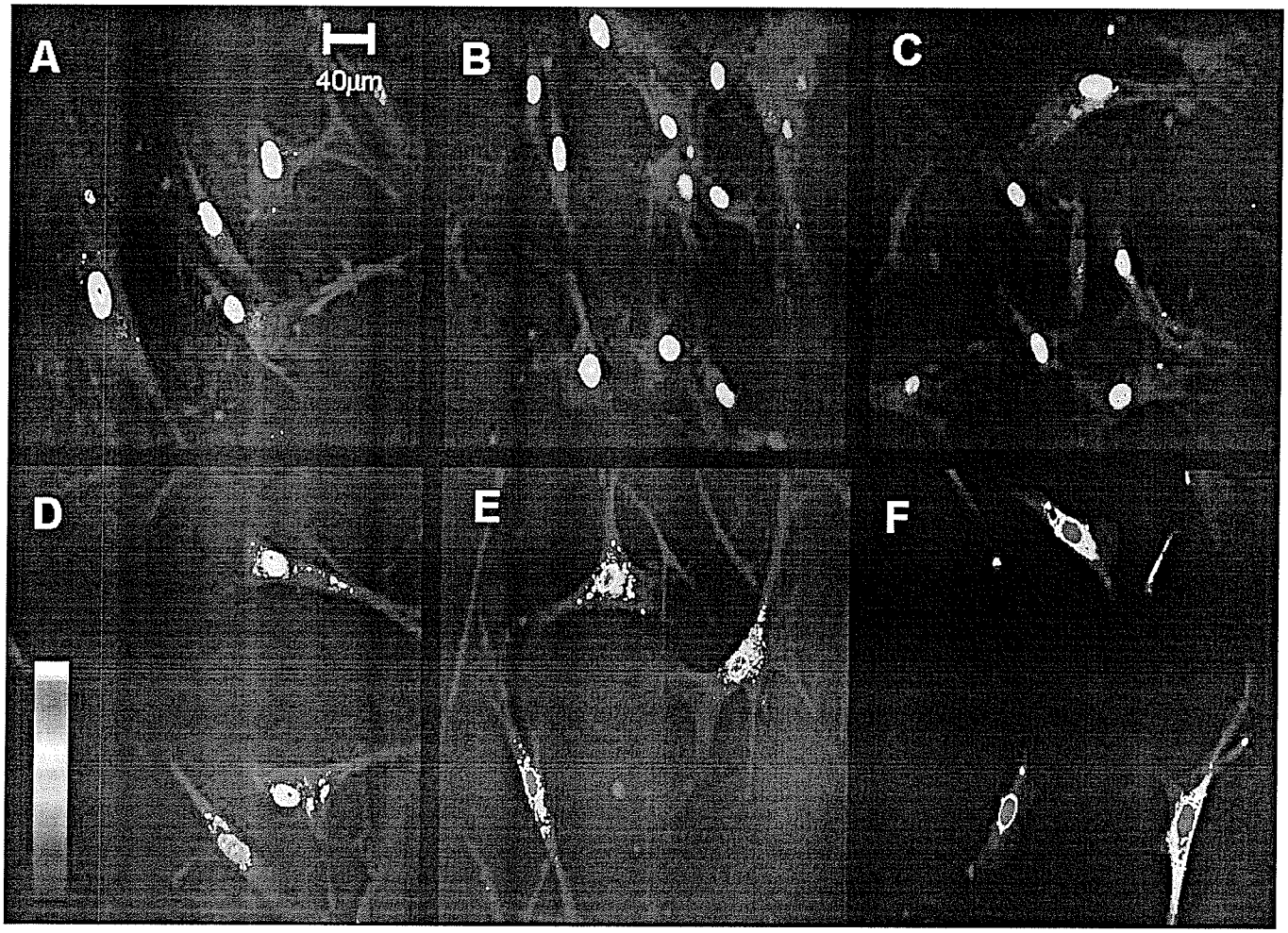

Figure 34. Exogenously treated cytosol increases nuclear import

Permeabilized vascular smooth muscle cells (A-C) were pre-treated with 1 µg/ml of exogenous MAP kinases (see Table 6) prior to use in the nuclear import assay and did not show any changes in the rate of nuclear import over 60 minutes. Representative figures using p38 treatment as an example are shown. (A) no pre-treatment, (B) 15 min, (C) 60 min. For experiments using treated import mix, (D-F) control cells in (D) exhibited a comparable level of import as seen in (A). Treatment of import mix containing 50% cytosol with exogenous MAP kinases, however, displayed a significant increase in nuclear import after 15 min (E) which was sustained after 60 min (F). D-F is representative of treatment with 1 µg/ml ERK-2. Color scale represents fluorescence intensity where blue indicates little to no fluorescence and red/white is indicative of high levels. Magnification: 40x (oil immersion)

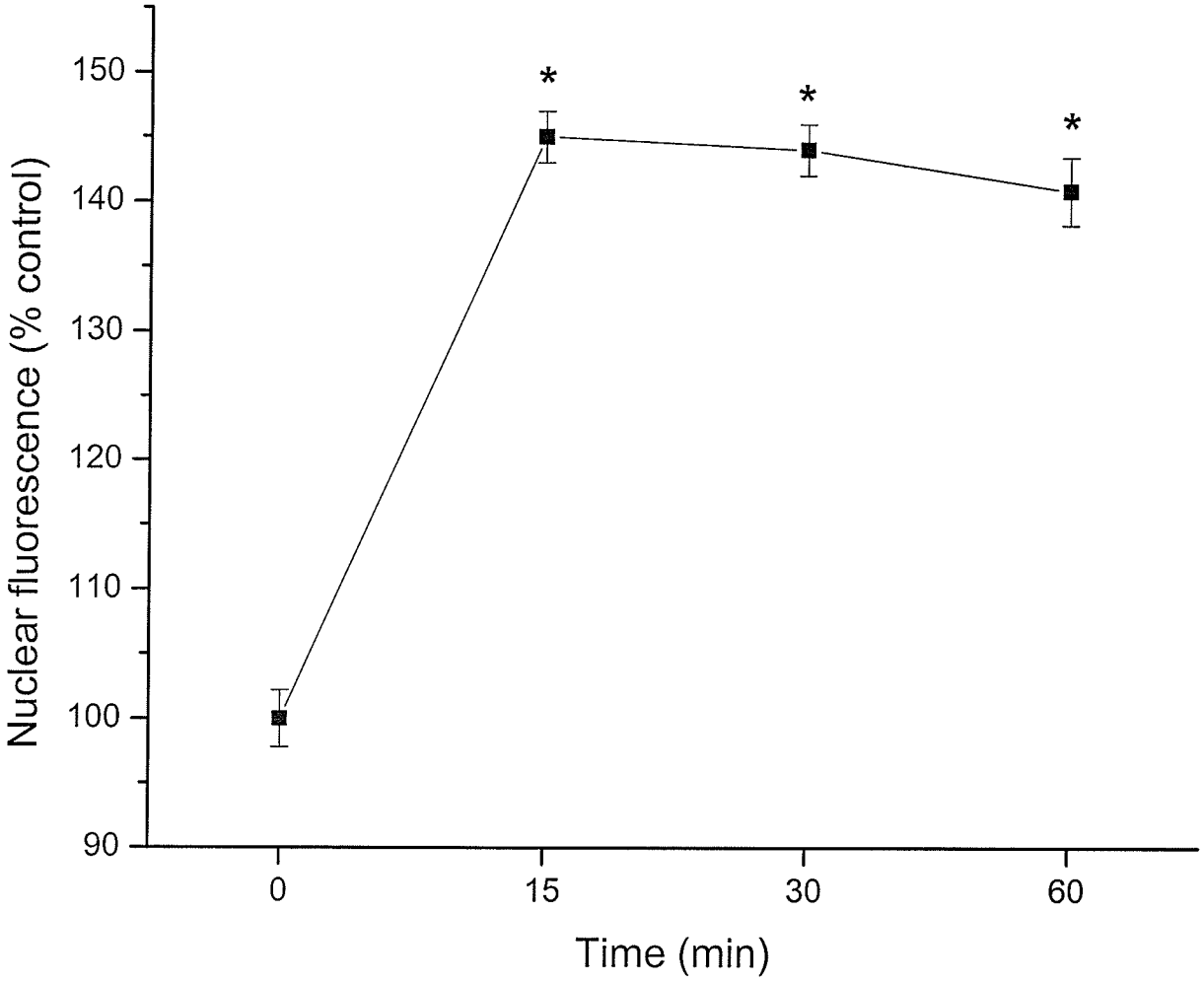

Figure 35. Nuclear import is significantly upregulated by ERK-2

Exogenously added cytosol was pre-treated for varying amounts of time with 1 μg/ml of activated ERK-2. A statistically relevant increase in nuclear import was observed at 15 min of pre-treatment which persisted for 60 min. Data were reported as mean ± SEM. *$p<0.05$ vs. control, $n = 3$.

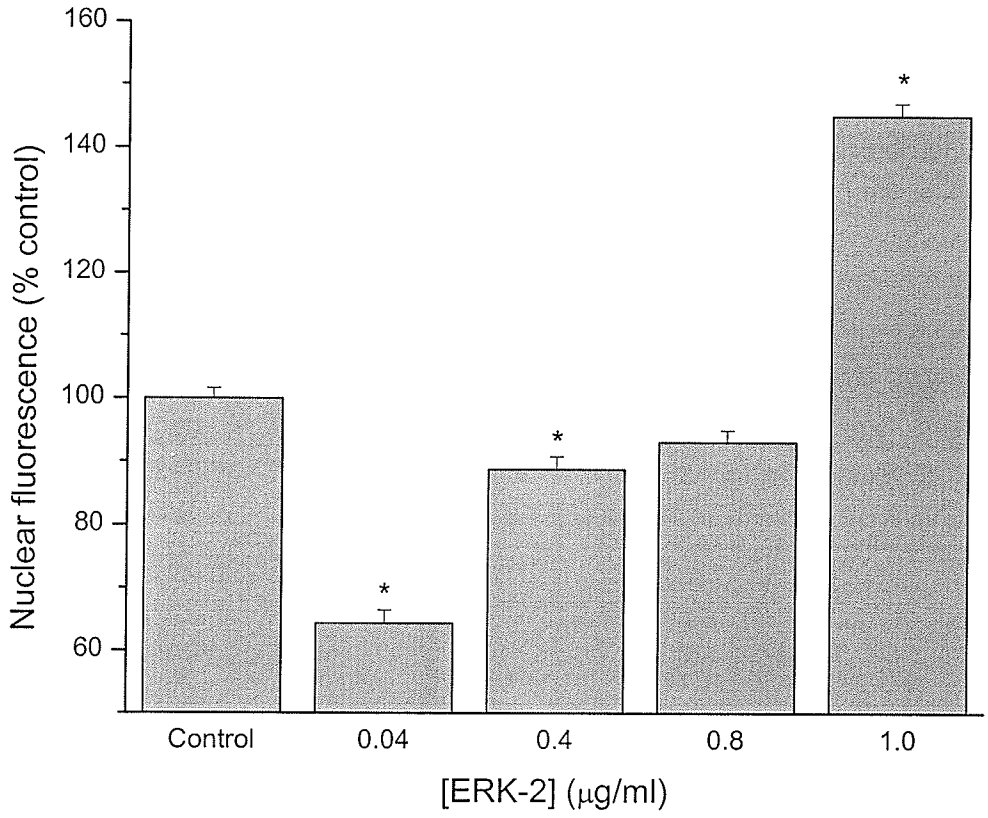

Figure 36. Dose dependent effects of ERK-2 on nuclear import

ERK-2 pre-treatment of import mix exhibits a dose-dependent effect on the rate of nuclear import. Pre-treatment time was held constant at 30 min and increasing doses of exogenous ERK-2 were used. Incubation with kinase buffer (vehicle) had no effect on nuclear import (not shown). Low concentrations (0.04 μg/ml) decreased the rate of nuclear import when compared to controls, while high concentrations (1.0 μg/ml) augmented nuclear import. Data were reported as mean ± SEM. *$p<0.05$ vs. control, $n = 3$.

to examine their effects *in situ*. Microinjection of vascular smooth muscle cells with 1 μg/ml of ERK-2 resulted in an increase in the rate of nuclear protein import over 30 min as compared to controls (Figure 37). Conversely, microinjection with 0.04μg/ml demonstrated a small decrease in the rate of nuclear protein import after 30 min.

It was important to determine if these effects induced by the ERK-2 MAP kinase were shared by other MAP kinase pathways. Exogenous cytosol was pre-treated for 30 min using 1 μg/ml (high) and 0.04 μg/ml (low) of exogenous p38, JNK or ERK-2. Vascular smooth muscle cells treated with high concentrations of these enzymes exhibited an augmented rate of nuclear protein import (Figure 38). Low concentrations caused a significant inhibition of nuclear protein import, similar to the inhibitory effects of MAP kinase activity on nuclear protein import observed previously (341).

The mechanisms mediating the effects of ERK-2 treatment were investigated. Since active ERK-2 changed its distribution in proliferating smooth muscle cells (Figure 31) smooth muscle cells were immunostained for several cytosolic transport proteins in order to determine changes in their localization under proliferating and quiescent conditions. CAS, NTF2 and Ran did not redistribute in proliferating or quiescent smooth muscle cells (Figures 39, 40). Anti-Rch1 recognizes importin-α and demonstrated slightly less cytosolic staining in quiescent cells (Figure 39). RanGAP was distributed to the nuclear envelope and diffusely within the cytosol (Figure 40) under proliferating conditions. Quiescence induced a nuclear relocalization of the protein (Figure 40).

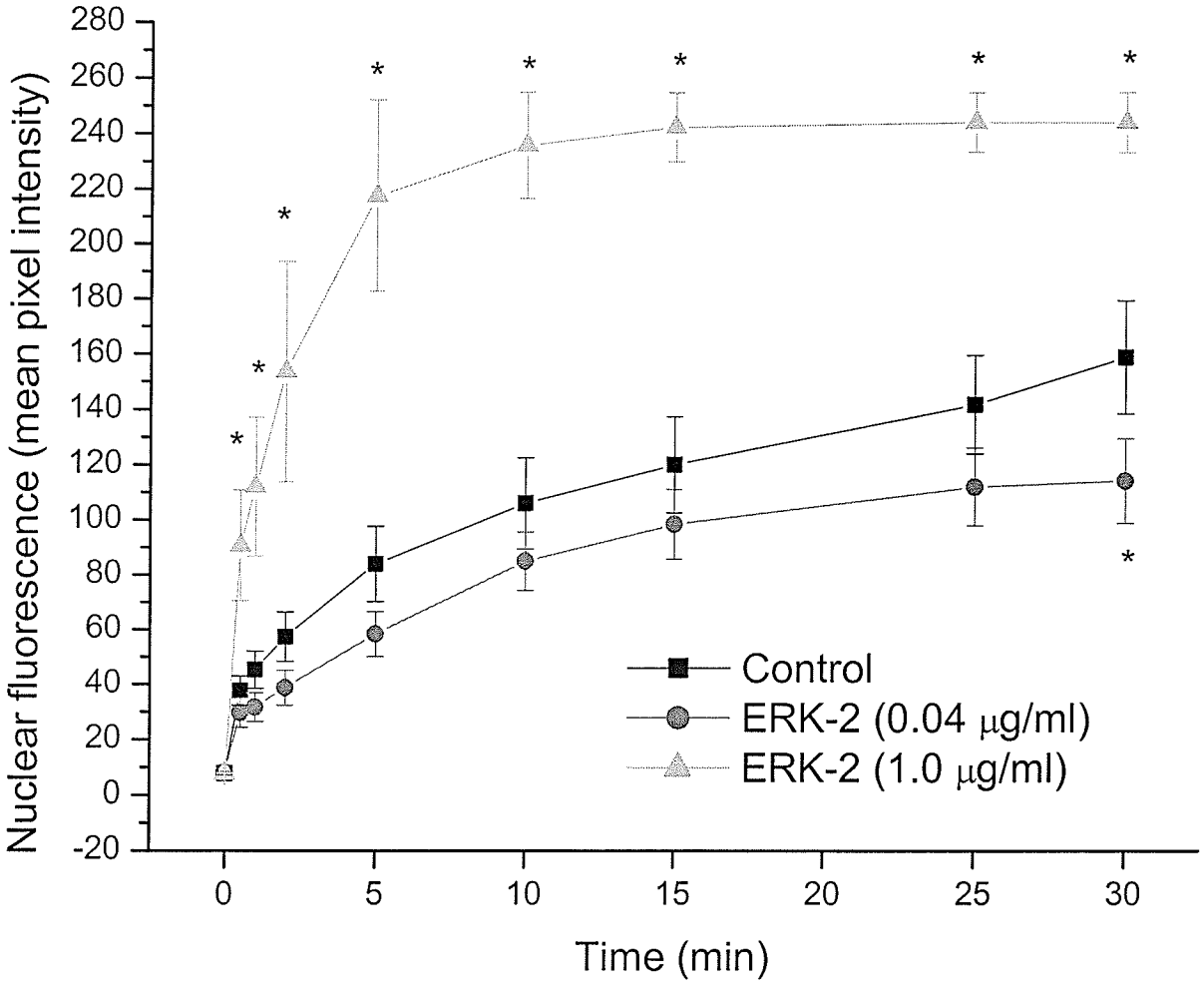

Figure 37. Microinjection of VSMCs with high and low concentrations of ERK-2

Vascular smooth muscle cells were microinjected with high and low concentrations of ERK-2 and the rate of nuclear import was observed for 30 min. Microinjection is a way of observing treatments in a more physiologically relevant context than the permeabilized cell system. Similar to the results observed with permeabilized cells, high concentrations of ERK-2 increased the rate of nuclear import above basal levels, while low concentrations inhibited nuclear protein import. Data were reported as mean ± SEM. *$p<0.05$ vs. control, $n = 3$.

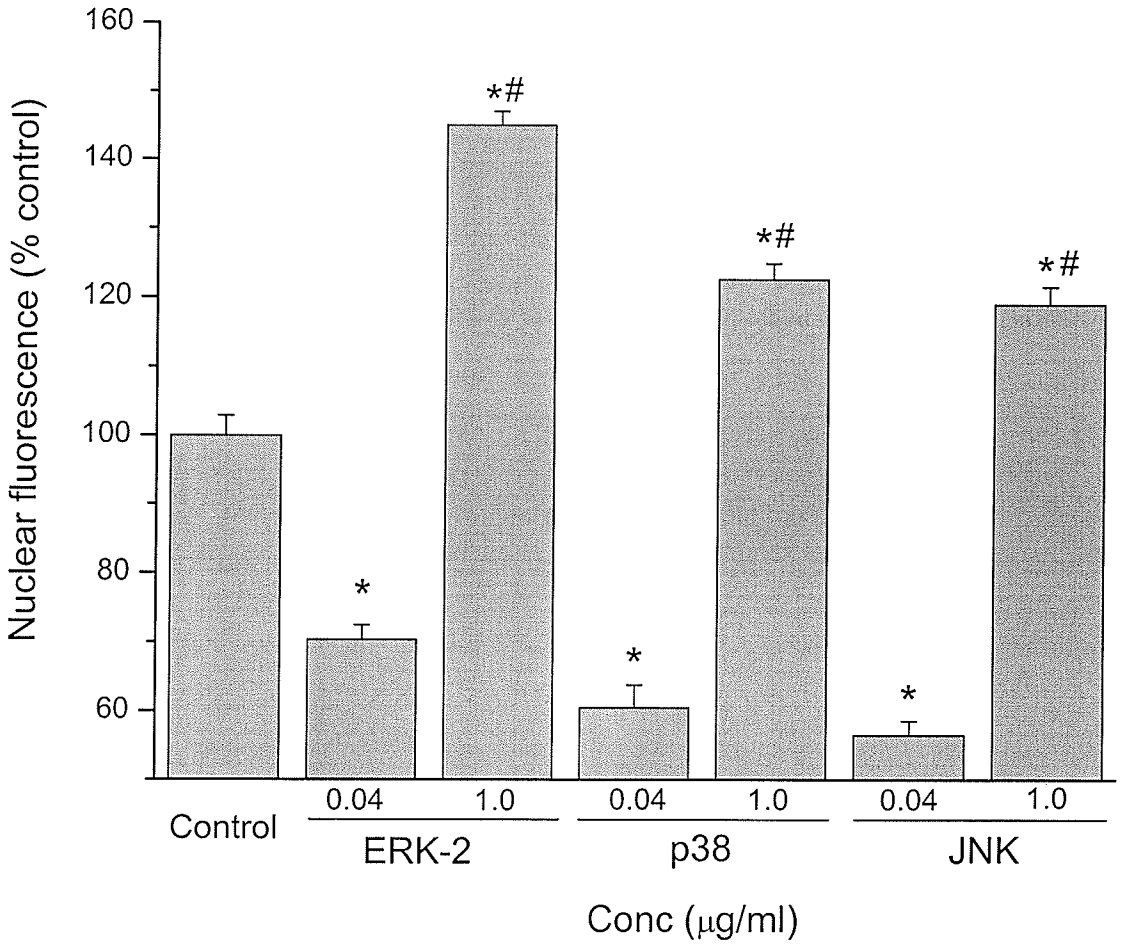

Figure 38. High and low concentrations of MAP kinases have differential effects on nuclear import

The dose dependent effects of other MAP kinases were tested on permeabilized smooth muscle cells. Similar to ERK-2, p38 and JNK displayed concentration dependent inhibition and augmentation of nuclear import.Data were reported as mean ± SEM. *$p<0.05$ vs. control, n = 3, #$p<0.05$ vs. low (0.04 μg/ml).

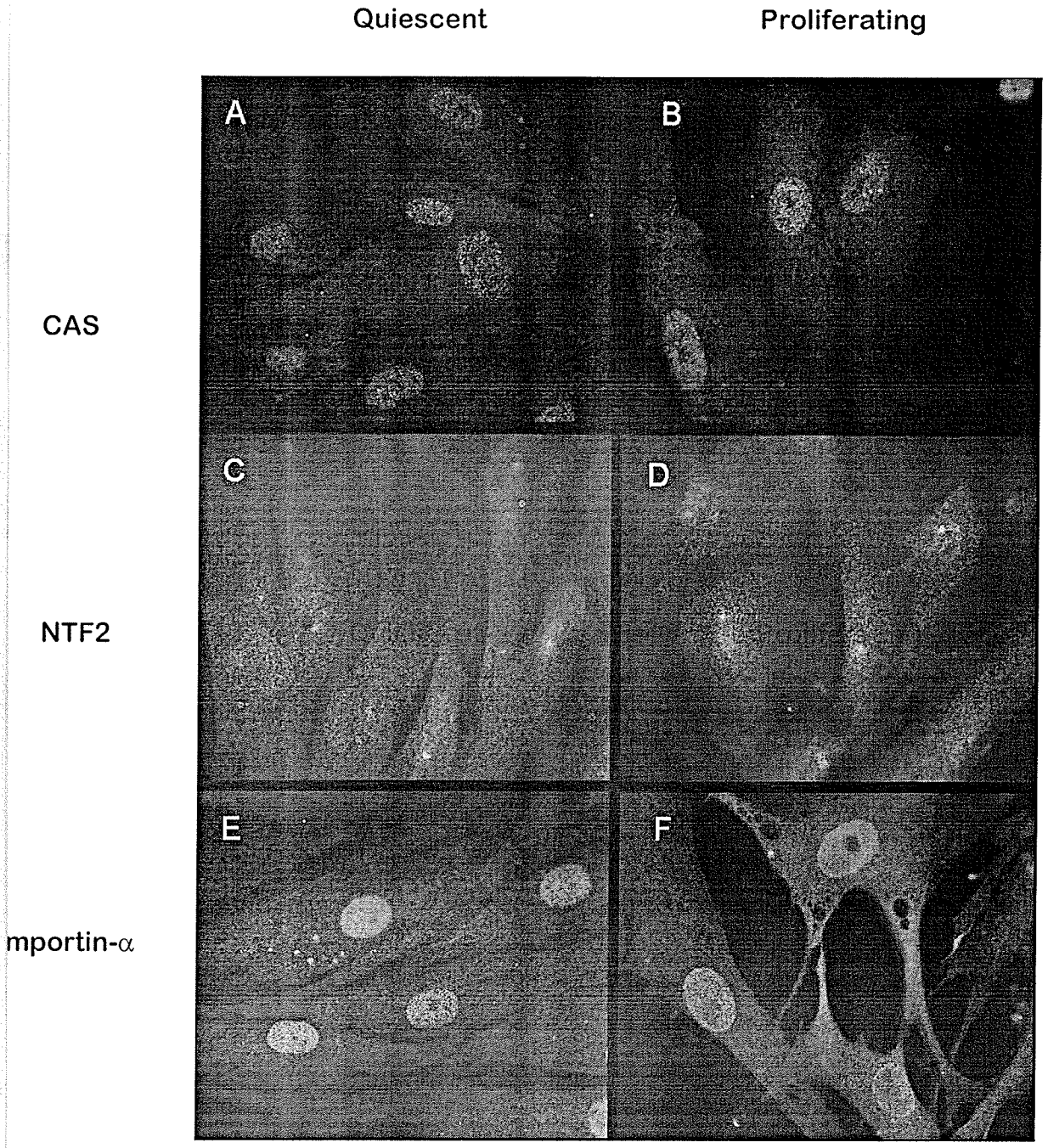

Figure 39. Localization of nuclear transport factors within quiescent and proliferating VSMCs

The distribution of nuclear transport factors were analyzed in quiescent and proliferating vascular smooth muscle cells. CAS displayed slightly more nuclear staining in proliferative cells compared to quiescent cells (A, B). NTF2 (C, D) and importin-α (E, F) did not show any redistribution associated with changes in metabolic activity. Magnification: 63x (oil immersion objective)

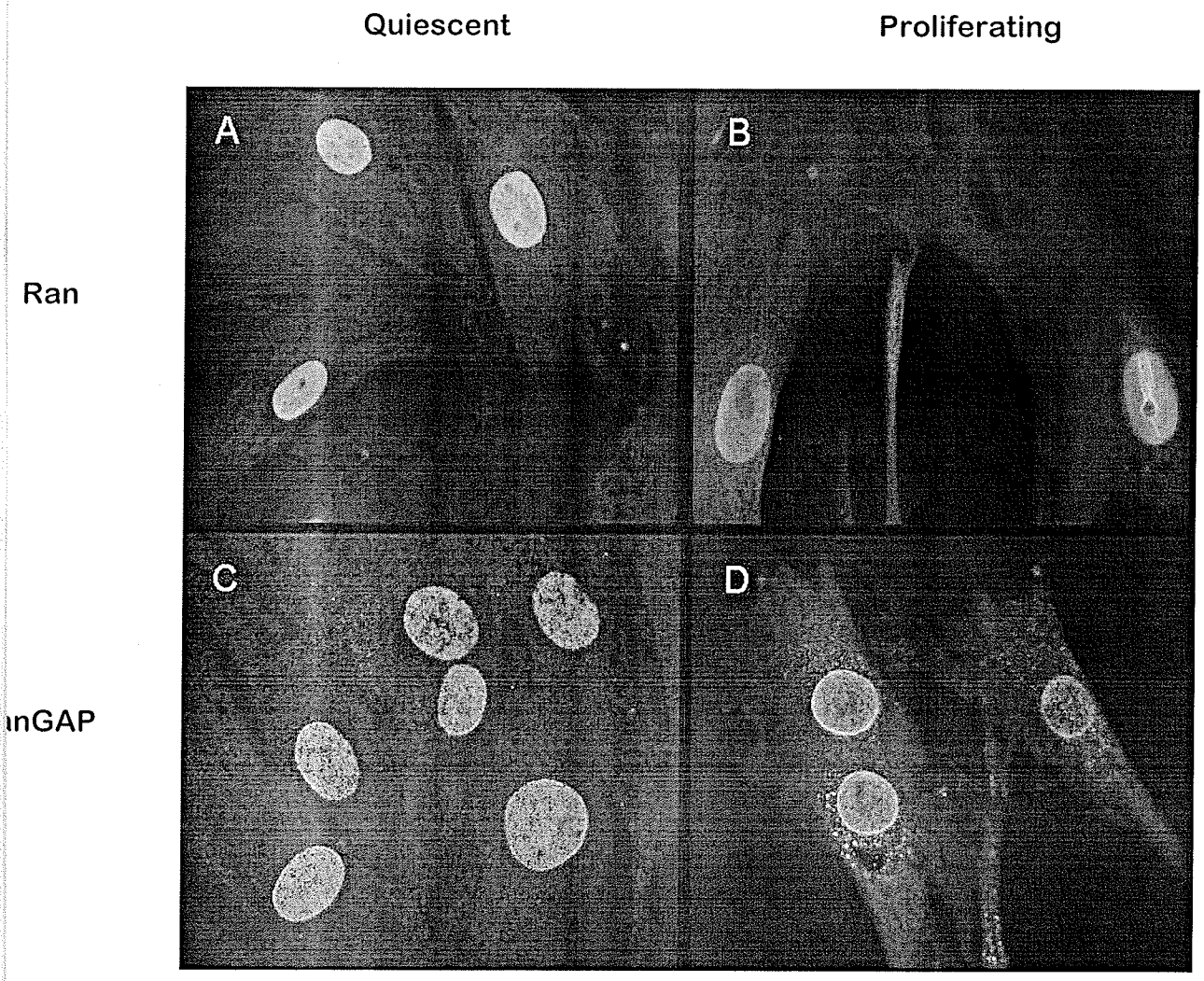

Figure 40. RanGAP shows a change in distribution in proliferating smooth muscle cells

Ran is localized to the nucleus in both quiescent and proliferating cells (A, B). RanGAP is also primarily nuclear in quiescent cells (C), but exhibits a predominant nuclear rim staining as well as diffuse cytosolic staining in proliferating vascular smooth muscle cells.

Potential cytosolic targets for the effects of the MAP kinases on nuclear protein import were studied. Phosphorylation of a >90 kDa protein in the cytosol by 1 μg/ml of exogenously added ERK-2 was observed (Figure 41). Western blotting of the cytosol revealed the presence of RanGAP (Figure 42), an essential molecule involved in nuclear protein import that migrates at >90 kDa. The >90 kDa protein that we observed being phosphorylated by ERK-2 was thought to be RanGAP, so ERK-2 was hypothesized to potentially mediate its effects on nuclear protein import via an effect on RanGAP. To investigate this further, cytosolic RanGAP activity was measured after pre-treatment with both high and low concentrations of ERK-2. Negative controls (ERK-2 without ATP) and buffer alone showed no differences in RanGAP activity (Figure 43). High concentrations of ERK-2 significantly augmented RanGAP activity whereas low concentrations of ERK-2 decreased RanGAP activity (Figure 44).

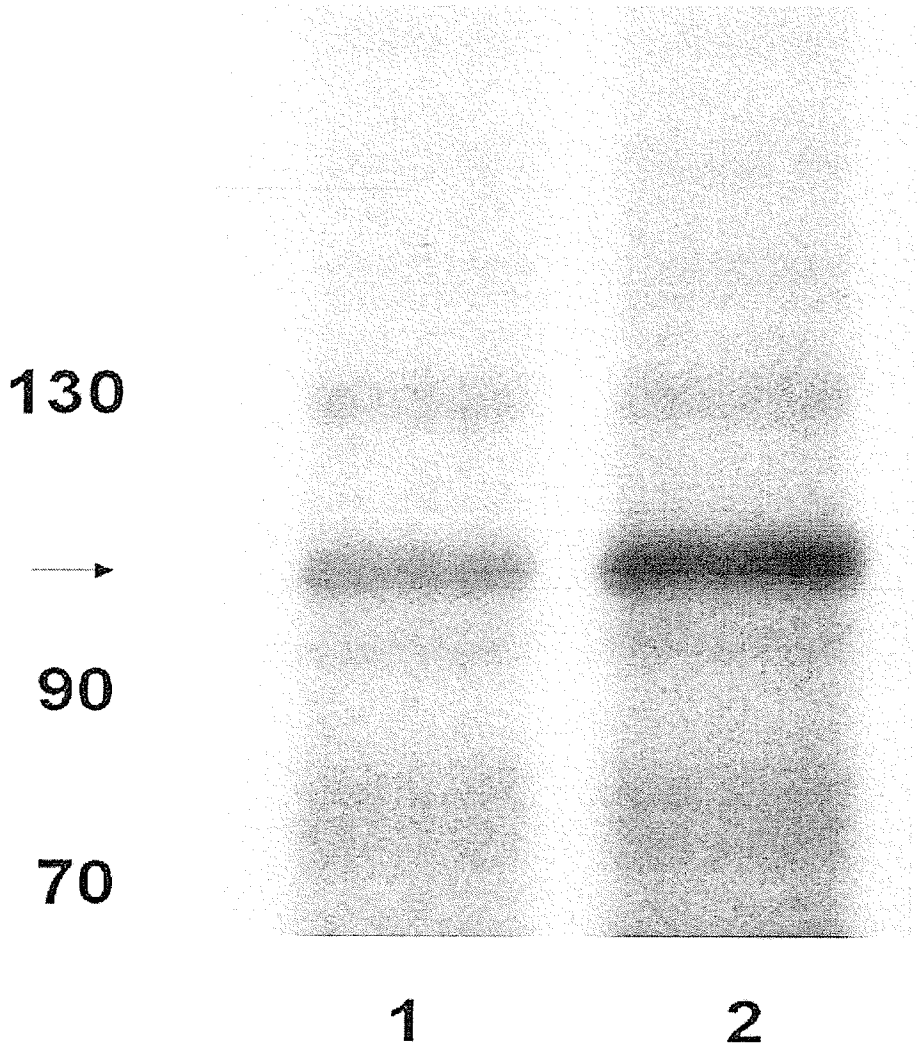

Figure 41. ERK-2 phosphorylation of a cytosolic protein

Isolated rat hepatic cytosol was incubated with ^{32}P and exogenous MAP kinase and subjected to SDS-PAGE. The gel was dried and exposed to film and the resulting autoradiogram demonstrated that pre-treatment of cytosolic mix with exogenous ERK-2 phosphorylates a ~95-97 kDa protein. *Lane 1* – cytosol with no ERK-2, *lane 2* – cytosol + 1μg/ml ERK-2. Arrow indicates what is believed to be phosphorylated RanGAP.

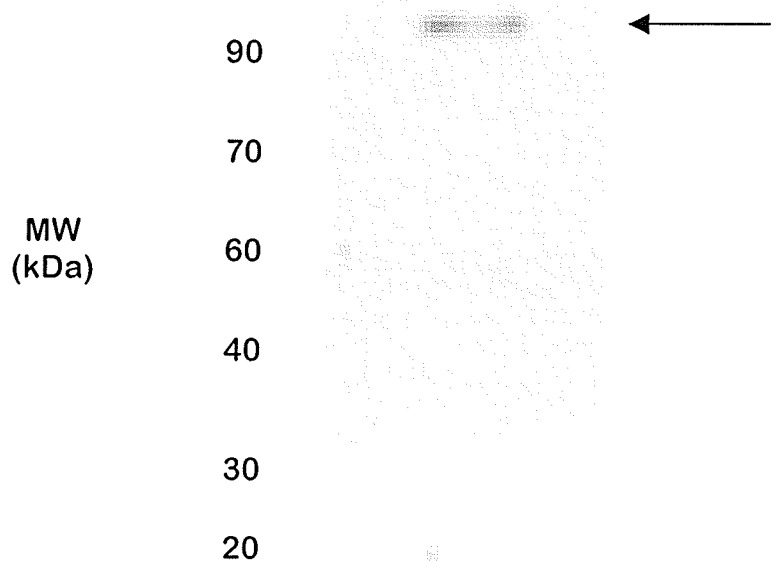

Figure 42. RanGAP is present in prepared cytosol

Cytosol (60 μg) used for preparing the import mix was run on SDS-PAGE and then immunoblotted for RanGAP. Molecular mass standards are given in kDa and are listed on the left. Arrow indicates RanGAP, demonstrating that it is not lost during the isolation procedure.

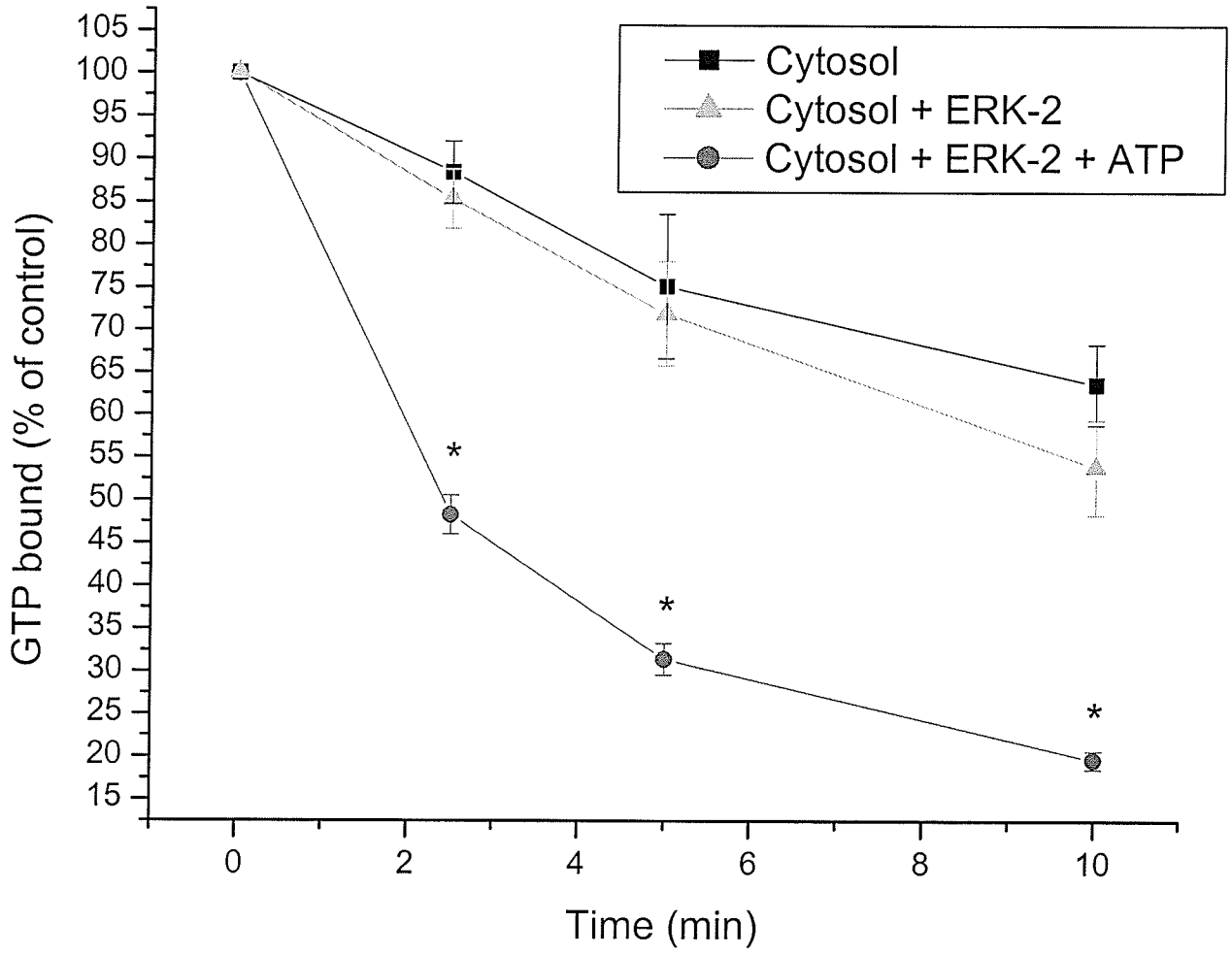

Figure 43. Exogenous ERK-2 activates RanGAP

RanGAP activity was observed for 10 min in untreated cytosolic mix (1.5% cytosol), cytosol + exogenous ERK-2 and cytosol + exogenous ERK-2 + ATP. Untreated cytosol displayed moderate RanGAP activity comparable to cytosol treated with ERK-2 alone. The addition of ATP increased RanGAP activity in a statistically significant manner, indicating that ERK-2 activity may moderate RanGAP function. Data were reported as mean ± SEM. *$p<0.05$ vs. control, $n = 3$.

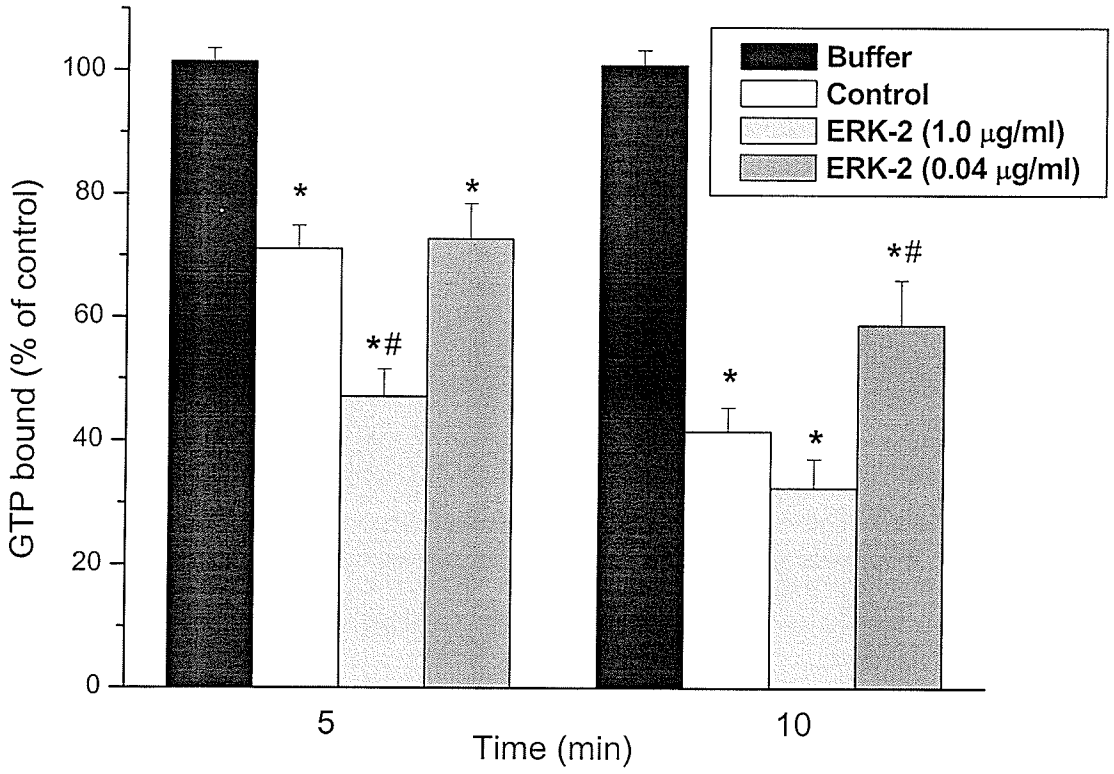

Figure 44. High and low concentrations of ERK-2 differentially activate RanGAP

RanGAP activity was assayed over 30 min. At 5 min, high ERK-2 significantly activated RanGAP activity and was sustained past 10 min, after which RanGAP activity was similar to that of untreated cytosol. Low concentrations of ERK-2 significantly depressed the activity of RanGAP at 10 min, resulting in a larger proportion of membrane bound GTP. Data were reported as mean ± SEM. *$p<0.05$ vs. buffer, #$p<0.05$ vs. control, $n = 3$.

Lipid Signaling

Lysophosphatidylcholine (LPC)

Lipids are important signaling molecules. For example, LPC is an important lysolipid that stimulates proliferation of smooth muscle cells (214, 292, 351). Its role in regulating nuclear transport has not been examined. We first investigated the *in situ* effects of lysophosphatidylcholine on nuclear import of a microinjected molecule in vascular smooth muscle cells. Cells were pre-incubated with DME alone or DME + LPC (1 μM) and then microinjected with $ALEXA_{488}$-BSA-NLS. Nuclear fluorescence, i.e. – nuclear import, was measured 30 min after microinjection of the import substrate. Microinjection of cells treated with LPC resulted in a marked increase in the nuclear accumulation of fluorescent substrate vs. control cells (Figure 45). High nuclear fluorescence is indicative of increased rates of nuclear transport. LPC treatment of cells in many separate experiments induced a statistically significant augmentation of nuclear protein import at all time points examined (Figure 45).

These results were re-examined using a conventional cell permeabilization assay. The advantage of this technique is that it allowed us to examine in greater detail the biochemical characteristics of the action of LPC and to isolate its effects to specific cytosolic components of the nuclear protein import pathway. Consistent with the microinjection results, LPC stimulated nuclear protein import (Figures 46, 47). Increasing the duration of treatment of import cocktail at 37° C with 10 μM LPC resulted in a steady rise in nuclear import, with a peak at 30 min (Figures 48, 49). The results from a number of experiments are presented in (Figure 49). Thirty min of incubation with LPC increased

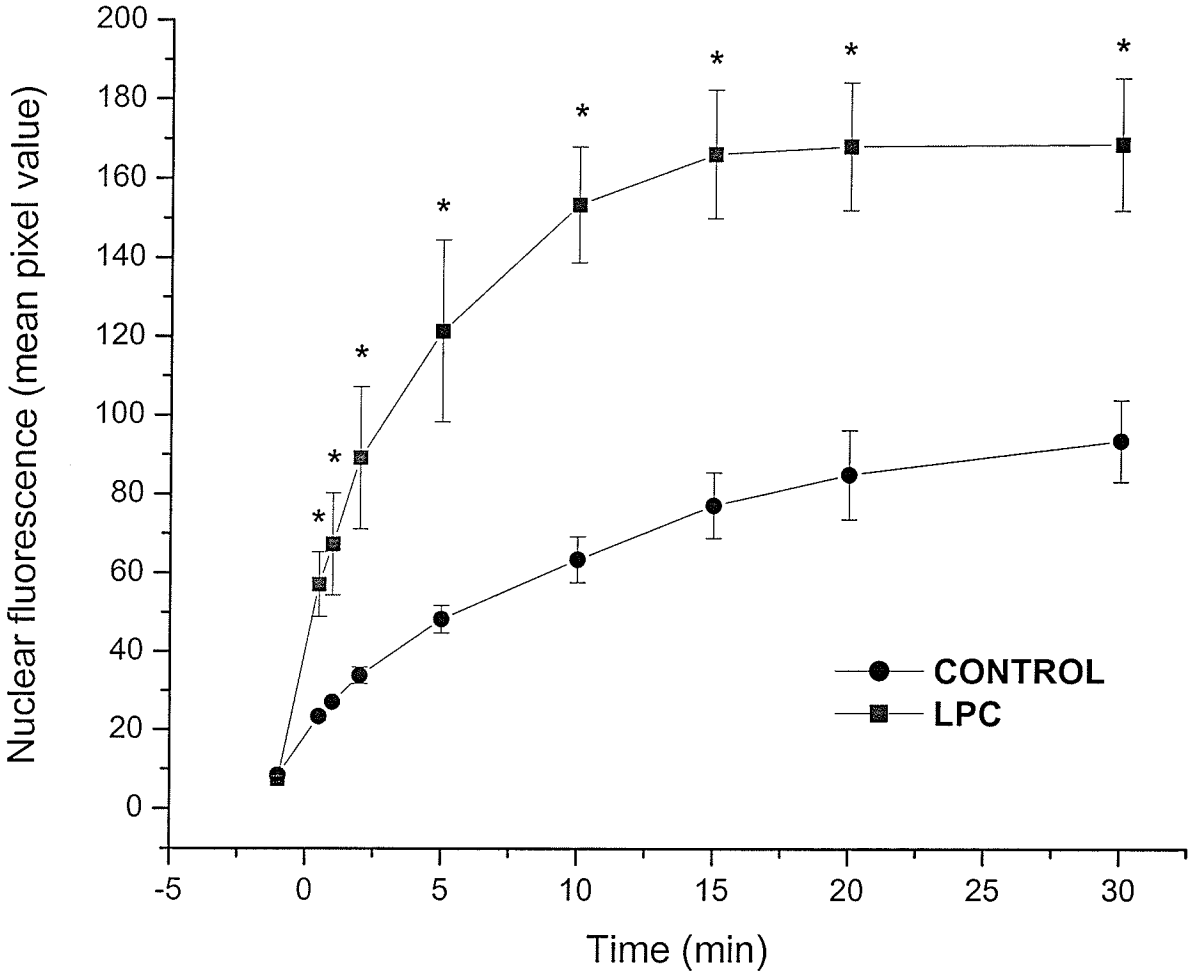

Figure 45. Microinjection of LPC augments the rate of nuclear import

To observe the effects of LPC treatment in a physiologically relevant context, cells were microinjected with fluorescent substrate following treatment with 1μM LPC and observed for 30 min. Treatment with LPC significantly increased the rate of nuclear protein import at all time points within the timecourse. Data were reported as mean ± SEM. *$p<0.05$ vs. control, $n = 3$.

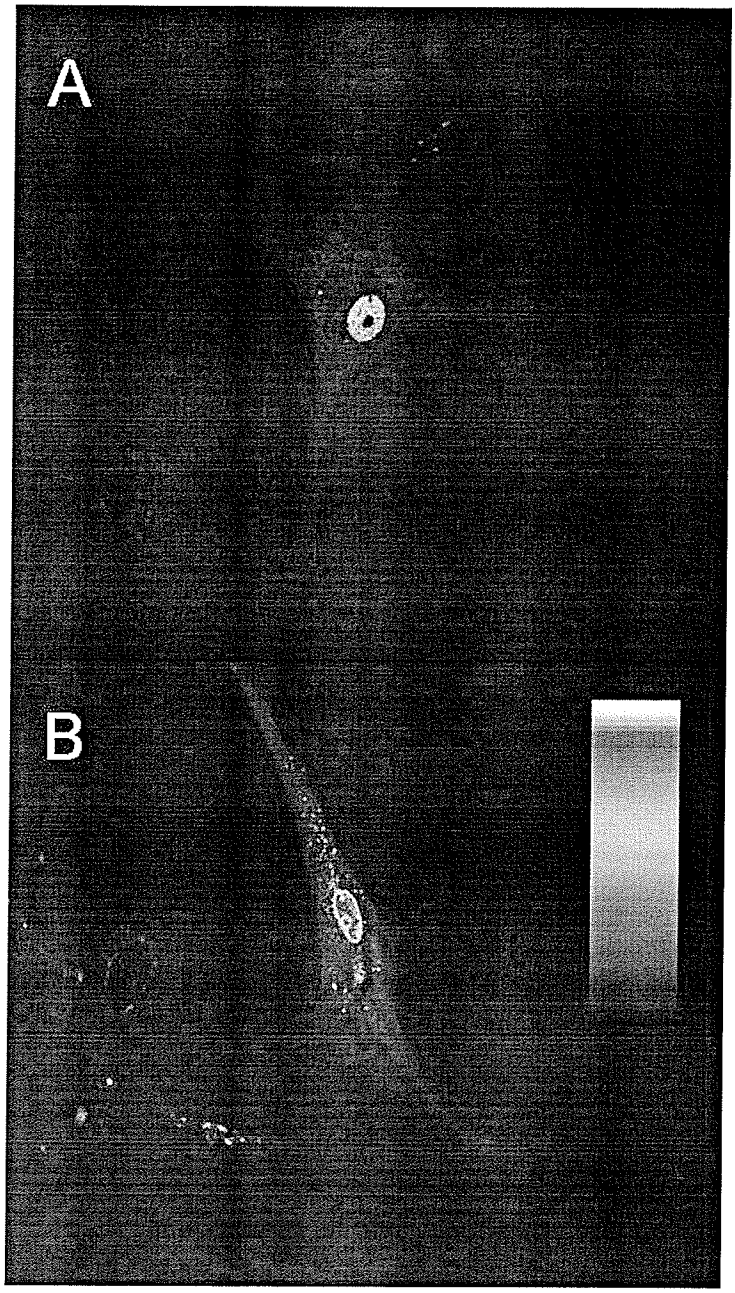

Figure 46. Lysophosphatidylcholine increases the rate of import in microinjected smooth muscle cells

Microinjected smooth muscle cells were treated with 1μM lysophosphatidylcholine (LPC) for 30 min prior to use in the nuclear import assay. (A) – control cells demonstrated distinct nuclear staining, and treatment with LPC (B) significantly increased nuclear fluorescence. *Inset*: color scale representing regions of low and high fluorescence, which are black/blue and red/white, respectively. Magnification: 40x

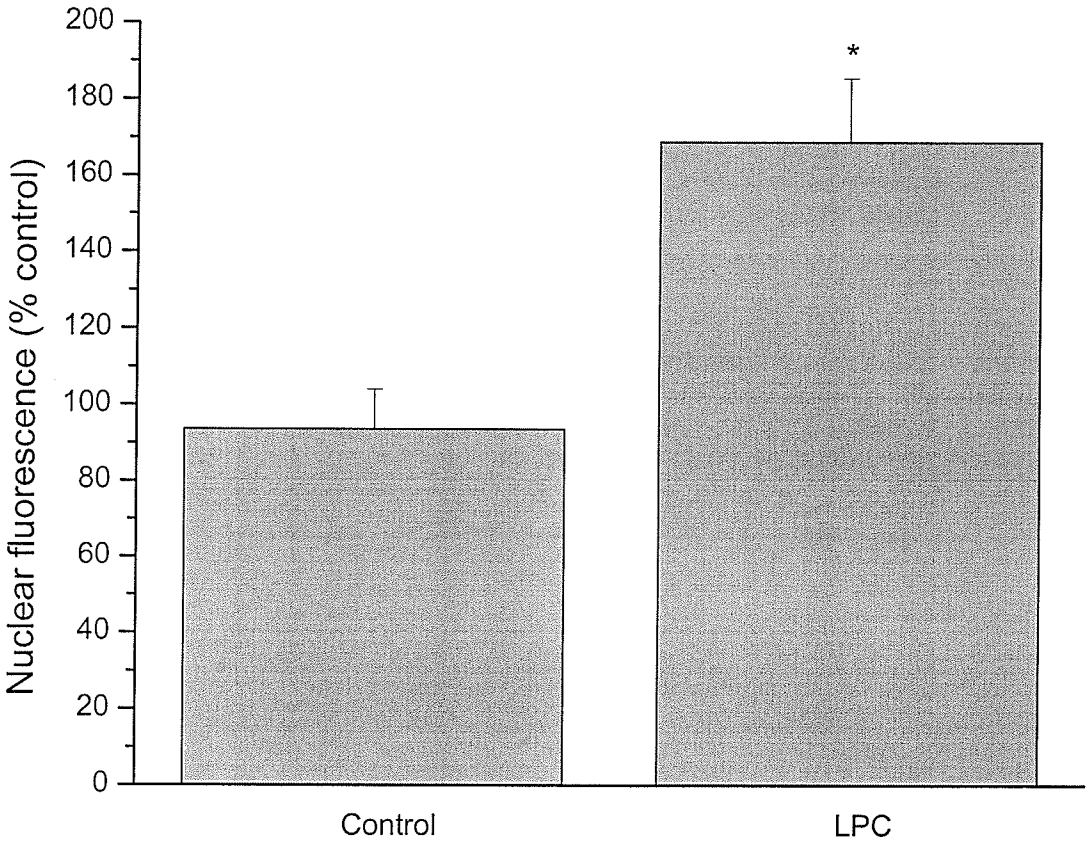

Figure 47. LPC significantly upregulates the rate of nuclear import in permeabilized cells

Analysis of nuclear fluorescence reveals that LPC treatment increases the rate of nuclear protein import by approximately 70% above basal levels of transport. Data were reported as mean ± SEM. *$p<0.05$ vs. control, $n = 3$.

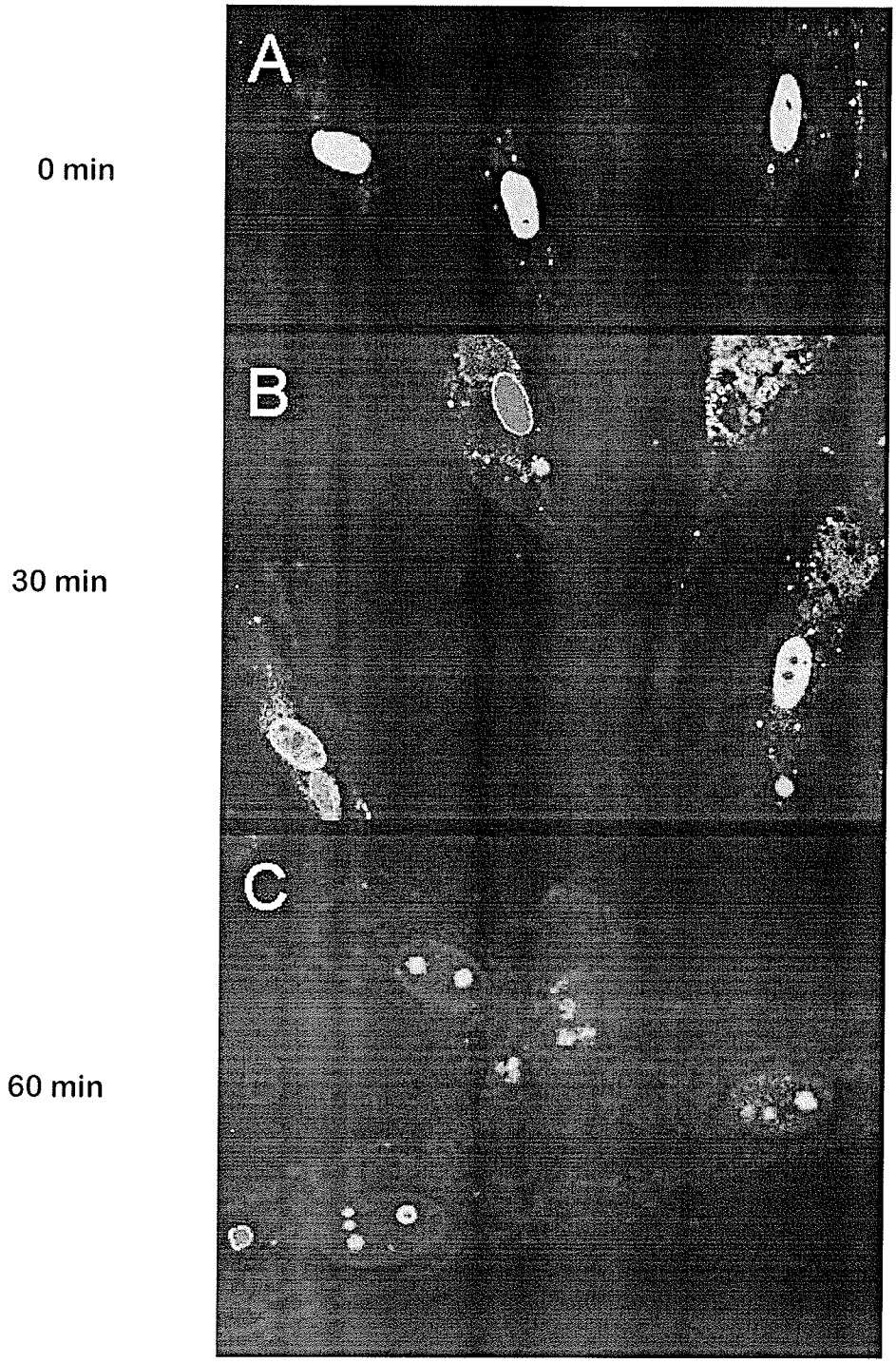

Figure 48. Nuclear import peaks at 30 min after exogenously treating cytosolic mix with LPC

Permeabilized cells were used to assess the effects of treated cytosol on protein import over 60 min. Nuclear fluorescence peaked after 30 min (B) and then significantly decreased after 60 min (C).

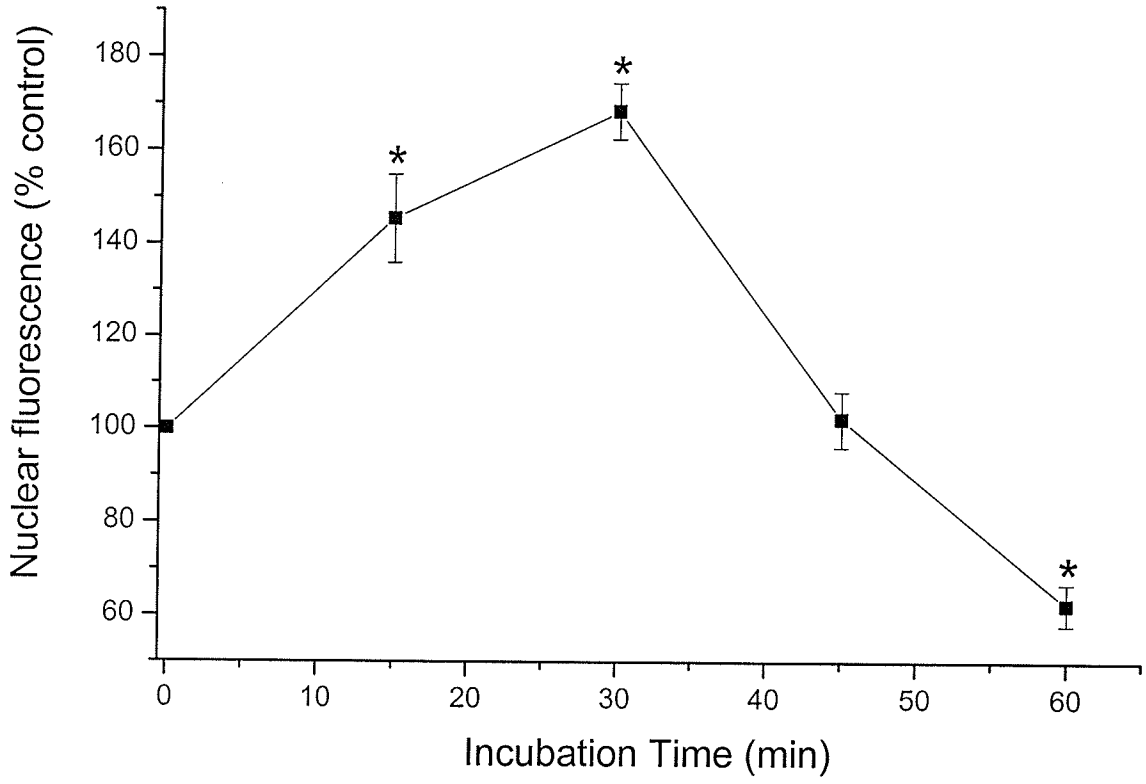

Figure 49. LPC demonstrates a biphasic, time-dependent effect on nuclear import

Exogenous cytosol was treated for various timepoints with 1 μM LPC before adding to the permeabilized cell assay system. Graphic analysis of LPC treatment on nuclear protein import reveals that LPC demonstrates a biphasic, time-dependent effect, showing statistically significant augmentation of nuclear transport at 30 min, and a significant inhibition at 60 min. Data were reported as mean ± SEM. *$p<0.05$ vs. control, $n = 3$.

nuclear protein import by ~70%. This degree of stimulation at 30 min was similar to that observed using the microinjection technique (Figure 45). Longer incubation times resulted in an attenuation of import (Figure 49). LPC did not stimulate import when incubated with the permeabilized cell, suggesting that the nuclear pore complex itself did not directly mediate its effects. This stimulation of import occurred only after pre-treatment of the cytosolic fraction and demonstrates that the effects of LPC are dependent upon an action of a specific cytosolic component.

The effects of different concentrations of LPC on nuclear protein import were studied with a constant pre-treatment time of 30 min (Figure 50). As little as 1 μM LPC significantly stimulated import. Import peaked at 10 μM LPC. At concentrations above the critical micelle concentration of LPC (>10 μM), non-specific detergent side-effects were observed. Thus, all subsequent experiments were performed at concentrations of LPC that were ≤10 μM.

It is possible that other lysophospholipid species may alter import as well. While pre-treatment of import cocktail with 10 μM LPC caused a striking increase in protein import, pre-treatment with any of 10 μM LPE, LPI, or LPS produced no effect (Figure 51). Pre-treatment with 10 μM LPLC, however, significantly increased import by ~30%.

The mechanism by which LPC was altering nuclear protein import was investigated. PD-98059, an inhibitor of the MAPK pathway, was included with 10 μM LPC and the rate of nuclear import was measured. LPC alone caused a significant increase in nuclear fluorescence, but the addition of PD-98059 significantly reversed this augmentation of nuclear protein import (Figure 52).

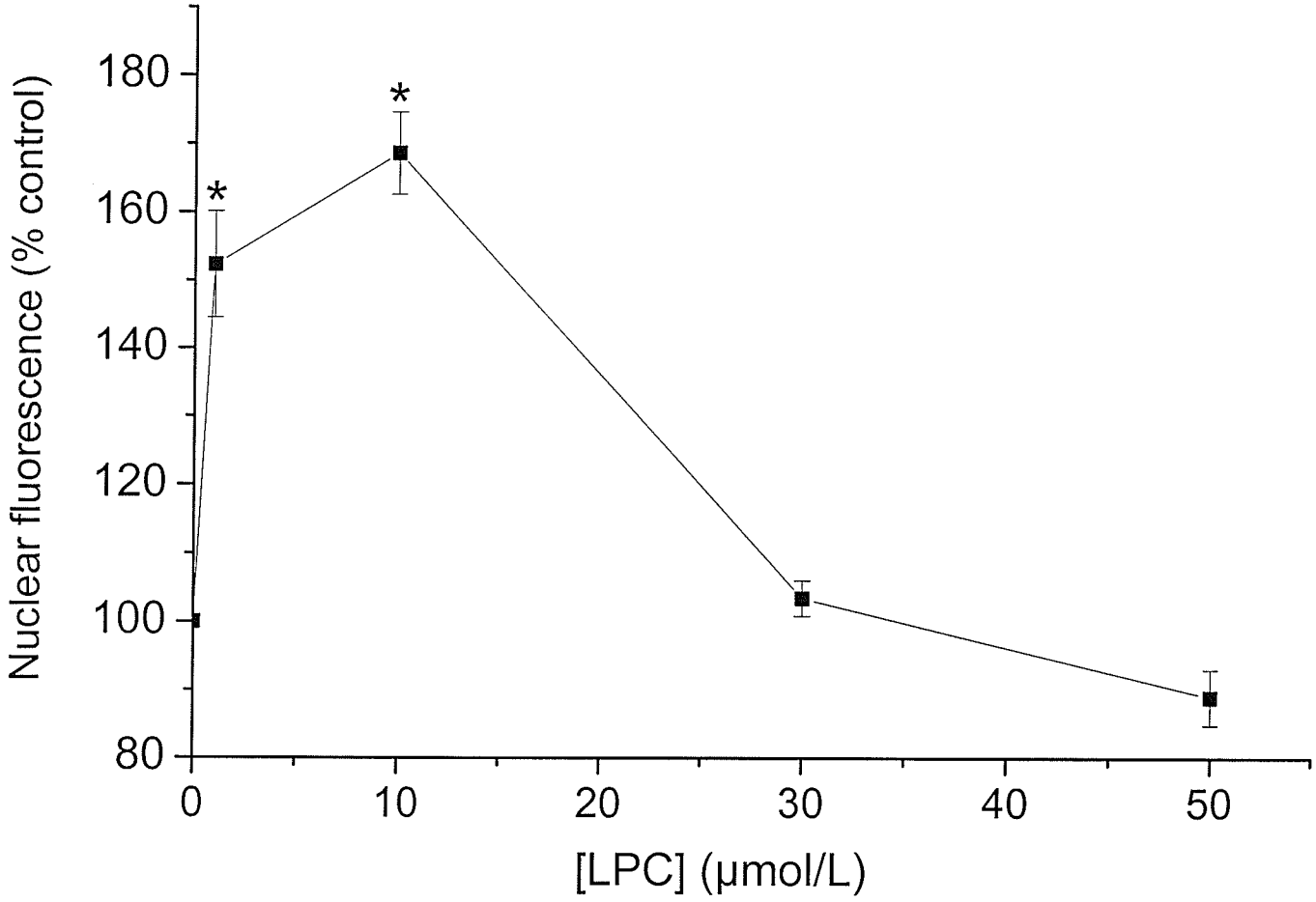

Figure 50. LPC affects nuclear import in a dose-dependent manner

Different concentrations of LPC were used and their effects on nuclear protein import in vascular smooth muscle cells were observed. 1 μM and 10 μM LPC both displayed a statistically significant increase in nuclear transport (keeping pre-treatment time constant at 30 min). Concentrations beyond 10 μM did not demonstrate significance or began exerting detergent-like effects. Data were reported as mean ± SEM. *$p<0.05$ vs. control, $n = 3$.

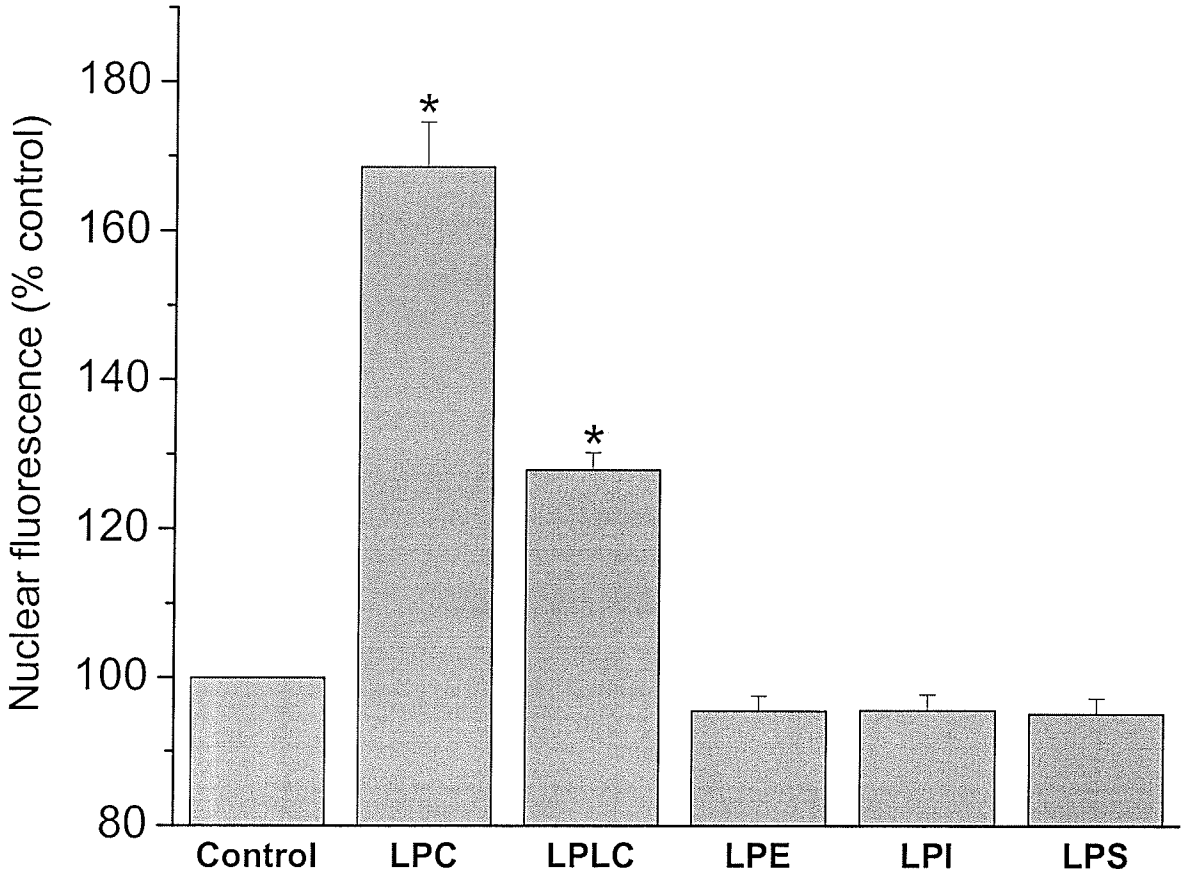

Figure 51. Effect of other lysolipids on nuclear import

Other lysolipids were tested to determine if they possessed any transport modifying activity. Lysoplasmenylcholine (LPLC), lysophosphatidylethanolamine (LPE), lysophosphatidylinositol (LPI) and lysophosphatidylserine (LPS) were assayed in addition to LPC and only LPLC demonstrated a statistically significant increase in nuclear import compared to controls. Data were reported as mean ± SEM. *$p<0.05$ vs. control, $n = 3$.

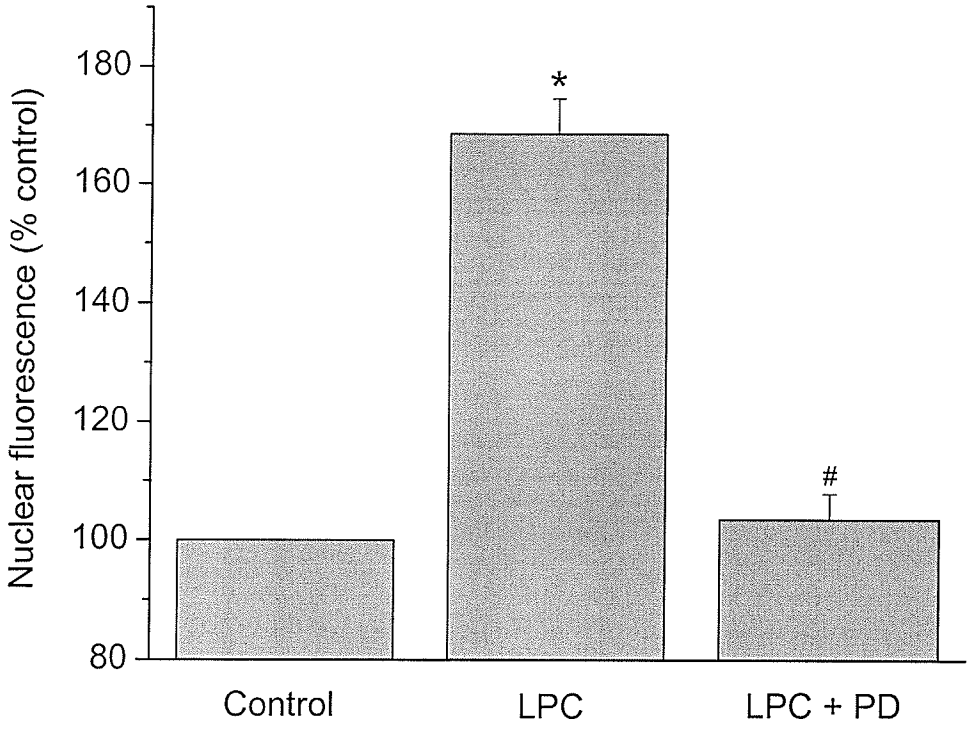

Figure 52. Lysophosphatidylcholine augments nuclear protein import in a reversible manner

Lysophosphatidylcholine (LPC) was incubated with exogenous cytosolic mix at a concentration of 10 μM for 30 min to ensure augmentation of nuclear protein import, which was increased by approximately 70% beyond control levels. This was reversed by the inclusion of 20 μM PD-98059 in the pre-treatment step. Data were reported as mean ± SEM. *$p<0.05$ vs. control, #$p<0.05$ vs. LPC, $n = 3$.

The generation and utilization of GTP is a critical regulatory point within the sequence of steps necessary for protein to be imported into the nucleus. RanGAP is an important protein that activates hydrolysis of Ran-bound GTP and was a logical site to investigate as a potential mediator for the effects of LPC. As shown in (Figure 53), incubation of cytosol with 1 μM LPC induced a significant increase in RanGAP activity when compared to the control, reflected by the decrease in GTP bound to the membrane over the incubation period. Incubation of exogenous, constitutively active ERK-2 induced a similar, significant increase in RanGAP activity (Figure 53).

Sphingolipids

Sphingolipids are a class of lipid molecules implicated in growth arrest and apoptosis. We wanted to investigate whether the effects of specific sphingolipids were mediated in part by influencing nuclear protein import. To study this, cells were microinjected with the ALEXA-BSA-NLS and ceramide. As shown in (Figure 54), ALEXA-BSA-NLS substrate delivered into the cytosol of control cells rapidly and selectively entered the nucleus, with a peak nuclear fluorescence at 30 min. Microinjection of vascular smooth muscle cells with substrate plus 1 μM ceramide decreased nuclear import (Figure 54). This inhibition was completely reversed by the addition of 1 μM SB-202190 (Figure 54). Nuclear fluorescence from a number of experiments was quantitated, confirming that microinjection of ceramide significantly inhibited nuclear import (~80%) and was abrogated by the addition of 1 μM SB-202190 (Figure 55).

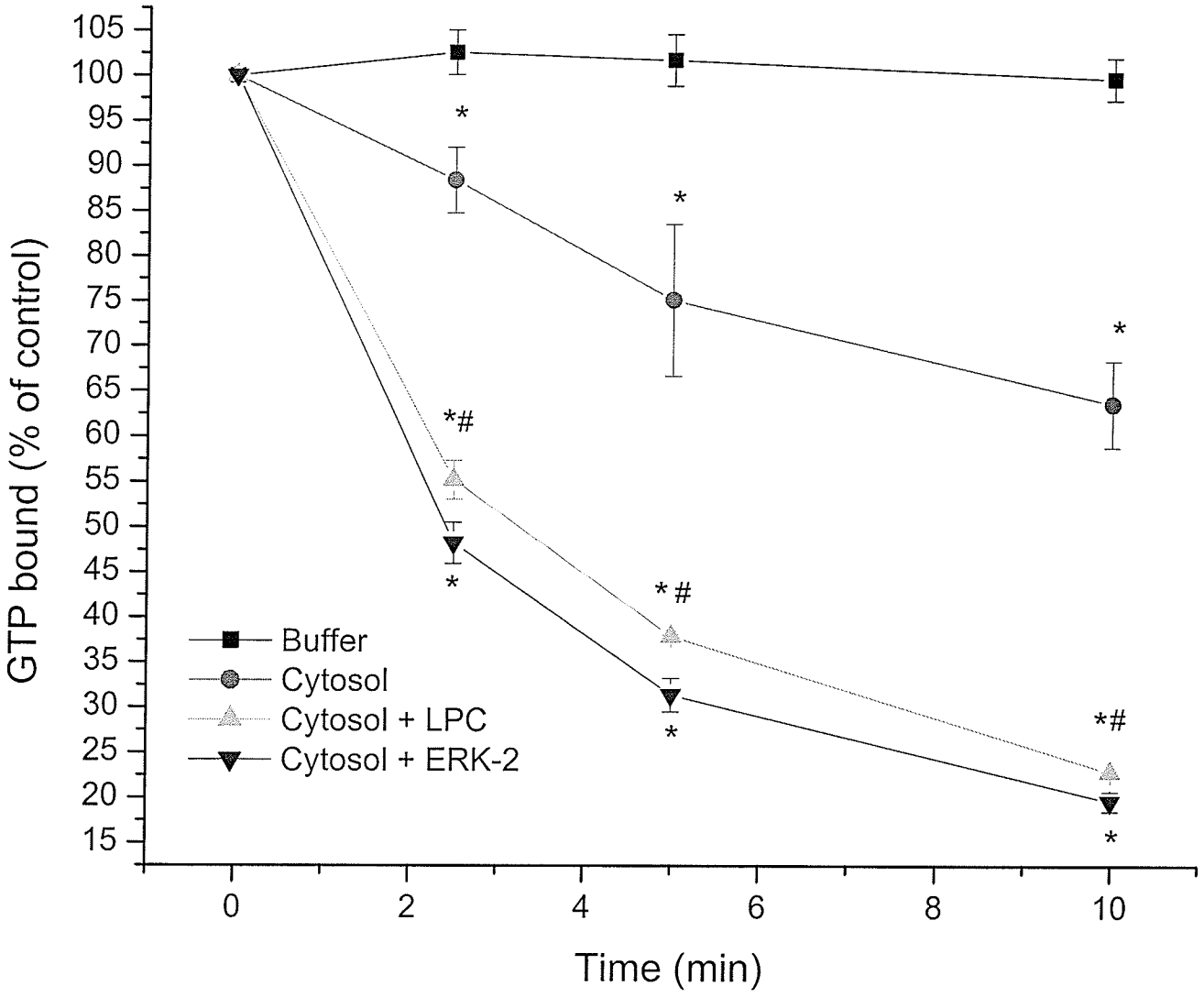

Figure 53. LPC stimulates RanGAP activity

The effect of LPC pre-treatment on RanGAP activity was assayed. Treatment of exogenously added cytosolic mix with 1 μM LPC significantly increased RanGAP activity. Similarly, treatment with high (1 μg/ml) concentrations of ERK-2 augmented RanGAP activity (described previously). Buffer was used as control. Data were reported as mean ± SEM. *$p<0.05$ vs. buffer, #$p<0.05$ vs. cytosol, n=3.

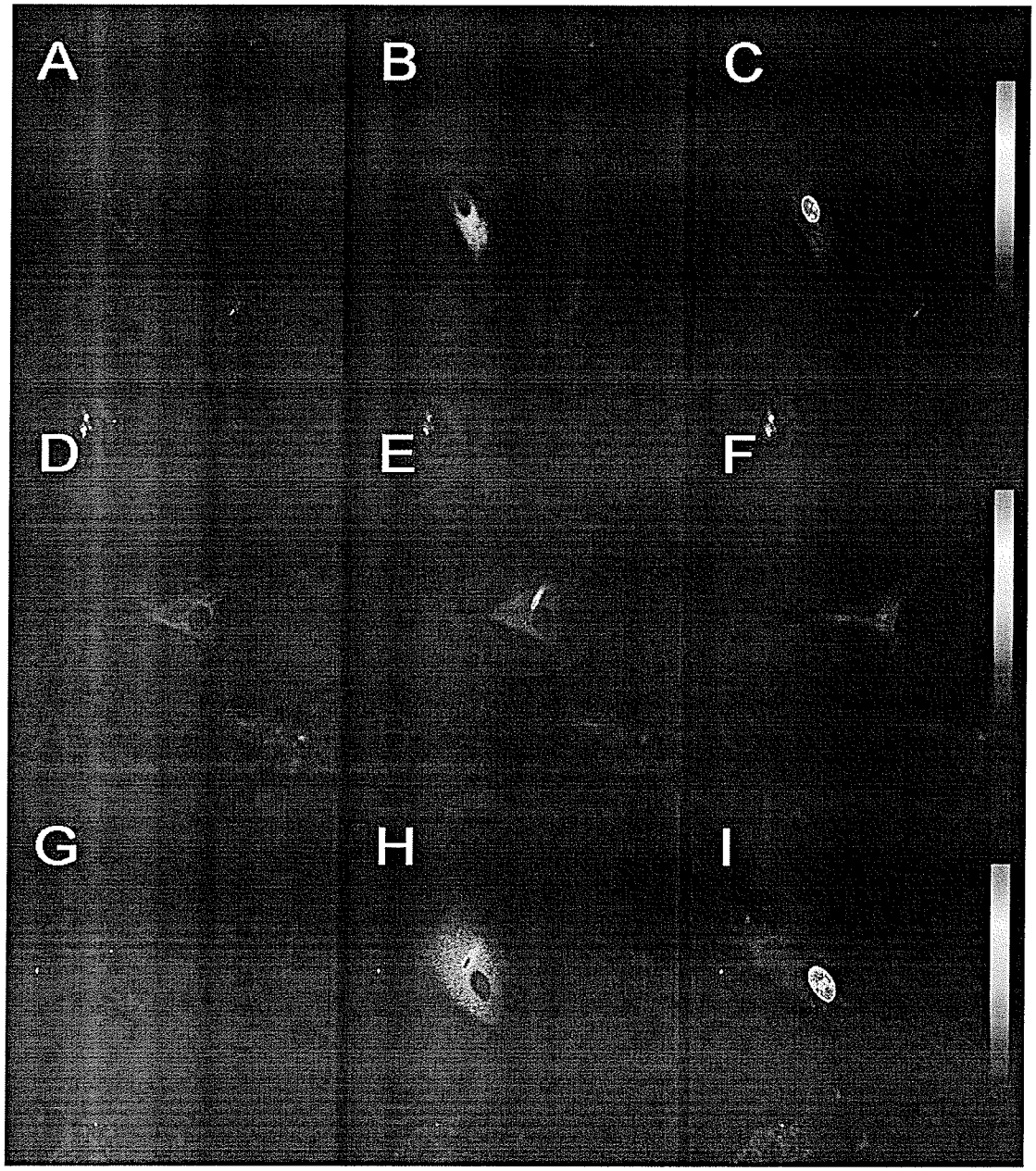

Figure 54. Microinjection of VSMC with ceramide decreases nuclear import in a SB-202190 reversible manner

Vascular smooth muscle cells were microinjected with ceramide or with ceramide + SB-202190. Microinjection with ceramide significantly decreased nuclear import after 30 min and was reversed by the addition of a p38 MAP kinase specific inhibitor.

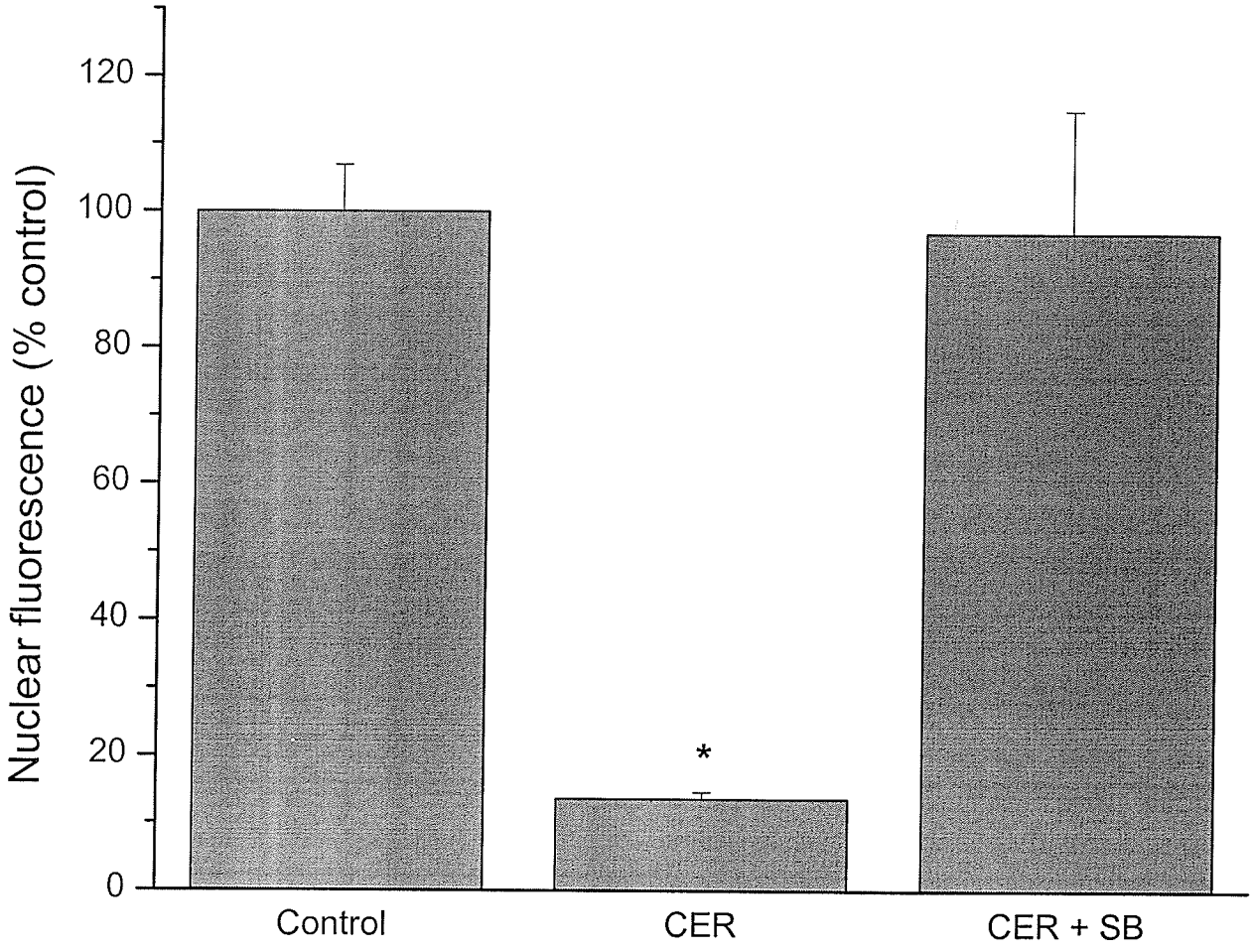

Figure 55. Ceramide significantly downregulates nuclear import in microinjected vascular smooth muscle cells

Analysis of nuclear fluorescence in control microinjected cells compared to cells injected with ceramide-treated cytosol (CER) exhibit a >80% decrease in the rate of nuclear transport. Treatment of cytosol with 1 μM SB-202190 (CER + SB) reversed the ceramide-mediated inhibition. Data were reported as mean ± SEM. *$p<0.05$ vs. control, n = 3.

The mechanism responsible for the ceramide-mediated inhibition of nuclear import in smooth muscle cells was investigated. The more conventional digitonin-permeablized cell preparation was now used to measure nuclear protein import instead of the cell microinjection technique. This allowed us to isolate specific cellular pathways better and to identify and characterize the targets for the ceramide action. For example, ceramide could be pre-incubated with only the cytosol to determine if the inhibitory action was due to an effect on the cytosolic fraction. The effect of 1 μM ceramide on nuclear import was examined (Figure 56). No significant difference was observed between control cells and cells treated with vehicle. Ceramide-treated cytosol, however, significantly inhibited import at 30 and 60 min (Figure 57). Cultured vascular smooth muscle cells were incubated with exogenous cytosol pre-treated for 30 min with 0.1, 1 and 10 μM of ceramide. Treatment with 0.1 μM ceramide had no significant effect on nuclear protein import. However, treatment with 1 and 10 μM ceramide both caused a significant inhibition of nuclear import (Figure 58).

Other sphingolipid metabolites and/or pathway inhibitors were tested for their effects on nuclear import. Ceramide-1-phosphate and sphingomyelin are downstream metabolites of ceramide and both inhibited nuclear import in a statistically significant manner (Figure 59). N-oleoylethanolamide (NOE) is a ceramidase antagonist which also inhibits the synthesis of glucosylceramide. Addition of NOE to our assay system should therefore increase the amount of endogenous ceramide by inhibiting its conversion or modification into downstream metabolites, and treatment with NOE would therefore be expected to inhibit nuclear import by increasing endogenous ceramide concentration. Pre-

Control

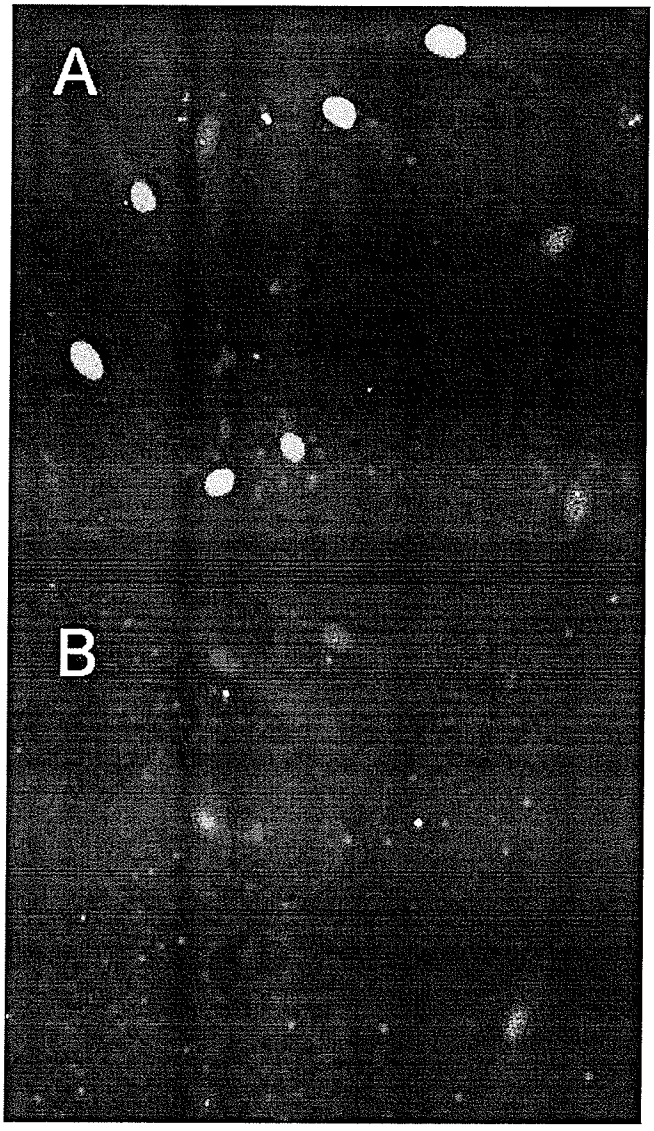

1 μM ceramide

Figure 56. Permeabilized smooth muscle cells display a downregulated rate of nuclear import upon treatment with ceramide

The effects of ceramide on import were assessed using the permeabilized cell assay. Treatment of exogenously added cytosol with 1 μM ceramide for 30 min decreased nuclear protein import in a statistically significant manner.

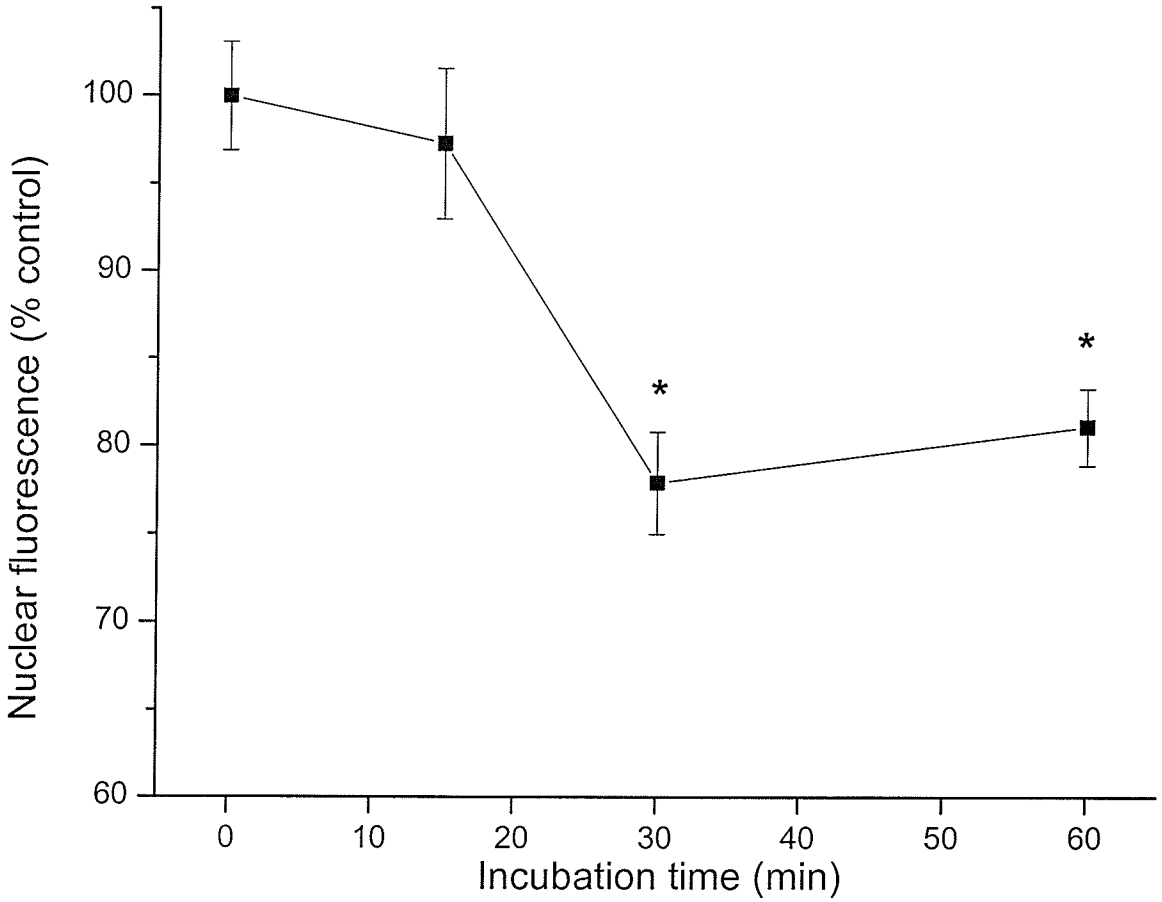

Figure 57. Nuclear import in VSMCs is significantly downregulated after ceramide treatment

Ceramide exhibits a time dependent effect on nuclear import in vascular smooth muscle cells. Exogenous cytosolic mix pre-treated for 30 and 60 min with 1 μM ceramide decreases nuclear protein import in a statistically significant manner. Data were reported as mean ± SEM. *$p<0.05$ vs. control, $n = 3$.

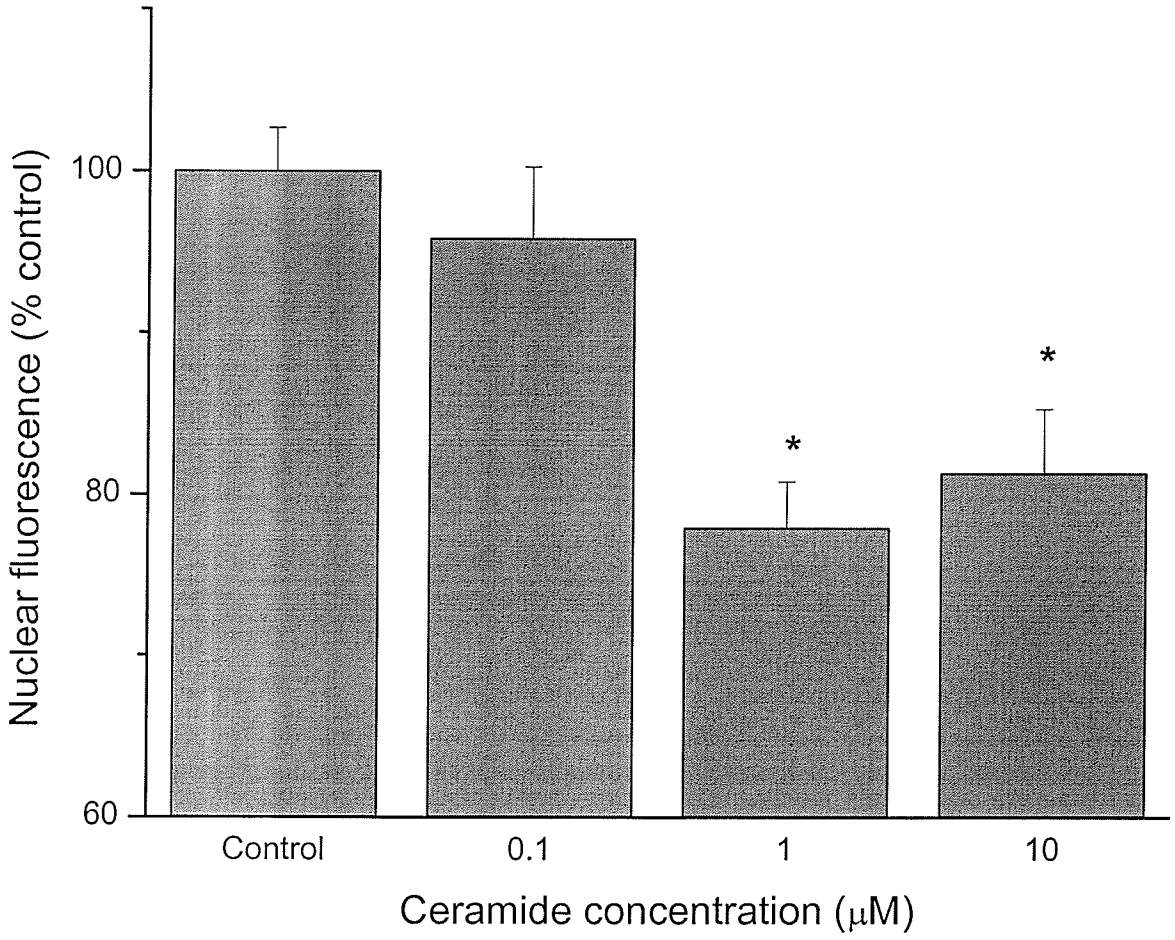

Figure 58. Dose-dependent effects of ceramide treatment on nuclear import

Cytosolic mix was treated with various concentrations of ceramide. A dose dependent effect was demonstrated. Similar inhibitory effects on nuclear protein import were observed for 1 μM and 10 μM ceramide. Data were reported as mean ± SEM. *$p<0.05$ vs. control, $n = 3$.

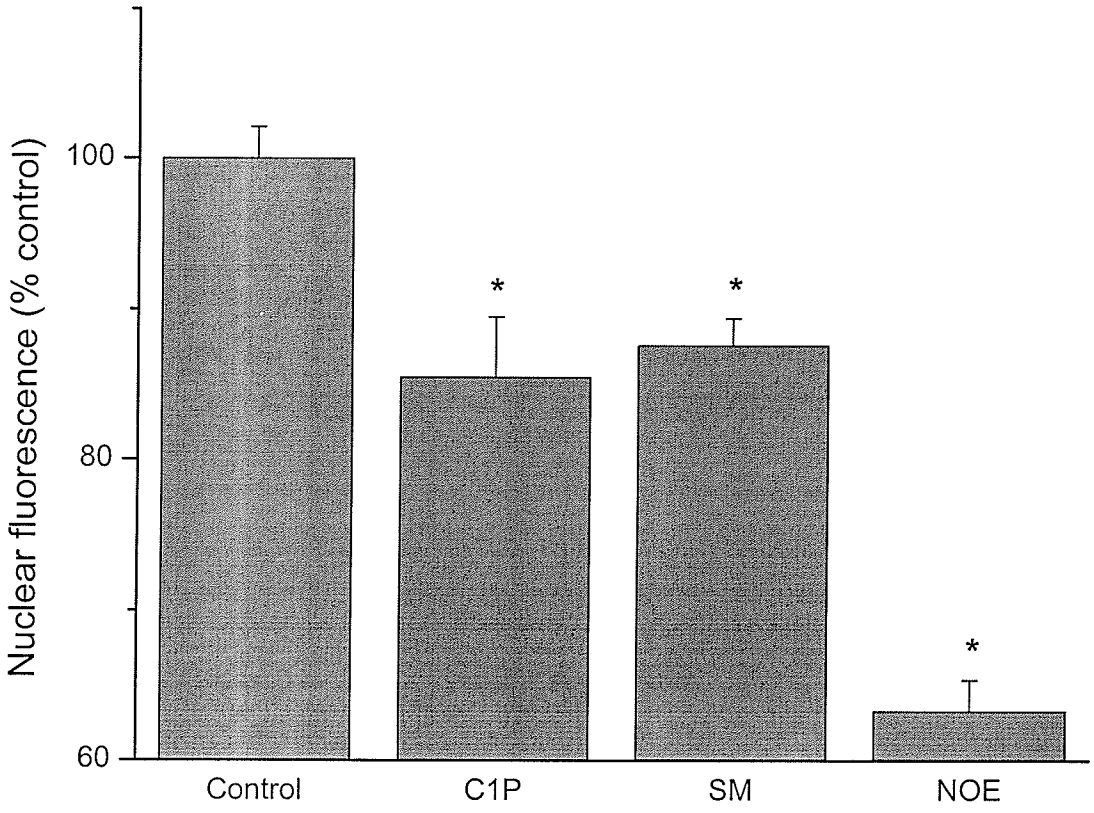

Figure 59. Effects of other sphingolipid metabolites on nuclear import

All compounds tested in this experiment were used at a final concentration of 1 μM. Ceramide-1-phosphate (C1P) and sphingomyelin (SM) are downstream metabolites of ceramide which demonstrated a significant inhibitory effect on nuclear import. N-oleoylethanolamide (NOE) inhibits the formation of glucosylceramides and ceramidase activity. In this study, it decreased the rate of import by ~40%. Data were reported as mean ± SEM. *$p<0.05$ vs. control, $n = 3$.

treatment of the cytosol with NOE significantly downregulated the rate of nuclear import (~40%) in vascular smooth muscle cells.

Ceramide was further studied and the involvement of the MAPK pathway was examined using specific pharmacological inhibitors. Incubation of ceramide plus 1 μM 5-iodotubercidin, a potent and specific ERK-2 inhibitor, did not show any difference with respect to treatment with ceramide alone (Figure 60). Consistent with the microinjection experiments (Figures 54, 55), ceramide dependent inhibition was reversed upon the addition of 1 μM SB-202190, a p38 MAP kinase inhibitor. It was also reversed with the addition of 20 μM PD-98059, a MEK specific inhibitor (Figure 60). These data strongly suggested that p38 MAPK activation was involved in the inhibition of import. To directly assess this possibility, we determined the effects of exogenously added p38 MAP kinase. Pre-treatment of permeablized VSMCs with recombinant p38 MAP kinase significantly decreased nuclear protein import. This effect was reversed upon the addition of 1 μM SB-202190 (Figure 61).

The molecular target for the action of MAP kinase was investigated. Since CAS plays a key role in cycling importin-α from the nucleus to the cytosol, it was hypothesized that CAS may be a potential substrate for MAP kinase activity with subsequent effects on nuclear protein import. For immunocytochemistry experiments, cells were treated with exogenous cytosol (± ceramide) as for the nuclear import assays except without the addition of the fluorescent reporter. After fixation, coverslips were rinsed and incubated with anti-CAS antibody for use in immunofluorescent studies. A nuclear/nuclear rim localization of CAS was observed in control cells (Figure 62). Treatment of the cytosol with 1 μM ceramide removed CAS from these nuclear sites (Figure 62). Treatment with

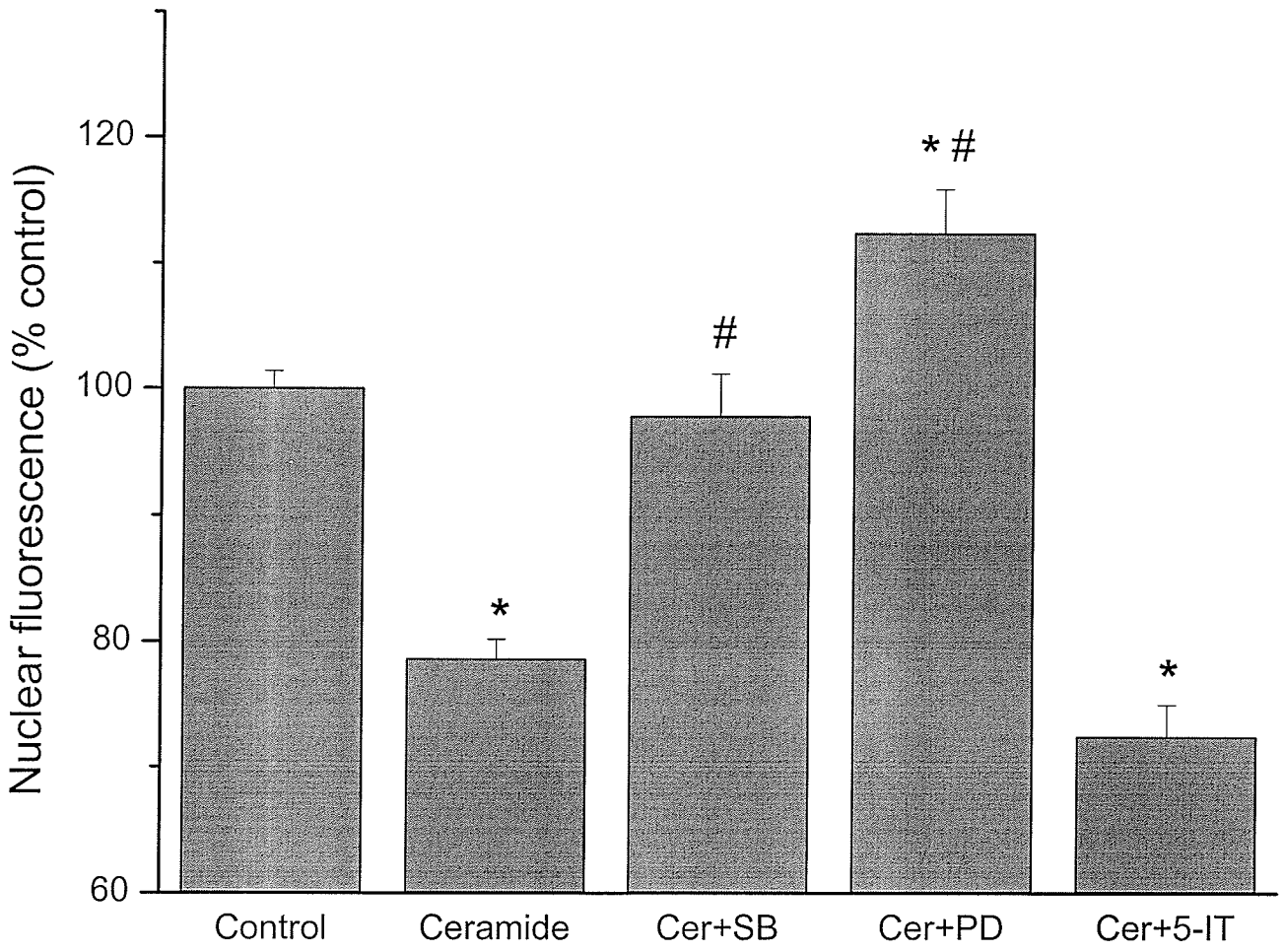

Figure 60. Pharmacological inhibition of the ceramide-mediated downregulation of nuclear import

Various MAP kinase inhibitors were used to determine if the effects of ceramide could be reversed. Incubation with SB-202190 (SB) reversed the effects of ceramide on nuclear protein import. Treatment with ceramide and PD-98059 (PD) showed a slight but significant increase in nuclear protein import compared to controls. Treatment with 5-iodotubercidin (5-IT), an ERK-2 specific inhibitor did not reverse the ceramide-mediated downregulation of nuclear import. Data were reported as mean ± SEM. *$p<0.05$ vs. control, #$p<0.05$ vs. ceramide, $n = 3$.

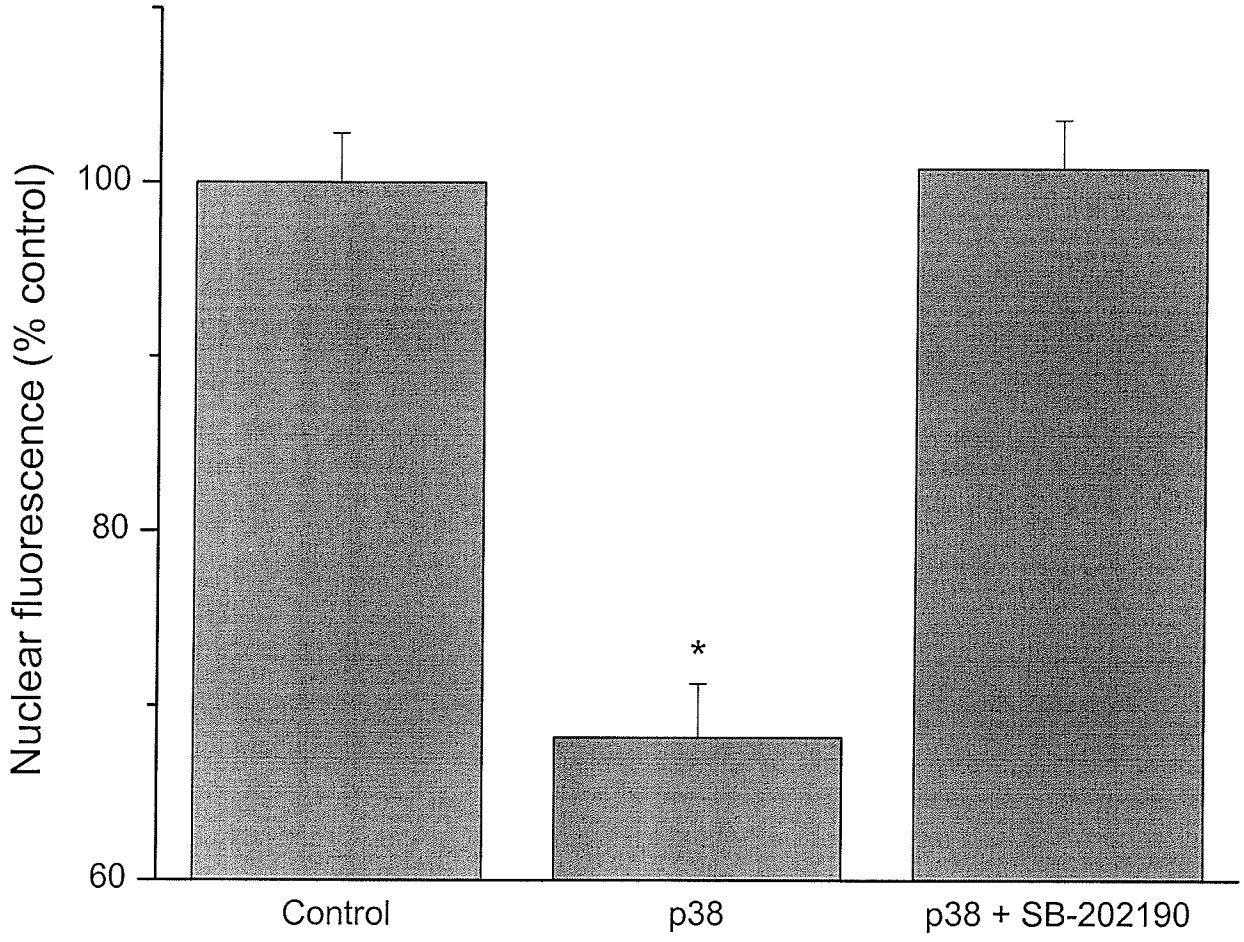

Figure 61. Exogenous p38 MAP kinase decreases nuclear import in a reversible manner

Cytosolic mix was treated with a low (0.04 μg/ml) concentration of exogenous p38 MAP kinase and exhibited a decrease in the rate of import. Addition of SB-202190 reversed the effects of p38 on nuclear transport. Data were reported as mean ± SEM. *$p<0.05$ vs. control, $n = 3$.

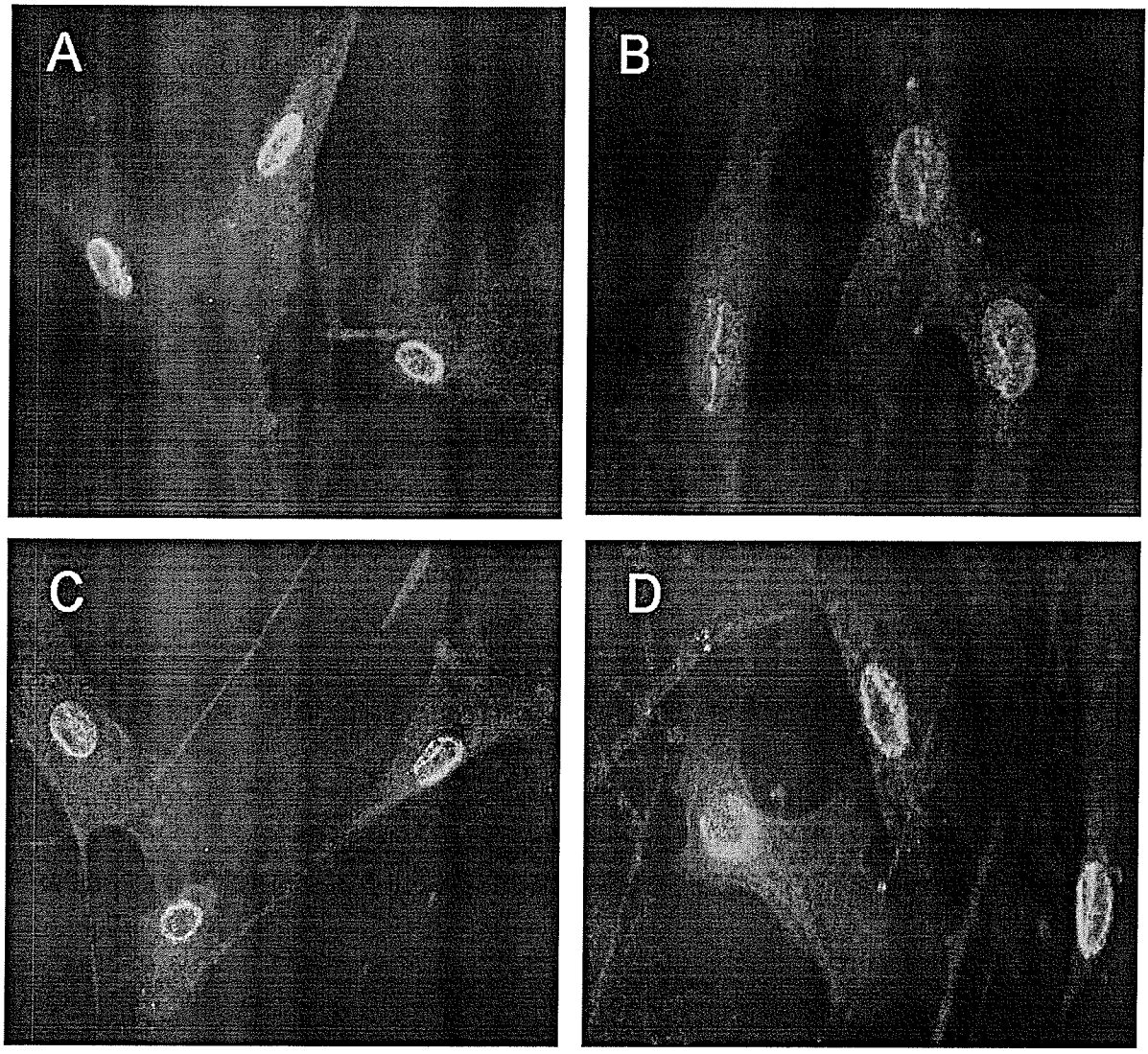

Figure 62. Pharmacological inhibition of CAS localization in ceramide treated vascular smooth muscle cells

Proliferating vascular smooth muscle cells were stained for CAS after treating with ceramide. Control cells exhibited a nuclear/nuclear rim staining (A). Pre-treatment with 1 μM ceramide eliminated the nuclear staining of CAS (B), which was restored by the addition of 1 μM SB-202190 or 20 μM PD-98059 (C and D, respectively) to the pre-treatment step.

ceramide and either SB-202190 or PD-98059 restored CAS localization predominantly to the nuclear periphery (Figure 62).

Since CAS is the nuclear export receptor for importin-α, the possibility that ceramide treatment would also cause a subsequent redistribution of importin-α was investigated. Cells were subjected to the sham import assay procedure described previously. An alteration in the distribution of importin-α in vascular smooth muscle cells with ceramide pre-treatment was observed. Cells receiving no ceramide were stained for importin-α and displayed a constitutive nuclear localization (Figure 63), whereas pre-treatment with 1 μM ceramide inhibited its nuclear localization (Figure 63).

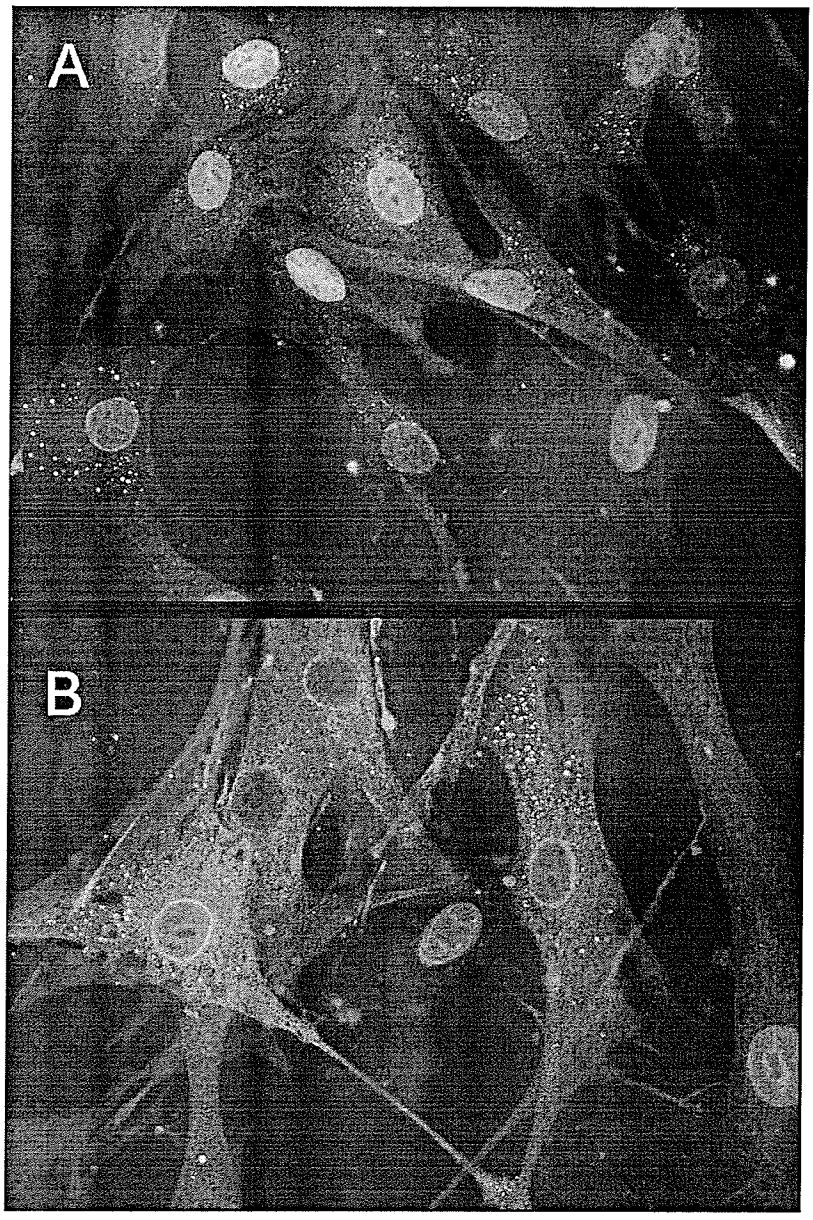

Figure 63. Relocalization of importin-α in ceramide treated cells

CAS is the export receptor for importin-α and inhibition of CAS cycling between the nuclear and cytosolic compartments will affect importin-α distribution. (A) Proliferating control cells exhibit a nuclear localization of importin-α. (B) Pre-treatment of exogenously added cytosol with 1 μM ceramide largely eliminates nuclear localization of importin-α and staining shows a more diffuse cytosolic distribution with nuclear rim staining in some cells.

DISCUSSION

Calcium and the nuclear pore complex

Calcium is associated with nuclear transport regulation as well as nuclear pore complex dynamics, but its specific role remains ambiguous. Also, the existence of a separate nuclear calcium store is a contested issue, since some investigators do not observe a discretely regulated nucleoplasmic pool of calcium (352), while other laboratories report a separate pool of nuclear calcium buffered against alterations in cytoplasmic calcium (353). The latter hypothesis is supported by the presence of calcium handling enzymes within the inner and outer nuclear membranes of the nuclear envelope (354-356). The identification of NPC-containing tubular structures associated with calcium signaling in the nucleus provided further evidence for the existence of a nuclear calcium handling system (357, 358). Work by Chamero *et al* suggested that a more refined calcium handling system exists at the nucleus (359). They proposed that a kinetic barrier exists which filters out high frequency calcium oscillations without impeding sustained increases (359). This would subsequently allow differential regulation of calcium dependent processes within the cytoplasm and the nucleus (359).

Calcium fluxes within the nucleus have been reported to affect the opening and closing of the nuclear pore complex (118, 119, 131, 360). Perez-Terzic *et al* originally demonstrated that depletion of nuclear calcium inhibited nuclear transport, concomitant with the appearance of a central plug within the aqueous channel of the NPC (119). Specifically, depletion of the calcium stores resulted in NPC occlusion, while repletion of nuclear calcium restored the NPC to an "open" conformation. Shahin *et al* provided

evidence for calcium sensitivity within the pore (121) and it was Wozniak *et al* who first identified a putative metal ion binding region within the nucleoporin gp210 (361). No group has determined if gp210 is a physiologically relevant calcium sensor within the NPC, however. The purpose of the present study was to identify calcium binding proteins within the nuclear pore complex fraction. Our results demonstrated that no calcium binding proteins could be identified within the pore.

Therefore, within the limitations of the approaches used, the nucleoporin gp210 was not identified as a calcium binding protein in rat hepatic nuclei and endogenous calcium-sensitive kinase activity was not present. These conclusions are limited by the relatively low sensitivity of the overlay assay to low affinity calcium binding proteins. However, we did detect Ca^{2+} binding to calsequestrin controls and this assay has been used successfully for the identification of other calcium binding proteins (337). This would demonstrate that the assay is capable of detecting significant calcium binding activity. It is also possible that loosely associated, peripheral calcium binding proteins may have been lost during the isolation procedure. However, the retention of many other proteins that would be loosely associated with the NPC, such as phosphatases and various MAP kinases (Table 5) argues against this.

An alternative, more indirect mechanism whereby the NPC may be regulated in a Ca^{2+}-sensitive manner was investigated. Kinase dependent phosphorylation of channels is well known to alter channel activity (362-364). We investigated the possibility that calmodulin dependent kinase (CaM) activity may induce phosphorylation of NPC proteins. Using divalent cation chelating agents as well as specific pharmacological inhibitors, we observed no endogenous CaM kinase activity associated with the NPC

fraction. Immunological analysis of the nuclear pore fraction confirmed the absence of endogenous CaM kinases (Table 5). Conversely, the addition of *exogenous* CaM kinase demonstrated a rapid, time dependent phosphorylation of a 60 kDa and 70 kDa protein within the nuclear pore complex fraction. CaM kinase is regulated by calmodulin, an essential cofactor for CaM kinase activity (30). Pruschy *et al* first demonstrated reversible nuclear transport of calmodulin (365) and subsequent work by Sweitzer and Hanover identified a calmodulin-dependent mode of nuclear transport (366). These observations suggest that calmodulin is physiologically associated with the process of nuclear trafficking in a relevant manner. Other studies identifying the presence of calcium handling enzymes within the nucleus and within the nuclear envelope (354, 355), the observed effects of calcium depletion and repletion on nuclear transport (118, 119, 131, 360) and our CaM kinase phosphorylation data suggest that a calcium sensing mechanism participates in nuclear pore function.

Identification of MAP kinase phosphoproteins within the nuclear pore complex

Nuclear pore complexes were isolated from rat hepatocytes and investigated for the presence of phosphoproteins. Previous studies have demonstrated the presence of substrates phosphorylated by mitotically regulated kinases (334, 335) as well as NPC regulation by PKA and PKC (336). However, the presence of MAP kinase phosphosubstrates within the NPC has not been identified. We have biochemically investigated MAP kinase phosphorylation of the nuclear pore complex fraction from rat hepatocytes and have found that several substrates exist for all three members of the MAP kinase family.

Screening of the NPC fraction with a battery of antibodies revealed the presence of kinases and phosphatases in addition to a large variety of unclassified proteins (Table 5, unclassified proteins not listed). It could be argued that some of the proteins identified in this screening process may be present because of cross-contamination with other subcellular fractions during the isolation procedure. However, the results from the enzyme marker assays suggest that significant cross contamination did not occur. It may also be argued that the MAP kinase substrates themselves were co-purified with the NPC from a discrete cellular compartment. The high degree of enrichment of nuclear proteins such as nuclear lamins and histones in addition to well characterized nuclear pore complex proteins such as p62 and p120 argues against this. The presence of kinases, phosphatases and MAP kinase specific phosphosubstrates within the NPC fraction implies that phosphorylation is a regulated and physiologically relevant process at the nuclear pore complex. Therefore, the role of nuclear pore phosphorylation on nuclear import using the permeabilized cell assay was studied. The majority of studies documenting the effects of phosphorylation on nuclear transport focus on the effects of kinase activity on the soluble components of the transport machinery (14, 332, 333, 336). After treating permeabilized smooth muscle cells with exogenous MAP kinase, we did not detect any alterations in nuclear import (Table 6). Several explanations may account for this lack of effect. If the pore is constitutively phosphorylated by the presence of endogenous kinase activity, adding excess MAP kinase may have no effect. Another possibility is that NPC phosphorylation may affect nuclear export processes and not nuclear import. Finally, it is possible that MAP kinase phosphorylation may be important in structural dynamics of the pore instead of regulating transport.

MAP kinases and nuclear import

While no effects on nuclear protein import were observed after phosphorylation of the permeabilized cell, pre-treatment of the cytosol with exogenous p38, JNK and ERK-2 induced changes in nuclear import. We have previously characterized a significant inhibitory effect of ERK-2 on nuclear protein import in vascular smooth muscle cells (341) so ERK-2 was selected for further study. We have found in the present study that ERK-2 induced phosphorylation of the cytosolic fraction cannot only inhibit import but it can also cause a significant stimulation of nuclear protein import under selected conditions. The dual effects of ERK-2 on nuclear protein import were found to be dose dependent. Permeabilized cell assays and microinjection using high (1 μg/ml) and low (0.04 μg/ml) concentrations of ERK-2 identified that ERK-2 possessed biphasic effects on nuclear transport. This dual effect may not be as unusual as one might believe at first. MAP kinase has been previously characterized as having both stimulatory and inhibitory effects on DNA synthesis (206) in rat hepatocytes. Tombes and co-workers discovered that acute phasic activation of the MAP kinase pathway in rat hepatocytes promoted DNA synthesis (206). Chronic activation, however, caused an inhibition of DNA synthesis by preventing entry of the cell cycle into S phase (206). These observations establish a precedent for the dual effects of MAP kinase on cellular growth in chronic versus acute exposure. In the current study, the differential effects of MAP kinase on nuclear protein import occur in an acute setting and this is the first report of such an occurrence.

Despite its utility in compartmentalizing the effects of MAP kinase treatment in our experiments to either the membrane bound phase or the soluble phase, the permeabilized cell assay does not allow an experimenter to observe treatments within a living system. Another limitation is the use of exogenous cytosol, which may be different from the normal cytoplasmic milieu of the cell. Microinjection circumvents these limitations and was used to observe the effects of exogenously added ERK-2 in an *in situ* context. Over 30 min, we observed that the dose-dependent effects of ERK-2 treatment in the permeabilized cell assay were recapitulated in the microinjection study. In whole living cells, regulatory structures and mechanisms remain intact and represent a physiological context in which to observe the effects of various treatments which is not available in the permeabilized cell model. The results for the microinjection experiments reflect those seen in the permeabilized cell assay. Therefore, the effects we observe identify a significant effect of ERK-2 on nuclear protein import via the soluble transport machinery.

In light of recent discoveries highlighting the emerging function of the nuclear transport proteins in mitosis (151, 152, 367), RanGAP regulation by MAP kinase establishes a potential mechanism by which nuclear transport may regulate cellular proliferation. ERK-2 phosphosubstrates share a docking sequence (321, 368). Sequence analysis of RanGAP revealed a similar putative docking site for ERK-2, so this protein was considered as a potential candidate for mediating the effects of ERK-2 on nuclear transport. A significant effect of both concentrations of ERK-2 was observed on RanGAP activity. RanGAP can exist in the cell in both unmodified, cytosolic and SUMO1-modified, NPC-associated forms (18), so a possible mode of action may involve an allosterically regulated association between ERK-2 and RanGAP. Alternatively, the

association between ERK-2 and RanGAP may be transient. It is also possible that one form of RanGAP may promote a higher affinity association between MAP kinase and RanGAP. RanGAP is allosterically regulated by SUMO (369), RanBP2 (370) and importin-β (186), so it is plausible that the association of ERK-2 may be regulated in a similar manner.

Lysophosphatidylcholine and nuclear import

Lysophosphatidylcholine (LPC) significantly altered nuclear protein import. The stimulatory effects of LPC were relatively large: 30 min of incubation with 10 μM LPC increased import by ~70%. The stimulation of import by LPC was observed irrespective of the methodology used to measure import. The effects of LPC were observed *in situ* in VSMC using the microinjection technique. This demonstrates its physiological relevance in VSMC and lends further confidence to the validity of the results. However, the possibility exists that several confounding artefacts associated with the use of LPC may have influenced our results. A potential source for concern is the use of BSA as our marker substrate for nuclear protein import. Lysophospholipids bind albumin (371), so it was possible that the effects on nuclear protein import were due to a non-specific association of LPC with the BSA portion of the fluorescent tracer. However, in the microinjection experiments, cells were pre-treated with LPC and rinsed off prior to microinjection. Nuclear protein import was significantly higher in LPC pre-treated cells than in controls. These results demonstrate that the LPC-stimulated augmentation of nuclear protein import is due to activation of an LPC dependent pathway rather than a non-specific association of lysolipid with the fluorophore.

Higher concentrations of LPC tend to form micelles, causing membrane breakdown (372) via a "detergent-like" action (373). A 16 carbon LPC chain (as was used in our study) does not induce critical micelle formation until LPC concentrations exceeded 10 μM. It is highly unlikely that the stimulatory effects we observed were associated with a non-specific detergent action. The lack of an effect of other lysophospholipids at 10 μM also makes it unlikely that the effects were due to a non-specific detergent action.

Conversely, the small inhibitory effects demonstrated by >10 μM LPC and during longer incubation times were likely the result of non-specific detergent effects.

Several lines of evidence suggest that the mechanism of action of LPC on nuclear protein import involves an intracellular pathway. The data acquired from the two different techniques for measuring nuclear protein import represents the first line of evidence in support of this hypothesis. In the microinjection experiments, LPC was applied to the outside of the cells and then the cells were injected with the protein import substrate. With this method, it is difficult to determine if the effects of LPC are due to an interaction with the extracellular surface of the cell or due to an intracellular mechanism of action. Either option is possible. LPC is known to passively cross the plasma membrane into the cell (297). Alternatively, LPC can interact with receptors on the cell surface to initiate a cascade of cell signaling to induce its effects (296). The cell permeabilization assay selectively examines the effects of LPC on the cell cytosol. The plasma membrane is effectively perforated by digitonin treatment of the cell and LPC is pre-incubated only with the cytosolic fraction. The stimulation of LPC in this assay system, therefore, minimizes the involvement of the cell surface in the effects of LPC on nuclear protein import in this context and instead implicates a target in the cytosol as the primary mechanism for its action.

The specificity of the stimulatory effects of the lysophosphatidylcholine and lysoplasmenylcholine species on nuclear protein import is interesting and provides another line of evidence identifying the cytosol as an important site for LPC action. The specificity of the stimulation to just LPC and LPLC suggests that the stimulation was due to a specific action of the choline head group on import. These data are consistent with

recent findings that the phosphocholine head group was necessary for the stimulation of DNA synthesis in smooth muscle cells (214). LPC can stimulate kinase activity (292) and kinases can affect nuclear protein import (341). The import substrate we constructed does not contain a phosphorylation substrate site within its NLS sequence (341). Therefore, the effects of LPC clearly did not involve phosphorylation of the imported protein itself. Instead, the results indicate, once again, a dependency upon a cytosolic factor.

The stimulation of nuclear protein import by LPC was blocked by PD-98059, strongly suggesting that MEK activity is involved in the process. Other investigators have demonstrated that LPC activates MAP kinases (291). However, the downstream target for the LPC-induced MAPK effects on nuclear transport was not as easily anticipated. A variety of proteins share a docking sequence for MAPK (321). A similar site was observed in RanGAP and was therefore selected as a candidate protein upon which to focus our attention. Our data demonstrate that LPC stimulated RanGAP activity, ostensibly through the action of the MAPK pathway (Figure 53). The involvement of MAPK in the LPC-induced stimulation of RanGAP activity is further strengthened by the observation that the addition of activated ERK-2 directly stimulates RanGAP activity (Figure 53). Although the effects of PD-98059 treatment on RanGAP activity was not assessed, it did show a significant inhibition of the LPC-mediated augmentation of nuclear import, returning levels of nuclear import to those seen in control cells (Figure 52). The effects of ERK-2 on RanGAP activity correlate well with its effects on nuclear import (Figures 37, 38, 52) and may be explained by the following mechanism. RanGAP is an upstream regulator of Ran (81, 374) and in concert with RanBP1, is essential in maintaining low levels of RanGTP in the cytosol (81, 375). As a result of the exclusively

cytoplasmic localization of RanGAP and RanBP1, a gradient is created across the nuclear envelope with low concentrations of RanGDP in the nucleus. In contrast, RanGTP concentrations are high in the nucleus and low in the cytosol (160). We hypothesize, therefore, that LPC stimulates ERK activity which in turn stimulates RanGAP activity to increase GTP hydrolysis by Ran. This will lead to a greater amount of RanGDP available for nuclear import. As more RanGDP is cycled back to the nucleus and converted to RanGTP, this will increase the nuclear concentration of RanGTP. More importin-β would then be exported in conjunction with RanGTP (either as part of trimeric export complex or bound to RanGTP alone) resulting in a greater cytoplasmic pool of importin-β available for import. The same increases in nuclear RanGTP would also affect CAS and importin-α cycling. An increase in the amount of available importin-α and β would then significantly increase nuclear import events within the cell (Figure 64). Our report is the first documentation of any lipid having such an effect on nuclear import and we have identified a unique interaction via the RanGAP pathway.

The results presented here have important functional implications during atherosclerosis. Proliferation of vascular smooth muscle cells is a critical event in atherosclerosis (351). Atherosclerotic molecules like oxidized LDL have been suggested to induce cell proliferation in a plaque through its LPC content (292, 351). LPC can also directly induce VSMC proliferation (214, 292). LPC may achieve this action by stimulating the expression of a variety of genes important in atherogenesis and cell proliferation (376, 377). In view of the key role that nucleocytoplasmic trafficking has on

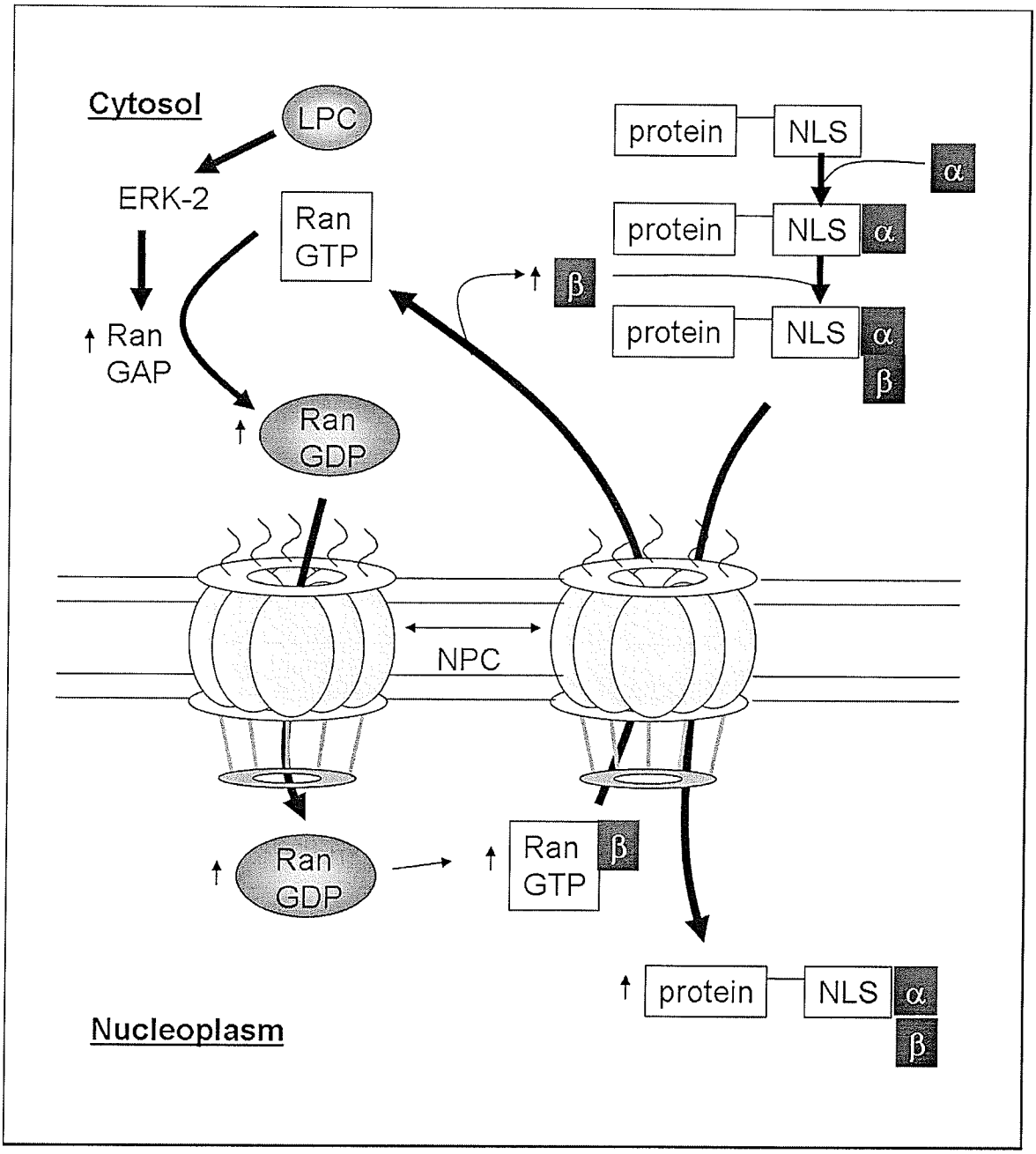

Figure 64. Hypothetical mechanism of LPC effects on nuclear import

.

In this scheme, LPC stimulates RanGAP activity which upregulates Ran-mediated GTP hydrolysis. This increases the amount of cycling RanGDP that can increase the amount of importin-β receptors cycled back to the cytoplasm. Increased cytosolic concentrations of importin-β can then lead to a global increase in nuclear protein import by the "classic" mode of import.

gene expression and protein translation, our results suggest one mechanism whereby LPC may affect VSMC proliferation through an action on nucleocytoplasmic trafficking.

The relevance of the present study may extend beyond the vasculature. The effects of LPC on nuclear protein import reported here may also partly explain the proliferative effects of LPC in cancer (378-380).

The capacity of LPC to stimulate nuclear protein import allows us to conclude that LPC may be a far more important signaling molecule in effecting changes in gene expression than previously appreciated. The relatively low concentrations of LPC that are thought to be generated *in vivo* (381) can produce a striking stimulation of nuclear protein import through an effect on the RanGAP signaling pathway. This could have important mechanistic implications for cell proliferation in atherosclerosis and other proliferative disorders.

Sphingolipids and nuclear import

The effects of ceramide on nuclear protein import were investigated in vascular smooth muscle cells. Ceramide exerted a time and dose-dependent inhibitory effect on the importin-α mediated nuclear import of a fluorescent tracer molecule bearing a "classical" (PKKKRKV) nuclear localization signal. The inhibition of nuclear protein import was even more striking (80% inhibition) (Figure 54, 55) in an *in situ* condition using cell microinjection. This further strengthens the relevance of this effect in vascular smooth muscle cells. This inhibition of nuclear protein import was not due to a non-specific, disruptive interaction of the sphingolipid with the nuclear membrane, though such an action is possible. For example, ceramide can create stable channels (266) in the

outer membrane of mitochondria (267) leading to an increase in membrane permeability. In our study, ceramide treatment induced a reversible inhibition of import. This argues strongly against a non-specific membrane disordering effect and instead suggests that the effects of ceramide were due to a specific signaling mechanism.

Although ceramide inhibition occurred in both the microinjection and permeabilized cell experiments, the degrees to which they downregulated nuclear import were significantly different. Preservation of the physiological milieu in the microinjected experiments may explain these differences, as ceramide is an essential precursor for other sphingolipids (Figure 11). Therefore, the possibility that a downstream product may affect nuclear import was considered. NOE inhibits the formation of sphingosine and glucosylceramide and would prevent ceramide from being metabolized by those branches of the sphingolipid pathway. Pre-treatment of the cytosol with NOE in the permeabilized cell assay demonstrated a significant decrease in nuclear import, approximating the levels seen with ceramide in the microinjected cell. Ceramide-1-phosphate and sphingomyelin induced a significant decrease in nuclear import and may synergistically contribute to the inhibitory effects of ceramide on nuclear import.

Previous work from our laboratory identified that H_2O_2 can inhibit nuclear protein import via an activation of MAP kinase activity (341). Therefore, it was logical to pursue the possibility that ceramide was working through the same pathway to inhibit import. Addition of the MEK inhibitor PD-98059 to the permeabilized cell assay significantly reversed ceramide dependent inhibition of nuclear protein import, suggesting that MEK kinase may be involved. However, the ERK-2 specific inhibitor, 5-iodotubercidin (327), did not reverse the inhibitory effect of ceramide. Modulation of nuclear protein import by

ceramide, therefore, did not involve ERK-2. Ceramide-dependent inhibition of nuclear protein import was reversed by the addition of SB-202190, a potent and specific p38 MAP kinase inhibitor. In support of this observation, the effects on nuclear protein import were mimicked using cytosol pre-treated with exogenously added, recombinant p38 MAP kinase. Together with the results observed above for other selective inhibitors, these data suggest that the effects of ceramide were achieved through a specific, not general, activation of the MAP kinase pathway. Ceramide, therefore, appears to target two distinctly different parts of the MAP kinase signaling system. These two sites may be complementary for the action of ceramide. Precedents exist for crosstalk between the p38 and MEK signaling pathway (382). Work by Ludwig *et al* reported that treatment of human embryonic kidney cells with arsenite caused an activation of ERK that was inhibited by the p38 MAP kinase inhibitor, SB-203580 (382). These observations were further supported by other experiments from the same study in which overexpression of a constitutively active form of p38 MAP kinase was found to stimulate ERK activity fivefold over control transfected cells in the absence of any stimuli (382). It is reasonable to propose that ceramide may stimulate p38 to activate MEK, which subsequently phosphorylates a substrate that inhibits nuclear protein import.

Although previous work has identified a MAPK-mediated inhibition of nuclear protein import by H_2O_2 (341), a target for the MAPK action was never clearly identified. CAS was selected as a potential candidate mediating the MAP kinase effects observed in our work. It is a 100 kDa protein (383) intimately involved with karyopherin dependent import (384) through its action as a nuclear exporter of importin-α (60, 85, 385). By recycling importin-α to the cytoplasm, another round of nuclear import can be initiated

(384). CAS levels change depending on the cell type as well as the metabolic state of the cell. Proliferating cells display a higher level of constitutive CAS than non-proliferating cells (83). In the present study, CAS was localized to the nucleus of untreated vascular smooth muscle cells. Scherf *et al* have demonstrated that CAS contains a MEK target motif and is a physiological phosphosubstrate for MEK (82). They demonstrated that constitutively phosphorylated CAS was localized predominantly in the cytoplasm of baby hamster kidney (BHK) cells. Upon treatment with PD-98059, CAS was redistributed to the nucleus (82). Consistent with these effects, in the present study CAS was found primarily along the nuclear periphery in vascular smooth muscle cells. This localization was not observed after treatment with 1 μM ceramide and was restored upon the addition of 20 μM PD-98059. These results suggest that the re-distribution of CAS was sensitive to MEK activation. As discussed above, the effects of p38 on CAS localization may also be attributed to crosstalk between the p38 and MEK signaling pathways. In support of this hypothesis, the distribution of CAS in ceramide-treated cells was also sensitive to treatment with 1 μM SB-202190. It is unknown if CAS possesses a motif for p38 phosphorylation. It is uncertain, therefore, if CAS may be a direct target for p38 MAP kinase activity or if it achieves its effects through crosstalk involving the MEK pathway. Alternatively, a common downstream target of both p38 and MEK may mediate the effects observed on nuclear protein import. A potential mediator is MAPKAP kinase-2. Also known as MAP kinase activated protein kinase-2, it is directly and indirectly phosphorylated by both p38 and MEK (via ERK), respectively (386, 387). These characteristics make it an attractive candidate for the proposed MAP kinase-dependent effects of ceramide on nuclear protein import. Presently, the effects of MAPKAPK-2 on

nuclear protein import have not been investigated. In light of the observations made in this thesis and current literature, the role of MAPKAPK-2 in nuclear transport regulation warrants further study.

Since CAS is the endogenous export receptor of importin-α (388) the redistribution of CAS would imply that importin-α may undergo a similar relocalization. In untreated vascular smooth muscle cells, importin-α distribution was constitutively nuclear. Pre-treatment with ceramide, however, caused a distinct non-nuclear localization of importin-α. Importin-α is critically important in shuttling proteins to the nucleus (85). Therefore, any irregularity in its localization would be expected to alter nucleocytoplasmic trafficking.

Our results identify an important action of ceramide that may have physiological and pathological relevance. Previous work has demonstrated that ceramide possesses apoptotic and anti-proliferative effects in a variety of cell types (253, 259, 260, 389, 390). Our data may in part explain this action. The results of the present study may have particular relevance for vascular smooth muscle cells. For example, Charpie *et al* demonstrated that the addition of exogenous cell-permeant ceramide exerted an anti-proliferative effect on smooth muscle cells (391). The mechanism by which this occurred, however, was unknown. Since alterations in nuclear protein import are related to changes in the proliferative state of the cell, we may conclude that one mechanism by which ceramide may exert its anti-proliferative effects is through a specific inhibition of nuclear protein import. Our data may have important implications for the proliferative status of the vasculature in various pathologic conditions. Schissel and co-workers first demonstrated that ceramide content was significantly enriched in atherosclerotic lesions

(392). This may have relevance for the increased incidence of apoptosis identified in VSMCs isolated from human atherosclerotic plaques (393). Furthermore, augmented ceramide signaling has been implicated in other conditions of accelerated vascular apoptosis (255). Conversely, impaired ceramide-mediated signaling has been suggested to be related to the intimal thickening associated with hypertension (256) and has also been presented as a treatment strategy to inhibit the neointimal hyperplasia that accompanies vascular injury (394). We propose, therefore, that one mechanism whereby ceramide may alter the vascular proliferative state and the subsequent vascular pathology is through a striking effect on nucleocytoplasmic trafficking.

The results presented here have demonstrated that regulation of nuclear transport can involve various aspects of the transport machinery. Lipids can have differential effects on nuclear protein import depending on their biochemical nature, length of exposure and concentration used in these experimental systems. The modulatory effects of lipids observed in this study were mediated by members of the MAP kinase family in a pharmacologically reversible manner. In this regard, more than one MAP kinase target was identified as responsible for the effects on nuclear protein import. Inhibition of nuclear import caused by ceramide treatment is mediated by phosphorylation of CAS, an essential factor involved in recycling of importin-α, whereas RanGAP phosphorylation was observed to participate in the LPC-mediated augmentation of nuclear transport. The targets identified for the two lipid species may also account for the biphasic, dose dependent effects of ERK-2 treatment on nuclear protein import. The data presented here demonstrate important and novel effects of lipids on nucleocytoplasmic transport in

vascular smooth muscle cells and this information will be of particular relevance in elucidating the mechanism of lipid mediated vascular pathologies.

REFERENCES

1. **M. Mazzanti, J. O. Bustamante and H. Oberleithner**. 2001. Electrical dimension of the nuclear envelope. *Physiol Rev.* 1:1-19.

2. **N. Panté and U. Aebi**. 1996. Molecular dissection of the nuclear pore complex. *Crit Rev Biochem Mol Biol.* 31:153-199.

3. **D. Kalderon, W. D. Richardson, A. F. Markham and A. E. Smith**. 1984. Sequence requirements for nuclear location of simian virus 40 large-T antigen. *Nature.* 311:33-8.

4. **C. Dingwall, S. V. Sharnick and R. A. Laskey**. 1982. A polypeptide domain that specifies migration of nucleoplasmin into the nucleus. *Cell.* 30:449-458.

5. **C. Dingwall, S. M. Dilworth, S. J. Black, S. E. Kearsey, L. S. Cox and R. A. Laskey**. 1987. Nucleoplasmin cDNA sequence reveals polyglutamic acid tracts and a cluster of sequences homologous to putative nuclear localization signals. *EMBO J.* 6:69-74.

6. **H. Siomi and G. Dreyfuss**. 1995. A nuclear localization domain in the hnRNP A1 protein. *J Cell Biol.* 129:551-560.

7. **J. Robbins, S. M. Dilworth, R. A. Laskey and C. Dingwall**. 1991. Two interdependent basic domains in nucleoplasmin nuclear targeting sequence: Identification of a class of bipartite nuclear targeting sequence. *Cell.* 64:615-623.

8. **N. Imamoto**. 2000. Diversity in nucleocytoplasmic transport pathways. *Cell Struct Funct.* 25:207-216.

9. **J. Huber, U. Cronshagen, M. Kadokura, C. Marshallsay, T. Wada, M. Sekine and R. Lührmann**. 1998. Snurportin1, an m_3G-cap-specific nuclear import receptor with a novel domain structure. *EMBO J.* 17:4114-4126.

10. **D. Jullien, D. Görlich, U. K. Laemmli and Y. Adachi**. 1999. Nuclear import of RPA in *Xenopus* egg extracts requires a novel protein XRIPα but not importin α. *EMBO J.* 18:4348-4358.

11. **B. R. Henderson and A. Eleftheriou**. 2000. A comparison of the activity, sequence specificity, and CRM1-dependence of different nuclear export signals. *Exp Cell Res.* 256:213-224.

12. **B. R. Cullen**. 2003. Nuclear RNA export. *J Cell Sci.* 116:587-597.

13. **J. Zhu, F. Shibasaki, R. Price, J. C. Guillemot, T. Yano, V. Dötsch, G. Wagner, P. Ferrara and F. McKeon**. 1998. Intramolecular masking of nuclear import signal on NF-AT4 by casein kinase I and MEKK1. *Cell.* 93:851-861.

14. **H. Okamura, J. Aramburu, C. Garcia-Rodriguez, J. P. Viola, A. Raghavan, M. Tahiliani, X. Zhang, J. Qin, P. G. Hogan and A. Rao**. 2000. Concerted dephosphorylation of the transcription factor NFAT1 induces a conformational switch that regulates transcriptional activity. *Mol Cell.* 6:539-550.

15. **P. G. d. Arco, S. Martínez-Martínez, J. L. Maldonado, I. Ortega-Pérez and J. M. Redondo**. 2000. A role for the p38 MAP kinase pathway in the nuclear shuttling of NFATp. *J Biol Chem.* 275:13872-13878.

16. **R. T. Hay, L. Vuillard, J. M. Desterro and M. S. Rodriguez**. 1999. Control of NF-kappa B transcriptional activation by signal induced proteolysis of I kappa B alpha. *Philos Trans R Soc Lond B Biol Sci.* 354:1601-9.

17. **H. P. Rihs, D. A. Jans, H. Fan and R. Peters**. 1991. The rate of nuclear cytoplasmic protein transport is determined by the casein kinase II site flanking the nuclear localization sequence of the SV40 T-antigen. *EMBO J.* 10:633-639.

18. **M. J. Matunis, J. Wu and G. Blobel**. 1998. SUMO-1 modification and its role in targeting the RanGTPase-activating protein, RanGAP1, to the nuclear pore complex. *J Cell Biol.* 140:499-509.

19. **F. Melchior, M. Schergaut and A. Pichler**. 2003. SUMO: ligases, isopeptidases and nuclear pores. *Trends Biochem Sci.* 28:612-618.

20. **C. Elfgang, O. Rosorius, L. Hofer, H. Jaksche, J. Hauber and D. Bevec**. 1999. Evidence for specific nucleocytoplasmic transport pathways used by leucine-rich nuclear export signals. *Proc Natl Acad Sci USA.* 96:6229-6234.

21. **W. Wen, J. L. Meinkoth, R. Y. Tsien and S. S. Taylor**. 1995. Identification of a signal for rapid export of proteins from the nucleus. *Cell.* 82:463-473.

22. **C. Julien, P. Coulombe and S. Meloche**. 2003. Nuclear export of ERK3 by a CRM1-dependent mechanism regulates its inhibitory action on cell cycle progression. *J Biol Chem.* 278:42615-42624.

23. **A. Herold, R. Truant, H. Wiegand and B. R. Cullen**. 1998. Determination of the functional domain organization of the importin α nuclear import factor. *J Cell Biol.* 143:309-318.

24. **J. M. Holaska, B. E. Black, D. C. Love, J. A. Hanover, J. Leszyk and B. M. Paschal**. 2001. Calreticulin is a receptor for nuclear export. *J Cell Biol.* 152:127-140.

25. **Y. Kang and B. R. Cullen**. 1999. The human TAP protein is a nuclear mRNA export factor that contains novel RNA-binding and nucleocytoplasmic transport sequences. *Genes Dev.* 13:1126-1139.

26. **A. Segref, K. Sharma, V. Doye, A. Hellwig, J. Huber, R. Lührmann and E. Hurt**. 1997. Mex67p, a novel factor for nuclear mRNA export, binds to both poly(A)$^+$ RNA and nuclear pores. *EMBO J.* 16:3256-3271.

27. **K. Tasken and E. M. Aandahl**. 2004. Localized effects of cAMP mediated by distinct routes of protein kinase A. *Physiol Rev.* 84:137-167.

28. **R. Feil, S. M. Lohmann, H. deJonge, U. Walter and F. Hofmann**. 2003. Cyclic GMP-dependent protein kinases and the cardiovascular system: insights from genetically modified mice. *Circ Res.* 93:907-916.

29. **J. Schlossmann, R. Feil and F. Hofmann**. 2003. Signaling through NO and cGMP-dependent protein kinases. *Ann Med.* 35:21-27.

30. **E. K. Heist and H. Schulman**. 1998. The role of Ca2+/calmodulin-dependent protein kinases within the nucleus. *Cell Calcium.* 23:103-114.

31. **M. Sugiura, K. Kono, H. Liu, T. Shimizugawa, H. Minekura, S. Spiegel and T. Kohama**. 2002. Ceramide kinase, a novel lipid kinase. Molecular cloning and functional characterization. *J Biol Chem.* 277:23294-23300.

32. **H. Kanoh, K. Yamada and F. Sakane**. 2002. Diacylglycerol kinases: emerging downstream regulators in cell signaling systems. *J Biochem (Tokyo).* 131:629-633.

33. **A. V. Alessenko and E. B. Burlakova**. 2002. Functional role of phospholipids in the nuclear events. *Bioelectrochemistry.* 58:13-21.

34. **S. Klumpp and J. Krieglstein**. 2002. Phosphorylation and dephosphorylation of histidine residues in proteins. *Eur J Biochem.* 269:1067-1071.

35. **A. V. Khokhlatchev, B. Canagarajah, J. Wilsbacher, M. Robinson, M. Atkinson, E. Goldsmith and M. H. Cobb**. 1998. Phosphorylation of the MAP kinase ERK2 promotes its homodimerization and nuclear translocation. *Cell.* 93:605-615.

36. **C.-Y. Xiao, S. Hübner and D. A. Jans**. 1997. SV40 large tumor antigen nuclear import is regulated by the double-stranded DNA-dependent protein kinase site

(serine 120) flanking the nuclear localization sequence. *J Biol Chem.* 272:22191-22198.

37. **D. Barford, A. K. Das and M.-P. Egloff**. 1998. The structure and mechanism of protein phosphatases: insights into catalysis and regulation. *Annu Rev Biophys Biomol Struct.* 27:133-164.

38. **N. K. Tonks and P. Cohen**. 1983. Calcineurin is a calcium ion-dependent, calmodulin-stimulated protein phosphatase. *Biochim Biophys Acta.* 747:191-193.

39. **M. Bollen and M. Beullens**. 2002. Signaling by protein phosphatases in the nucleus. *Trends Cell Biol.* 12:138-145.

40. **E. J. Lubert and K. D. Sarge**. 2003. Interaction between protein phosphatase 2A and members of the importin β superfamily. *Biochem Biophys Res Comm.* 303:908-913.

41. **D. Görlich and U. Kutay**. 1999. Transport between the cell nucleus and the cytoplasm. *Annu Rev Cell Dev Biol.* 15:607-660.

42. **E. J. H. Adam and S. A. Adam**. 1994. Identification of cytosolic factors required for nuclear location sequence-mediated binding to the nuclear envelope. *J Cell Biol.* 125:547-555.

43. **A. Radu, G. Blobel and M. S. Moore**. 1995. Identification of a protein complex that is required for nuclear protein import and mediates docking of import substrate to distinct nucleoporins. *Proc Natl Acad Sci USA.* 92:1769-1773.

44. **N. C. Chi, E. J. H. Adam and S. A. Adam**. 1995. Sequence and characterization of cytoplasmic nuclear protein import factor p97. *J Cell Biol.* 130:265-274.

45. **G. Cingolani, C. Petosa, K. Weis and C. W. Müller**. 1999. Structure of importin-β bound to the IBB domain of importin-α. *Nature.* 399:221-229.

46. **U. Kutay, E. Izaurralde, F. R. Bischoff, I. W. Mattaj and D. Görlich**. 1997. Dominant-negative mutants of importin-β block multiple pathways of import and export through the nuclear pore complex. *EMBO J.* 16:1153-1163.

47. **N. C. Chi and S. A. Adam**. 1997. Functional domains in nuclear import factor p97 for binding the nuclear localization sequence receptor and the nuclear pore. *Mol Biol Cell.* 8:945-956.

48. **N. C. Chi, E. J. H. Adam and S. A. Adam**. 1997. Different binding domains for Ran-GTP and Ran-GDP/RanBP1 on nuclear import factor p97. *J Biol Chem.* 272:6818-6822.

49. **S. A. Adam and L. Gerace**. 1991. Cytosolic proteins that specifically bind nuclear location signals are receptors for nuclear import. *Cell*. 66:837-847.

50. **G. Cingolani, H. A. Lashuel, L. Gerace and C. W. Müller**. 2000. Nuclear import factors importin α and importin β undergo mutually induced conformational changes upon association. *FEBS Lett*. 484:291-298.

51. **D. Palmeri and M. H. Malim**. 1999. Importin beta can mediate the nuclear import of an arginine-rich nuclear localization signal in the absence of importin alpha. *Mol Cell Biol*. 19.

52. **B. R. Henderson and P. P.** 1997. Interactions between HIV Rev and nuclear import and export factors: the Rev nuclear localisation signal mediates specific binding to human importin-beta. *J Mol Biol*. 274.

53. **R. Truant and B. R. Cullen**. 1999. The arginine-rich domains present in human immunodeficiency virus type 1 tat and rev function as direct importin beta-dependent nuclear localization signals. *Mol Cell Biol*. 19.

54. **S. Jäkel and D. Görlich**. 1998. Importin beta, transportin, RanBP5 and RanBP7 mediate nuclear import of ribosomal proteins in mammalian cells. *EMBO J*. 17:4491-4502.

55. **M. H. C. Lam, L. J. Briggs, W. Hu, T. J. Martin, M. T. Gillespie and D. A. Jans**. 1999. Importin β recognizes parathyroid hormone-related protein with high affinity and mediates its nuclear import in the absence of importin α. *J Biol Chem*. 274:7391-7398.

56. **E. Conti, M. Uy, L. Leighton, G. Blobel and J. Kuriyan**. 1998. Crystallographic analysis of the recognition of a nuclear localization signal by the nuclear import factor karyopherin α. *Cell*. 94:193-204.

57. **M. R. M. Fontes, T. Teh and B. Kobe**. 2000. Structural basis of recognition of monopartite and bipartite nuclear localization sequences by mammalian importin-α. *J Mol Biol*. 297:1183-1194.

58. **K. Melén, R. Fagerlund, J. Franke, M. Köhler, L. Kinnunen and I. Julkunnen**. 2003. Importin α nuclear localization signal binding sites for STAT1, STAT2, and influenza A virus nucleoprotein. *J Biol Chem*. 278:28193-28200.

59. **J. K. Hood and P. A. Silver**. 1998. Cse1p is required for export of Srp1p/importin-α from the nucleus in *Saccharomyces cerevisiae*. *J Biol Chem*. 273:35142-35146.

60. **U. Kutay, F. R. Bischoff, S. Kostka, R. Kraft and D. Görlich**. 1997. Export of importin α from the nucleus is mediated by a specific nuclear transport factor. *Cell*. 90:1061-1071.

61. **B. Kobe**. 1999. Autoinhibition by an internal nuclear localization signal revealed by the crystal structure of mammalian importin α. *Nat Struct Biol.* 6:388-397.

62. **M. T. Harreman, M. R. Hodel, P. Fanara, A. E. Hodel and A. H. Corbett**. 2003. The auto-inhibitory function of importin α is essential *in vivo*. *J Biol Chem.* 278:5854-5863.

63. **M. Köhler, C. Speck, M. Christiansen, F. R. Bischoff, S. Prehn, H. Haller, D. Görlich and E. Hartmann**. 1999. Evidence for distinct substrate specificities of importin α family members in nuclear protein import. *Mol Cell Biol.* 19:7782-7791.

64. **Y. Kamei, S. Yuba, T. Nakayama and Y. Yoneda**. 1999. Three distinct classes of the α-subunit of the nuclear pore-targeting complex (importin-α) are differentially expressed in adult mouse tissues. *J Histochem Cytochem.* 47:363-372.

65. **B. Talcott and M. S. Moore**. 2000. The nuclear import of RCC1 requires a specific nuclear localization sequence receptor, karyopherin α3/Qip. *J Biol Chem.* 275:10099-10104.

66. **J. Huber, A. Dickmanns and R. Lührmann**. 2002. The importin-β binding domain of snurportin1 is responsible for the Ran- and energy-independent nuclear import of spliceosomal U snRNPs in vitro. *J Cell Biol.* 156:467-479.

67. **A. Belmont**. 2003. Dynamics of chromatin, proteins, and bodies within the cell nucleus. *Curr Opin Cell Biol.* 15:304-310.

68. **M. Bäuerle, D. Doenecke and W. Albig**. 2002. The requirement of H1 histones for a heterodimeric nuclear import receptor. *J Biol Chem.* 277:32480-32489.

69. **D. T. Brown**. 2003. Histone H1 and the dynamic regulation of chromatin function. *Biochem Cell Biol.* 81:221-227.

70. **S. Jäkel, W. Albig, U. Kutay, F. R. Bischoff, K. Schwamborn, D. Doenecke and D. Görlich**. 1999. The importin beta/importin 7 heterodimer is a functional nuclear import receptor for histone H1. *EMBO J.* 18:2411-2423.

71. **M. S. Wold**. 1997. Replication protein A: heterotrimeric, single-stranded DNA-binding protein required for eukaryotic DNA metabolism. *Annu Rev Biochem.* 66:61-92.

72. **Y. Adachi and U. K. Laemmli**. 1994. Study of the cell cycle-dependent assembly of the DNA pre-replication centers in *Xenopus* egg extracts. *EMBO J.* 13:4153-4164.

73. **S. P. Moore, L. Erdile, T. Kelly and R. Fishel**. 1991. The human homologous pairing protein HPP-1 is specifically stimulated by the cognate single-stranded binding protein hRP-A. *Proc Natl Acad Sci USA*. 88:9067-9071.

74. **A. Shinohara, M. Shinohara, T. Ohta, S. Matsuda and T. Ogawa**. 1998. Rad52 forms ring structures and co-operates with RPA in single-strand DNA annealing. *Genes Cells*. 3:145-156.

75. **M. P. Longhese, P. Plevani and G. Lucchini**. 1994. Replication factor A is required *in vivo* for DNA replication, repair and recombination. *Mol Cell Biol*. 14:7884-7890.

76. **J. H. New, T. Sugiyama, E. Zaitseva and S. C. Kowalczykowski**. 1998. Rad52 protein stimulates DNA strand exchange by Rad51 and replication protein A. *Nature*. 391:407-410.

77. **H. M. Fried and U. Kutay**. 2003. Nucleocytoplasmic transport: taking an inventory. *Cell Mol Life Sci*. 60:1659-1688.

78. **M. Fornerod, M. Ohno, M. Yoshida and I. W. Mattaj**. 1997. CRM1 is an export receptor for leucine-rich nuclear export signals. *Cell*. 90:1051-1060.

79. **U. Fischer, J. Huber, W. C. Boelens, I. W. Mattaj and R. Lührmann**. 1995. The HIV-1 Rev activation domain is a nuclear export signal that accesses an export pathway used by specific cellular RNAs. *Cell*. 82:475-483.

80. **K. S. Ullman, S. Shah, M. A. Powers and D. J. Forbes**. 1999. The nucleoporin nup153 plays a critical role in multiple types of nuclear export. *Mol Biol Cell*. 10:649-664.

81. **F. R. Bischoff, C. Klebe, J. Kretschmer, A. Wittinghofer and H. Ponstingl**. 1994. RanGAP1 induces GTPase activity of nuclear ras-related Ran. *Proc Natl Acad Sci USA*. 91:2587-2591.

82. **U. Scherf, P. Kalab, M. Dasso, I. Pastan and U. Brinkmann**. 1998. The hCSE1/CAS protein is phosphorylated by HeLa extracts and MEK-1: MEK-1 phosphorylation may modulate the intracelluar localization of CAS. *Biochem Biophys Res Comm*. 250:623-628.

83. **U. Scherf, I. Pastan, M. C. Willingham and U. Brinkmann**. 1996. The human CAS protein which is homologous to the CSE1 yeast chromosome segregation gene product is associated with microtubules and mitotic spindle. *Proc Natl Acad Sci USA*. 93:2670-2674.

84. **V. V. Ogryzko, E. Brinkmann, B. H. Howard, I. Pastan and U. Brinkmann**. 1997. Antisense inhibition of CAS, the human homologue of the yeast

chromosome segregation gene CSE1, interferes with mitosis in HeLa cells. *Biochemistry*. 36:9493-9500.

85. **P. Behrens, U. Brinkmann and A. Wellmann**. 2003. CSE1L/CAS: Its role in proliferation and apoptosis. *Apoptosis*. 8:39-44.

86. **N. Mesaeli, K. Nakamura, E. Zvaritch, P. Dickie, E. Dziak, K.-H. Krause, M. Opas, D. H. MacLennan and M. Michalak**. 1999. Calreticulin is essential for cardiac development. *J Cell Biol*. 144:857-868.

87. **J. Li, M. Pucéat, C. Perez-Terzic, A. Mery, K. Nakamura, M. Michalak, K.-H. Krause and M. E. Jaconi**. 2002. Calreticulin reveals a critical Ca^{2+} checkpoint in cardiac myofibrillogenesis. *J Cell Biol*. 158:103-113.

88. **R. E. Walther, C. Lamprecht, A. Ridsdale, I. Groulx, S. Lee, Y. A. Lefebvre and R. J. G. Haché**. 2003. Nuclear export of the glucocorticoid receptor is accelerated by cell fusion-dependent release of calreticulin. *J Biol Chem*. 278:37858-37864.

89. **D. B. DeFranco**. 2001. Nuclear export: DNA-binding domains find a surprising partner. *Curr Biol*. 11:R1036-R1037.

90. **J. M. Holaska, B. E. Black, F. Rastinejad and B. M. Paschal**. 2002. Ca^{2+}-dependent nuclear export mediated by calreticulin. *Mol Cell Biol*. 22:6286-6297.

91. **M. Michalak, E. F. Corbett, N. Mesaeli, K. Nakamura and M. Opas**. 1999. Calreticulin: one protein, one gene, many functions. *Biochem J*. 344:281-292.

92. **G.-J. Arts, S. Kuersten, P. Romby, B. Ehresmann and I. W. Mattaj**. 1998. The role of exportin-t in selective nuclear export of mature tRNAs. *EMBO J*.

93. **U. Kutay, G. Lipowsky, E. Izaurralde, F. R. Bischoff, P. Schwarzmaier, E. Hartmann and D. Görlich**. 1998. Identification of a tRNA-specific nuclear export receptor. *Mol Cell*. 1:359-369.

94. **A. Calado, N. Treichel, E. C. Müller, A. Otto and U. Kutay**. 2002. Exportin-5-mediated nuclear export of eukaryotic elongation factor 1A and tRNA. *EMBO J*. 21:6216-6224.

95. **I. Schmitt and L. Gerace**. 2001. *In vitro* analysis of nuclear transport mediated by the C-terminal shuttle domain of Tap. *J Biol Chem*. 276.

96. **L. Lévesque, B. Guzik, T. Guan, J. Coyle, B. E. Black, D. Rekosh, M.-L. Hammarskjöld and B. M. Paschal**. 2001. RNA export mediated by Tap involves NXT1-dependent interactions with the nuclear pore complex. *J Biol Chem*. 276:44953-44962.

97. **B. W. Guzik, L. Levesque, S. Prasad, Y. C. Bor, B. E. Black, B. M. Paschal, D. Rekosh and M. L. Hammarskjöld**. 2001. NXT1 (p15) is a crucial cellular cofactor in TAP-dependent export of intron-containing RNA in mammalian cells. *Mol Cell Biol.* 21:2545-2554.

98. **H. L. Wiegand, G. A. Coburn, Y. Zeng, Y. Kang, H. P. Bogerd and B. R. Cullen**. 2002. Formation of Tap/NXT1 heterodimers activates Tap-dependent nuclear mRNA export by enhancing recruitment to nuclear pore complexes. *Mol Cell Biol.* 22:245-256.

99. **W. Gilbert and C. Guthrie**. 2004. The Glc7p nuclear phosphatase promotes mRNA export by facilitating association of Mex67p with mRNA. *Mol Cell.* 13:201-212.

100. **E. Hurt, M. J. Luo, S. Rother, R. Reed and K. Strasser**. 2004. Cotranscriptional recruitment of the serine-arginine-rich (SR)-like proteins Gbp2 and Hrb1 to nascent mRNA via the TREX complex. *Proc Natl Acad Sci USA.* 101:1858-1862.

101. **K. A. Dean, O. vonAhsen, D. Görlich and H. M. Fried**. 2001. Signal recognition particle protein 19 is imported into the nucleus by importin 8 (RanBP8) and transportin. *J Cell Sci.* 114:3479-3485.

102. **R. H. Kehlenbach and L. Gerace**. 2000. Phosphorylation of the nuclear transport machinery down-regulates nuclear protein import *in vitro*. *J Biol Chem.* 275:17848-17856.

103. **D. J. Forbes**. 1992. Structure and function of the nuclear pore complex. *Annu Rev Cell Biol.* 8.

104. **J. E. Hinshaw**. 1994. Architecture of the nuclear pore complex and its involvement in nucleocytoplasmic transport. *Biochem Pharmacol.* 47:15-20.

105. **J. E. Hinshaw, B. O. Carragher and R. A. Milligan**. 1992. Architecture and design of the nuclear pore complex. *Cell.* 69:1133-1141.

106. **N. Panté and U. Aebi**. 1993. The nuclear pore complex. *J Cell Biol.* 122:977-984.

107. **N. Panté and U. Aebi**. 1995. Exploring nuclear pore complex structure and function in molecular detail. *J Cell Sci.* Supplement 19:1-11.

108. **S. A. Adam**. 2001. The nuclear pore complex. *Genome Biol.* 2:1-6.

109. **M. Miller, M. K. Park and J. A. Hanover**. 1991. Nuclear pore complex: structure, function, and regulation. *Physiol Rev.* 71:909-949.

110. **K. J. Ryan and S. R. Wente**. 2000. The nuclear pore complex: a protein machine bridging the nucleus and cytoplasm. *Curr Opin Cell Biol.* 12:361-371.

111. **M. P. Rout, J. D. Aitchison, A. Suprapto, K. Hjertaas, Y. Zhao and B. T. Chait.** 2000. The yeast nuclear pore complex: composition, architecture, and transport mechanism. *J Cell Biol.* 148:635-651.

112. **N. Panté, F. Thomas, U. Aebi, B. Burke and R. Bastos**. 2000. Recombinant Nup153 incorporates *in vivo* into *Xenopus* oocyte nuclear pore complexes. *J Struct Biol.* 129:306-312.

113. **C. W. Akey and M. Radermacher**. 1993. Architecture of the *Xenopus* nuclear pore complex revealed by three-dimensional cryo-electron microscopy. *J Cell Biol.* 122:1-19.

114. **T. Danker and H. Oberleithner**. 2000. Nuclear pore function viewed with atomic force microscopy. *Pflugers Arch.* 439:671-681.

115. **N. Panté and M. Kann**. 2002. Nuclear pore complex is able to transport macromolecules with diameters of ~39 nm. *Mol Biol Cell.* 13:425-434.

116. **C. Feldherr, D. Akin and M. S. Moore**. 1998. The nuclear import factor p10 regulates the functional size of the nuclear pore complex during oogenesis. *J Cell Sci.* 111:1889-1896.

117. **C. M. Feldherr, D. Akin and R. J. Cohen**. 2001. Regulation of functional nuclear pore size in fibroblasts. *J Cell Sci.* 114:4621-4627.

118. **C. Perez-Terzic, M. Jaconi and D. E. Clapham**. 1997. Nuclear calcium and the regulation of the nuclear pore complex. *Bioessays.* 19:787-792.

119. **C. Perez-Terzic, J. Pyle, M. Jaconi, L. Stehno-Bittel and D. E. Clapham**. 1996. Conformational states of the nuclear pore complex induced by depletion of nuclear Ca^{2+}stores. *Science.* 273:1875-1877.

120. **O. Keminer and R. Peters**. 1999. Permeability of single nuclear pores. *Biophys J.* 77:217-228.

121. **V. Shahin, T. Danker, K. Enss, R. Ossig and H. Oberleithner**. 2001. Evidence for Ca^{2+}- and ATP-sensitive peripheral channels in nuclear pore complexes. *FASEB J.* 15:1895-1901.

122. **D. Stoffler, B. Feja, B. Fahrenkrog, J. Walz, D. Typke and U. Aebi**. 2003. Cryo-electron tomography provides novel insights into nuclear pore architecture: implications for nucleocytoplasmic transport. *J Mol Biol.* 328:119-130.

123. **N. Yokoyama, N. Hayashi, T. Seki, N. Panté, T. Ohba, K. Nishii, K. Kuma, T. Hayashida, T. Miyata, U. Aebi, M. Fukui and T. Nishimoto**. 1995. A giant nucleopore protein that binds Ran/TC4. *Nature*. 376:184-188.

124. **N. R. Yaseen and G. Blobel**. 1999. Two distinct classes of Ran-binding sites on the nucleoporin Nup-358. *Proc Natl Acad Sci USA*. 96:5516-5521.

125. **N. R. Yaseen and G. Blobel**. 1999. GTP hydrolysis links initiation and termination of nuclear import on the nucleoporin Nup358. *J Biol Chem*. 274:26493-26502.

126. **J. Wu, M. J. Matunis, D. Kraemer, G. Blobel and E. Coutavas**. 1995. Nup358, a cytoplasmically exposed nucleoporin with peptide repeats, Ran-GTP binding sites, zinc fingers, a cyclophilin A homologous domain, and a leucine rich region. *J Biol Chem*. 270:14209-14213.

127. **M. W. Goldberg and T. D. Allen**. 1992. High resolution scanning electron microscopy of the nuclear envelope: demonstration of a new, regular, fibrous lattice attached to the baskets of the nucleoplasmic face of the nuclear pores. *J Cell Biol*. 119:1429-1440.

128. **B. Fahrenkrog, B. Maco, A. M. Fager, J. Köser, U. Sauder, K. S. Ullman and U. Aebi**. 2002. Domain-specific antibodies reveal multiple-site topology of Nup153 within the nuclear pore complex. *J Struct Biol*. 140:254-267.

129. **N. Daigle, J. Beaudouin, L. Hartnell, G. Imreh, E. Hallberg, J. Lippincott-Schwartz and J. Ellenberg**. 2001. Nuclear pore complexes form immobile networks and have a very low turnover in live mammalian cells. *J Cell Biol*. 154:71-84.

130. **D. Moore-Nichols, A. Arnott and R. C. Dunn**. 2002. Regulation of nuclear pore complex conformation by IP_3 receptor activation. *Biophys J*. 83:1421-1428.

131. **C. Perez-Terzic, A. M. Gacy, R. Bortolon, P. P. Dzeja, M. Puceat, M. Jaconi, F. G. Prendergast and A. Terzic**. 1999. Structural plasticity of the cardiac nuclear pore complex in response to regulators of nuclear import. *Circ Res*. 84:1292-1301.

132. **M. W. Goldberg, S. A. Rutherford, M. Hughes, L. A. Cotter, S. Bagley, E. Kiseleva, T. D. Allen and P. R. Clarke**. 2000. Ran alters nuclear pore complex conformation. *J Mol Biol*. 300:519-529.

133. **D. Stoffler, K. N. Goldie, B. Feja and U. Aebi**. 1999. Calcium-mediated structural changes of native nuclear pore complexes monitored by time-lapse atomic force microscopy. *J Mol Biol*. 287:741-752.

134. **J. O. Bustamante, E. R. F. Michelette, J. P. Geibel, D. A. Dean, J. A. Hanover and T. J. McDonnell**. 2000. Calcium, ATP and nuclear pore channel gating. *Pflügers Arch*. 439:433-444.

135. **T. C. Walther, P. Askjaer, M. Gentzel, A. Habermann, G. Griffiths, M. Wilm, I. W. Mattaj and M. Hetzer**. 2003. RanGTP mediates nuclear pore complex assembly. *Nature*. 424:689-694.

136. **A. Harel, R. C. Chan, A. Lachish-Zalait, E. Zimmerman, M. Elbaum and D. J. Forbes**. 2003. Importin β negatively regulates nuclear membrane fusion and nuclear pore complex assembly. *Mol Biol Cell*. 14:4387-4396.

137. **V. C. Cordes, H.-R. Rackwitz and S. Reidenbach**. 1997. Mediators of nuclear protein import target karyophilic proteins to pore complexes of cytoplasmic annulate lamellae. *Exp Cell Res*. 237:419-433.

138. **G. Imreh and E. Hallberg**. 2000. An integral membrane protein from the nuclear pore complex is also present in the annulate lamellae: implications for annulate lamellae formation. *Exp Cell Res*. 259:180-190.

139. **A. Ewald, U. Kossner, U. Scheer and M. C. Dabauvalle**. 1996. A biochemical and immunological comparison of nuclear and cytoplasmic pore complexes. *J Cell Sci*. 109:1813-1824.

140. **N. Belgareh and V. Doye**. 1997. Dynamics of nuclear pore distribution in nucleoporin mutant yeast cells. *J Cell Biol*. 136:747-759.

141. **C. Favreau, R. Bastos, J. Cartaud, J. C. Courvalin and P. Mustonen**. 2001. Biochemical characterization of nuclear pore complex protein gp210. *Eur J Biochem*. 268:3883-3889.

142. **M. Kihlmark, G. Imreh and E. Hallberg**. 2001. Sequential degradation of proteins from the nuclear envelope during apoptosis. *J Cell Sci*. 114:3643-3653.

143. **B. Lenz-Böhme, J. Wismar, S. Fuchs, R. Reifegerste, E. Buchner, H. Betz and B. Schmitt**. 1997. Insertional mutation of the *Drosophila* nuclear lamin Dm_0 gene results in defective nuclear envelopes, clustering of nuclear pore complexes, and accumulation of annulate lamellae. *J Cell Biol*. 137:1001-1016.

144. **C. V. Heath, C. S. Copeland, D. C. Amberg, V. D. Priore, M. Snyder and C. N. Cole**. 1995. Nuclear pore complex clustering and nuclear accumulation of poly(A)+ RNA associated with mutation of the *Saccharomyces cerevisiae RAT2/NUP120* gene. *J Cell Biol*. 131:1677-1697.

145. **J. D. Aitchison, G. Blobel and M. P. Rout**. 1995. Nup120p: a yeast nucleoporin required for NPC distribution and mRNA transport. *J Cell Biol*. 131:1659-1675.

146. **L. F. Pemberton, M. P. Rout and G. Blobel**. 1995. Disruption of the nucleoporin gene *NUP133* results in clustering of nuclear pore complexes. *Proc Natl Acad Sci USA*. 92:1187-1191.

147. **G. D. Maul and L. Deaven**. 1977. Quantitative determination of nuclear pore complexes in cycling cells with differing DNA content. *J Cell Biol*. 73:748-760.

148. **G. G. Maul, L. L. Deaven, J. J. Freed, G. L. M. Campbell and W. Beçak**. 1980. Investigation of the determinants of nuclear pore number. *Cytogenet Cell Genet*. 26:175-190.

149. **H. M. Maul, B. Y. L. Hsu, T. M. Borun and G. G. Maul**. 1973. Effect of metabolic inhibitors on nuclear pore formation during the HeLa S_3 cycle. *J Cell Biol*. 59:669-676.

150. **T. Iouk, O. Kerscher, R. J. Scott, M. A. Basrai and R. W. Wozniak**. 2002. The yeast nuclear pore complex functionally interacts with components of the spindle assembly checkpoint. *J Cell Biol*. 159:807-819.

151. **D. Salina, P. Enarson, J. B. Rattner and B. Burke**. 2003. Nup358 integrates nuclear envelope breakdown with kinetochore assembly. *J Cell Biol*. 162:991-1001.

152. **P. T. Stukenberg and I. G. Macara**. 2003. The kinetochore NUPtials. *Nat Cell Biol*. 5:945-947.

153. **M. P. Rout and S. R. Wente**. 1994. Pores for thought: nuclear pore complex proteins. *Trends Cell Biol*. 4:357-365.

154. **X. Wu, L. H. Kasper, R. T. Mantcheva, G. T. Mantchev, M. J. Springett and J. M. A. vanDeursen**. 2001. Disruption of the FG nucleoporin NUP98 causes selective changes in nuclear pore complex stoichiometry and function. *Proc Natl Acad Sci USA*. 98:3191-3196.

155. **M. A. Powers, D. J. Forbes, J. E. Dahlberg and E. Lund**. 1997. The vertebrate GLFG nucleoporin, Nup98, is an essential component of multiple RNA export pathways. *J Cell Biol*. 136:241-250.

156. **R. Bayliss, T. Littlewood and M. Stewart**. 2000. Structural basis for the interaction between FxFG nucleoporin repeats and importin-β in nuclear trafficking. *Cell*. 102:99-108.

157. **I. Ben-Efraim and L. Gerace**. 2001. Gradient of increasing affinity of importin beta for nucleoporins along the pathway of nuclear import. *Journal of Cell Biology*. 152:411-417.

158. **K. Ribbeck and D. Görlich**. 2001. Kinetic analysis of translocation through nuclear pore complexes. *EMBO J.* 20:1320-1330.

159. **I. G. Macara**. 2001. Transport into and out of the nucleus. *Microbiol Mol Biol Rev.* 65:570-594.

160. **E. Izaurralde, U. Kutay, C. vonKobbe, I. W. Mattaj and D. Görlich**. 1997. The asymmetric distribution of the constituents of the Ran system is essential for transport into and out of the nucleus. *EMBO J.* 16:6535-6547.

161. **R. T. Pu and M. Dasso**. 1997. The balance of RanBP1 and RCC1 is critical for nuclear assembly and nuclear transport. *Mol Biol Cell.* 8:1955-1970.

162. **J. M. Avis and P. R. Clarke**. 1996. Ran, a GTPase involved in nuclear processes: its regulators and effectors. *J Cell Sci.* 109:2423-2427.

163. **Y. Azuma and M. Dasso**. 2000. The role of Ran in nuclear function. *Curr Opin Cell Biol.* 12:302-307.

164. **M. V. Nachury and K. Weis**. 1999. The direction of transport through the nuclear pore can be inverted. *Proc Natl Acad Sci USA.* 96:9622-9627.

165. **R. H. Kehlenbach, A. Dickmanns, A. Kehlenbach, T. Guan and L. Gerace**. 1999. A role for RanBP1 in the release of CRM1 from the nuclear pore complex in a terminal step of nuclear export. *J Cell Biol.* 145:645-657.

166. **B. B. Singh, H. H. Patel, R. Roepman, D. Schick and P. A. Ferreira**. 1999. The zinc finger cluster domain of RanBP2 is a specific docking site for the nuclear export factor, exportin-1. *J Biol Chem.* 274:37370-37378.

167. **S. Shah and D. J. Forbes**. 1998. Separate nuclear import pathways converge on the nucleoporin Nup153 and can be dissected with dominant-negative inhibitors. *Curr Biol.* 8:1376-1386.

168. **U. Stochaj and K. L. Rother**. 1999. Nucleocytoplasmic trafficking of proteins: with or without Ran? *Bioessays.* 21:579-589.

169. **F. Melchior, B. Paschal, J. Evans and L. Gerace**. 1993. Inhibition of nuclear protein import by nonhydrolyzable analogues of GTP and identification of the small GTPase Ran/TC4 as an essential transport factor. *J Cell Biol.* 123:1649-1659.

170. **B. B. Quimby, T. Lamitina, S. W. L'Hernault and A. H. Corbett**. 2000. The mechanism of Ran import into the nucleus by nuclear transport factor 2. *J Biol Chem.* 275:28575-28582.

171. **Y. Yoneda, M. Hieda, E. Nagoshi and Y. Miyamoto**. 1999. Nucleocytoplasmic protein transport and recycling of Ran. *Cell Struct Funct*. 24:425-433.

172. **S. A. Richards, K. L. Carey and I. G. Macara**. 1997. Requirement of guanosine triphosphate-bound Ran for signal-mediated nuclear protein export. *Science*. 276:1842-1844.

173. **A. H. Corbett, D. M. Koepp, G. Schlenstedt, M. S. Lee, A. K. Hopper and P. A. Silver**. 1995. Rna1p, a Ran/TC4 GTPase activating protein, is required for nuclear import. *J Cell Biol*. 130:1017-1026.

174. **U. Nehrbass and G. Blobel**. 1996. Role of the nuclear transport factor p10 in nuclear import. *Science*. 272:120-122.

175. **C. Chaillan-Huntington, C. V. Braslavsky, J. Kuhlmann and M. Stewart**. 2000. Dissecting the interactions between NTF2, RanGDP, and the nucleoporin XFXFG repeats. *J Biol Chem*. 275:5874-5879.

176. **R. Bayliss, K. Ribbeck, D. Akin, H. M. Kent, C. M. Feldherr, D. Görlich and M. Stewart**. 1999. Interaction between NTF2 and xFxFG-containing nucleoporins is required to mediate nuclear import of RanGDP. *J Mol Biol*. 293:579-593.

177. **K. Ribbeck, G. Lipowsky, H. M. Kent, M. Stewart and D. Görlich**. 1998. NTF2 mediates nuclear import of Ran. *EMBO J*. 17:6587-6598.

178. **A. Smith, A. Brownawell and I. G. Macara**. 1998. Nuclear import of Ran is mediated by the transport factor NTF2. *Curr Biol*. 8:1403-1406.

179. **S. M. Steggerda, B. E. Black and B. M. Paschal**. 2000. Monoclonal antibodies to NTF2 inhibit nuclear protein import by preventing nuclear translocation of the GTPase Ran. *Mol Biol Cell*. 11:703-719.

180. **M. Geyer, R. Assheuer, C. Klebe, J. Kuhlmann, J. Becker, A. Wittinghofer and H. R. Kalbitzer**. 1999. Conformational states of the nuclear GTP-binding protein Ran and its complexes with the exchange factor RCC1 and the effector protein RanBP1. *Biochemistry*. 38:11250-11260.

181. **M. Ohtsubo, H. Okazaki and T. Nishimoto**. 1989. The RCC1 protein, a regulator for the onset of chromosome condensation locates in the nucleus and binds to DNA. *J Cell Biol*. 109:1389-1397.

182. **C. Klebe, F. R. Bischoff, H. Ponstingl and A. Wittinghofer**. 1995. Interaction of the nuclear GTP-binding protein Ran with its regulatory proteins RCC1 and RanGAP1. *Biochemistry*. 34:639-647.

183. **Y. Yoneda**. 2000. Nucleocytoplasmic protein traffic and its significance to cell function. *Genes Cells*. 5:777-787.

184. **J. Moroianu and G. Blobel**. 1995. Protein export from the nucleus requires the GTPase Ran and GTP hydrolysis. *Proc Natl Acad Sci USA*. 92:4318-4322.

185. **M. E. Nemergut and I. G. Macara**. 2000. Nuclear import of Ran exchange factor, RCC1, is mediated by at least two distinct mechanisms. *J Cell Biol*. 149:835-849.

186. **K. M. Lounsbury and I. G. Macara**. 1997. Ran-binding protein 1 (RanBP1) forms a ternary complex with Ran and karyopherin β and reduces Ran GTPase-activating protein (RanGAP) inhibition by karyopherin β. *J Biol Chem*. 272:551-555.

187. **P. Kalab, K. Weis and R. Heald**. 2002. Visualization of a Ran-GTP gradient in interphase and mitotic Xenopus egg extracts. *Science*. 295:2452-2456.

188. **C. G. Takizawa, K. Weis and D. O. Morgan**. 1999. Ran-independent nuclear import of cyclin B1-Cdc2 by importin β. *Proc Natl Acad Sci USA*. 96:7938-7943.

189. **K. Ribbeck, U. Kutay, E. Paraskeva and D. Görlich**. 1999. The translocation of transportin-cargo complexes through nuclear pores is independent of both Ran and energy. *Curr Biol*. 9:47-50.

190. **S. Sachdev, S. Bagchi, D. D. Zhang, A. C. Mings and M. Hannink**. 2000. Nuclear import of IκBα is accomplished by a Ran-independent transport pathway. *Mol Cell Biol*. 20:1571-1582.

191. **F. Yokoya, N. Imamoto, T. Tachibana and Y. Yoneda**. 1999. β-catenin can be transported into the nucleus in a Ran-unassisted manner. *Mol Biol Cell*. 10:1119-1131.

192. **M. Hetzer and I. W. Mattaj**. 2000. An ATP-dependent, Ran-independent mechanism for nuclear import of the U1A and U2B" spliceosome proteins. *J Cell Biol*. 148:293-303.

193. **B. C. Berk**. 2001. Vascular smooth muscle growth: autocrine growth mechanisms. *Physiol Rev*. 81:999-1030.

194. **P. Sipkema, P. J. W. vanderLinden, N. Westerhof and F. C. P. Yin**. 2003. Effect of cyclic axial stretch of rat arteries on endothelial cytoskeletal morphology and vascular reactivity. *J Biomech*. 36:653-659.

195. **S. D. Rybalkin, C. Yan, K. E. Bornfeldt and J. A. Beavo**. 2003. Cyclic GMP phosphodiesterases and regulation of smooth muscle function. *Circ Res*. 93:280-291.

196. **A. Bayes-Genis, R. S. Schwartz, L. K. Bale and C. A. Conover**. 2003. Effects of insulin-like growth factor-I on cultured human coronary artery smooth muscle cells. *Growth Horm IGF Res*. 13:246-253.

197. **I. Zachary**. 2001. Signaling mechanisms mediating vascular protective actions of vascular endothelial growth factor. *Am J Physiol Cell Physiol*. 280:C1375-C1386.

198. **M. R. Weir and V. J. Dzau**. 1999. The renin-angiotensin-aldosterone system: a specific target for hypertension management. *Am J Hypertens*. 12:205S-213S.

199. **M. Takahashi, K. i. Hayashi, K. Yoshida, Y. Ohkawa, T. Komurasaki, A. Kitabatake, A. Ogawa, W. Nishida, M. Yano, M. Monden and K. Sobue**. 2003. Epiregulin as a major autocrine/paracrine factor released from ERK- and p38MAPK-activated vascular smooth muscle cells. *Circulation*. 108:2524-2529.

200. **J. J. Wentzel, F. J. H. Gijsen, N. Stergiopulos, P. W. Serruys, C. J. Slager and R. Krams**. 2003. Shear stress, vascular remodeling and neointimal formation. *J Biomech*. 36:681-688.

201. **A. Kapus, C. DiCiano, J. Sun, X. Zhan, L. Kim, T. W. Wong and O. D. Rotstein**. 2000. Cell volume-dependent phosphorylation of proteins of the cortical cytoskeleton and cell-cell contact sites. *J Biol Chem*. 275:32289-32298.

202. **X. A. Li, C. Bianchi and F. W. Sellke**. 2001. Rat aortic smooth muscle cell density affects activation of MAP kinase and Akt by menadione and PDGF homodimer BB. *J Surg Res*. 100:197-204.

203. **P. J. Garl, J. M. Wenzlau, H. A. Walker, J. M. Whitelock, M. Costell and M. C. M. Weiser-Evans**. 2004. Perlecan-induced suppression of smooth muscle cell proliferation is mediated through increased activity of the tumor suppressor PTEN. *Circ Res*. 94:175-183.

204. **J. Figueroa, J. Oubre and P. Vijayagopal**. 2004. Modulation of vascular smooth muscle cells proteoglycan synthesis by the extracellular matrix. *J Cell Physiol*. 198:302-309.

205. **J. B. Michel**. 2003. Anoïkis in the cardiovascular system. *Arterioscler Thromb Vasc Biol*. 23:2146-2154.

206. **R. M. Tombes, K. L. Auer, R. Mikkelsen, K. Valerie, M. P. Wymann, C. J. Marshall, M. McMahon and P. Dent**. 1998. The mitogen-activated protein (MAP) kinase cascade can either stimulate or inhibit DNA synthesis in primary cultures of rat hepatocytes depending upon whether its activation is acute/phasic or chronic. *Biochem J*. 330:1451-1460.

207. **A. Hipper and G. Isenberg**. 2000. Cyclic mechanical strain decreases the DNA synthesis of vascular smooth muscle cells. *Pflugers Arch.* 440:19-27.

208. **A. Zeidan, J. Broman, P. Hellstrand and K. Swärd**. 2003. Cholesterol dependence of vascular ERK1/2 activation and growth in response to stretch: role of endothelin-1. *Arterioscler Thromb Vasc Biol.* 23:1528-1534.

209. **K. Hamada, N. Takuwa, K. Yokoyama and Y. Takuwa**. 1998. Stretch activates jun N-terminal kinase/stress-activated proein kinase in vascular smooth muscle cells through mechanisms involving autocrine ATP stimulation of purinoceptors. *J Biol Chem.* 273:6334-6340.

210. **H. P. Reusch, G. Chan, H. E. Ives and R. A. Nemenoff**. 1997. Activation of JNK/SAPK and ERK by mechanical strain in vascular smooth muscle cells depends on extracellular matrix composition. *Biochem Biophys Res Comm.* 237:239-244.

211. **C. Li, Y. Hu, M. Mayr and Q. Xu**. 1999. Cyclic strain stress-induced mitogen-activated protein kinase (MAPK) phosphatase 1 expression in vascular smooth muscle cells is regulated by Ras/Rac-MAPK pathways. *J Biol Chem.* 274:25273-25280.

212. **A. G. Vouyouka, S. S. Salib, S. Cala, J. D. Marsh and M. D. Basson**. 2003. Chronic high pressure potentiates the antiproliferative effect and abolishes contractile phenotypic changes caused by endothelial cells in cocultured smooth muscle cells. *J Surg Res.* 110:344-351.

213. **Y.-C. Chai, D. G. Binion, R. Macklis and G. M. Chisolm**. 2002. Smooth muscle cell proliferation induced by oxidized LDL-borne lysophosphatidylcholine. *Vasc Pharmacol.* 38:229-237.

214. **Y. Chai, D. G. Binion and G. M. Chisolm**. 2000. Relationship of molecular structure to the mechanism of lysophospholipid-induced smooth muscle cell proliferation. *Am J Physiol.* 279:H1830-H1838.

215. **C. Michiels**. 2003. Endothelial cell functions. *J Cell Physiol.* 196:430-443.

216. **F. Grinnell**. 2003. Fibroblast biology in three-dimensional collagen matrices. *Trends Cell Biol.* 13:264-269.

217. **B. Fernandez, A. Kampmann, F. Pipp, R. Zimmermann and W. Schaper**. 2003. Osteoglycin expression and localization in rabbit tissues and atherosclerotic plaques. *Mol Cell Biochem.* 246:3-11.

218. **H. Wilkens, W. Regelson and F. S. Hoffmeister**. 1962. The physiologic importance of pulsatile blood flow. *N Eng J Med.* 267:443-446.

219. **C. M. Brophy, D. A. Woodrum, J. Pollock, M. Dickinson, P. Komalavilas, T. L. Cornwell and T. M. Lincoln**. 2002. cGMP-dependent protein kinase expression restores contractile function in cultured vascular smooth muscle cells. *J Vasc Res*. 39:95-103.

220. **C. Kimura, W. Cheng, K. Hisadome, Y.-P. Wang, T. Koyama, Y. Karashima, M. Oike and Y. Ito**. 2002. Superoxide anion impairs contractility in cultured aortic smooth muscle cells. *Am J Physiol Heart Circ Physiol*. 283:H382-H390.

221. **E. B. Okon, T. Szado, I. Laher, B. McManus and C. vanBreemen**. 2003. Augmented contractile response of vascular smooth muscle in a diabetic mouse model. *J Vasc Res*. 40:520-530.

222. **A. J. Halayko and J. Solway**. 2001. Molecular mechanisms of phenotypic plasticity in smooth muscle cells. *J Appl Physiol*. 90:358-368.

223. **S. Li, S. Sims, Y. Jiao, L. H. Chow and J. G. Pickering**. 1999. Evidence from a novel human cell clone that adult vascular smooth muscle cells can convert reversibly between noncontractile and contractile phenotypes. *Circ Res*. 85:338-348.

224. **K. Sobue, K. i. Hayashi and W. Nishida**. 1998. Molecular mechanism of phenotypic modulation of smooth muscle cells. *Horm Res*. 50:15-24.

225. **H. Hao, G. Gabbiani and M.-L. Bochaton-Piallat**. 2003. Arterial smooth muscle cell heterogeneity: implications for atherosclerosis and restenosis development. *Arterioscler Thromb Vasc Biol*. 23:1510-1520.

226. **C. Indolfi, A. Mongiardo, A. Curcio and D. Torella**. 2003. Molecular mechanisms of in-stent restenosis and approach to therapy with eluting stents. *Trends Cardiovasc Med*. 13:142-148.

227. **V. Rajagopal and S. G.Rockson**. 2003. Coronary restenosis: a review of mechanisms and management. *Am J Med*. 115:547-553.

228. **J. S. Ross, N. E. Stagliano, M. J. Donovan, R. E. Bretibart and G. S. Ginsburg**. 2001. Atherosclerosis: a cancer of the blood vessels? *Am J Clin Pathol*. 116:S97-S107.

229. **M. Hamon, C. Bauters, E. P. McFadden, N. Wernert, J. M. Lablanche, B. Dupuis and M. E. Bertrand**. 1995. Restenosis after coronary angioplasty. *Eur Heart J*. 16:33-48.

230. **J. Wöhrle, M. Kochs, C. Vollmer, H. A. Kestler, V. Hombach and M. Höher**. 2004. Re-angioplasty of in-stent restenosis versus balloon restenoses - matched pair comparison. *Int J Cardiol*. 93:257-262.

231. **C. Casey and D. P. Faxon**. 2004. Multi-vessel coronary disease and percutaneous coronary intervention. *Heart*. 90:341-346.

232. **J. C. Tardif, J. Gregoire and P. L. L'Allier**. 2002. Prevention of restenosis with antioxidants: mechanisms and implications. *Am J Cardiovasc Drugs*. 2:323-324.

233. **E. P. Benditt and J. M. Benditt**. 1973. Evidence for a monoclonal origin of human atherosclerotic plaques. *Proc Natl Acad Sci USA*. 70:1753-1756.

234. **S. M. Schwartz, M. W. Majesky and C. E. Murry**. 1995. The intima: development and monoclonal responses to injury. *Atherosclerosis*. 118:S125-S140.

235. **S. Jono, M. D. McKee, C. E. Murry, A. Shioi, Y. Nishizawa, K. Mori, H. Morii and C. M. Giachelli**. 2000. Phosphate regulation of vascular smooth muscle cell calcification. *Circ Res*. 87:E10-E17.

236. **M. J. Barnes and R. W. Farndale**. 1999. Collagens and atherosclerosis. *Exp Gerontol*. 34:513-525.

237. **M. Klouche, S. Rose-John, W. Schmiedt and S. Bhakdi**. 2000. Enzymatically degraded, nonoxidized LDL induces human vascular smooth muscle cell activation, foam cell transformation, and proliferation. *Circulation*. 101:1799-1805.

238. **K. Burger, G. Gimpl and F. Fahrenholz**. 2000. Regulation of receptor function by cholesterol. *Cell Mol Life Sci*. 57:1577-1592.

239. **D. Brown**. 2002. Structure and function of membrane rafts. *Int J Med Micro*. 291:433-437.

240. **K. Schoonjans, C. Brendel, D. Mangelsdorf and J. Auwerx**. 2000. Sterols and gene expression: control of affluence. *Biochim Biophys Acta*. 1529:114-125.

241. **D. M. Stocco**. 2000. The role of the StAR protein in steroidogenesis: challenges for the future. *J Endocrinol*. 164:247-253.

242. **M. S. Brown, J. R. Faust and J. L. Goldstein**. 1975. Role of the low density lipoprotein receptor in regulating the content of free and esterified cholesterol in human fibroblasts. *J Clin Invest*. 55:783-793.

243. **M. S. Brown and J. L. Goldstein**. 1975. Regulation of the activity of the low density lipoprotein receptor in human fibroblasts. *Cell*. 6:307-316.

244. **M. Chen, T. Masaki and T. Sawamura**. 2002. LOX-1, the receptor for oxidized low-density lipoprotein identified from endothelial cells: implications in endothelial dysfunction and atherosclerosis. *Pharmacol Ther*. 95:89-100.

245. **H. Itabe**. 2003. Oxidized low-density lipoproteins: what is understood and what remains to be clarified. *Biol Pharm Bull*. 26:1-9.

246. **N. Murata, K. Sato, J. Kon, H. Tomura, M. Yanagita, A. Kuwabra, M. Ui and F. Okajima**. 2000. Interaction of sphingosine-1-phosphate with plasma components, including lipoproteins, regulates the lipid receptor-mediated actions. *Biochem J*. 352:809-815.

247. **B. Boyanovsky, A. Karakashian, K. King, N. Giltiay and M. Nikolova-Karakashian**. 2003. Uptake and metabolism of low density lipoproteins with elevated ceramide content by human microvascular endothelial cell: implications for the regulation of apoptosis. *J Biol Chem*. 278:26992-26999.

248. **S. Lightle, R. Tosheva, A. Lee, J. Queen-Baker, B. Boyanovksy, S. Shedlofsky and M. Nikolova-Karakashian**. 2003. Elevation of ceramide in serum lipoproteins during acute phase response in humans and mice: role of serine-palmitoyl transferase. *Arch Biochem Biophys*. 419:120-128.

249. **J. Schiller, O. Zschörnig, M. Petkovic, M. Müller, J. Arnhold and K. Arnold**. 2001. Lipid analysis of human HDL and LDL by MALDI-TOF mass spectrometry and ^{31}P-NMR. *J Lipid Res*. 42:1501-1508.

250. **W. L. Smith and J. Alfred H. Merrill**. 2002. Sphingolipid metabolism and signaling minireview series. *J Biol Chem*. 277:25841-25842.

251. **T. Levade, N. Augé, R. J. Veldman, O. Cuvillier, A. Nègre-Salvayre and R. Salvayre**. 2001. Sphingolipid mediators in cardiovascular cell biology and pathology. *Circ Res*. 89:957-968.

252. **Y. A. Hannun, C. Luberto and K. M. Argraves**. 2001. Enzymes of sphingolipid metabolism: from modular to integrative signaling. *Biochemistry*. 40:4893-4903.

253. **G. vanEchten-Deckert, A. Klein, T. Linke, T. Heinemann, J. Weisgerber and K. Sandhoff**. 1997. Turnover of endogenous ceramide in cultured normal and Farber fibroblasts. *J Lipid Res*. 38:2569-2579.

254. **S. Willaime, P. Vanhoutte, J. Caboche, Y. Lemaigre-Dubreuil, J. Mariani and B. Brugg**. 2001. Ceramide-induced apoptosis in cortical neurons is mediated by

an increase in p38 phosphorylation and not by the decrease in ERK phosphorylation. *Eur J Neurosci.* 13:2037-2046.

255. **A. Erdreich-Epstein, L. B. Tran, N. N. Bowman, H. Wang, M. C. Cabot, D. L. Durden, J. Vlckova, C. P. Reynolds, M. F. Stins, S. Groshen and M. Millard.** 2002. Ceramide signaling in fenretinide-induced endothelial cell apoptosis. *J Biol Chem.* 277:49531-49537.

256. **D. G. Johns, R. C. Webb and J. R. Charpie.** 2001. Impaired ceramide signalling in spontaneously hypertensive rat vascular smooth muscle: a possible mechanism for augmented cell proliferation. *J Hypertens.* 19:63-70.

257. **R. K. Malik, B. A. Thornhill, A. Y. Chuang, S. C. Kiley and R. L. Chevalier.** 2000. Apoptosis parallels ceramide content in the developing rat kidney. *Dev Biol.* 15:188-191.

258. **C. Mazière, M.-A. Conte, L. Leborgne, T. Levade, W. Hornebeck, R. Santus and J.-C. Mazière.** 2001. UVA radiation stimulates ceramide production: relationship to oxidative stress and potential role in ERK, JNK, and p38 activation. *Biochem Biophys Res Comm.* 281.

259. **Y. Uchida, A. D. Nardo, V. Collins, P. M. Elias and W. M. Holleran.** 2003. *De novo* ceramide synthesis participates in the ultraviolet B irradiation-induced apoptosis in undifferentiated cultured human keratinocytes. *J Invest Dermatol.* 120:662-669.

260. **S. S. Castillo and D. Teegarden.** 2001. Ceramide conversion to sphingosine-1-phosphate is essential for survival in C3H10T½ cells. *J Nutr.* 131:2826-2830.

261. **S. Willaime-Morawek, K. Brami-Cherrier, J. Mariani, J. Caboche and B. Brugg.** 2003. C-Jun N-terminal kinases/c-Jun and p38 pathways cooperate in ceramide-induced apoptosis. *Neuroscience.* 119:387-397.

262. **S. P. Li, M. R. Juntilla, J. Han, V. M. Kahari and J. Westermarck.** 2003. p38 mitogen-activated protein kinase pathway suppresses cell survival by inducing dephosphorylation of mitogen-activated protein/extracellular signal-regulated kinase kinase 1,2. *Cancer Res.* 63:3473-3477.

263. **B. Brenner, U. Koppenhoefer, C. Weinstock, O. Linderkamp, F. Lang and E. Gulbin.** 1997. Fas- or ceramide-induced apoptosis is mediated by a Rac1-regulated activation of Jun N-terminal kinase/p38 kinases and GADD153. *J Biol Chem.* 272:22173-22181.

264. **S. Mathias, K. A. Dressler and R. N. Kolesnick.** 1991. Characterization of a ceramide-activated protein kinase: stimulation by tumor necrosis factor α. *Proc Natl Acad Sci USA.* 88:10009-10013.

265. **S. Galadari, A. Hago and M. Patel**. 2001. Effects of cations on ceramide-activated protein phosphatase 2A. *Exp Mol Med*. 33:240-244.

266. **L. J. Siskind and M. Colombini**. 2000. The lipids C_2-and C_{16}- ceramide form large stable channels. *J Biol Chem*. 275:38640-38644.

267. **L. J. Siskind, R. N. Kolesnick and M. Colombini**. 2002. Ceramide channels increase the permeability of the mitochondrial outer membrane to small proteins. *J Biol Chem*. 277:26796-26803.

268. **W. Martinet, D. M. Schrivers, G. R. De Meyer, J. Thielemans, M. W. Knaapen, A. G. Herman and M. M. Kockx**. 2002. Gene expression profiling of apoptosis-related genes in human atherosclerosis: upregulation of death-associated protein kinase. *Arterioscler Thromb Vasc Biol*. 22:2023-2029.

269. **T. Hla**. 2003. Signaling and biological actions of sphingosine-1-phosphate. *Pharmacol Res*. 47:401-407.

270. **H. Zhang, N. N. Desai, A. Olivera, T. Seki, G. Booker and S. Spiegel**. 1991. Sphingosine-1-phosphate, a novel lipid, involved in cellular proliferation. *J Cell Biol*. 114:155-167.

271. **N. Augé, M. Nikolova-Karakashian, S. Carpentier, S. Parthasarathy, A. Nègre-Salvayre, R. Salvayre, J. Alfred H. Merrill and T. Levade**. 1999. Role of sphingosine-1-phosphate in the mitogenesis induced by oxidized low density lipoprotein in smooth muscle cells via activation of sphingomyelinase, ceramidase, and sphingosine kinase. *J Biol Chem*. 274:21533-21538.

272. **V. Thamilselvan, W. Li, B. E. Sumpio and M. D. Basson**. 2002. Sphingosine-1-phosphate stimulates human Caco-2 intestinal epithelial proliferation via p38 activation and activates ERK by an independent mechanism. *In Vitro Cell Dev Biol Anim*. 38:246-253.

273. **D.-S. Kim, E.-S. Hwang, J.-E. Lee, S.-Y. Kim and K.-C. Park**. 2003. Sphingosine-1-phosphate promotes mouse melanocyte survival via ERK and Akt activation. *Cell Signal*. 15:919-926.

274. **Y. Rikitake, K. Hirata, S. Kawashima, M. Ozaki, T. Takahashi, W. Ogawa, N. Inoue and M. Yokoyama**. 2001. Involvement of endothelial nitric oxide in sphingosine-1-phosphate-induced angiogenesis. *Arterioscler Thromb Vasc Biol*. 22:108-114.

275. **S. Spiegel and S. Milstien**. 2002. Sphingosine-1-phosphate, a key cell signaling molecule. *J Biol Chem*. 277:25851-25854.

276. **S. Pyne and N. J. Pyne**. 2000. Sphingosine 1-phosphate signalling in mammalian cells. *Biochem J.* 349:385-402.

277. **G. Murugesan, M. R. S. Rani, C. E. Gerber, C. Mukhopadhyay, R. M. Ransohoff, G. M. Chisolm and K. Kottke-Marchant**. 2003. Lysophosphatidylcholine regulates human microvascular endothelial cell expression of chemokines. *J Mol Cell Cardiol.* 35:1375-1384.

278. **B. Engelmann, S. Zieseniss, K. Brand, S. Page, A. Lentschat, A. J. Ulmer and E. Gerlach**. 1999. Tissue factor expression of human monocytes is suppressed by lysophosphatidylcholine. *Arterioscler Thromb Vasc Biol.* 19:47-53.

279. **G. Sekas, G. M. Patton, E. C. Lincoln and S. J. Robins**. 1985. Origin of plasma lysophosphatidylcholine: evidence for direct hepatic secretion in the rat. *J Lab Clin Med.* 105:190-194.

280. **L. Yu, T. Netticadan, Y.-J. Xu, V. Panagia and N. S. Dhalla**. 1998. Mechanisms of lysophosphatidylcholine-induced increase in intracellular calcium in rat cardiomyocytes. *J Pharmcaol Exp Ther.* 286:1-8.

281. **R. I. Jabr, J. Yamazaki and J. R. Hume**. 2000. Lysophosphatidylcholine triggers intracellular calcium release and activation of non-selective cation channels in renal arterial smooth muscle cells. *Pflugers Arch.* 439:495-500.

282. **N. V. Prokazova, N. D. Zvedzina and A. A. Korotaeva**. 1998. Effect of lysophosphatidylcholine on transmembrane signal transduction. *Biochemistry (Mosc).* 63:31-7.

283. **C. G. Radu, L. V. Yang, M. Riedinger, M. Au and O. N. Witte**. 2004. T cell chemotaxis to lysophosphatidylcholine through the G2A receptor. *Proc Natl Acad Sci USA.* 101:245-250.

284. **R. Scalia, T. Murohara, B. Campbell, A. Kaji and A. M. Lefer**. 1997. Lysophosphatidylcholine stimulates leukocyte rolling and adherence in rat mesenteric microvasculature. *Am J Physiol.* 276:H2584-H2590.

285. **C. Weber, W. Erl and P. C. Weber**. 1995. Enhancement of monocyte adhesion to endothelial cells by oxidatively modified low-density lipoprotein is mediated by activation of CD11b. *Biochem Biophys Res Comm.* 206:621-628.

286. **F. Kinard, K. Jaworski, T. Sergent-Engelen, D. Goldstein, P. P. V. Veldhoven, P. Holvoet, A. Trouet, Y.-J. Schneider and C. Remacle**. 2001. Smooth muscle cells influence monocyte response to LDL as well as their adhesion and transmigration in a coculture model of the arterial wall. *J Vasc Res.* 38.

287. **J. X. Rong, J. W. Berman, M. B. Taubman and E. A. Fisher**. 2002. Lysophosphatidylcholine stimulates monocyte chemoattractant protein-1 gene expression in rat aortic smooth muscle cells. *Arterioscler Thromb Vasc Biol.* 22:1617-1623.

288. **Y. Rikitake, K. Hirata, T. Yamashita, K. Iwai, S. Kobayashi, H. Itoh, M. Ozaki, J. Ejiri, M. Shiomi, N. Inoue, S. Kawashima and M. Yokoyama**. 2002. Expression of G2A, a receptor for lysophosphatidylcholine, by macrophages in murine, rabbit, and human atherosclerotic plaques. *Arterioscler Thromb Vasc Biol.* 22:2049-2053.

289. **T. Watanabe, R. Pakala, T. Katagiri and C. R. Benedict**. 2002. Lysophosphatidylcholine is a major contributor to the synergistic effect of mildly oxidized low-density lipoprotein with endothelin-1 on vascular smooth muscle cell proliferation. *J Cardiovasc Pharmacol.* 39:449-459.

290. **B. V. Bassa, D. D. Roh, N. D. Vaziri, M. A. Kirschenbaum and V. S. Kamanna**. 1999. Lysophosphatidylcholine activates mesangial cell PKC and MAP kinase by PLCγ-1 and tyrosine kinase-Ras pathways. *Am J Physiol Renal Physiol.* 277:F328-F337.

291. **Q. Jing, S.-M. Xin, W.-B. Zhang, P. Wang, Y.-W. Qin and G. Pei**. 2000. Lysophosphatidylcholine activates p38 and p42/44 mitogen-activated protein kinases in monocytic THP-1 cells, but only p38 activation is involved in its stimulated chemotaxis. *Circ Res.* 87:52-59.

292. **T. Yamakawa, S. Eguchi, Y. Yamakawa, E. D. Motley, K. Numaguchi, H. Utsunomiya and T. Inagami**. 1998. Lysophosphatidylcholine stimulates MAP kinase activity in rat vascular smooth muscle cells. *Hypertension.* 31:248-253.

293. **J. H. S. Kabarowski, Y. Xu and O. N. Witte**. 2002. Lysophosphatidylcholine as a ligand for immunoregulation. *Biochem Pharmacol.* 64:161-167.

294. **J. H. S. Kabarowski, K. Zhu, L. Q. Le, O. N. Witte and Y. Xu**. 2001. Lysophosphatidylcholine as a ligand for the immunoregulatory receptor G2A. *Science.* 293:702-705.

295. **K. Zhu, L. M. Baudhuin, G. Hong, F. S. Williams, K. L. Cristina, J. H. S. Kabarowski, O. N. Witte and Y. Xu**. 2001. Sphingosylphosphorylcholine and lysophosphatidylcholine are ligands for the G protein-coupled receptor GPR4. *J Biol Chem.* 276:41325-41335.

296. **M. Sakai, A. Miyazaki, H. Hakamata, T. Kodama, H. Suzuki, S. Kobori, M. Shichiri and S. Horiuchi**. 1996. The scavenger receptor serves as a route for internalization of lysophosphatidylcholine in oxidized low density lipoprotein-induced macrophage proliferation. *J Biol Chem.* 271:27346-27352.

297. **A. H. vanderLuit, M. Budde, M. Verheij and W. J. vanBlitterswijk**. 2003. Different modes of internalization of apoptotic alkyl-lysophospholipid and cell-rescuing lysophosphatidylcholine. *Biochem J.* 374:747-753.

298. **A. K. Menon, W. E. Watkins and S. Hrafnsdottir**. 2000. Specific proteins are required to translocate phosphatidylcholine bidirectionally across the endoplasmic reticulum. *Curr Biol.* 10:241-252.

299. **J. English, G. Pearson, J. Wilsbacher, J. Swantek, M. Karandikar, S. Xu and M. H. Cobb**. 1999. New insights into the control of MAP kinase pathways. *Exp Cell Res.* 253:255-270.

300. **W. Woessmann, Y.-H. Meng and N. F. Mivechi**. 1999. An essential role for mitogen-activated protein kinases, ERKs, in preventing heat-induced cell death. *J Cell Biochem.* 74:648-662.

301. **S. Chiri, C. D. Nadai and B. Ciapa**. 1998. Evidence for MAP kinase activation during mitotic activation. *J Cell Sci.* 111:2519-2527.

302. **G. Pearson, F. Robinson, T. B. Gibson, B.-E. Xu, M. Karandikar, K. Berman and M. H. Cobb**. 2001. Mitogen-activated protein (MAP) kinase pathways: regulation and physiological functions. *Endocr Rev.* 22:153-183.

303. **C. Mendez, C. Jaffray, V. Wong, K. F. Salhab, A. A. Kramer, L. C. Carey and J. G. Norman**. 2000. Involvement of p38 mitogen-activated protein kinase in the induction of tolerance to hemorrhagic and endotoxic shock. *J Surg Res.* 91:165-70.

304. **B. Dérijard, M. Hibi, I.-H. Wu, T. Barrett, B. Su, T. Deng, M. Karin and R. J. Davis**. 1994. JNK1: A protein kinase stimulated by UV light and Ha-Ras that binds and phosphorylates the c-Jun activation domain. *Cell.* 76:1025-1037.

305. **J. Han, J. D. Lee, L. Bibbs and R. J. Ulevitch**. 1994. A MAP kinase targeted by endotoxin and hyperosmolarity in mammalian cells. *Science.* 265:808-811.

306. **M. Fisher, B. Liu, P. E. Glennon, K. M. Southgate, E. M. Sale, G. J. Sale, M. J. Lewis and P. H. Groves**. 2001. Downregulation of the ERK 1 and 2 mitogen activated protein kinases using antisense oligonucleotides inhibits proliferation of porcine vascular smooth muscle cells. *Atherosclerosis.* 156:289-295.

307. **P. Lenormand, J.-M. Brondello, A. Brunet and J. Pouysségur**. 1998. Growth factor-induced p42/p44 MAPK nuclear translocation and retention requires both MAPK activation and neosynthesis of nuclear anchoring proteins. *J Cell Biol.* 142:625-633.

308. **M. G. Wilkinson and J. B. A. Millar**. 2000. Control of the eukaryotic cell cycle by MAP kinase signaling pathways. *FASEB J.* 14.

309. **M. Buehr and A. Smith**. 2003. Genesis of embryonic stem cells. *Philos Trans R Soc Lond B Biol Sci.* 358:1397-1402.

310. **Y. Yao, W. Li, J. Wu, U. A. Germann, M. S. S. Su, K. Kuida and D. M. Boucher**. 2003. Extracellular signal-regulated kinase 2 is necessary for mesoderm differentiation. *Proc Natl Acad Sci USA.* 100:12759-12764.

311. **T. Burdon, A. Smith and P. Savatier**. 2002. Signalling, cell cycle and pluripotency in embryonic stem cells. *Trends Cell Biol.* 12:432-438.

312. **L. Jirmanova, M. Afanassieff, S. Gobert-Gosse, S. Markossian and P. Savatier**. 2002. Differential contributions of ERK and PI3-kinase to the regulation of cyclin D1 expression and to the control of the G1/S transition in mouse embryonic stem cells. *Oncogene.* 21:5515-5528.

313. **H. Kook, H. Itoh, B. S. Choi, N. Sawada, K. Doi, T. J. Hwang, K. K. Kim, H. Arai, Y. H. Baik and K. Nakao**. 2003. Physiological concentration of atrial natriuretic peptide induces endothelial regeneration in vitro. *Am J Physiol Heart Circ Physiol.* 284:H1388-H1397.

314. **G.-D. Sharma, J. He and H. E. P. Bazan**. 2003. p38 and ERK1/2 coordinate cellular migration and proliferation in epithelial wound healing. *J Biol Chem.* 278:21989-21997.

315. **S. Yates and T. E. Rayner**. 2002. Transcription factor activation in response to cutaneous injury: role of AP-1 in reepithelialization. *Wound Repair Regen.* 10:5-15.

316. **O. F. Bueno and J. D. Molkentin**. 2002. Involvement of extracellular signal-related kinases 1/2 in cardiac hypertrophy and cell death. *Circ Res.* 91:776-781.

317. **G. A. Nader and K. A. Esser**. 2001. Intracellular signaling specificity in skeletal muscle in response to different modes of exercises. *J Appl Physiol.* 90:1936-1942.

318. **M. C. Michel, Y. Li and G. Heusch**. 2001. Mitogen-activated protein kinases in the heart. *Arch Pharmacol.* 363:245-266.

319. **T. Wada and J. M. Peninger**. 2004. Mitogen-activated protein kinases in apoptosis regulation. *Oncogene.* 23:2838-2849.

320. **C. C. Franklin and A. S. Kraft**. 1997. Conditional expression of the mitogen-activated protein kinase (MAPK) phosphatase MKP-1 preferentially inhibits p38

MAPK and stress-activated protein kinase in U937 cells. *J Biol Chem.* 272:16917-16923.

321. **D. Jacobs, D. Glossip, H. Xing, A. J. Muslin and K. Kornfeld**. 1999. Multiple docking sites on substrate proteins form a modular system that mediates recognition by ERK MAP kinase. *Genes Dev.* 13:163-175.

322. **M. L. Kuo and N. C. Yang**. 1995. Reversion of v-H-ras-transformed NIH 3T3 cells by apigenin through inhibiting mitogen activated protein kinase and its downstream oncogenes. *Biochem Biophys Res Comm.* 212:767-775.

323. **F. Yin, A. E. Giuliano, R. E. Law and A. J. Van Herle**. 2001. Apigenin inhibits growth and induces G2/M arrest by modulating cyclin-CDK regulators and ERK MAP kinase activation in breast carcinoma cells. *Anticancer Research.* 21:413-420.

324. **F. Yin, A. E. Giuliano and A. J. Van Herle**. 1999. Signal pathways involved in apigenin inhibition of growth and induction of apoptosis of human anaplastic thyroid cancer cells (ARO). *Anticancer Research.* 19:4297-4303.

325. **D. R. Alessi, A. Cuenda, P. Cohen, D. T. Dudley and A. R. Saltiel**. 1995. PD 098059 is a specific inhibitor of the activation of mitogen-activated protein kinase kinase *in vitro* and *in vivo*. *J Biol Chem.* 270:27489-27494.

326. **D. T. Dudley, L. Pang, S. J. Decker, A. J. Bridges and A. R. Saltiel**. 1995. A synthetic inhibitor of the mitogen-activated protein kinase cascade. *Proc Natl Acad Sci USA.* 92:7686-7689.

327. **T. Fox, J. T. Coll, X. Xie, P. J. Ford, U. A. Germann, M. D. Porter, S. Pazhanisamy, M. A. Fleming, V. Galullo, M. S. Su and K. P. Wilson**. 1998. A single amino acid substitution makes ERK2 susceptible to pyridinyl imidazole inhibitors of p38 MAP kinase. *Protein Science.* 7:2249-2255.

328. **D. Massillon, W. Stalmans, G. van de Werve and M. Bollen**. 1994. Identification of the glycogenic compound 5-iodotubercidin as a general protein kinase inhibitor. *Biochem J.* 299:123-128.

329. **F. E. Parkinson and J. D. Geiger**. 1996. Effects of iodotubercidin on adenosine kinase activity and nucleoside transport in DDT1 MF-2 smooth muscle cells. *J Pharmcaol Exp Ther.* 277:1397-1401.

330. **S. Nemoto, J. Xiang, S. Huang and A. Lin**. 1998. Induction of apoptosis by SB202190 through inhibition of p38β mitogen-activated protein kinase. *J Biol Chem.* 273:16415-16420.

331. **K. Subbaramaiah, T. P. Marmo, D. A. Dixon and A. J. Dannenberg**. 2003. Regulation of cyclooxygenase-2 mRNA stability by taxanes. *J Biol Chem.* 278:37637-37647.

332. **D. A. Jans**. 1995. The regulation of protein transport to the nucleus by phosphorylation. *Biochem J.* 311:705-716.

333. **D. A. Jans and S. Hübner**. 1996. Regulation of protein transport to the nucleus: central role of phosphorylation. *Physiol Rev.* 76:651-685.

334. **C. Favreau, H. J. Worman, R. W. Wozniak, T. Frappier and J.-C. Courvalin**. 1996. Cell cycle-dependent phosphorylation of nucleoporins and nuclear pore membrane protein gp210. *Biochemistry.* 35:8035-8044.

335. **C. Macaulay, E. Meier and D. J. Forbes**. 1995. Differential mitotic phosphorylation of proteins of the nuclear pore complex. *J Biol Chem.* 270:254-262.

336. **K. Mishra and V. K. Parnaik**. 1995. Essential role of phosphorylation in nuclear transport. *Exp Cell Res.* 216:124-134.

337. **J. S. C. Gilchrist and G. N. Pierce**. 1993. Identification and purification of a calcium-binding protein in hepatic nuclear membranes. *J Biol Chem.* 268:4291-4299.

338. **M. P. Czubryt, B. Ramjiawan, J. S. C. Gilchrist, H. Massaeli and G. N. Pierce**. 1996. The presence and partitioning of calcium binding proteins in hepatic and cardiac nuclei. *J Mol Cell Cardiol.* 28:455-465.

339. **G. N. Pierce, P. S. Sekhon, H. P. Meng and T. G. Maddaford**. 1989. Effects of chronic swimming training on cardiac sarcolemmal function and composition. *J Appl Physiol.* 66:1715-1721.

340. **G. N. Pierce, M. K. Lockwood and C. D. Eckhert**. 1989. Cardiac contractile protein ATPase activity in a diet induced model of noninsulin dependent diabetes mellitus. *Can J Cardiol.* 5:117-120.

341. **M. P. Czubryt, J. A. Austria and G. N. Pierce**. 2000. Hydrogen peroxide inhibition of nuclear import is mediated by the mitogen-activated protein kinase, ERK-2. *J Cell Biol.* 148:7 - 15.

342. **M. Berrios**. 1998. Isolation and characterization of karyoskeletal protein-enriched fractions from vertebrate livers. *In* Methods in cell biology: nuclear structure and function. Vol. 53. M. Berrios, editor. Academic Press, San Diego. 3-22.

343. **S. A. Adam, R. Sterne-Marr and L. Gerace**. 1991. *In vitro* nuclear protein import using permeablized mammalian cells. *Meth Cell Biol.* 35:469-482.

344. **S. A. Richards, K. M. Lounsbury and I. G. Macara**. 1995. The C terminus of the nuclear RAN/TC4 GTPase stabilizes the GDP-bound state and mediates interactions with RCC1, Ran-GAP, and HTF9A/RanBP1. *J Biol Chem.* 270:14405-14411.

345. **S. K. Lyman, T. Guan, J. Bednenko, H. Wodrich and L. Gerace**. 2002. Influence of cargo size on Ran and energy requirements for nuclear protein import. *J Cell Biol.* 159:55-67.

346. **M. E. Zettler, M. A. Prociuk, J. A. Austria, H. Massaeli, G. Zhong and G. N. Pierce**. 2003. OxLDL stimulates cell proliferation through a general induction of cell cycle proteins. *Am J Physiol Heart Circ Physiol.* 284:H644-H653.

347. **L. I. Davis and G. Blobel**. 1986. Identification and characterization of a nuclear pore complex protein. *Cell.* 45:699-709.

348. **G. E. Ward and M. W. Kirschner**. 1990. Identification of cell cycle-regulated phosphorylation sites on nuclear lamin C. *Cell.* 61:561-577.

349. **R. Heald and F. McKeon**. 1990. Mutations of phosphorylation sites in lamin A that prevent nuclear lamina disassembly in mitosis. *Cell.* 61:579-589.

350. **B. A. Hocevar, D. J. Burns and A. P. Fields**. 1993. Identification of protein kinase C (PKC) phosphorylation sites on human lamin B. *J Biol Chem.* 268:7545-7552.

351. **Y. Chai, P. H. Howe, P. E. DiCorleto and G. M. Chisolm**. 1996. Oxidized low density lipoprotein and lysophosphatidylcholine stimulate cell cycle entry in vascular smooth muscle cells. *J Biol Chem.* 271:17791-17797.

352. **N. L. Allbritton, E. Oancea, M. A. Kuhn and T. Meyer**. 1994. Source of nuclear calcium signals. *Proc Natl Acad Sci USA.* 91:12458-12462.

353. **B. Abrenica and J. S. C. Gilchrist**. 2002. Nucleoplasmic Ca^{2+} loading is regulated by mobilization of perinuclear Ca^{2+}. *Cell Calcium.* 28:127-136.

354. **O. V. Gerasimenko, J. V. Gerasimenko, A. V. Tepikin and O. H. Petersen**. 1996. Calcium transport pathways in the nucleus. *Pflugers Arch.* 432:1-6.

355. **L. Santella and E. Carafoli**. 1997. Calcium signaling in the cell nucleus. *FASEB J.* 11:1091-1109.

356. **W. Echevarria, M. F. Leite, M. T. Guerra, W. R. Zipfel and M. H. Nathanson**. 2003. Regulation of calcium signals in the nucleus by a nucleoplasmic reticulum. *Nat Cell Biol.* 5:440-446.

357. **P. P. Y. Lui, S. K. Kong, T. T. Kwok and C. Y. Lee**. 1998. The nucleus of HeLa cell contains tubular structures for Ca^{2+} signalling. *Biochem Biophys Res Comm.* 247:88-93.

358. **P. P. Y. Lui, C. Y. Lee, D. Tsang and S. K. Kong**. 1998. Ca^{2+} is released from the nuclear tubular structure into nucleoplasm in C6 glioma cells after stimulation with phorbol ester. *FEBS Lett.* 432:82-87.

359. **P. Chamero, C. Villalobos, M. T. Alonso and J. García-Sancho**. 2002. Dampening of cytosolic Ca^{2+} oscillations on propagation to nucleus. *J Biol Chem.* 277:50226-50229.

360. **H. Wang and D. E. Clapham**. 1999. Conformational changes of the in situ nuclear pore complex. *Biophys J.* 77:241-247.

361. **R. W. Wozniak, E. Bartnik and G. Blobel**. 1989. Primary structure analysis of an integral membrane glycoprotein of the nuclear pore. *J Cell Biol.* 108:2083-2092.

362. **I. B. Levitan**. 1994. Modulation of ion channels by protein phosphorylation and dephosphorylation. *Annu Rev Physiol.* 56:193-212.

363. **P. Light**. 1996. Regulation of ATP-sensitive potassium channels by phosphorylation. *Biochim Biophys Acta.* 1286:65-73.

364. **Y. Qu, J. C. Rogers, T. N. Tanada, W. A. Catterall and T. Scheuer**. 1996. Phosphorylation of S1505 in the cardiac Na^{+} channel inactivation gate is required for modulation by protein kinase C. *J Gen Physiol.* 108:375-379.

365. **M. Pruschy, Y. Ju, L. Spitz, E. Carafoli and D. S. Goldfarb**. 1994. Facilitated nuclear transport of calmodulin in tissue culture cells. *J Cell Biol.* 127:1527-1536.

366. **T. D. Sweitzer and J. A. Hanover**. 1996. Calmodulin activates nuclear protein import: a link between signal transduction and nuclear transport. *Proc Natl Acad Sci USA.* 93:14574-14579.

367. **J. Joseph, S.-H. Tan, T. S. Karpova, J. G. McNally and M. Dasso**. 2002. SUMO-1 targets RanGAP1 to kinetochores and mitotic spindles. *J Cell Biol.* 156:595-602.

368. **A. D. Sharrocks, S.-H. Yang and A. Galanis**. 2000. Docking domains and substrate-specificity determination for MAP kinases. *Trends Biochem Sci.* 25:448-453.

369. **R. Mahajan, C. Delphin, T. Guan, L. Gerace and F. Melchior**. 1997. A small ubiquitin-related polypeptide involved in targeting RanGAP1 to nuclear pore complex protein RanBP2. *Cell.* 88:97-107.

370. **H. Saitoh, R. Pu, M. Cavenagh and M. Dasso**. 1997. RanBP2 associates with Ubc9p and a modified form of RanGAP1. *Proc Natl Acad Sci USA.* 94:3736-3741.

371. **A. E. A. Thumser, J. E. Voysey and D. C. Wilton**. 1994. The binding of lysophospholipids to rat liver fatty acid-binding protein and albumin. *Biochem J.* 301:801-806.

372. **J. X. Kang and A. Leaf**. 1996. Protective effects of free polyunsaturated fatty acids on arrhythmias induced by lysophosphatidylcholine or palmitoylcarnitine in neonatal rat cardiac myocytes. *Eur J Pharmacol.* 297:97-106.

373. **A. M. Katz and F. C. Messineo**. 1981. Lipid-membrane interactions and the pathogenesis of ischemic damage in the myocardium. *Circ Res.* 48:1-16.

374. **T. Nishimoto**. 2000. Upstream and downstream of RanGTPase. *Biol Chem.* 381:397-405.

375. **F. R. Bischoff, H. Krebber, E. Smirnova, W. Dong and H. Ponstingl**. 1995. Co-activation of RanGTPase and inhibition of GTP dissociation by Ran-GTP binding protein RanBP1. *EMBO J.* 14:705-715.

376. **T. Aoyama, M. Chen, H. Fujiwara, T. Masaki and T. Sawamura**. 2000. LOX-1 mediates lysophosphatidylcholine-induced oxidized LDL uptake in smooth muscle cells. *FEBS Lett.* 467:217-220.

377. **N. Kume and J. Gimbrone, M.A.** 1994. Lysophosphatidylcholine transcriptionally induces growth factor gene expression in cultured human endothelial cells. *J Clin Invest.* 93:907-911.

378. **X. Fang, M. Gaudette, T. Furui, M. Mao, V. Estrella, A. Eder, T. Pustilnik, T. Sasagawa, R. Lapushin, S. Yu, R. B. Jaffe, J. R. Wiener, J. R. Erickson and G. B. Mills**. 2000. Lysophospholipid growth factors in the initiation, progression, metastases, and management of ovarian cancer. *Ann N Y Acad Sci.* 905:188-208.

379. **M. Okita, M. Gaudette, G. B. Mills and B. J. Holub**. 1997. Elevated levels and altered fatty acid composition of plasma lysophosphatidylcholine (LysoPC) in ovarian cancer patients. *Int J Cancer.* 71:31-34.

380. **T. Sasagawa, M. Okita, J. Murakami, T. Kato and A. Watanabe**. 1999. Abnormal serum lysophospholipids in multiple myeloma patients. *Lipids*. 34:17-21.

381. **S. Liu, C. Yu, J. Hays, V. Panagia and N. S. Dhalla**. 1997. Modification of heart sarcolemmal phosphoinositide pathway by lysophosphatidylcholine. *Biochim Biophys Acta*. 1349:264-274.

382. **S. Ludwig, A. Hoffmeyer, M. Goebeler, K. Kilian, H. Häfner, B. Neufeld, J. Han and U. R. Rapp**. 1998. The stress inducer arsenite activates mitogen-activated protein kinases extracellular signal-regulated kinases 1 and 2 via a MAPK Kinase 6/p38-dependent pathway. *J Biol Chem*. 273:1917-1922.

383. **U. Brinkmann, E. Brinkmann, M. Gallo and I. Pastan**. 1995. Cloning and characterization of a cellular apoptosis susceptibility gene, the human homologue to the yeast chromosome segregation gene *CSE1*. *Proc Natl Acad Sci USA*. 92:10427-10431.

384. **J. Moroianu**. 1998. Distinct nuclear import and export pathways mediated by members of the karyopherin β family. *J Cell Biochem*. 70:231-239.

385. **J. Solsbacher, P. Maurer, F. R. Bischoff and G. Schlenstedt**. 1998. Cse1p is involved in export of yeast importin α from the nucleus. *Mol Cell Biol*. 18:6805-6815.

386. **A. Cuenda, J. Rouse, Y. N. Doza, R. Meier, P. Cohen, T. F. Gallagher, P. R. Young and J. C. Lee**. 1995. SB 203580 is a specific inhibitor of a MAP kinase homologue which is stimulated by cellular stresses and interleukin-1. *FEBS Lett*. 364:229-233.

387. **R. Ben-Levy, I. A. Leighton, Y. N. Doza, P. Attwood, N. Morrice, C. J. Marshall and P. Cohen**. 1995. Identification of novel phosphorylation sites required for activation of MAPKAP kinase-2. *EMBO J*. 14:5920-5930.

388. **D. Görlich**. 1997. Nuclear protein import. *Curr Opin Cell Biol*. 9:412-419.

389. **R. Buccoliero and A. H. Futerman**. 2003. The roles of ceramide and complex sphingolipids in neruonal cell function. *Pharmacol Res*. 47:409-419.

390. **S. Geley, B. L. Hartmann and R. Kofler**. 1997. Ceramides induce a form of apoptosis in human acute lymphoblastic leukemia cells that is inhibited by Bcl-2, but not by CrmA. *FEBS Lett*. 400:15-18.

391. **J. R. Charpie, D. G. Johns and R. C. Webb**. 1999. Tumor necrosis factor-alpha inhibits human coronary artery smooth muscle cell proliferation by generation of intracellular ceramide. *FASEB J*. 13:A39.

392. **S. L. Schissel, J. Tweedie-Hardman, J. H. Rapp, G. Graham, K. J. Williams and I. Tabas**. 1996. Rabbit aorta and human atherosclerotic lesions hydrolyze the sphingomyelin of retained low-density lipoproteins. *J Clin Invest*. 98:1455-1464.

393. **M. R. Bennet, K. Macdonald, S.-W. Chan, J. J. Boyle and P. L. Weissberg**. 1998. Cooperative interactions between RB and p53 regulate cell proliferation, cell senescence, and apoptosis in human vascular smooth muscle cells from atherosclerotic plaques. *Circ Res*. 82:704-712.

394. **N. A. Bourbon, L. Sandirasegarane and M. Kester**. 2002. Ceramide-induced inhibition of Akt is mediated through protein kinase Cζ. *J Biol Chem*. 277:3286-3292.